Low Cost Drinking Water Treatment Using Indigenous Materials for Remote Communities in Developing Countries

A thesis submitted in fulfilment of the requirements for the degree of Doctor of Philosophy

Nur Adila Ab Aziz

Bachelor of Civil Engineering (Honours), Master of Civil Engineering

Universiti Tun Hussein Onn Malaysia

School of Engineering

College of Science, Engineering and Health

RMIT University

March 2017

Declaration

I, Nur Adila Ab Aziz hereby certify that; except where due acknowledgment has been made, the work is that of the author alone, the work has not been submitted previously, in whole or in part, to qualify for any other academic award, the content of this thesis is the result of work which has been carried out since the official commencement date of the approved research program, any editorial work, paid or unpaid, carried out by a third party is acknowledged; and ethics procedures and guidelines have been followed.

Signed.....

On.....

Acknowledgements

Firstly, I would like to convey my most sincere gratitude to my principal supervisor Dr. Niranjali Jayasuriya for the continuous support towards my Ph.D. study and related research, for her patience, motivation, and vast knowledge. Her guidance helped me in my research and writing of this thesis. I could not ask for a better supervisor and mentor for my Ph.D. study.

In addition, I would like to acknowledge my second supervisor, Dr. Linhua Fan and members of Water Research group for their insightful comments and encouragement, as well as for the tough questions which motivated me to widen my research to cover various perspectives and taught me how to boost my confidence in delivering presentations in front of peers and professionals. Special appreciation also goes to Dr. Babu, Dr. Sandro, Cameron and Paul Morrison for their guidance throughout the experiments and analyses in the laboratories.

I could not thank enough for the funding received towards my Ph.D. from Ministry of Higher Education, Malaysia and Universiti Tun Hussein Onn Malaysia for the 3.5 years. Without the scholarships, I would not be able to experience this great opportunity especially in developing my research skills, being independent and appreciating different cultures while overseas.

I would like to thank my fellow lab mates and other friends in the School of Engineering (Civil, Environmental and Chemical Disciplines) at RMIT University namely Sugeesha, Shovana, Sivanandhan, Chamila, Farouk, Sakinul, Kaniz, Shakila, Biplob, Yufei, Xiao Lei, Maha Al-Ali, Malindu and many others. Not to forget, my

fellow colleagues at Universiti Tun Hussein Onn Malaysia namely Nurul, Faniza, Salwa, Hamizah, Hafizal, Faizal, Firdaus and Azuan who are always there whenever I need a helping hand. I am grateful to have all of you throughout this journey especially for enlightening me with ideas, solutions and motivation during my most difficult times.

Last but not least, I would like to thank my family including my beloved husband (Mohd Faizuan) for his sacrifices and my lovely daughters (Nur Hannani & Nur Tihany), my supportive parents (Ab Aziz & Fauziah), my siblings (Shahidah, Shafiq, Sharah & Nuha), my in-laws and my relatives for constantly supporting me throughout this journey.

I would also like to convey my utmost gratitude to the Malaysian community in Melbourne, particularly the residents of Kampung (Village) Victoria North Melbourne (KVNM) who have been very supportive and had created a family-like environment during our 3.5 years' stay in Melbourne.

List of publications

1. Aziz, N.A.A., Jayasuriya, N. & Fan, L. (2014). Effectiveness of plant-based indigenous materials for the removal of heavy metals and fluoride from drinking water. *In 5th International Conference on Sustainable Built Environment Proceedings*. Kandy, Sri Lanka, *3*, 34-41.
2. Aziz, N.A.A., Jayasuriya, N. and Fan, L (2015). Application of *Moringa oleifera* seeds and *Musa cavendish* as coagulants for lead, nickel and cadmium removal from drinking water. *In: Asia Pacific Confederation of Chemical Engineering Congress 2015: APCChE 2015, incorporating CHEMECA 2015*. Melbourne: Engineers Australia, 2015: 1774-1781.
3. Aziz, N. A. A., Jayasuriya, N., & Fan, L. (2016). Adsorption study on *Moringa oleifera* seeds and *Musa cavendish* as natural water purification agents for removal of lead, nickel and cadmium from drinking water. *IOP Conference Series: Materials Science and Engineering*, *136*, 12044.
4. Aziz, N. A. A., Jayasuriya, N., & Fan, L. Application of plant-based materials for the removal of heavy metals, turbidity and fluoride from drinking water at household level in remote areas. (under preparation)
5. Aziz, N. A. A., Jayasuriya, N., & Fan, L. Adsorption of lead, nickel and cadmium on *Moringa oleifera* and *Musa cavendish* from contaminated drinking water sources. (under preparation)

Table of contents

List of figures

List of tables

List of nomenclature

Å	Unit of pore diameter
a_{ij}	Competition coefficient for the adsorption of element i in the existence of element j
a_R	Redlich-Peterson isotherm constant (1/mg)
A_T	Tempkin isotherm equilibrium binding constant (L/g)
b	Langmuir isotherm constant (dm^3/mg)
C	Dissolved concentration (mg/L)
C_0	Initial concentration of contaminant in the solution (μmol/L)
C_{BET}	BET adsorption isotherm relating to the energy of surface interaction (L/mg)
C_e	Equilibrium concentration of contaminant (mg/L) or (μmol/L)
$C_{e\ experiment}$	Final concentration of contaminant (μmol/L)
$C_{e\ model}$	Calculated (model) final concentration of contaminant (μmol/L)
C_i	Concentration of element i in the equilibrium solution in (μmol/L)
C_j	Concentration of element j in the equilibrium solution in (μmol/L)
C_s	Adsorbate monolayer saturation concentration (mg/L)
$d.f.$	Degree of freedom
g	Redlich-Peterson isotherm exponent
i	Metal components i
j	Metal components j
k_{ad}	Dubinin-Radushkevich isotherm constant (mol^2/kJ^2)
keV	Kilo Electron Volt
K_F	Freundlich isotherm constant (mg/g)(dm^3/g)
kg	Kilogram
k_i	Freundlich constants obtained for i in single-element system
K_L	Langmuir constant (L/μmol)
K_R	Redlich-Peterson isotherm constant (L/g)
kV	Kilo Volt
L	Litre

l	Total number of components
M	Molar
m	Mass of the biomass used (g)
min	Minute
mL	Millilitre
N	Number of sample (count)
n	Adsorption intensity
n_F	Freundlich constant
n_i	Freundlich constants obtained for i in single-element system
n^{th}	Rank of Sample
Q_0	Maximum monolayer coverage capacities (mg/g)
Q_e	Amount of heavy metal adsorbed (μmol/g)
q_e	Amount of adsorbate in the adsorbent at equilibrium (mg/g)
Qm	Monolayer adsorption capacity (μmol/g)
q_i	Adsorption of element i per gram (μmol/g)
q_s	Theoretical isotherm saturation capacity (mg/g)
R	Universal gas constant (8.314 J/mol K)
R^2	Coefficient of determination
R_L	Separation factor
S	Amount of adsorption (mg/kg)
T	Temperature (K)
t_c	Critical-T (t_c =1.962 for $\alpha = 95\%$)
V	Volume of the solution (L)
α	Confidence level
σ^2	Variance
σ	Standard deviation
°C	Degree Celsius
ε	Dubinin-Radushkevich isotherm constant
μ	Mean
%	Percentage
%Wt	Percentage weight

List of abbreviations

ANSI	American National Standards Institute
ATR-FTIR	Attenuated Total Reflectance-Fourier Transform Infrared
AUD	Australian dollar
BET	Brunauer-Emmett-Teller
BGS	British Geological Survey
BIS	Bureau of Indian Standards
CA	*Cicer arietinum* (chickpeas)
CKDu	Chronic Kidney Disease of unknown aetiology
CN	*Cocos nucifera* (coconut solid endosperm)
COD	Chemical oxygen demand
CTAB	Cetyl trimethyl ammonium bromide
CTS	Coconut tree sawdust
DOC	Dissolved organic carbon
DPHE	Department of Public Health Engineering
EC	Electroconductivity
ES	Eggshell
EDX	Energy Dispersive X-ray
FAO	Food and Agriculture Organization of the United Nations
GAC	Granular activated carbon
GW	Groundwater
HMAA	Hydroxyapatite-modified activated alumina
HWTS	Household water treatment systems
ICP-MS	Inductively Coupled Plasma Mass Spectrometry
ISEF	Fluoride Ion Selective Electrode
IWRA	International Water Resources Association
LE	*Lentinus edodes* (Shiitake mushroom)
MC	*Musa cavendish* (banana peel)
ME	Multi-element
MIAA	Modified immobilized activated alumina
MO	*Moringa oleifera* (Moringa seeds)

NDWQS	National Drinking Water Quality Standard
NOM	Natural organic matter
NSDWQ	National Standards for Drinking Water Quality
NSF	National Science Foundation
NTU	Nephelometric Turbidity Units
PAC	Powdered activated carbon
PANI/SD	Saw dust coated with polyaniline
PDF	Probability density function
POE	Point of entry
POU	Point of use
RMIT	Royal Melbourne Institute of Technology
RWH	Rainwater harvesting
SB	Sugarcane bagasse
SDS	Sodium dodecyl sulfate
SE	Single-element
SEM	Scanning Electron Microscopy
SLS	Sri Lanka Standards
SRS	Sheindorf-Rebhun-Sheintuch
SSS	Small scale systems
TOC	Total organic carbon
TSS	Total suspended solids
UNICEF	United Nations International Children's Emergency Fund
USD	United States (Dollar)
USEPA	United States Environmental Protection Agency
USGS	United States Geological Survey
UV	Ultraviolet
UVA_{254}	Ultraviolet 254 nm absorbance
WHO	World Health Organisation
XMCS	Xanthate-modified magnetic chitosan

Executive summary

Groundwater in many remote areas in developing countries was polluted with various harmful contaminants such as heavy metals and fluoride. The existence of these contaminants in polluted groundwater usually exceeds the standard limit recommended by the World Health Organisation (WHO) for drinking water quality. The primary objective of this study was to examine the use of indigenous natural products that are locally available, non-toxic, easy to prepare and biodegradable. It was expected that natural material can be an alternative to the expensive and harmful chemicals used for drinking water treatment.

Based on previous studies, *Moringa oleifera* (Moringa seeds), *Cicer arietinum* (chickpeas), *Musa Cavendish* (banana peel), *Cocos nucifera* (coconut's solid endosperm) and *Lentinus edodes* (Shiitake mushroom) were selected as natural water purification agents to examine their potential of removing various contaminants from polluted groundwater. However, it is important to realise that the effectiveness of each biomass tends to vary, depending on the contaminant. For this study, coagulation was selected as the key treatment process due to its practicality and simplicity to be used by non-skilled remote communities with small-scale water treatment systems.

This research focused on groundwater as it is a major source of drinking water supply especially for many remote areas in the developing countries such as Pakistan, India, Sri Lanka and Bangladesh. It was documented in the literature that arsenic (As) and fluoride were the most concerned water contaminants due to their excessive level in groundwater, followed by other heavy metals such as lead (Pb), nickel (Ni) and cadmium (Cd). These harmful chemicals will lead to long-term effects on human

health. Turbidity is generally not an issue for groundwater quality because the underground water has been filtered through the natural soil filtration system. Only in certain cases, groundwater was found turbid and aesthetically unpleasant due to the improper groundwater abstraction. In this study, the effectiveness of plant-based materials for the removal of low concentrations of As, Pb, Cd, Ni, fluoride and turbidity were investigated.

Batch tests with individual biomass and their combinations were conducted at a pH of 7. Synthetic groundwater samples with known concentration of As, Pb, Ni, Cd, fluoride and turbidity was prepared, each with different biomass dosages ranging from 100 mg/L to 600 mg/L and different biomass dosing methods (single, combination and sequential manners) were attempted. Based on the preliminary screening, *Moringa oleifera* (MO) and *Musa cavendish* (MC) have been chosen to be used for the study based on their efficiency in removing target contaminants. The optimum efficiency was achieved by using combination of MO and MC (MO+MC), which dosed either in a mixing or in a sequential manner. The optimum biomass dosage was 200 mg/L for the individual biomass and 200:200 mg/L for the combined biomass. Unlike chemical coagulants such as alum, natural materials did not significantly affect the pH of water during treatment. Treatment tests were also conducted on actual groundwater samples to verify the applicability of the studied treatment process on actual applications. The results suggested that the MO+MC was capable of treating actual groundwater samples to meet the required WHO standards.

Characterisation study of the combined biomass (MO+MC) before and after the treatment process was conducted using Attenuated Total Reflectance-Fourier Transform Infrared (ATR-FTIR), Scanning Electron Microscopy (SEM), and Energy Dispersive X-ray (EDX) in order to determine the possible mechanisms behind the

removal of each contaminant. Based on the FTIR spectral analysis, carboxylic acids, primary and secondary amines as well as carbonyl (amides) were identified as the dominant functional groups in MO, MC and MO+MC which were favoured during the adsorption of the contaminants. SEM exhibited that there was an abundant availability of porous and irregular surfaces which provide binding sites that facilitate the accumulation of target contaminants on the biomass. On the other hand, through EDX analysis, EDX spectra of the contaminant-loaded biomass (after treatment) exhibited specific feature (element) which corresponded to the presence of the target contaminants through adsorption. It was revealed that adsorption (chemisorption and physisorption) was the main mechanism for the removal of target contaminants besides ion exchange and surface complexation. Therefore, existing adsorption models were evaluated by fitting the experimental adsorption data of single-contaminant and multi-contaminant elements to predict the treated groundwater quality. Based on the results, most of the experimental adsorption data provided an agreement with the Freundlich model, which was then selected to predict the final groundwater quality. Variations of input water quality were generated using a simple Monte Carlo simulation method (random number generation) to simulate the actual groundwater quality. These water quality samples were subjected to the selected treatment process. The probability of the groundwater quality (after the treatment with MO, MC and MO+MC) complied with WHO standards were also predicted. The results showed that 94% and 91% from 1000 samples of groundwater contaminated with Pb were complied with WHO standards after treated using MO and MO+MC respectively. Furthermore, 98% and 84% from 1000 samples of groundwater contaminated with Ni and Cd, respectively, complied with WHO standards.

At the final stage of the research, cost estimation of the proposed treatment method (MO and MC dosed in a mixing manner) was carried out. It was assumed that there would be no cost incurred on the natural materials of biomass as they would be freely available in the selected countries. The only cost that might be incurred during the treatment process was the investment on raw groundwater storage, coagulation reactor and sand filter containers, grinder (i.e., pestle and mortar) as well as the siever. The contaminant-loaded biomass was managed using native earthworms called *Perionyx excavatus* which was previously reported capable of converting arsenic from plant available form to plant unavailable form. Therefore, after cost estimation analysis, it appears that the proposed treatment would be economically feasible for the remote communities in the developing countries.

To sum up, this research had demonstrated that tropical plant-based materials had the potential in removing target contaminants from contaminated groundwater to meet WHO standards for drinking water. The understanding of the whole process was essential in developing an operational scale decentralised treatment system in the future. Further extensive investigations on the low-cost sludge management methods would be important and useful to minimise the impact of untreated sludge on the environment.

CHAPTER 1 Introduction

Communities living in remote areas mostly in developing countries rarely have the access to treated drinking water supply. These countries often lack of resources to fund large centralised water treatment systems to supply the remote areas (Berger et al., 2009). As a result, groundwater wells were left as the primary source of drinking water available. However, groundwater was polluted in some regions, particularly in South Asian countries where harmful contaminants, including heavy metals, exceed World Health Organisation (WHO) standards for drinking water. The degrading quality of drinking water sources in some of the South Asian countries has become a major public health concern.

India, Pakistan, Bangladesh and Sri Lanka has renewable groundwater resources with an average of 432, 55, 21 and 8 billion cubic meters per year, respectively (FAO, 2015). The groundwater can be contaminated with various pollutants such as heavy metals and turbidity. Heavy metals are present in groundwater due to the untreated wastewater and poor practices of land used including the excessive use of agrochemicals. In some cases, harmful heavy metals such as arsenic can be occurring naturally in groundwater. Pandey et al. (2016) reported that arsenic and fluoride occurred in the groundwater by the natural process of mineral dissolutions from the aquifers.

In recent decades, elevated concentration of heavy metals and other problematic ions in drinking water supply had been identified in rural areas especially in India, Pakistan, Bangladesh and Sri Lanka. The average level of lead (Pb) recorded in groundwater samples collected from areas in India and Pakistan was 287 µg/L and 330 µg/L, respectively (Buragohain et al., 2010; Midrar-Ul-Haq et al., 2005). Midrar-Ul-Haq et

al. (2005) also reported that the average level of nickel (Ni) in groundwater in Pakistan was as high as 960 μg/L. In Sri Lanka, average levels of cadmium (Cd) in groundwater have been recorded between 5 to 23 μg/L (Bandara et al., 2010) and arsenic (As) concentration level at certain locations was as high as 40 μg/L (Rajasooriyar et al., 2013). The concentration of heavy metals exceeds the recommended standards by WHO for drinking water (10 μg/L, 20 μg/L, 3 μg/L, 10 μg/L for Pb, Ni, Cd and As, respectively). Excessive level of As in drinking water can cause arsenic skin lesions.

The north central province in Sri Lanka faced a controversial issue regarding high contents of fluoride in the groundwater. The fatal Chronic Kidney Disease of unknown aetiology (CKDu) had been detected over ten years ago in certain parts of the dry zone regions (Aturaliya et al., 2006; Chandrajith et al., 2011). However, factors that contributed to the increasing number of people suffering from kidney failure were still not fully understood. The highest concentration of fluoride recorded was 8 mg/L, significantly exceeds WHO drinking water standard which is 1.5 mg/L. Higher concentration of fluoride in drinking water can cause dental and skeletal fluorosis (Jayawardana et al., 2012). Therefore, it was extremely important to remove these harmful substances from drinking water to prevent adverse effects to human health.

Millions of people are living in poverty in arid and semi-arid zones of these tropical countries. These countries are not only among the fastest growing country in the world but also among the poorest. Apart from the drinking water quality issues, poor economic and political situations in some developing countries disrupted the development of centralised low-cost drinking water treatment methods which uses fewer chemicals and energy. The centralised low-cost drinking water treatment allows the vast majority of people living away from urban cities to have potable water. Even

though claims have been made that there were viable low-cost water treatment methods, scientific evidence to support most of these claims was very limited.

Coagulation is a simple treatment process and relatively cost-effective for the point-of-use system. Conventional chemical treatment of contaminated water may not be feasible for remote communities in the region due to its technical and financial constraints. The use of plant-based materials for drinking water treatment is environmentally sustainable, cost-effective as they are locally available, non-toxic, easy to prepare and the generated residual is easy to be disposed. Unlike removing contaminants from wastewater, little attention has been paid to the use of natural materials to remove low concentration of contaminants from groundwater.

Various plant-based materials have been studied recently as a potential low-cost water purification agents (Chen et al., 2008; Anwar et al., 2010; Sengupta et al., 2012; Fatombi et al., 2013; Kale, 2013). These studies reported that different types of plant-based materials could remove specific contaminants in the water. Furthermore, the use of these materials can overcome the drawbacks when using chemical agents in conventional water treatment methods. Other than high cost incurred, the major challenge in using aluminium-based coagulants is the high volume of sludge produced at the end of the treatment process as well as the significant effects on the acidity of water (Flaten, 2001).

Based on the previous studies, *Moringa oleifera* (MO) seeds were widely known for its effectiveness in removing various pollutants from water. In the early stage of the introduction of MO for water purification, Ndabigengesere et al. (1995) stated that MO had a mechanism of coagulation that consists of adsorption and neutralisation of the colloidal charges. The promising mechanism created significant opportunities for

the researchers to conduct the study in their respective areas. MO could also produce four to five times less sludge volume compared to alum (Ndabigengesere et al., 1995). MO was reported to be effective in removing turbidity as reported by several studies (Ndabigengesere et al., 1995; Beltrán-Heredia & Sánchez-Martín, 2009; Ali et al., 2010; Pritchard et al., 2010; Sengupta et al., 2012). Also, there were several studies which investigated the removal of heavy metals such as Cd (Sharma et al., 2006), Zn (Bhatti et al., 2007), Cu, Ni, Zn (Kalavathy & Miranda, 2010) and Pb using MO (Reddy et al., 2010). *Cicer arietinum* (CA), which commonly known as chickpeas, was also reported able to remove turbidity and As up to a satisfactory level (Asrafuzzaman et al., 2011; Saqib et al., 2013), providing a practical alternative to MO. *Musa cavendish* (MC) known as banana peel appeared to be a promising water purification agent in removing Pb and Cd (Anwar et al., 2010). The use of banana peel in water treatment fits well with the concept of environmental sustainability since the agricultural waste were recycled to minimise the waste in an eco-friendly way (Okoro & Okoro, 2011). Fatombi et al. (2013) reported that *Cocos nucifera* (CN) (coconut's solid endosperm) provided a competitive result to MO in terms of turbidity removal. Attractively, coconut is widely available in tropical countries. Chen et al. (2006, 2008) reported that *Lentinus edodes* (LE), which also known as Shiitake mushroom is effective for chromium (Cr) and Cd removal from metal-contaminated wastewater. The above mentioned indigenous plant-based materials have fulfilled the criteria of plant-based materials selection and were therefore tested in the present study.

While some studies investigated the effectiveness of low-cost water treatment methods using indigenous materials, little has been written about the principal mechanism underneath the treatment process to enhance the understanding of pollutant removal mechanism which is essential in designing low-cost water treatment systems in the

future. This study aims in contributing to more comprehensive understanding of the treatment mechanisms for designing low-cost treatment process using indigenous materials.

The applicability of the existing mathematical adsorption models to predict water quality after being treated by the selected treatment process was also evaluated. After the verification process, a suitable model was used to predict the water quality outputs for a range of simulated water quality inputs. A Monte Carlo random number generation technique was used to simulate variations of a large number of water quality input. Furthermore, the assessment on the probability of treated water quality exceeding or complying with WHO drinking water quality standards was carried out to minimise the risk of unsafe water reaching the end users.

At the end of the thesis, estimation on the cost incurred during drinking water treatment was calculated to provide an assessment on the cost related to the use of indigenous materials for water treatment. The methodology of the study is illustrated in the flow chart (Figure 1.1).

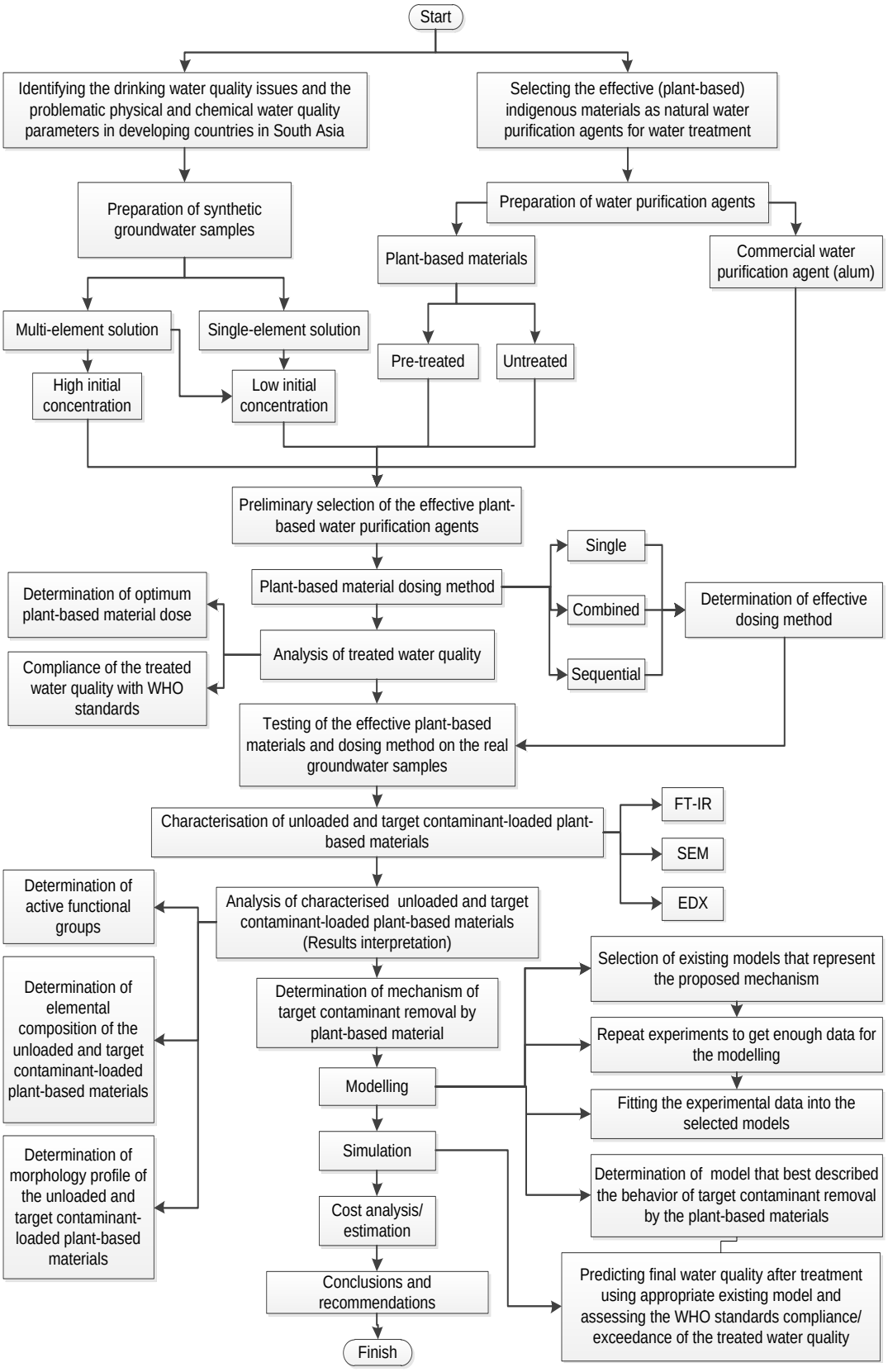

Figure 1.1 Flow chart of research methodology

1.1 Research questions

Research questions that formulate the entire design of this study are as follows:

1. Could WHO standards for drinking water be achieved using the indigenous plant-based material as the water purification agent to remove turbidity, fluoride, arsenic, cadmium, lead and nickel during water treatment process?
2. If so, which natural material(s) can meet the treatment targets, and how to maximise the treatment efficiency?
3. Can output water quality concentration be predicted if input water quality concentration and optimum treatment conditions were known?
4. Is it possible to develop a decentralised drinking water treatment system which is affordable to rural communities in developing countries?

1.2 Objective of the Study

The primary objective of the study was to examine the use of widely available indigenous natural products as an alternative to expensive chemicals in contaminated groundwater treatment and to improve the understanding of factors contributing to a decentralised and low-cost water treatment systems using indigenous materials. In this study, coagulation was selected to be the key treatment process. This study will:

1. Identify effective biomass and optimum conditions such as biomass concentration (dose) and biomass dosing method as well as the initial concentration of target contaminants in the removal of target contaminants from polluted groundwater.

2. Determine the chemical composition, active functional groups and surface morphology of the biomass before and after the treatment process to understand the removal mechanism of the target contaminants.
3. Select a suitable mathematical model to predict the final water quality (contaminant concentrations) knowing the input water quality concentrations for a given dosage of biomass and a particular type of treatment medium.
4. Determine the probability of treated water quality parameters exceeding the WHO recommended water quality standards; and
5. Estimate the costs of the proposed treatment method including the disposal of the sludge.

1.3 Thesis outline

Chapter 1 describes the background, rationale and objectives of the research. The research questions were formulated to guide the flow of research conducted in this study.

Chapter 2 provides a review of current literatures related to drinking water quality issues in developing countries, followed by a discussion on conventional drinking water treatment materials and technologies related to low-cost drinking water treatment. This chapter also provides a review and a discussion on the effectiveness of plant-based indigenous materials in removing pollutants from water followed by a brief introduction on the existing adsorption models. Furthermore, a discussion on the importance of biomass characterisation before and after treatment process, as well as cost estimation of the proposed treatment method was conducted. Finally, the current state of the knowledge and research gaps in low-cost water treatment system using plant-based indigenous materials was identified.

Chapter 3 describes materials and methods involved throughout this research.

Chapter 4 presents the preliminary experimental results investigating the effectiveness of selected biomass and their optimum treatment conditions in removing the target contaminants from a synthetic groundwater sample. The optimum biomass conditions were then used on actual groundwater collected from the field to investigate the performance efficiency, and the results were presented. Investigations on the pre-treatment of biomass with acid, base and thermal in removing problematic contaminants according to WHO standards were also carried out. Furthermore, the use of a considerably small dosage of alum has been investigated to ensure that these problematic pollutants can be reduced to meet WHO standards for drinking water.

Chapter 5 examines the possible mechanisms involved in the treatment process by characterising the unloaded and contaminant loaded-biomass using FTIR, SEM, and EDX instruments.

Chapter 6 reports on the adsorption study of target heavy metals (lead, nickel, and cadmium) on *Moringa oleifera, Musa cavendish* and their mixing in single-element and multi-element systems. In this chapter, Langmuir, Freundlich and Sheindorf-Rebhun-Sheintuch (SRS) adsorption models were evaluated to detail out the behaviour of the adsorption process. Furthermore, this chapter also investigates the reliability of treatment on the incoming target contaminant concentrations with predetermined optimum doses of biomass within WHO standards.

Chapter 7 reveals the cost estimation for the proposed drinking water treatment. This chapter also compares the costs of the treatment using plant-based indigenous materials with conventional alum.

Chapter 8 summarises the findings of the research and relates the implications of this research on treating polluted groundwater in developing countries to supply rural communities with treated water. Recommendations are also included in this chapter to provide guide for future research.

CHAPTER 2 Literature review

This chapter provides a review of the current literature on the drinking water sources and quality issues in developing countries, followed by a discussion on the conventional drinking water treatment materials and technologies related to low-cost drinking water treatment. The chapter also discusses the effectiveness of plant-based indigenous materials in removing water pollutants followed by a brief introduction of the existing adsorption models and their applications. This chapter also reveals the importance of characterising biomass before and after the treatment process and estimates the cost of the proposed treatment method. Finally, the chapter identifies the current state of the knowledge and research gaps in low-cost water treatment using plant-based indigenous materials.

2.1 Introduction

An individual requires no less than 20 to 50 litres of water per day for drinking, food preparation and personal hygiene (Gleick & IWRA, 1996). Many people in remote areas in developing countries (particularly South Asian and African countries) are known to be lacking access to proper water treatment facilities which eventually lead them to various issues due to unsafe quality of drinking water.

Unlike the urban communities who are normally provided with treated drinking water, rural communities are often lagging and undersupplied with drinking water due to lack of financial resources. Furthermore, the contamination of drinking water sources due to various natural and anthropogenic factors deteriorate the water quality. To address the increasing demand for safe quality of drinking water, low-cost, decentralised drinking water treatment facilities should be introduced to serve rural communities.

Natural materials (plant-based biomass) are low in cost and freely available in targeted countries compared to expensive chemicals that are normally used during alternative conventional water treatment. It was proven that plant-based materials possess a potential to be applied as a water purification agent due to their effectiveness to remove pollutants from water and wastewater as documented in literature (Chen et al., 2008; Asrafuzzaman et al., 2011; Sengupta et al., 2012; Kamsonlian et al., 2012; Fatombi et al., 2013).

However, it is known that the effectiveness of a specific biomass depends on the type of water quality contaminant that needs to be treated. Thus, it is important to investigate the effectiveness of the selected biomass in treating specific pollutants in contaminated drinking water. Furthermore, it is also essential to determine the physical and chemical properties of the biomass to maximise the treatment efficiency prior to application in water treatment.

2.2 Drinking water sources in remote areas in developing countries

In 2015, 134 million people in Southern Asia still lacked clean drinking water sources followed by people in Eastern Asia (65 million) and South-Eastern Asia (61 million) (WHO & UNICEF, 2015). This statistic shows that people living in South Asian countries particularly in remote regions are vulnerable to drinking water scarcely.

Unfortunately, due to economic and financial constraints, conventional water treatment plants are often limited in remote areas in developing countries. These unfavourable situations have led these communities to depend on various kinds of reliable water sources for drinking water including surface water, groundwater, rainwater and desalinated water (Delpla et al., 2009; Chakraborti et al., 2010; Basu &

Van Meter, 2013; Naddeo et al., 2013; Kim et al., 2015). Besides, submarine groundwater is also identified as a potential supply of drinking water as it might be present in large quantities and also possess lower salinity compared to the sea water (Bakken et al., 2012).

Even though there is easy access to surface water, there are high concentrations of toxic and harmful contaminants in agricultural and industrial residues which are discharged to water bodies (i.e., river, dam, lake) without proper treatment (Chau et al., 2015). Surface water is also known as a source that is prone to bacterial and enteric viruses contamination such as *Salmonella* and bovine enteric virus (Gibson & Schwab, 2011; Levantesi et al., 2012). Accordingly, these drawbacks have led to the need for surface water to be treated before consumption.

Rainwater harvesting (RWH) is also a popular approach to storing water at household or community levels in urban and remote areas for daily activities (Naddeo et al., 2013; Akter & Ahmed, 2015). RWH is greatly dependent on the intensity and frequency of storm events. Despite of its cost effectiveness, it possesses a number of disadvantages including (i) the reliance on storm events; (ii) the uncertainty of quantity and quality of rainwater; (iii) susceptible to undesired health hazards due to uncertain durations (long period) of rainwater storage before it reaches the consumers (Zhu et al., 2004).

Over the years, groundwater has always been chosen as a reliable drinking water source due to its quality (Nagarajan et al., 2010; Hashim et al., 2011). Eighty percent (80%) of the total population of Sri Lanka live in rural regions with 30% considered to be liable to the untreated drinking water supply (Rajapakse et al., 2014). Most of the water that is been used in these areas is coming from groundwater followed by rain

water. Groundwater is less prone to bacterial contamination compared to the other sources of untreated drinking water.

Groundwater usually can be consumed untreated because it is considered to be treated as the water flows through the natural soil filtration system. During this process, it collects necessary minerals such as sodium, calcium, magnesium, potassium and chloride which are essential minerals for functioning of the human body. However, the level of these dissolved mineral substances should not be more than 1000 mg/L as this level can be hazardous to the living organisms such as plants and animals (USGS, 2013).

Based on the above water sources which are suitable to be used for drinking, cooking and personal hygiene purposes, groundwater is identified to be the most suitable compared to surface water, rainwater and other sources such as desalinated sea water and submarine groundwater due to cost in treating the water to WHO compliance levels.

2.3 Drinking water quality issues in developing countries in Asia

Although the groundwater is considered to be of drinking water standard (Naddeo et al., 2013; Chowdhury et al., 2016), a number of factors have contributed in providing safe quality of drinking water in many remote areas of developing countries in Asia. One of the major issues hindering providing with quality drinking water is the poor economic condition and the ongoing cycle of poverty (WHO, 2006). Furthermore, the water sources are degraded due to pollutants entering water sources from rapid urbanisation, industrialisation and poor land use practices such as the uncontrolled

application of agrochemicals (i.e., fertilisers and pesticides) in agriculture (Gupta, 2008).

Midrar-Ul-Haq et al. (2005) reported that 88% and 100% of the groundwater samples in North-west Frontier Province and Sindh, Pakistan, respectively were polluted with lead (Pb) (average concentrations of 330 µg/L and 150 µg/L, respectively). On the other hand, most of the groundwater samples (100%) that had been collected from these locations also were found to be contaminated with the excessive concentrations of cadmium (Cd) (average concentrations of 40 and 30 µg/L in North-west Frontier Province and Sindh, Pakistan, respectively). The groundwater samples were collected from wells (depth: 50 to 60 feet) at various sites in the above areas. Hence, it was assumed that the risk of groundwater contaminations could be coming from industrial or municipal sources.

Buragohain et al. (2010) reported that the maximum levels of Pb (360 µg/L) and Cd (120 µg/L) in dry season exceeded the recommended levels by WHO standards of 10 µg/L and 3 µg/L respectively in Assam, India. The groundwater samples were taken from 20 different sites in dry and wet seasons. Most of the high concentrations of metal contaminants were detected in the dry season. The reason could be due to the dilution effects of contaminants during the rainy season. The above authors reported that the location of the above study area was within the sedimentary basins and the contamination could be due to the deposition of sediments from the surface erosion of the surrounding rocks or aquifers. The authors also argued that the anthropogenic sources could not be the cause for high metal contamination in the study area.

In West Bengal, Bangladesh, 48.1% out of 46,321 hand tube wells were exceeded the WHO recommended concentration for arsenic (As) of 10 µg/L (Chakraborti et al.,

2010). While in a study conducted by Ghoraba & Khan (2013) reported that 25 out of 120 groundwater samples in Balochistan province, Pakistan, had shown fluoride values above the maximum WHO acceptable limit of 1.5 mg/L.

In Karachi, Pakistan, 86% of 216 groundwater and surface water wells contain excessive levels of Pb (Ul-Haq et al., 2011). The concentration levels are as high as 146±119 µg/L and 77.1±54 µg/L in groundwater and surface water respectively (WHO recommended value is 10 µg/L). The authors claimed that the excessive level of Pb in the groundwater and surface water was mainly due to the discharge of untreated effluents from industrial activities and leaching from pipeline materials into the groundwater.

On the other hand, Memon et al. (2011) reported that the level of turbidity in groundwater exceeded the recommended WHO standard of 5 NTU in the southern province of Pakistan. This is due to intrusion of soils and organic matter from the surrounding into the groundwater source. The prevalence of diseases such as gastroenteritis, diarrhea and vomiting, kidney and skin problems in the study area could be attributed to the excessive level of turbidity in the groundwater sources. Adhikary et al. (2012) reported that 78 NTU (turbidity) was found as the maximum recorded level among the water samples collected from 42 shallow wells (majorly from open wells) in Bangladesh during pre-monsoon period with the average level of turbidity of 5.91 NTU (considerably high since the level exceeds the WHO standard of 5 NTU). While in Sri Lanka, Mayilswami et al. (2012) reported that the level of turbidity also was found to be considerably high (14.5 NTU) which exceeds the WHO standard. The groundwater samples also were taken from shallow wells. Table 2.1

presents the other recorded concentrations of water quality contaminants in groundwater in Asian countries.

Table 2.1 Concentrations of contaminants of concern in groundwater in the selected Asian countries

Parameter	Location	Concentration ([a]µg/L, [b]mg/L, [c]NTU)			WHO maximum concentration limit	Reference
		Min	Max	Mean		
Lead[a]	Pakistan	20	730	330	10 µg/L	(Midrar-Ul-Haq et al., 2005)
	Pakistan	100	240	150		(Midrar-Ul-Haq et al., 2005)
	Pakistan	200	970	660		(Tariq et al., 2006)
	Pakistan	-	260	-		(Tariq et al., 2008)
	India	200	360	287		(Buragohain et al., 2010)
	Pakistan	-	43.17	24.1		(Muhammad et al., 2011)
	Pakistan	-	-	30.7+17.4		(Khan et al., 2013)
	Bangladesh	0.10	0.38	0.17		(Rahman et al., 2013)
Arsenic[a]	Pakistan	7	28	15	10 µg/L	(Afzal et al., 2000)
	Bangladesh	-	1670	55		(BGS & DPHE, 2001)
	Bangladesh	30	750	410		(Anawar et al., 2003)
	Bangladesh	-	555	-		(Zheng et al. 2005)
	China	-	5.98	0.91		(Xu et al., 2006)
	Pakistan	23.3	96.3	60.2+12.5		(Arain et al., 2009)
	India	1	16	8		(Buragohain et al., 2010)
	Philippines					(Hosono et al., 2010)
	Shallow	2.4	22.5	-		
	Deep	1.1	19.8	-		
	Bangladesh	-	-	366		(Sarker, 2012)
	Taiwan	-	350	-		(Chung et al., 2013)
	Bangladesh	14	772	328		(Rahman et al., 2013)
	India	<1	875	-		(Halder et al., 2013)
	Sri Lanka	-	-	40		(Rajasooriyar et al., 2013)
Nickel[a]	Pakistan	-	220	-	20 µg/L	(Ullah et al., 2009)
	Pakistan	0.24	14.42	4.7		(Muhammad et al., 2011)
	Pakistan	0.63	6.01	2.72		(Muhammad et al., 2011)
	Pakistan	2.18	10.26	4.93		(Muhammad et al., 2011)
	Bangladesh	0.68	2.57	1.24		(Rahman et al., 2013)
	Pakistan	0.089	25.89	-		(Khan et al., 2013)
Cadmium[a]	Pakistan	10	70	40	3 µg/L	(Midrar-Ul-Haq et al., 2005)
	Pakistan	20	40	30		(Midrar-Ul-Haq et al., 2005)
	Pakistan	-	25	-		(Nasrullah et al., 2006)
	Pakistan	-	27	-		(Tariq et al. 2008)
	India	-	120	39		(Buragohain et al., 2010)
	Sri Lanka	5.1	23	-		(Bandara, et al., 2010)
	Pakistan	-	3.9	2		(Muhammad et al., 2011)
	Pakistan	-	20.38	-		(Khan et al., 2013)
Fluoride[b]	India	-	6.9	-	1.5 mg/L	(Meenakshi et al., 2004)
	India	-	5.2	-		(Singh et al., 2007)
	Pakistan	-	21.1	-		(Farooqi et al., 2007)
	India	-	3.24	-		(Viswanathan et al., 2009)
	India	-	8.5	-		(Chaudhary et al., 2010)
	Sri Lanka	-	8	-		(Jayawardana et al., 2012)
	India	-	6.6	-		(Arif et al., 2012)
	Sri Lanka	-	9.2	-		(Rajasooriyar et al., 2013)
	Pakistan	-	4.89	1.04		(Ghoraba & Khan, 2013)

Table 2.1 (Continued)

Parameter	Location	Concentration ([a]μg/L, [b]mg/L, [c]NTU)			WHO maximum concentration limit	Reference
		Min	Max	Mean		
Turbidity[c]	Sri Lanka	-	14.8	0.92	5 NTU	(Mayilswami et al., 2012)
	Bangladesh	0.76	78	5.91		(Adhikary et al., 2012)
pH	Pakistan	-	8.7	-	6.5-8.5	(Afzal et al., 2000)
	India	-	8.44	-		(Meenakshi et al., 2004)
	Bangladesh	-	7.31	-		(Zheng et al., 2005)
	India	-	7.61	-		(Viswanathan et al., 2009)
	Sri Lanka	-	8.2	-		(Jayawardanaa et al., 2010)
	Sri Lanka	-	7.9	-		(Jayawardana et al., 2012)
	Bangladesh	-	8.7	-		(Adhikary et al., 2012)
	Sri Lanka	-	7.9	-		(Rajasooriyar et al., 2013)
	Pakistan	6.8	8.75	7.93		(Ghoraba & Khan, 2013)

The contamination of groundwater with parameters reported in Table 2.1 may be due to natural and anthropogenic factors. For example, the presence of Pb and Ni in groundwater is usually associated with the leaching of lead and nickel materials from pipe fittings and poor practices of industrial waste disposal into the environment (WHO, 2005, 2011).

Meanwhile, As and fluoride are introduced into groundwater through natural and anthropogenic factors (i.e., poor practices of land use during agricultural activities and unsafe disposal of industrial effluents). The natural factor is by the dissolution of minerals from rocks during the groundwater flow in the aquifer that is confined within hard bedrock layers. The uncontrolled application of agrochemicals such as fertilisers and pesticides have also been attributed to the intrusion of these two chemicals into the groundwater (WHO, 2004, 2011).

Joshi & Sahu (2014) reported that in India, rapid industrialisation has led to the intrusion of undesired chemical substances such as lead, chromium, mercury, uranium, selenium, zinc, arsenic, cadmium, gold, silver, copper and nickel into the groundwater. Table 2.2 depicts further details of physicochemical properties of groundwater quality contaminants of concern and their major uses.

Table 2.2 Physicochemical properties of groundwater quality contaminants of concern and their sources of origin

Contaminant	Identity	Major uses	Reference
Lead	• The commonest of the heavy elements • Accounting for 13 mg/kg of earth's crust	• Lead acid batteries, solder, alloys, cable sheathing, pigments, rust inhibitors, plastic stabilizers	(WHO, 2005, 2011d)
Nickel	A lustrous white, hard, ferromagnetic metal.	• Leaching of metals in contact with drinking-water, such as pipes and fittings • Dissolution from nickel ore-bearing rocks.	(WHO, 2005)
Cadmium	• Metal with an oxidation state of +2 • Chemically similar to zinc and occurs naturally with zinc and lead in sulfide ores	• Mainly used as an anticorrosive and electroplated onto steel, pigments in plastics and in electric batteries, electronic components and nuclear reactors	(WHO, 2011b)
Arsenic	• Exists in oxidation states of −3, 0, 3 and 5 • Widely distributed throughout earth's crust, most often as arsenic sulfide or as metal arsenates and arsenides	• Commercially and industrially used as alloying agents in the manufacture of transistors, lasers and semiconductors, processing of glass, pigments, textiles, paper, metal adhesives, wood preservatives and ammunition.	(WHO, 2011a)
Fluoride	• A common element that does not occur in the elemental state in nature because of its high reactivity • Accounts for about 0.3 g/kg of the earth's crust and exists in the form of fluorides in a number of minerals • The oxidation state of the fluoride ion is -1	• Used in aluminium production and as a flux in the steel and glass fibre industries can also be released into the environment during the production of phosphate fertilizers, bricks, tiles and ceramics.	(WHO, 2004)

2.4 Impact of excessive levels of chemical contaminants in groundwater sources on human health

The presence of heavy metals and other undesired substances in drinking water is of risk to human health. Human beings could be exposed to heavy metals primarily through drinking water consumption and food, but few heavy metals can bio-accumulate in the human body (e.g., in lipids and the gastrointestinal system) and may induce cancer and other health risks (Chowdhury et al., 2016).

Based on a study conducted between 1996 to 2002, around 80 million people in the As-affected areas of Bangladesh (WHO standard of 10 µg/L) were possibly at risk from As-contaminated groundwater (Chakraborti et al., 2010). According to above authors arsenical skin lesions depends on several factors including (i) the concentration of As in drinking water; (ii) the volume of water consumed (including cooking water); (iii) duration of water consumption and (iv) health and nutritional status of the individuals.

The effect of toxicity of As-contaminated drinking water on human health is often reported to be prevalent among adults which is related to the excessive levels of As in drinking water. This can cause non-malignant lung disease and cardiovascular disease (Smith & Steinmaus, 2009; van Halem et al., 2009; Dauphiné et al., 2011). However, toxicity of As in drinking water was also identified to be a cause for the health problem among chidren including skin abnormalities, pulmonary interstitial fibrosis (in Chile) and affection of intellectual function (in Thailand, Bangladeh and India) (Majumdar & Mazumder, 2012).

In another earlier study, Ryan et al. (2000), claimed that prolonged ingestion of As-, Cd- and Pb-contaminated drinking water have been linked with numerous cases of cancer, nephrotoxicity, central nervous system effects, and cardiovascular disease in humans. Cd is usually exposed to humans through food, tobacco smoke and house dust and consequently led to the disease associated with lung cancer in adults and adverse effects on motoric and perceptual behaviour in children, kidney damage, renal disorder, human carcinogen (Schoeters et al., 2006; Bandara et al., 2010). The carcinogenicity of Ni in the human body is seen to cause trouble in the nasal cavity, larynx and lungs (Cempel & Nikel, 2006).

High fluoride exposure via drinking water can cause dental and skeletal fluorosis. The findings revealed that fluoride content in hair is highly correlated with fluoride content in drinking water and dental fluorosis level (Fewtrell et al., 2006; Mandinic et al., 2010). Mann et al. (2007) reported that the excessive levels of turbidity in drinking water can cause acute gastrointestinal illnesses which are generally due to presence of undesired organic content in drinking water sources.

Removal of these heavy metals and other harmful water quality pollutants from drinking water sources particularly groundwater has been a great challenge to environmentalists in affected areas. It is a great challenge to ensure that the quality of drinking water fit the stringent international and national standards (Table 2.3).

Table 2.3 Comparison World Health Organisation (WHO) Drinking Water Quality Guidelines and national drinking water standard from different countries

Parameter	Unit	Maximum Permissible level				
		WHO[a]	Pakistan[b]	India[c]	Sri Lanka[d]	Bangladesh[e]
pH	-	6.5-8.5	6.5-8.5	6.5-8.5	6.5-9.0	6.5-8.5
Turbidity	NTU/JTU*	5	5	5	2	10* (4 NTU)[f]
Arsenic	µg/L	10	50	100	10	50
Fluoride	mg/L	1.5	1.5	1.0	1.0	1.0
Nickel	µg/L	20	20	20	20	100
Lead	µg/L	10	50	10	10	50
Cadmium	µg/L	3	10	3	3	5

[a] WHO, (2011),[b](NSDWQ, 2008) , [c](BIS, 2012), [d](SLS, 2013),[e](WQPBS, 2012), [f] 1 NTU=2.5 JTU

Based on the above information, it is revealed that the exposure to excessive levels of heavy metals, turbidity and fluoride in drinking water has led to various adverse impacts on human health. Therefore, it is of importance to treat the groundwater prior to drinking, cooking and for personal hygiene purposes. The subsequent section discusses the wide range of conventional and new approaches to treating drinking water sources contaminated with the target groundwater quality contaminants which have been identified in Section 2.3.

2.5 Existing water treatment technologies adopted for the removal of heavy metals, fluoride and turbidity

Excessive levels of heavy metals (lead, arsenic, nickel, cadmium), fluoride and turbidity seem to be present in groundwater in many places in South Asian countries. As a result, it is important that the water is treated before it is consumed by people. There are various treatment methods proposed to remove these target contaminants from various water sources. Conventional treatment methods primarily consist of chemical, physical and biological technologies (Gautam et al., 2014). However, the cost-effectiveness of the conventional methods for the removal of heavy metals, fluoride and turbidity from contaminated groundwater need to be evaluated despite their proven efficiencies in treating the contaminants.

2.5.1 Heavy metal removal

In this section, a few treatment techniques for removal of heavy metals have been reviewed. The recommended treatment of heavy metals from different sources of water have been documented including chemical precipitation or coagulation (Pang et al., 2009; Oehmen et al., 2011), filtration (Lombardo & Brigano, 2014), ion exchange (Inglezakis & Loizidou, 2007), membrane separation (Sang et al., 2008) and adsorption on activated carbon (Karnib et al., 2014).

2.5.1.1 Chemical precipitation or coagulation

Fundamentally, coagulation is a process where small particles combine into larger flocs and for adsorbing dissolved organic matter onto particulate aggregates so that these impurities can be removed in subsequent solid/liquid separation processes (Jiang, 2015).

A study conducted by Pang et al. (2009) on the effectiveness of hydroxide precipitation and coagulation-flocculation methods for removing of Pb, Zn, Cu and Fe from wastewater reported that up to 99% removal of Pb was achieved by the dose of 1200 mg/L (alum), 150 mg/L (PACl) and 2000 mg/L ($MgCl_2$) in a pH ranges of 6.5 to 7.8, 8.1 to 8.9, and 9.7 to 10.9, respectively. In contrast to the impact on the environment which might introduced by the application of high dose of chemical coagulants as recommended above, Oehmen et al. (2011) suggested a hybrid process which is a combination of ion exchange membrane and coagulation for reducing arsenate from drinking water below the maximum contaminant level (6.6 ± 2.8 µg/L) during periods with and without alum addition. Alum was reported to be more effective than ferric at preventing membrane scaling. The reason was likely due to the contrasting charges of the precipitates. The technique successfully improved the water quality as well as prevented the secondary pollutants produced by the coagulant (i.e., alum and ferric) and pH controlling agents.

2.5.1.2 Filtration

Gao et al. (2011) used modified graphite-oxide (GO) nano sheets with a thiol group (through diazonium chemistry) to remove mercury (Hg) from aqueous solutions. The results indicated that the modified GO was capable of removing Hg six-fold higher than the unmodified GO. Besides, GO was also assembled with the sand particles in a usable filtration column which resulted in five-fold higher retention of Hg and organic dye than the uncoated sand. Although the results were promising, the preparation of filtration media involved a complex process which could only be handled by skilful personnel. In another study, Lombardo & Brigano (2014) attempted at designing a filter system which consists of multiple layers to ensure the removal of soluble, insoluble and complex species of heavy metals in water . The designed filter removes

most of lead (Pb) species (soluble, particulate and semi-insoluble Pb). Complex solutions of Pb were prepared in accordance with Standard 53 of the National Science Foundation (NSF)/American National Standards Institute (ANSI) for the removal of Pb at pH 8.5. The results showed that the filter is capable of removing more than 80 gallons (equivalent to 303 L) of Pb to meet the WHO drinking water standard of 10 µg/L compared to a typical filter.

2.5.1.3 Ion exchange

Ion exchange is a process in which ions between ion-containing solutions are exchanged. Inglezakis & Loizidou (2007) investigated the possibility of ion exchange of heavy metals (Cu, Cr and Fe) using polar organic solvents (pure ethanol and acetone) and natural zeolite clinoptilolite. The level of ion exchanged was higher for Fe (53.1%) compared to ethanol (12.5%) and acetone (3.1%). Similarly, 46.8% of Cr exchanged compared to 27.4% ethanol and 23.8% of Cu was exchanged compared to 26.6% acetone. It was also found that different complexes were formed depending on the type of solvent. Furthermore, zeolite was able to be used in ion exchange of metals which conducted in polar organic solvents.

2.5.1.4 Membrane separation

Membrane technology is known to be an advanced treatment technology in water treatment. The media used in the membrane system is usually made up of expensive materials that are prepared using advanced technology. For examples, the membrane used in a study conducted by Sang et al. (2008) was prepared from chloridised polyvinyl chloride by high-voltage electrospinning process. The membrane was used to couple with another filtration system named micellar enhanced filtration. The Cu, Pb and Cd removal were more than 73%, 82% and 91% respectively in synthetic

groundwater samples. Maher et al. (2014) reported that a polyamide nanofiltration membrane was successful in removing 93% of Ni and 86% of Pb when the initial concentrations of each Ni and Pb were 1 mg/L.

2.5.1.5 Adsorption on activated carbon

Adsorption is regarded as the most innovative component in water purification. Currently, there were increasing number of adsorption studies have been conducted on various type of adsorbents. It is an emerging water research field that investigates the potential use of low-cost activated carbon for water treatment which is derived from many natural products and by-products (Kadirvelu et al., 2001; Sekar et al., 2004). The typical activated carbon that is used in a conventional water treatment system is very expensive and the process involved in regeneration activated carbon is complex (Beyene, 2014). An adsorption study of Pb, Cd, Ni, Cr and Zn on activated carbon, silica and silica/activated carbon (2:3) composites were conducted by Karnib et al. (2014). The results showed that Ni had the highest removal efficiencies for all tested concentrations. Silica/activated carbon (2:3) composite showed the better performance in removing Ni compared to individual activated carbon and silica. Mondal et al. (2007) investigated the use of iron impregnated granular activated carbon (GAC-Fe) in adsorption of As (initial concentration of 200 µg/L) from a synthetic groundwater sample. The maximum removals of As(Total), arsenite [As (III)], arsenate [As (V)] were found to be 95.5%, 93% and 98% respectively and 56%, 41%, 71% respectively when GAC was used.

2.5.2 Fluoride removal

There are few adsorptive media that have been recommended for the fluoride removal including zeolites and activated alumina (Rafique et al., 2013; Zhou et al., 2014).

Tomar et al., 2015). For example, the use of modified immobilized activated alumina (MIAA) prepared by sol-gel method (by adding a specific amount of alum during the sol formation step) was effective in removing fluoride from drinking water. The removal efficiency of more than 90% was achieved within 60 minutes. Another finding from this study also shows that MIAA was 10% more effective than activated charcoal (Rafique et al., 2013). In another study, the removal of fluoride by using a zirconium modified zeolite composite was found to be 97.62% from the initial concentration of 10 mg/L which was better than that of removed by raw zeolite (32.94%) and acid modified zeolite (57.05%) (Zhou et al., 2014). Tomar et al. (2015) reported that a hydroxyapatite-modified activated alumina (HMAA) prepared by dispersing nanoparticles of hydroxyapatite inside activated alumina granules had resulted in improving the adsorption capacity at least five-fold higher than that adsorbed by virgin-activated alumina.

2.5.3 Turbidity removal

Coagulation is commonly regarded as the key treatment process in conventional water treatment. Chemical-based coagulants such as alum and ferric are typically used as water treatment agents. They were proven to be effective at removing a wide range of water quality pollutants particularly turbidity, pathogens and other colloidal substances from water and wastewater (Choy et al., 2015). Hu et al. (2015) found that Fe-based coagulant was more effective than the Al-based coagulant for selenium (Se) removal from water. On the other hand, coagulation appears as the most popular method to date when dealing with turbidity. For example, the feasibility of coagulation coupling with inorganic metal microfiltration membranes in submerged membrane manner for the removal of natural organic matter (NOM) was investigated by Leiknes et al., (2004). The findings indicated that the methods were efficient since more than

95% of colour, 85% of UV, 65 to 75% of total organic carbon (TOC), less than 0.2 NTU of turbidity and non-detectable suspended solids removal in the permeate were achieved.

Sultana & Ahmed, (2016) reported that turbidity levels (in most of 20 sites) were reduced to 5 NTU from the initial levels of 50 to 150 NTU from pond water in the southern deltaic plains of Bangladesh. Pond water was treated by a treatment system which designed with an over ground double chambered filtration tank with a graded sand filter in one chamber for the managed aquifer recharge (for drinking water purpose). In another study, Moringa oleifera extracted with 0.5 Molar (M) of NaCl was tested as natural macromolecular coagulant for the removal of turbidity from groundwater. The results showed that the Moringa oleifera was successful in reducing the level of turbidity from 100 to 500 NTU to the level of less than 5 NTU. It was observed that flocs formed to be bigger and it settled faster when compared to alum (Sasikala & Muthuraman, 2016).

In another study conducted by Sarparastzadeh et al. (2007) reported that the removal of chemical oxygen demand (COD), phosphorus, turbidity and total suspended solids (TSS) were increased when the doses of aluminum sulfate (alum) and ferric chloride (ferric) were increased. 38% of COD, 66% of phosphorus, 68% of turbidity and 69% of TSS were removed by using optimum dose of 80 mg/L of alum, at pH of 8.2. At the same pH condition, 60% of COD, 73% of phosphorus, 49% of turbidity and 48% of TSS were removed by using ferric chloride at an optimum dose of 70 mg/L.

The above studies revealed that the chemical coagulants such as alum and ferric were efficient in removing various types of parameters particularly organic matters. However, it is a concern that the high dose of these chemicals would produce a large

amount of sludge which needs to be treated appropriately to avoid the adverse impact on the environment and consequently increasing the cost of treating the sludge.

As discussed earlier, the conventional treatment methods for heavy metals, fluoride and turbidity removal have limitations to be implemented in rural areas because of the high costs in chemicals used in the treatment process and complexity of operation (involving the use of advanced instruments and complex step of preparation of materials or media for the treatment). Besides, the conventional methods usually deal with wastewater and sludge which contains high concentrations of contaminants. The effectiveness of the conventional treatment methods is expected to vary when dealing with groundwater which usually contains very low concentrations of contaminants. The quality of drinkable water usually depends on the stringent WHO drinking water quality standards as shown in Table 2.3.

Given the performance (effectiveness) and the drawbacks of the reviewed conventional and new water treatment technologies to treat different water quality contaminants, it is proposed that coagulation method would be the most suitable treatment process to be applied in remote communities in developing countries. Coagulation is a simple treatment technique and considered as a preliminary treatment process in a water treatment system. However, the chemical water purification agents need to be substituted with the native and freely available natural materials to ensure the implementation of this treatment method is feasible and affordable in the outback regions of developing countries.

2.6 Low-cost materials as drinking water purification agents (non-chemical substitutes)

The use of plant-based biomass as water purification agents used more than 2000 years ago in certain countries such as India, China and Africa (Asrafuzzaman et al., 2011). Globally it has become an emerging trend among the current researchers to investigate the potential use of various low-cost materials (biomass) for water treatment purposes as this can be beneficial to the people living in remote areas with economically disadvantaged. It is evident from the rapidly increasing publications in indexed journals especially in past 16 years (Figure 2.1).

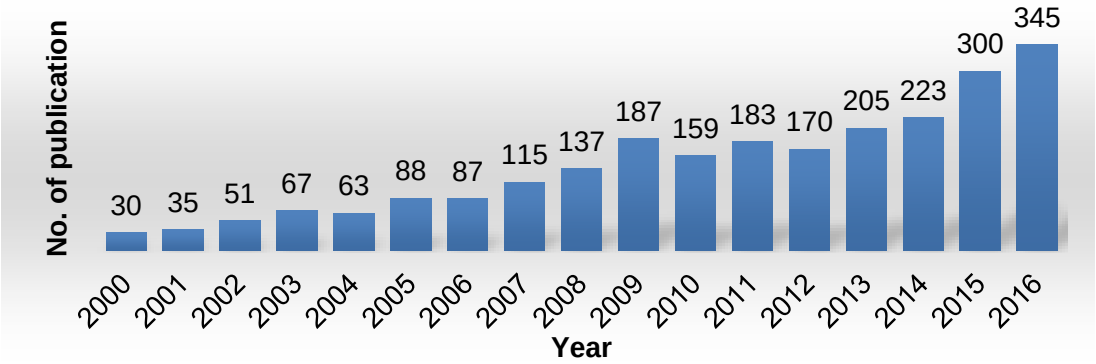

Figure 2.1 Record of the number of publications in indexed journals between 2000 and 2016 searched using keywords "plant-based material", "biomass", "heavy metal" and "drinking water". (Source: Sciencedirect, searched on 10 March 2017)

In the literature, numerous plant-based biomass have been studied to be used as water treatment agents including *Moringa oleifera* (Moringa seeds), *Jatropha curcas* (purging nuts), *Strychnos potatorum* (nirmali), tannin, cactus, *Solanum torvum* (Sundakai seeds), *Cicer arietinum* (chickpeas), *Musa cavendish* (banana peel), *Cocos nucifera* (coconut's solid endosperm), *Lentinus edodes* (Shiitake mushroom) and many more to remove various water quality pollutants. For example, *Moringa oleifera* tree can produce about 2000 seeds per year. This number of seeds would be able to

treat about 6000 L of water using a 50 mg/L dose. Trees can, however, be cultivated to produce about five to ten times this yield (i.e. 10,000–20,000 seeds) (Pritchard et al., 2010). Table 2.4 depicts the countries that have studied the use of some plant-based materials as water treatment agents.

Table 2.4 Plant-based materials used in previous researches and their countries of origin

Plant-based material	Countries of origin	Reference
Solanum torvum (Sundakai seeds)	India, Malaya, China, Philippines and tropical America	(Sivapriya & Leela, 2007)
Moringa oleifera	India, Asia, sub-Saharan Africa, Sudan and Latin America	(Yin, 2010)
Strychnos potatorum (nirmali)	Southern and central parts of India, Sri Lanka, and Burma	
Tannin	Asia Minor	
Cactus	Mexico, North America	
Jatropha curcas (purging nuts)	Regions of India such as Uttrakhand, Gujarat, Rajasthan, Bihar, Chhattisgarh, Punjab, Himachal Pradesh, Andhra Pradesh, Madhya Pradesh, Orissa and North-East states of India	(Bajrang Singh et al., 2013)

2.6.1 *Moringa oleifera* seeds as a plant-based material used in water purification

Recently, there had been an increased interest in the use of *Moringa oleifera* (MO) application for water treatment in remote regions in developing countries. Many parts of this plant are used for unique purposes such as herbal medicine and water purification agents (Ndibewu et al., 2011). This plant also is common in some of the South Asian countries such as Sri Lanka, India and Bangladesh and is consumed as a vegetable.

Ndabigengesere et al. (1995) introduced MO as a water purification agent and reported that MO has a mechanism of coagulation which consists of adsorption and neutralisation of the colloidal charges. This promising mechanism created significant opportunities for the researchers to conduct studies with MO in their specific research areas. Also, this miracle plant could also produce four to five times less in sludge volume as compared to sludge volume generated by alum (Ndabigengesere et al.,

1995). This is one of the most significant findings from the use of MO as a water purification agent. It possesses an advantage by reducing the amount of disposable sludge which usually is a problem at the end of a conventional water treatment process.

Unlike chemical-based water purification agents such as alum and ferric coagulants, MO is proven to be non-toxic, biodegradable and it does not significantly affect the pH and conductivity of the water after the treatment process (Ndabigengesere et al., 1995). According to above authors the sludge produced by MO is four to five times less in volume than the sludge produced by alum coagulation. The use of plant-based materials was initiated long before the introduction of chemical salts. However, they have not been used effectively because of the lack of scientific understanding of their effectiveness and mechanism of action removing pollutants (Ndabigengesere & Subba Narasiah, 1998). Above authors also discovered that MO seed is more effective than alum and the zeta potential measurements indicating that the primary mechanism of the coagulation with MO appeared to be adsorption and charge neutralisation.

The optimisation of MO treatment dose was studied by Katayon et al. (2006). The authors claimed that for removal of high (194 ± 3.8 NTU) and very high (390 ± 4.5 NTU) turbid water, the optimum dosage of MO was between 300 mg/L to 400 mg/L. For medium (87.8 ± 2.1 NTU) turbid water, 160 mg/L of MO produced the highest turbidity removal. Increasing in MO dose did not improve the removal of turbidity, instead reduced the treatment efficiency as a result of excessive amount of MO than that is required. Ali et al. (2010) and Sánchez-Martín et al. (2010) also confirmed that MO was effective in removing turbidity from water.

According to Pritchard et al. (2009), MO showed the best performance compared to *Jatropha curcas* (purging nut) and *Guar gum* (cluster bean) in a study of turbidity

removal from the synthetic turbid water. The results showed that 90% of turbidity removal was achieved by all three natural materials from the initial concentration of turbidity of 49 NTU. Furthermore, these materials were also effective in removing coliforms with an 80% removal efficiency. This finding suggests that MO was not only effective for the removal of turbidity but also is effective in the removal of coliform from water sources. Lürling & Beekman (2010) conducted a study investigating antimicrobial property of MO. The study found that the growth rates of *Microcystis aeruginosa* were negative and on average -0.23 (±0.05) day for 120 to 160 mg/L of crushed Moringa seeds filtrate. A number of researchers also investigated the use of MO for the removal of heavy metals such as Cd (Sharma et al., 2006), Zn (Bhatti et al., 2007), Cu, Ni, Zn (Kalavathy & Miranda, 2010) and Pb (Reddy et al., 2010). Hussain et al., (2012) also reported that MO seeds removed 90% of Cu, 80 %of Pb, 60 % of Cd and 50 % of Zn and Cr, respectively.

Based on the above review and other published material, it is evident that MO can be regarded as an effective plant-derived biomass due to its exceptional performance in removing various types of water quality contaminants such as heavy metals, turbidity and other organic matters. However, the effectiveness of other biomass that also had gained attention due to their effectiveness in removing water quality pollutants should not be disregarded.

2.6.2 Other biomass

An agricultural waste product, banana peel (*Musa cavendish*, MC) appears to be a good candidate for the application in water (Mohammed & Chong, 2014). Anwar et al. (2010) found that MC can achieve more than 80% removal of Cd and Pb from the initial concentrations of 50 µg/L of heavy metal. The optimum dose of MC for the

removal of Cd and Pb were found to be 30 and 40 mg/L and at pH of 3 and 5 respectively. Kamsonlian et al. (2012) reported that 82% of As was removed from its initial concentration of 10 mg/L using 8 g/L of MC at pH 7. It is important that low-cost water treatment, eliminate the use of chemicals for pH adjustments in pre- and post-treatment in order to reduce the overall treatment costs. Therefore, it is suggested that the effectiveness of MC to remove target contaminants at the typical pH of groundwater (pH 7) should be investigated. On the other hand, referring to result obtained by Kamsonlian et al. (2012), the concentration of As was very high (10 mg/L) compared to the typical concentrations (< 0.5 mg/L) of As in groundwater. Therefore, it is essential to investigate further the effectiveness and optimum dosage of MC for treating As with lower initial concentrations.

Furthermore, Asrafuzzaman et al. (2011) claimed that *Cicer arietinum* (chickpeas) had a comparable performance to MO in removing turbidity. Fatombi et al. (2013), reported that *Cocos nucifera* (copra) a novel plant-based material possesses similar material properties to Moringa oleifera since it produced comparable performance in removing turbidity from water. The use of coconut as a water purification agent would be beneficial in the target developing countries (South Asian countries) as it is commonly found in Asia, Africa, Caribbean and Latin America. On the other hand, the application of *Lentinus edodes* (Shiitake mushroom, an edible mushroom) in water treatment was proven to be capable of removing heavy metals such as chromium (Cr) and Cd (Chen et al., 2006, 2008).

The use of *Eichhornia crassipes* (water hyacinth) biomass for the removal of Zn, Cd and Cr in single, binary and tertiary aqueous systems were studied by Saraswat & Rai (2010). The treatments were found to be optimised at pH 5 and 6 for Cd and Zn,

respectively and at pH 2 for Cr. The dose of biomass used to achieve the optimum removal of these three metals was 0.5 g with the agitation time of 120 minutes for Cd and Zn and 180 minutes for Cr. The above authors also found that the removal of Cd was better in the binary system while the removal of Cr and Zn were reduced in binary and tertiary systems. The treatments were optimised with 0.5 g of biomass and mixing time of 120 minutes for Zn and Cd and 180 minutes for Cr. The findings suggest that there might be interaction or competition between metals' ions present in the same system which improved or reduced the removal efficiencies of the studied metal ions from the multi-metal aqueous systems.

Kiliç et al. (2013) investigated using a by-product of almond shell pyrolysis (bio-char) in removing Ni and cobalt (Co). Pyrolysis is a process carried out in a fixed-bed Heinze retort under nitrogen (N_2) flow of 100 cm^3/min with a heating rate of 10°C/min at 650°C to obtain porous bio-chars. The results indicated that the maximum adsorption of Ni and Co happened at pH of around 6. Adsorption of both metals was rapid when the time was increased from 0 to 30 minutes and the maximum adsorption for both metals was achieved at 150 minutes for all tested temperatures of 20, 30 and 40°C. In spite of its efficiency in treating Ni and Co, the pyrolysis process of the bio-char seems hard to be applied in the remote areas and the costs of implementation for the whole treatment process also tends to be expensive.

The use of saw dust coated with polyaniline (PANI/SD) claimed to be effective for Cd removal with the maximum adsorption capacity of 430 mg/g. The adsorption of Cd ion was rapid in the first 20 minutes when the concentration of Cd was between 10 to 40 mg/L. The maximum removal of Cd was found to be at pH 5 (Mansour et al., 2011).

Table 2.5 presents the performance of various plant-based materials in removing various water quality contaminants.

Table 2.5 Performance of various plant-based materials in removing various water quality contaminants

Plant-based material	Plant-based material dose	Contaminant	Contaminant initial concentration	Removal efficiency	pH	Reference
MO Lamarck seeds[a]	2 g/200 mL	As (III) As (V)	25 mg/L	60.21% 85.60%	7.5 2.5	(Kumari, et al., 2006)
MO Lamarck seeds[a]	0.5 g/200 mL	As (III)	1 mg/L	31.89%	7.5	(Kumari et al., 2006)
MO Lamarck seeds[a]	4 g/200 mL	Cd	25 µg/mL	85.10%	6.5	(Sharma et al., 2006)
MO wood[a]	0.2 g/100 mL	Cu Ni Zn	30 mg/L	55.60% 88.36% 63.90%	7	(Kalavathy & Miranda, 2010)
MO seeds[b]	0.4 mg/L	Turbidity	34-36 NTU	96.23%	7.5	(Ali et al., 2010)
MO seeds[a]	75 mg/L	Turbidity	146 NTU	84%	7.5	(Pritchard et al., 2010)
MO seeds (NaOH)[a]	0.5 g/L	Zn(II)	50 mg/L	91.52%	7	(Bhatti et al., 2007)
MO seeds[a]	100 mL of 3% (w/v) in 1L seed extract	Turbidity	>150 NTU	96%	6.8-7.5	(Sengupta et al., 2012)
[c]MO leaves (NaOH)[a]	0.04 g/100 mL	Pb(II)	50 mg/L	99%	5	(Reddy et al., 2010)
Cicer arietinum[a]	100 mg/L	Turbidity	95 NTU 49 NTU 31 NTU	95.89% 81.63% 71.29%	7.0-7.5	(Asrafuzzaman et al., 2011)
Cicer arietinum (sulphonated)[a]	5 g/100 mL	Pb	0.00202 g/mL	76%	6	(Kale, 2013)
Banana peel[a]	8 g/L	As (III)	10 mg/L	82.23%	7	(Kamsonlian et al., 2012)
Banana peel[a]	30 mg/L 40 mg/L	Cd Pb	50 µg/mL 50 µg/mL	89.2% 85.3%	3 5	(Anwar et al., 2010)
Cocos nucifera[a]	100 mg/L	Turbidity	250 mg/L silica nano colloids suspensions	>80%	6	(Fatombi et al., 2013)
Blue pine Walnut[a]	20 g/L 40 g/L	As	100 µg/L	94% 88%	8.5	(Saqib et al., 2013)

[a]Batch mode
[b]Ion exchange column
[c]Desorption (regeneration): More than 65% desorption of Pb occurred by 0.1M HCl, complete desorption (>98%) was achieved with 0.4M HCl, indicating that moderately higher concentration of HCl was more efficient in releasing Pb(II) ions.

2.6.3 Selection of plant-based materials for the study

Several criteria have been set prior to the selection of natural materials to be tested in the study. The selected natural materials should be (i) freely available or native to the targeted developing countries; (ii) ease of preparation prior to use in the treatment process; (iii) biodegradable; (iv) cheap (if not freely available) and (v) showed in previous studies a promising potential in removing water quality contaminants. Among the reviewed natural material, five materials have been selected for the study namely *Moringa oleifera* (Moringa seeds), *Cicer arietinum* (chickpeas), *Musa cavendish* (banana peel), *Cocos nucifera* (coconut solid endosperm), *and Lentinus edodes* (edible Shiitake mushroom). These plant-based indigenous materials were selected based on checking against the set criteria. As reported in literature each of these plant-based materials can remove various water pollutants including some of the target contaminants.

2.6.4 Preparation of biomass

Low-cost plant-based materials show a promising performance in substituting the chemicals such as alum and ferric that are commonly used for water treatment. Figure 2.2 shows the schematic diagram of steps involved in preparation of plant-based materials (Yin, 2010).

The steps in the preparation of biomass usually are simple and feasible to be applied by people living in remote areas. The steps involved are cleaning, cutting, drying and grinding the raw plant-based materials. This would minimise the need to purchase and operate advanced equipment or complex operations.

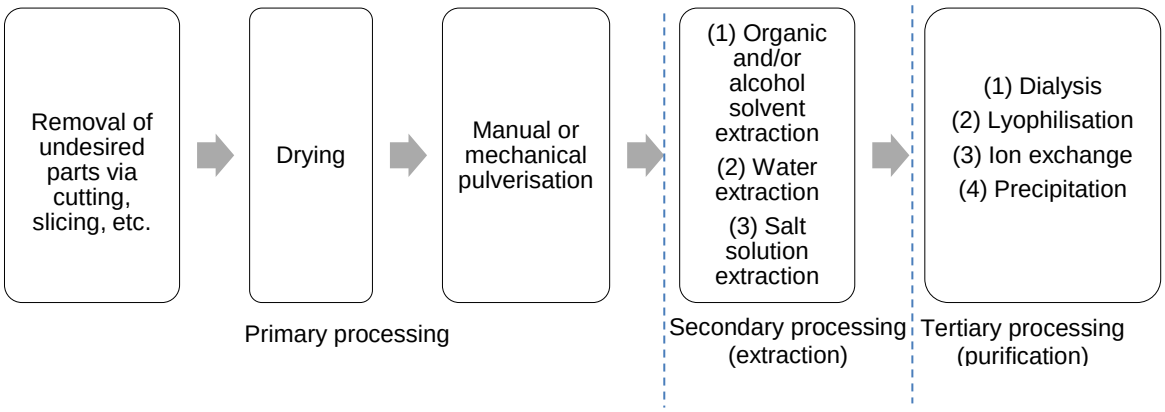

Figure 2.2 General processing stages in the preparation of plant-based materials. Adopted from Yin (2010)

2.6.5 Sludge management

It is important to understand not only the removal performance of the targeted contaminants using such plant based material but also their availability in large quantities for full scale applications, durability (replacement frequency), safe discharge strategies of contaminated biomass after filtration. The contaminant-loaded biomass can be managed by using native earthworms namely *Perionyx excavatus* (Chakravarty et al., 2002). The study reported that native earthworms convert arsenic from plant available to plant unavailable form. This method may be applicable to manage the sludge produced at the end of the proposed water treatment system.

2.6.6 Pre-treatment of biomass

In certain circumstances, the use of untreated biomass are incapable of treating the water to meet the WHO compliance limits. Pre-treatment or modification of biomass is aimed to enhance the treatment efficiency. However, due to the additional process of pre-treatment itself or the chemicals used in the processes, increases the overall costs incurred in the treatment process. As depicted in Figure 2.3 Nguyen et al. (2013)

summarised the methods recommended to modify the properties of biomass to enhance the efficiency of the biomass.

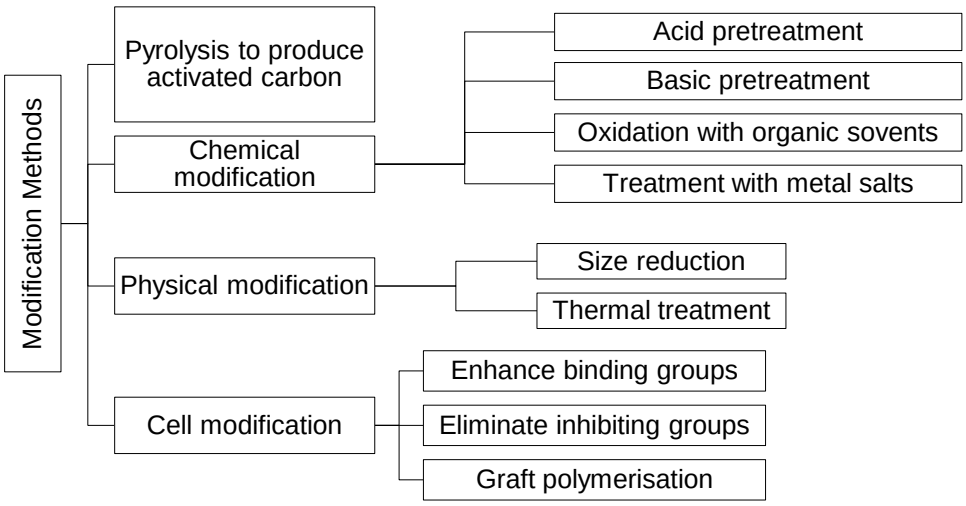

Figure 2.3 Modification methods for producing a better performance of biomass. Adopted from Nguyen et al. (2013)

Bhatti et al. (2007) reported MO biomass treated with sulfuric acid (H_2SO_4) and sodium hydroxide (NaOH) exhibited better removal of Zn with removal efficiencies of 90% and 92% respectively, compared to that demonstrated by the untreated MO (74%), hydrochloric acid (74%), phosphoric acid (82%), calcium hydroxide (85%), aluminium oxide (82%), sodium dodecyl sulfate (SDS, 81%), cetyl trimethyl ammonium bromide (CTAB, 86%) and Triton X-100 (84%). According to above authors the minerals and functional groups on the biomass are dissolved and modified in chemical pre-treatments. The removal of minerals from the biomass surface would result in the formation of complexes of hydrogen on the biomass surface. This would modify the chemistry of the biomass surface and enhanced the porosity and surface area. In basic pre-treatment, H^+ ions were removed from the surface of the biomass and consequently, this increases the negative charge surface which improves the attachment of Zn from the solutions. On the other hand, the capacity of pores and

surface area had improved in thermal pre-treatments at 573 K (equivalent to 300°C) for an hour (Akhtar et al., 2007).

Gautam et al. (2014) also have summarised technical advantages and disadvantages of existing modification (pre-treatment) techniques on biomass (Table 2.6).

Table 2.6 Technical advantages and disadvantages of existing modification (pre-treatment) techniques. Adopted from Gautam et al. (2014)

Modification	Treatment	Advantages	Disadvantages
Chemical	Acidic	Increases acidic functional groups on biomass surface, enhances chelation ability with metal species	May decrease surface area and pore volume
	Basic	Enhances uptake of organics	May, in some cases, decrease the uptake of metal ions
	Impregnation of foreign materials	Enhances in-built catalytic oxidation capability	May decrease surface area and pore volume
Physical	Heat	Increases surface area and pore volume	Decreases oxygen functional groups
Biological	Bioadsorption	Prolongs biomass bed life by rapid oxidation of organics by bacteria before the material can occupy adsorption sites	Thick biofilm encapsulating biomass may impede biomass diffusion of adsorbate species

The physical and chemical pre-treatments of biomass could alter the morphological profile of the biomass surface and functional groups either by eliminating or concealing the groups or by revealing more contaminant binding surface area site.

Given the performance of the pre-treated biomass compared to the untreated biomass, it is demonstrated that basic, acidic and thermal pre-treatments were among the most commonly applied methods by the researchers to improve treatment efficiency in their studies. The reasons might be due to the simplicity of the treatment process and their proven effectiveness in improving the treatment efficiency of the biomass (Rinta-Kanto et al., 2004; Akhtar et al., 2007; Bhatti et al., 2007; Kalavathy & Miranda, 2010; Mohammed & Chong, 2014).

2.6.7 Treatment mechanisms by plant-based materials

The mechanism of contaminant removal by each biomass can vary, depending on the nature of the biomass and the contaminant since each biomass may possess unique chemical properties to each other (Ahluwalia & Goyal, 2007). Therefore, it is important to understand the mechanism of contaminant removal by each individual biomass in order to improve the treatment efficiency of the biomass. The most common characterisation techniques for biomass include Fourier transform infrared (FTIR), scanning electron microscopy (SEM) and energy dispersive x-ray (EDX) (Araújo et al., 2010; Moreno-Tovar et al., 2014; Tibolla et al., 2014).

Functional groups on the biomass can be identified using FTIR. Active groups which are responsible for the binding of contaminant on the biomass can be determined based on the: (i) change of adsorption peak intensity, (ii) shift of wavenumber, (iii) appearance of new adsorption peak or (iv) absence of peak on the spectrum of the contaminant-loaded-biomass compared to the unloaded biomass (Bhende & Jadhav, 2012).

In the interpretation of FTIR spectrum, four zones can be considered for the assignment of respective functional groups. On the FTIR spectrum, the frequency term is used for band or peak position throughout the spectrum with the units of wavenumber (cm^{-1}) (Coates, 2000). The four zones on the FTIR spectrum are described in Table 2.7.

Table 2.7 Description of the corresponding zones on FTIR spectrum (Coates, 2000)

Zone	Wavenumber range (cm^{-1})	Description
1	4000-2500	Single bond stretch (Examples: O-H stretch, N-H stretch, C-H stretch)
2	2500-200	Triple bonds (Examples: nitriles, carbenes)
3	2000-1500	Double bonds (Examples: C=O bend, C=C bend, C=N bend)
4	1500-400	Fingerprint region (skeletal vibrations)

Based on FTIR spectrum, specific functional groups that responsible for the removal of one contaminant can be identified based on the positions of the significant peak. For example, a characterisation study on raw MO seed which was conducted by Araújo et al. (2010) revealed the significant peaks assigned to O-H stretch (3420 cm^{-1}), symmetrical and asymmetrical stretch of C-H (2923 and 2852 cm^{-1}), C=O stretch (1800 to 1600 cm^{-1}), fatty acids (1740 and 1715 cm^{-1}), amides (1658 cm^{-1}), and C-N stretch or N-H deformation (1587 cm^{-1}) (Figure 2.4).

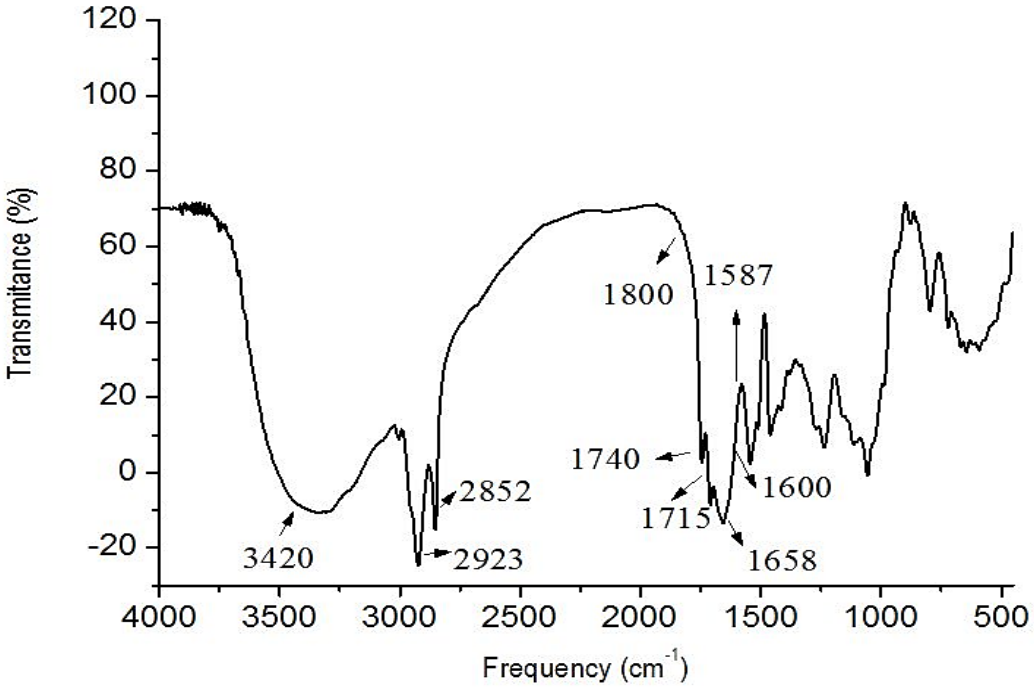

Figure 2.4 FTIR spectrum of raw MO seed. Adopted from Araújo et al. (2010)

In a study by Memon et al. (2008), the FTIR spectrum of MC peel exhibited significant adsorption peaks at 3313, 2920, 2851,1614, 1317, 1035, and 885 cm^{-1}, correspond to the presence of O-H stretch, C-H stretch of alkane, C-H and C O stretch of carboxylic acid or ester, COO- stretch, O-H bend, C-O stretch of ester or ether and N–H deformation of amines, respectively (Figure 2.5). The spectrum profile of MC was comparable to that reported by Gopi et al. (2014). Kaewsarn et al. (2008)

identified the presence of carboxyl, hydroxyl, and amide groups on the MC surface, which were suggested to be responsible for the adsorption of Cd on MC.

FTIR spectrum of an unloaded biomass can generally be used as a basis for studying the change in the spectrum of the contaminant-loaded biomass. The active functional groups corresponding to the removal of one contaminant by a biomass can then be identified based on the alterations of the FTIR spectra.

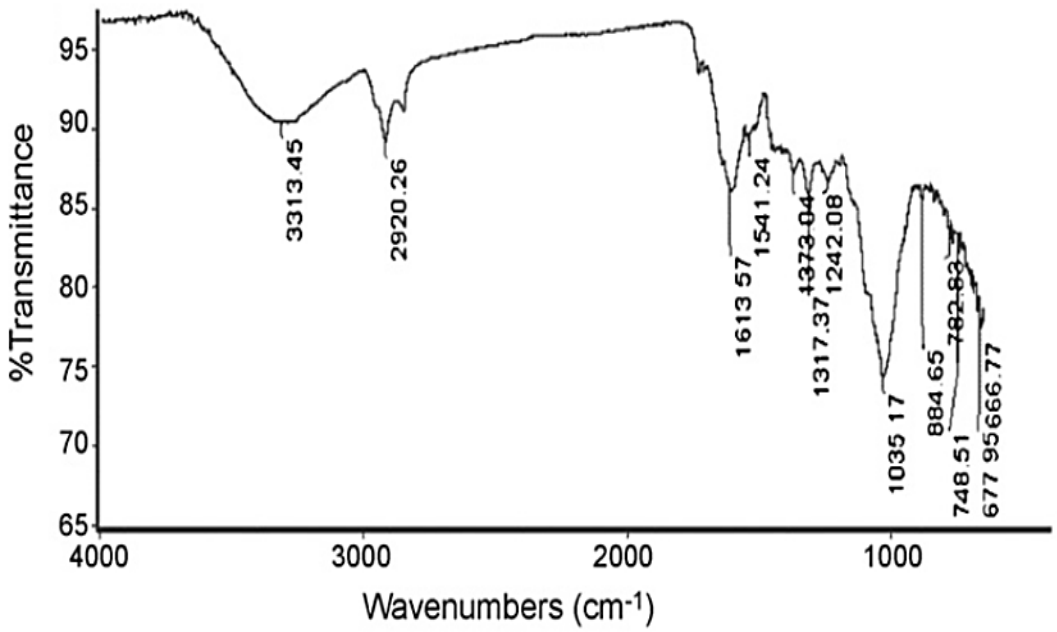

Figure 2.5 FTIR spectrum of raw MC peel. Adopted from Memon et al. (2008)

The adsorption of a contaminant on a biomass may be confirmed through a morphological study with SEM technique. For example, the presence of cavities on the surface of used black tea leaves suggests that there are possible available sites for the adsorption of Cr ion (Hossain et al., 2010). In another study conducted by Putra et al. (2014) confirmed the adsorption of Zn and Pb on egg shell and coconut tree sawdust, respectively since lump-like deposits and tiny nodules were observed on the biomass surface after loaded with Zn and Pb, respectively.

The chemical composition of biomass can be obtained via EDX. In EDX analysis, adsorption of one contaminant on a biomass can be confirmed based on the detection of additional peaks on the EDX spectrum of the biomass before and after the adsorption. For example, it is confirmed that Cd was adsorbed on MC surface based on the detection of an additional peak which corresponds to Cd element on the EDX spectrum of MC after Cd adsorption (Memon et al., 2008).

Verma et al. (2008) proposed that ion exchange was the prominent mechanism for the removal of Cd, Ni, Zn, Cu, Cr and Pb from synthetic industrial wastewater by using the oven dried biomass of *Eichhornia crassipes* (water hyacinth), *Valisneria spiralis* (tape grass) and *Pistia stratiotes* (water cabbage) at pH 6. According to the authors, there was a strong ionic balance between the adsorbed (H^+ and M^{2+}) to the released ions (Na^+ and K^+). Araujo et al. (2013) illustrated the mechanism of heavy metal adsorption on biomass as shown in Figure 2.6. Although the adsorption of heavy metals on biomass is often associated with ion exchange mechanism, there is also an indication that the adsorption occurs via simple surface precipitation of metal hydroxide species (Schneider et al., 2001).

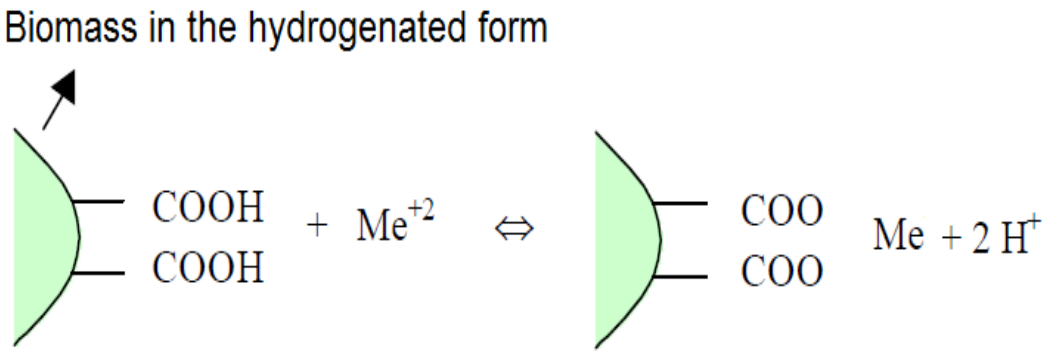

Figure 2.6 Schematic diagram of ion exchange mechanism. Adopted from Araujo et al. (2013)

It is suggested that the contaminant removal mechanisms of natural plant materials are usually complex and the dominant mechanism may be difficult to identify. It is commonly considered that more than one mechanisms would involve in the adsorption of contaminants on the biomass (Singh et al., 2006). Ndibewu et al. (2011) emphasised that it is essential to understand the chemical structure of the active chemical composition of a biomass so that suitable modification of the biomass may be conducted to improve its contaminant removal efficiency.

2.7 Existing adsorption models

There are numbers of adsorption models in the field that have been used for determining adsorption capacity of an adsorbent including Langmuir, Freundlich, Brunauer-Emmett-Teller, Redlich-Peterson, Dubinin-Radushkevich, and Temkin isotherm models (Freundlich, 1906; Langmuir, 1916; Bruanuer et al., 1938; Tempkin & Pyzhev, 1940); Dubinin & Radushkevich, 1947; Redlich & Peterson, 1959) (Table 2.8).

Among the adsorption models (Table 2.8), Langmuir and Freundlich models are the most popular adsorption models that have been widely applied in the field of water treatment due to their simplicity in application and the mechanism of process in obtaining the required parameters and constants. The applications of these two adsorption models are well documented for single-adsorbate aqueous systems as presented in Table 2.9.

Table 2.8 Existing adsorption models and their respective descriptions and nonlinear form equations

Model	Description	References
Langmuir	• assumes monolayer adsorption • adsorption can only occur at a finite (fixed) number of definite localized sites, that are identical and equivalent, • no lateral interaction and steric hindrance between the adsorbed molecules, even on adjacent sites $q_e = \frac{Q_0 b C_e}{1 + b C_e}$ Equation 2.1	(Langmuir, 1916)
Freundlich	• assumes multilayer adsorption • non-uniform distribution of adsorption heat and affinities over the heterogeneous surface $q_e = K_F C e_e^{\frac{1}{n}}$ Equation 2.2	(Freundlich, 1906)
Brunauer-Emmett-Teller (BET)	• developed to derive multilayer adsorption systems with relative pressure ranges from 0.05 to 0.30 corresponding to a monolayer coverage lying between 0.50 and 1.50. $q_e = \frac{q_s C_{BET} C_e}{(C_s - C_e)[1 + (C_{BET} - 1)(C_e / C_s)]}$ Equation 2.3	(Bruanuer et al., 1938)
Redlich–Peterson	• a hybrid isotherm featuring both Langmuir and Freundlich isotherms, which incorporate three parameters into an empirical equation • represent adsorption equilibria over a wide concentration range, that can be applied either in homogeneous or heterogeneous systems due to its versatility $q_e = \frac{K_R C_e}{1 + a_R C_e^g}$ Equation 2.4	(Redlich & Peterson, 1959)
Dubinin–Radushkevich	• considered for the adsorption of subcritical vapors onto micropore solids following a pore filling mechanism • generally applied to express the adsorption mechanism with a Gaussian energy distribution onto a heterogeneous surface $q_e = (q_s)\exp(-k_{ad}\varepsilon^2)$ Equation 2.5	(Dubinin & Radushkevich, 1947)
Tempkin	• contains a factor that is explicitly taking into the account of adsorbent–adsorbate interactions • by ignoring the extremely low and large value of concentrations, the model assumes that heat of adsorption (a function of temperature) of all molecules in the layer would decrease linearly rather than logarithmic with coverage $q_e = \frac{RT}{b_T} ln\mathrm{A}_T C_e$ Equation 2.6	(Tempkin & Pyzhev, 1940)

q_e :amount of adsorbate in the adsorbent at equilibrium (mg/g), Q_0: maximum monolayer coverage capacities (mg/g), b: Langmuir isotherm constant (dm^3/mg), C_e: equilibrium concentration (mg/L), K_F: Freundlich isotherm constant (mg/g) (dm^3/g) related to adsorption capacity, n: adsorption intensity, q_s: theoretical isotherm saturation capacity (mg/g), C_{BET}: BET adsorption isotherm relating to the energy of surface interaction (L/mg), C_s: adsorbate monolayer saturation concentration (mg/L), K_R: Redlich-Peterson isotherm constant (L/g), a_R: Redlich-Peterson isotherm constant (1/mg), g: Redlich-Peterson isotherm exponent, k_{ad}: Dubinin-Radushkevich isotherm constant (mol^2/kJ^2), ε: Dubinin-Radushkevich isotherm constant, R: universal gas constant (8.314 J/mol K), T: temperature (K), A_T: Tempkin isotherm equilibrium binding constant (L/g)

Table 2.9 Adsorption of various contaminants on biomass

Contaminant	Biomass	Adsorption model	Findings	Reference
Cd	Polyaniline-coated on sawdust	Freundlich	• Adsorption was rapid and occurred within 20 min for a cadmium concentration range of 10 to 40 mg/L. Maximum adsorption capacity was fund to be 430 mg/g.	(Mansour et al., 2011)
Cu and Pb	Banana peel	Langmuir	• Maximum uptake capacities for Cu and Pb ions were 20.97 and 41.44 mg/g, respectively. • The specific surface area was found to be 2.0 ± 0.01 m^2/g and pore diameters was 10.5 Å.	(Castro et al., 2011)
Pb, Cd and Ni	Grafted copolymerisation-modified orange peel	Langmuir	• Maximum uptake capacities for Pb,Cd and Ni were 476.1, 293.3 and 162.6 mg/g, respectively. • FTIR demonstrated that carboxyl and hydroxyl groups were involved in the biosorption of the metal ions.	(Feng et al., 2011)
Cu and Cd	Switchgrass biochar	Resulted plots that did not fit isotherm models such as Langmuir and Freundlich.	• Functional groups such as C=O demonstrate high coordination with Cu and Cd. • The adsorption of positively charged Cu and Cd ions might have occurred via attraction to negatively charged surface groups or through the formation of direct surface complexes to biochar.	(Regmi et al., 2012)
As	Banana peel	Freundlich	• Maximum percentage removal (82.23%) of As was obtained at optimized pH 7, contact time of 90 min, the dosage of 8 g, the temperature of 35°C and 10 mg/L As concentration, respectively.	(Kamsonlian et al., 2012)
Cu, Pb and Zn	Coconut tree sawdust (CTS), eggshell (ES) and sugarcane bagasse (SB)	Freundlich and Langmuir	• Maximum adsorption capacities were found to be 3.89, 25.00 and 23.81 mg/g for CTS, 34.48, 90.90 and 35.71 mg/g for ES, and 3.65, 21.28 and 40.00 mg/g for SB • The Freundlich constant (n_F) and separation factor (R_L) values suggest that the metal ions were favourably adsorbed onto biosorbents.	(Putra et al., 2014)

Based on Table 2.9, adsorption of different contaminant on the same biomass tends to follow a different type of adsorption model. The reason might be due to the unique functional groups present on the biomass surface that react differently with one contaminant to another. For example, the adsorption of Cu and Pb on banana peel followed Langmuir model while the adsorption of As on the same biomass followed the Freundlich model (Castro et al., 2011; Kamsonlian et al., 2012).

Zhu et al. (2012) applied Langmuir and Freundlich adsorption models for a multi-metal system containing Pb, Cu and Zn. The study found that maximum adsorption capacities were found to be 76.9 mg/g (Pb), 34.5 mg/g (Cu) and 20.8 mg/g (Zn) when treated using Novel xanthate-modified magnetic chitosan (XMCS). It is shown that the single-metal system followed Langmuir while multi-metal systems followed the Freundlich model.

Although Langmuir and Freundlich models were applicable in predicting adsorption capacity of a biomass, there are several other models that have also been developed to account for competitive adsorption systems. Some of these models are the Sheindorf-Rebhun-Sheintuch model (Sheindorf et al., 1981) and competitive Langmuir model (Murali & Aylmore, 1983).

The description of these models and the respective equations are presented in Table 2.10. As a rule, the applicability of the competitive adsorption model will be determined based on the model that the single contaminant adsorption followed. For example, in a non-competitive system, an adsorption of one contaminant on a biomass followed the Freundlich model assumptions then the Freundlich-type competitive adsorption (SRS model) should be chosen for further evaluation in competitive adsorption system (Sheindorf et al., 1981). Similarly, in a non-competitive system, if the adsorption of the contaminant on the biomass followed the Langmuir model's assumptions, then the competitive Langmuir model should be chosen for further evaluation in a competitive adsorption system.

Table 2.10 Existing competitive adsorption models and their respective descriptions and general equations

Model	Description	References
Sheindorf-Rebhun-Sheintuch (SRS)	• assumed that single-component sorption follows the Freundlich equation • specifically, the SRS model was developed to describe competitive equilibrium sorption for multicomponent systems where the sorption isotherms of a single component follow the Freundlich equation. $S_i = K_i C_i \left(\sum_{j=1}^{l} \alpha_{i,j} C_j \right)^{n_i}$ Equation 2.7	(Sheindorf et al., 1981)
Competitive Langmuir Model	• assumes that there is only one set of sorption sites for all competing ions. • the model also assumes that the presence of competing ions does not affect the sorption affinity of other ions. $S_i = \frac{K_{Li} C_i S_{max}}{1 + \sum_j K_L C_j}$ Equation 2.8	(Murali & Aylmore, 1983)

i and j: metal components i and j, l: is the total number of components, $\alpha_{i,j}$: dimensionless competition coefficient for the adsorption of component i in the presence of component j, K_i and n_i: Freundlich parameters representing a single-component system i, K_L: Langmuir parameter, S: the amount of adsorption (mg/kg), C is the dissolved concentration (mg/L)

2.8 Assessment of WHO drinking water quality exceedance and compliance probabilities

The quality of groundwater could vary spatially and temporarily. Irrespective of the groundwater quality it is important to ensure that the treated water meets the WHO water quality guidelines. Probability Density Functions (PDF) are created to establish the variation of input (groundwater) and output (treated water) water quality parameters. The Monte Carlo simulation technique will be used to generate random samples from a PDF (Khan, 2010).

2.9 Cost estimation

To conduct a cost estimation for drinking water treatment unit, there are several cost components need to be taken into account. The first cost component is the construction

or installation costs. The installation costs include the costs for pipes, valves, steel, concrete and many more. The second cost component accounts for costs involved in the operation and maintenance such as the costs for maintenance material, process, labour etc. (Sethi & Clark, 1998). Therefore, it is essential to identify all the materials and instruments that are involved in the proposed treatment unit so that an estimation of the overall costs involved can be evaluated. For a drinking water treatment unit, it is important to take account of the typical volume of the amount of water that a household needs per day.

According to Rajapakse et al. (2014), decentralised water supply systems are broadly categorised into household water treatment systems (HWTS) and small scale systems (SSS). The HWTS are further classified into the point of use (POU) systems and point of entry (POE) systems. This categorisation is shown schematically in Figure 2.7.

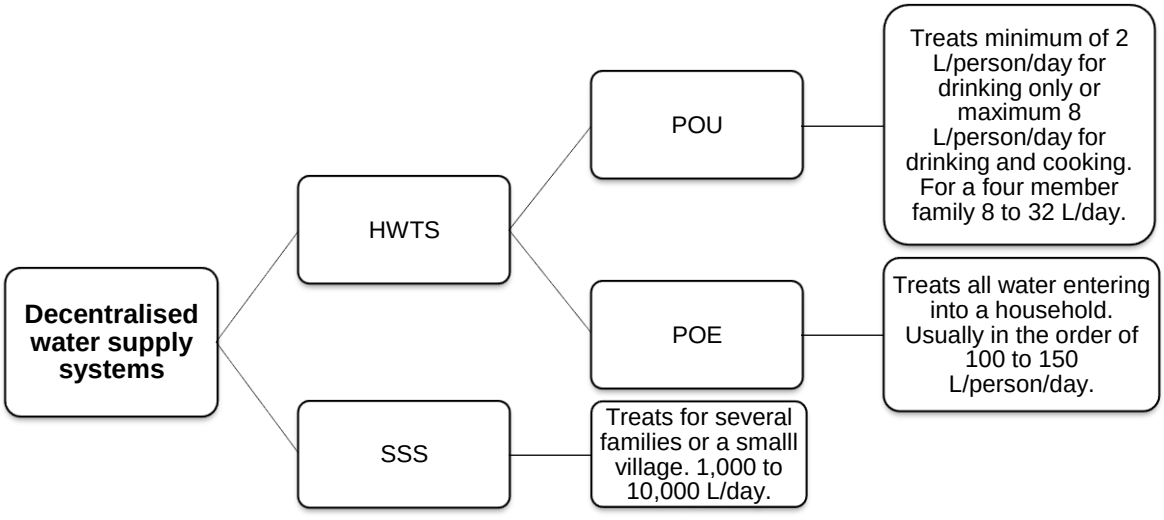

Figure 2.7 Classification of decentralized remote community water supply systems (Rajapakse et al., 2014)

This information is important for the cost estimation of the proposed treatment unit. By knowing the quantity of water that needs to be treated the dose of the proposed water purification agents can be calculated.

A cost comparison study carried out by Lantagne et al. (2006) reported that the cost of installation of bio-sand filtration unit for a household in Cambodia was USD 67. On the other hand, there was no cost involved for installation of ceramic filtration in Nicaragua and solar disinfection treatment in Indonesia because these treatment methods only used the reusable materials (Lantagne et al., 2006).

2.10 Conclusions

This chapter presents comprehensive information regarding drinking water quality issues associated with the excessive levels of heavy metals (lead, nickel, cadmium and arsenic), problematic fluoride ion and turbidity which have been found to be the parameters of concern in groundwater in many remote regions in South Asian countries such as Pakistan, India, Bangladesh and Sri Lanka over the past years. A broad range of conventional water treatment techniques for the removal of target contaminants has been discussed in detail. Most of these methods offer unique advantages and disadvantages. Furthermore, a wide range of low-cost materials and their effectiveness in removing various water quality pollutants from different water sources have been reviewed. Based on the review, use of natural materials in removing various kinds of contaminants from groundwater sources was considered in this research. It is also evident from previous studies that basic, acidic and thermal pre-treatments were among the most commonly applied methods by the researchers to improve treatment efficiency in their studies. The reasons might be due to the simplicity of the treatment process and their proven effectiveness in improving the treatment efficiency of the biomass. It is obvious that the use of natural materials as a low-cost alternative to the typically expensive chemicals could be considered as an important discovery in the field of low-cost drinking water treatment technologies.

2.11 Research Gaps

There are increasing concerns of health threats among people living in remote areas due to consumption of untreated water. Thus, there is an urgent need to provide low-cost drinking water treatment methods to community in remote areas. The review also demonstrated that different biomass possesses different capability in removing specific contaminants. Therefore, there is a need to study the effectiveness of biomass in removing contaminants. Also, it is interesting to determine the effect of combining different biomass to improve the treatment efficiency. Furthermore, extensive investigations are required to explain the efficiency of low-cost drinking water treatment using natural freely available materials (plant-based) on groundwater which usually has a lower concentration of contaminants of concern. Furthermore, mechanisms behind the treatment process and cost estimation (based on current market prices) for the proposed drinking water treatment unit need to be determined to ensure its applicability and affordability to people living in remote areas in countries which are financially disadvantaged.

CHAPTER 3 Methods and materials for determining effective plant-based materials and optimum operating conditions, characterisations, modelling and cost analysis

This chapter describes the plant-based materials and methods used throughout this research. Figure 1.1 (Chapter 1) depicts the flow chart of research methodology. Preliminary experiments were carried out to determine the optimum dosage of biomass used in the study. Preparation of synthetic groundwater samples and biomass used in the treatment process were fully explained. Experiments were carried out to determine the optimum dosage of biomass in order to remove target pollutants in synthetic groundwater to meet World Health Organisation (WHO) recommended standards. The experimental procedure of the treatment process for both synthetic and actual groundwater samples was described in detail. The preparation methods for pre-treated biomass were described to test the problematic contaminants which fail to meet the recommended WHO standards when treated with natural biomass. Experimental methods used to analyse the concentration of target contaminants (heavy metals, fluoride and turbidity), pH, dissolved organic carbon (DOC) and ultraviolet 254 nm absorbance (UVA_{254}) were also included in this chapter.

It is important to know the possible mechanisms involved in the treatment process. A study on original (unloaded) and contaminant (loaded) biomass characteristic was carried out. Experimental procedures and analytical instruments involved in the characterisation study were fully described. The characterisation study identified ‘adsorption’ as the main mechanism to remove target contaminants.

Pollutant concentrations in groundwater vary with seasons throughout the year and also with the location (aquifer). Thus, it is important to investigate the reliability of the treatment in order to achieve the recommended WHO standards with the predetermined biomass dosage. An adsorption model was selected for this purpose. The selection of the adsorption model was made based on its capability in predicting the final concentration of target contaminants with a known biomass dosage. Model parameters were determined by conducting laboratory experiments. Monte Carlo random number generation procedure was selected to generate different combinations of target contaminants in the groundwater quality. The experimental procedure of the adsorption study was explained in this chapter. Furthermore, quality estimation of the treated groundwater and calculation for the probability of exceeding WHO drinking water quality standard were also explained.

3.1 Preparation of synthetic groundwater samples and biomass in treatment process

3.1.1 Chemicals (analytical grade)

Synthetic groundwater samples containing arsenic (As), lead (Pb), nickel (Ni), cadmium (Cd), fluoride and turbidity were prepared with deionised water, since these were the target contaminants in groundwater especially in developing countries. All the above chemicals applied in this study were of analytical reagent grade. Arsenic trioxide (AsO_3), lead carbonate ($PbNO_3$), nickel carbonate ($NiCO_3$), cadmium nitrate tetrahydrate ($Cd(NO_3)_2.4H_2O$), sodium fluoride (NaF) and kaolin powder ($Al_2Si_2O_5(OH)_4$) were obtained from Sigma-Aldrich (Australia). The chemical stock solutions of target contaminants were prepared by dissolving the desired amount of each analytical reagent grade in deionised water. The range of concentration for each individual element prepared from the stock solutions varied based on the concentration

targeted for each respective experiment. Consequently, the required synthetic groundwater samples; either a single-element or multi-element were prepared by diluting the stock solution, which had a concentration of 1000 mg/L, for each heavy metal with deionised water, as per needed by the experiment. The purpose of testing with multi-element solutions was to examine the effects of using more than one element on the treatment performance. On the other hand, the purpose of testing single-element solutions was to determine the optimum dosage of biomass needed when treating a specific target contaminant without the presence of other contaminants. This eliminates the interference effects between different target contaminants present in the same sample solution. The other chemicals used were 0.1 Molar (M) of sulfuric acid (H_2SO_4) and 0.1 M of sodium hydroxide (NaOH) to adjust the pH of the solution. Certain target contaminants could not be removed by using the selected plant-based biomass to meet WHO standards. Thus, alum ($Al_2(SO_4)_3.18H_2O$) was used to pre-treat the biomass. Alum was supplied by Chem-Supply, Pty-Ltd., Australia. Concentration of alum reported in this study were in the form of Al^{3+} ion mg/L. 1 M of nitric acid (HNO_3) and 1 M of NaOH were used for the pre-treatment of plant-based materials.

3.1.2 Preparation of biomass (plant-based material) as a treatment agent

Moringa oleifera (Moringa seeds, MO), *Cicer arietinum* (chickpeas, CA), *Musa cavendish* (banana peel, MC), *Cocos nucifera* (coconut solid endosperm, CN) and *Lentinus edodes* (Shiitake mushroom, LE) were chosen as plant-based biomass based on their performances in treating various type of pollutants in water as reported in Chapter 2. One gram of prepared biomass powder was added to 1000 mL of deionised water. The mixture was then stirred at 1000 rpm for 10 minutes using a magnetic stirrer to generate an active ingredient. The mixture yields a stock solution with 1000 mg/L

concentration of the respective biomass. The stock solution was freshly prepared before each run in the experiment to avoid aging effects (Chen et al., 2006, 2008). Specific description on the preparation of each biomass (MO, CA, MC, CN, and LE) used in the study are described next.

3.1.2.1 Moringa oleifera (MO)

Moringa oleifera (MO) seeds were purchased from Pacific Blue Consulting Pty. Ltd. (The Moringa Shop, Australia). High-quality seeds were selected and cleaned from debris. Husks and outer coats were removed as recommended by Okuda et al. (2001). The selected MO seeds were then rinsed with deionised water and dried in an oven at 100°C for 1 hour. The dried seeds were ground to a fine powder and sieved through a 300 μm stainless steel mesh to obtain MO particles with similar size (Vardhan & Karthikeyan, 2011).

3.1.2.2 Cicer arietinum (CA)

Chickpeas (CA) were bought from a local market. They were cleaned and then dried in an oven for 1 hour at 105°C. Dried chickpeas were then grounded to a fine powder (Saqib et al., 2013). Then, the chickpeas powder was sieved through a 300 μm stainless-steel mesh to get a homogenous size of chickpea particles.

3.1.2.3 Musa cavendish (MC)

Ripe bananas (MC) were also bought from a local market. The peels were gently removed from the fruits. The peels were cleaned and dried in an oven for 1 hour at 100°C. Following that, the dried peels were cut into small pieces, ground and sieved through a 300 μm stainless steel mesh to produce a homogenous size of banana peel particles (Liu et al., 2012).

3.1.2.4 Cocos nucifera (CN)

The coconuts were bought from a local market. Coconut husks were removed, and the coconut was cracked to remove the water (Fatombi et al., 2013). The solid coconut endosperm was cut into small pieces and dried in an oven for 1 hour at 100°C. Small pieces of dried coconut solid endosperm were then ground to a fine powder and sieved through a 300 µm stainless-steel mesh to prepare a homogenous size of coconut solid endosperm powder.

3.1.2.5 Lentinus edodes (LE)

Lentinus edodes or Shiitake mushrooms (LE) were also bought from a local market. The mushrooms were then cleaned and oven-dried at 100°C for 1 hour. The dried Shiitake mushrooms were ground to fine powder and sieved through a 300 µm stainless steel to obtain a homogenous size of the mushroom powder.

3.1.2.6 Selection of effective plant-based materials for the study

The effective plant-based materials for the preliminary study were selected based on the criteria as described in Section 2.6.3. Then, the effective plant-based materials to be used for the proposed treatment methods were selected based on the performance of selected plant-based materials in treating target contaminants to comply with the respective WHO standards.

3.2 Batch experiments

Batch experiments were carried out to investigate the possibility of removing target contaminants to meet the recommended WHO standards by using plant-based biomass. Experiments were initially carried out on synthetic groundwater samples

prepared in the laboratory. Concentration of the target contaminants and biomass dosage were varied until the desired concentration of contaminants was obtained. The optimum biomass conditions identified through the experiment on synthetic groundwater samples were tested with actual groundwater to investigate the applicability of the treatment under actual conditions. It was not possible to reduce the concentration of arsenic (As) and fluoride to meet the required WHO standards by using the selected biomass dosage. Thus, the biomass was pre-treated and batch experiments were then conducted to determine the possibility of reducing As and fluoride to the desired concentration. Furthermore, conventional treatment with Alum was also carried out to determine the treatment efficiency.

3.2.1 Preparation of groundwater samples

3.2.1.1 Synthetic groundwater samples

Synthetic groundwater samples containing target contaminants of As, Pb, Ni, Cd, fluoride and turbidity were prepared by using deionised water. All chemicals used in the study, including arsenic trioxide, lead carbonate, nickel carbonate, cadmium nitrate tetrahydrate, sodium fluoride and kaolin powder were of analytical grade and obtained from Sigma-Aldrich (Australia). The chemical stock solutions with a concentration of 1000 mg/L was prepared and diluted to meet the target concentration as needed for the experiment. The preparation of the synthetic groundwater samples followed the method reported previously (USEPA, 2002). All glassware and bottles utilised in the experiments were cleaned by soaking them into 20% nitric acid solution and were then rinsed with deionised water before being used. The pH of the water sample was adjusted to 7.00 ± 0.02 using either 0.1 M of H_2SO_4 or 0.1 M of NaOH. Two types of solution matrix were tested throughout the study namely single-element solutions and multi-element solutions. For single-element solutions, desired concentration of the

target contaminants was prepared by diluting the prepared chemical stock solution with deionised water. Similarly, the same procedure was conducted on a multi-element solution in order to prepare the desired concentration of target contaminants. Initial characteristics of multi-element and single element synthetic groundwater samples are presented in Table 3.1 and Table 3.2.

Table 3.1 Initial characteristics of multi-element synthetic groundwater samples

Parameter	High initial concentration (Average: *N*=3)	Low initial concentration (Average: *N*=3)	World Health Organisation (WHO) drinking water quality standard
	Biomass dose: 10-100 mg/L	Biomass dose: 10-200 mg/L	
Arsenic (As)	655.9 µg/L	40.1 µg/L	10 µg/L
Lead (Pb)	125.0 µg/L	39.6 µg/L	10 µg/L
Nickel (Ni)	112.0 µg/L	28.6 µg/L	20 µg/L
Cadmium (Cd)	11.7 µg/L	5.1 µg/L	3 µg/L
Fluoride	14.0 mg/L	3.5 mg/L	1.5 mg/L
Turbidity	36.7 NTU	15.0 NTU	5 NTU
pH	7.0	7.0	6.5-8.5

Table 3.2 Initial characteristics of single-element synthetic groundwater samples

Parameter	Initial concentration (Average: *N*=3)	WHO drinking water quality standard
	Biomass dose: 100-600 mg/L	
Arsenic	20.7 µg/L	10 µg/L
Lead	19.3 µg/L	10 µg/L
Nickel	30.6 µg/L	20 µg/L
Cadmium	5.0 µg/L	3 µg/L
Fluoride	3.0 mg/L	1.5 mg/L
Turbidity	14.8 NTU	5 NTU
pH	7.0	6.5-8.5

3.2.1.2 Actual groundwater samples

In addition to the target contaminants, actual groundwater samples might also contain dissolved organic carbon, salts and organic matter. The behaviour of target contaminants differs in the presence of above parameters especially in actual conditions. The optimum biomass conditions identified using synthetic groundwater samples were tested with actual groundwater to investigate the applicability of the treatment performance under actual conditions. The actual groundwater samples were

taken from three different locations around Victoria, Australia. The groundwater samples were obtained from another project carried out at the RMIT University. Their locations and dissolve organic carbon (DOC), electroconductivity (representing the salinity of water) and ultraviolet absorbance (measured by UVA_{254}) are presented in Table 3.3.

Table 3.3 Characteristics of real groundwater samples

Parameter	pH	EC	As	Pb	Ni	Cd	Fluoride	Turbidity	DOC	UVA_{254}
Unit	-	µS/cm	µg/L	µg/L	µg/L	µg/L	mg/L	NTU	mg/L	cm^{-1}
Location of sampling										
East Gippsland (Site 1)	6.7	1944	0.1	2.0	0.8	0.2	0.1	2.2	9.9	0.058
East Gippsland (Site 2)	7.1	365	0.1	2.0	0.8	0.1	0.1	2.5	8.6	0.036
Cranbourne	9.1	9370	0.1	0.6	24.4	0.0	0.1	0.3	11.1	0.025

The concentration of all targeted contaminants in the actual groundwater samples meet the required WHO drinking water standards (Table 3.3), except for Ni concentration in the sample taken from a bore in Cranbourne. This bore is located at Clyde Reserve, south east of Melbourne. The bore is 49-meter-deep with inactive volcanic geology. Hence, the actual groundwater samples were spiked with the target contaminants of heavy metals, where the concentrations of each contaminant are shown in Table 3.4. The pH of the actual groundwater samples was adjusted to 7.0 using either 0.1 M of H_2SO_4 or 0.1 M of NaOH to be consistent with the pH of the synthetic groundwater samples.

Table 3.4 Characteristics of real groundwater sample (after spiking and pH adjustment)

Parameter	pH	EC	As	Pb	Ni	Cd	Fluoride	Turbidity
Unit	-	µS/cm	µg/L	µg/L	µg/L	µg/L	mg/L	NTU
Location of sampling								
East Gippsland (Site 1)	7.0	1891	19.7	19.3	29.8	5.1	2.98	14.8
East Gippsland (Site 2)	7.0	336	20.3	19.8	30.2	4.9	3.02	15.1
Cranbourne	7.0	8400	20.1	19.3	29.8	5.0	2.99	15.0

3.2.2 Pre-treatment of biomass

As reported in Chapter 4, the selected biomass were not capable to reduce the concentration of arsenic and fluoride to meet the recommended WHO standards. Pre-treatment of the biomass can improve the treatment efficiency (Kumar et al., 2009). Chemical and physical pre-treatments were expected to change the chemical composition and surface morphology of the biomass in order to provide extra capacity for the retention of some problematic contaminants. Bhatti et al. (2007) reported that zinc (Zn) removal of acidic pre-treated MO biomass was in following order: H_2SO_4 (90%) > H_3PO_4 (82%) > HCl (74%) > non-treated bio-mass (74%). On the other hand, Zn uptake by basic pre-treated MO biomass was in following order: NaOH (91.52%) > $Ca(OH)^2$ (85.20%) > $Al(OH)^3$ (82.08%) > non-treated biomass (74%). Study conducted by Akhtar et al. (2007) also reported that MO pods which was pre-treated with chemicals increased the surface area and pore diameter of the biomass, while thermal activation improves porosity of the MO pods. These facilitate the attachment of contaminants due to the greater availability of binding sites on the biomass. Therefore, the following three methods of pre-treatment were applied based on their capability in improving the treatment efficiency:

3.2.2.1 Acidic and basic pre-treatment

For acidic or basic pre-treatments, one gram of biomass was dissolved in 200 mL of 1 M of HNO_3 and 1 M of NaOH solution, respectively in a volumetric flask for 24 hours (Bhatti et al., 2007). The acid- or basic-dissolved biomass was filtered and washed with deionised water until the pH of the filtrated solution reached the pH of 7.00 ± 0.02. The retained biomass was dried at 60°C for 24 hours in a furnace.

3.2.2.2 Thermal pre-treatment

One gram of biomass was dried at 300°C for one hour in the furnace (Akhtar et al., 2007).

3.2.3 Coagulation (jar tests)

A standard jar tester (Lovibond, Phipps & Bird) was conducted to investigate the removal of target contaminants from both synthetic and actual groundwater samples by using the selected biomass. Series of experiments were conducted to investigate the removal of target contaminants by using the selected biomass. The combination and sequential dosing for more than one biomass method were also attempted in this study, with the intention to improve the treatment efficiency. All experiments were performed using 1 L groundwater sample solution in a 2 L acrylic jars under a room temperature of 20°C±1°C. The pH of each sample was adjusted to 7.00±0.02 with 0.1 M of NaOH or 0.1 M of H_2SO_4 before all experiments were conducted. The pH of the adjusted samples was dosed according to the desired amount of biomass as presented in Table 3.1 and Table 3.2. The samples were stirred at 150 rpm for 3 minutes. This process was followed by reducing the mixing speed to 30 rpm and stirred for an additional of 30 minutes. The agitated solutions were allowed to settle for 30 minutes before the supernatant layer was filtered through 0.45 μm Advantec fibreglass membrane filters. The treated sample was tested for the removal of target contaminants by using the selected biomass or alum. For experiments with the combined biomass (i.e., MO+MC), both biomass were added to the water sample simultaneously. It is noteworthy that the dose applied for combined biomass (MO+MC) was used in the ratio of 1:1. For example, 200 mg/L dose of MO+MC means that 100 mg/L of MO was dosed concurrently with 100 mg/L of MC. Thus, the combined total dose for

MO+MC is 200 mg/L. For the sequential dosing methods (i.e., MO→MC and MC→MO), the first biomass was dosed, and following that, the supernatant of the treated sample was withdrawn and sequentially treated using other biomass. All batch test experiments were conducted in triplicate (*N=3*) in order to analyse the results obtained. The mean outcome statistics were reported.

3.3 Analytical methods for determining concentrations of target contaminants, pH, DOC and UVA_{254}

3.3.1 Heavy metals

Concentrations of As, Pb, Ni and Cd in the treated solutions were determined using Agilent 7700 series Inductively Coupled Plasma Mass Spectrometry (ICP-MS). The ICP-MS was calibrated for each target element before the analysis. Results of ICP-MS standard calibrations were presented in Figure A1.1 (Appendix A1).

3.3.2 Fluoride

Fluoride was measured using HQ14d portable with ISEF121 Fluoride Ion Selective Electrode. For calibration purpose, fluoride concentration of 1, 2, 3, 5 and 10 mg/L were prepared using sodium fluoride (NaF) and deionised water. For the analysis, 25 mg of fluoride ionic strength adjuster was added to at least 25 mL of the fluoride samples before the analysis to maintain the fluoride reading during the measurement was taken. It is a standard procedure in performing the reading when using the fluoride probe. The mixture was stirred using a magnetic stirrer during measurements to generate a homogenous mixture for a stable and accurate reading.

3.3.3 Turbidity

Turbidity measurement was carried out using HACH turbidity meter 2100AN. Sample flask was cleaned thoroughly with deionised water and filled with the sample. The blank sample for HACH was prepared using deionised water. The blank sample reading was taken before each turbidity readings for both synthetic and treated groundwater samples to eliminate any irregular reading in turbidity.

3.3.4 pH

pH was measured using Seven Compact Mettler Toledo pH and conductivity meter. For calibration purpose, buffer solutions with pH of 4.01, 7.00 and 10.01 (Ajax Chemicals) were used to maintain the accuracy of pH measurement.

3.3.5 Dissolved organic carbon (DOC)

Dissolved organic carbon (DOC) level in the actual groundwater samples were measured using a total organic carbon analyser (Sievers Model 5310 C) equipped with an automatic sampler and inorganic carbon remover (Sievers 900). All samples were diluted using MilliQ water (Milli-Q Gradient A10 unit Millipore) before the DOC analysis.

3.3.6 Ultraviolet (UVA) 254 nm absorbance

Absorbance at 254 nm (UVA_{254}) was measured using a double beam scanning UV/vis spectrophotometer (UV2 Unicam) with a matched pair of 1 cm path length of quartz cuvettes.

3.4 Characterisation study

Characterisation of biomass is necessary to understand the mechanism(s) behind the treatment process. The Attenuated Total Reflectance-Fourier Transform Infrared (ATR-FTIR), Scanning electron Microscopy (SEM) and Energy Dispersive X-ray (EDX) analyses were carried out with natural (unloaded) and treated (contaminant-loaded) biomass for above purpose. For this study, unloaded biomass was applied directly without any treatment for the characterisation of biomass before the treatment process. However, the contaminant-loaded biomass was collected at the end of the treatment process and was dried at 60°C for 24 hours before the characterisation.

3.4.1 Attenuated Total Reflectance-Fourier Transform Infrared (ATR-FTIR) analysis

The FTIR analysis of biomass before and after the treatment process could provide valuable information about the mechanism underlying the contaminant removal process (Pandey et al., 2008). Accordingly, the FTIR analysis was conducted on both unloaded and contaminant-loaded biomass using Attenuated Total Reflectance-Fourier Transform Infrared (ATR-FTIR) Spectrum 100 spectroscopy (Figure 3.1). For FTIR analysis, a desired amount of unloaded biomass or contaminant loaded biomass that has been dried was placed on the crystal diamond disc mounted on the FTIR spectroscopy. All infrared spectra were recorded between wavenumber of 4000 to 600 cm^{-1} with 16 numbers of scans for each analysis and resolution of 4 cm^{-1}. Interpretation of the results were made based on the appearance of the specific bands on the FTIR spectra which correspond to the specific type of functional groups. The observed specific bands were assigned to the specific functional group according to the wavenumbers as classified by Silverstein et al. (1981), Kwaambwa & Maikokera

(2008), Reddy et al. (2012), Bhende & Jadhav (2012), Sharma & Paliwal (2013) and Bhutada et al. (2016).

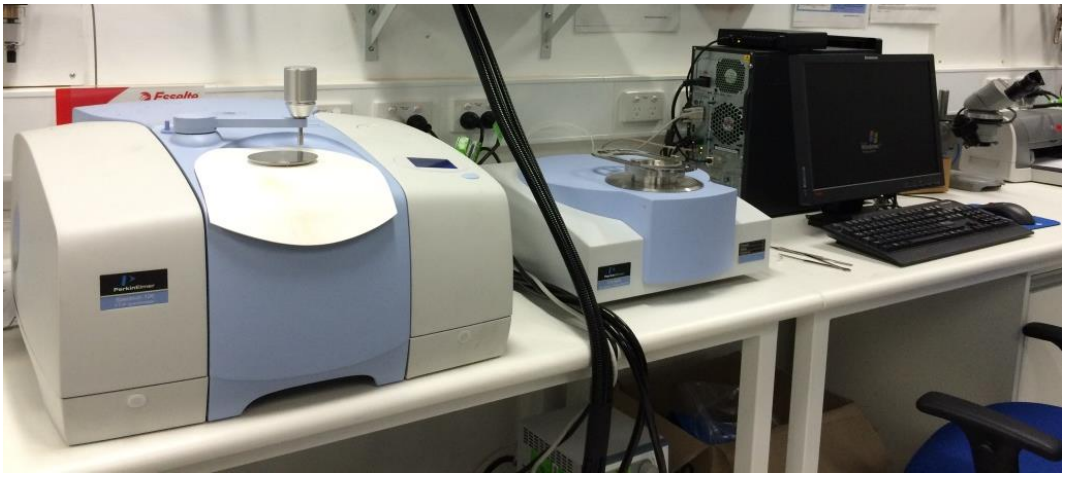

Figure 3.1 ATR-FTIR Spectrum 100 spectroscopy

3.4.2 Scanning Electron Microscopy (SEM) and Energy Dispersive X-ray (EDX) analyses

Analysis of biomass surface before and after the treatment process is important to observe the morphological profile of biomass to ensure its capability in retaining the target contaminant on its surface. This analysis was done using scanning electron microscopy (SEM) FEI Quanta 200. The scanning was carried out at a high voltage of 30 kV. For the preparation of the sample, the specimens were deposited on a double-sided carbon tape to a sample stub. Then, the samples were gold coated with SPI sputter coater to a thickness of approximately 20 nm to avoid electron charging during the scanning process. The elemental composition of the unloaded and contaminant-loaded biomass was observed by using EDX instrument which attached to the SEM (Figure 3.2). EDX spectra of the unloaded and contaminant-loaded biomass will be produced during the analysis so that the adsorption of the target contaminant on the biomass can be confirmed based on the composition of elements obtained from the analysis.

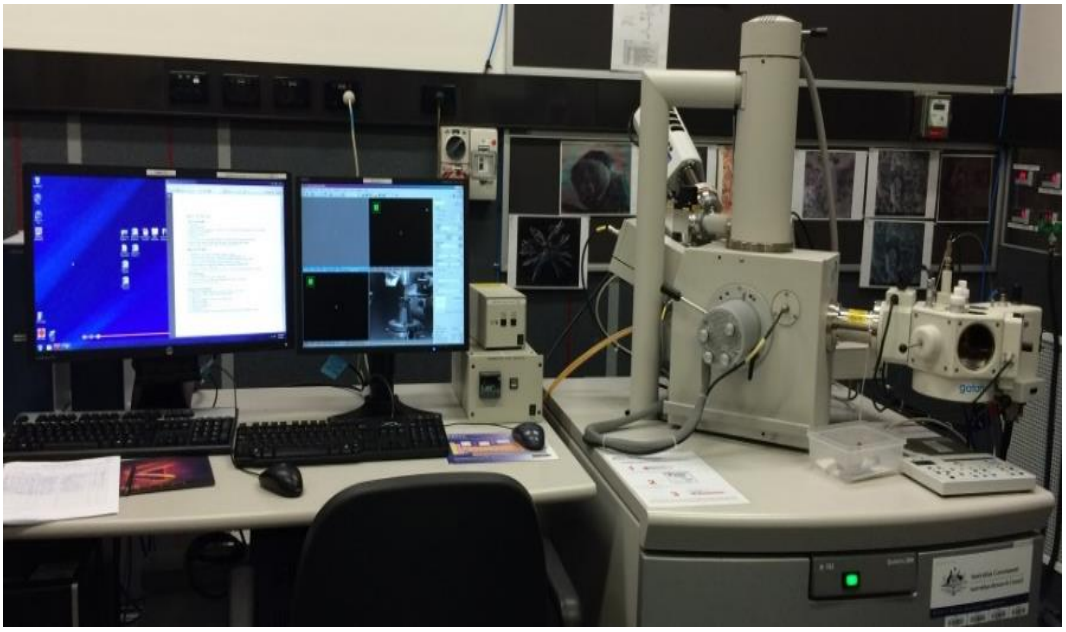

Figure 3.2 SEM FEI Quanta 200 equipped with EDX instrument

3.5 Adsorption batch tests

From the characterisation of the biomass (Chapter 5) it was determined that adsorption was the principal mechanism for the removal of target contaminant. A process similar to what was described in Section 3.2.3 was followed in conducting adsorption tests. As reported in Chapter 4 and Aziz et al. (2014 and 2015) the optimum biomass doses for removing As, Pb, Ni, Cd, fluoride and turbidity from single and multi-element synthetic groundwater samples were evaluated. The optimum biomass doses obtained were 200 mg/L for individual MO and MC biomass, and 200:200 mg/L in the ratio for MO+MC. The above biomass concentrations were therefore used in the adsorption batch tests to determine the final concentrations of the treated water.

Only Pb, Ni, and Cd were selected for adsorption tests as it was not possible to treat As and fluoride to meet the WHO standards from the above-mentioned biomass dosages. Synthetic groundwater samples containing individual (single-element) and mixture (multi-element) of Pb, Ni and Cd of known concentrations were prepared with

deionised water (Aziz et al., 2016). The mode of adsorption operation for this study referred to the concept of powdered activated carbon (PAC). PAC adsorption is usually less complex than that of granular activated carbon (GAC) adsorption process (Najm, 1996). Moreover, all biomass used for the current study were in powder form. Thus, it is expected that similar conditions to Najm (1996) study would work for the biomass in the current study. In PAC adsorption process, static adsorption is usually applied. Static adsorption is called batch adsorption which occurs in a closed system containing the desired amount of adsorbent, contacting with a particular concentration of target contaminant in a solution (Xu et al., 2013).

3.5.1 Adsorption in single-element solutions

In each experiment, 200 mg/L (MO or MC) or 200:200 mg/L (MO+MC) of the dried biomass were dosed into 1 L of prepared single-element synthetic groundwater samples, which contain a molar concentration of individual heavy metals described in Table 3.5.

Table 3.5 Initial concentrations (in molarity) of single-element samples

Parameter	Unit	Initial concentration (µmol/L)	WHO drinking water quality standard
Pb	µg/L	0.024 - 0.483	10 µg/L (0.048 µmol/L)
Ni	µg/L	0.170 - 1.704	20 µg/L (0.341 µmol/L)
Cd	µg/L	0.009 - 0.098	3 µg/L (0.027 µmol/L)
pH	-	7.0+0.1	6.5-8.5

3.5.2 Adsorption in multi-element solutions

Multi-element adsorption experiments were conducted by using sample solutions containing combined molar concentrations of each heavy metal (Pb, Ni and Cd) in the range described in Table 3.6. The experiments were conducted under similar experimental conditions to the single-element solution.

Table 3.6 Initial concentrations (in molarity) of multi-element samples (*independent test)

Sample	Initial concentrations (µmol/L)		
	Pb	Ni	Cd
1	0.024	0.170	0.009
2	0.097	0.511	0.044
3	0.193	0.682	0.062
4	0.290	0.852	0.080
5	0.483	1.704	0.098
6*	0.048	0.341	0.027
7*	0.386	1.363	0.089

3.6 Determination of final concentration of treated water using existing adsorption mathematical models

It is important to investigate the reliability of the treatment in achieving recommended WHO standards with the predetermined biomass dosage for an unknown input contaminant concentration. The experimental batch adsorption data were analysed with known isotherms models based on previous literature to find out the mechanism of adsorption replicated by the selected biomass. The experimental data were fitted to the selected isotherm models and the best fit model was obtained through regression. In an actual condition, groundwater source rarely contains only a single heavy metal substance. Usually, it contains several heavy metals or substances. Hence, the experiments were carried out for both single-element as well as multi-element solutions.

3.6.1 Single-element adsorption mathematical model

Adsorption isotherm batch experiments were conducted as described in the previous section. The adsorption data have been subjected to Langmuir (Langmuir, 1916) and Freundlich (Freundlich, 1906) isotherm models. Langmuir and Freundlich models were chosen based on their applicability to describe the behaviour of the adsorption process for a single-element solution using a biomass.

3.6.1.1 Langmuir adsorption model

Langmuir theory assumed that the adsorption process took place on a structurally homogeneous surface of the adsorbent and a set of distinct localised adsorption sites within the natural material. The theory also highlighted that there were no interactions between adsorbate molecules on adjacent sites. Furthermore, the assumption made in this model was that the adsorption layer will be one molecule thick and each of the adsorbent molecules was capable of adsorbing one molecule of adsorbate. The linear form of the Langmuir model is given in Equation 3.1.

$$\frac{C_e}{Q_e} = \frac{1}{Q_m} C_e + \frac{1}{K_L Q_m}$$

Equation 3.1

Where, *Qm* and K_L are the Langmuir constants. *Qm* is the monolayer adsorption capacity (μmol/g), K_L is adsorption constant (L/μmol), C_e is the equilibrium concentration of the heavy metal (μmol/L) and Q_e is the amount of heavy metal adsorbed (μmol/g) calculated as given in Equation 3.2.

$$Q_e = \frac{(C_0 - C_e)V}{m}$$

Equation 3.2

where C_0 is the initial concentration of heavy metal in the solution (μmol/L), *V* is the volume of the solution (L), and *m* is the mass of the biomass used (g). The Q_m and K_L can be determined from the gradient and the intercept of the linear graph between $\frac{C_e}{Q_e}$ and C_e in Equation 3.1.

3.6.1.2 Freundlich adsorption model

The Freundlich isotherm accounts for a multiple sites adsorption for heterogeneous surfaces (Equation 3.3 and Equation 3.4). It assumes that adsorbent has a heterogeneous surface composed of different classes of adsorption sites (Freundlich, 1906).

$$ln\,(Q_e) \;=\; ln\,(K_F) \;+\; (\tfrac{1}{n_F})\,ln(C_e)$$

Equation 3.3

or in linear form:

$$Q_e \;=\; K_F\,C_e^{\frac{1}{n_F}}$$

Equation 3.4

Where, n_F (dimensionless) and K_F (L/mmol) can be determined from the gradient and the intercept of the linear graph between *ln* (Q_e) and *ln* (C_e).

Percentage removal of heavy metal was calculated using Equation 3.5.

$$\%\,Removal = \frac{(C_0 - C_e)}{C_0}\,x100$$

Equation 3.5

where C_0 and C_e are as defined earlier in Equation 3.2 and Equation 3.1, respectively.

3.6.2 Multi-element adsorption mathematical model

As mentioned in Chapter 2 (Section 2.7), there are a number of developed competitive adsorption models available for the evaluation of competitiveness or multi-element adsorption. This includes Sheindorf-Rebhun-Sheintuch (SRS) model (modified Freundlich-type of adsorption model for the multi-element system), competitive

Langmuir model, competitive multi-reaction model, ion-exchange model and the surface complexation model (Selim & Zhang, 2013).

3.6.2.1 Sheindorf-Rebhun-Sheintuch (SRS) model

The SRS model (modified Freundlich model), which is the multi-element adsorption model (Sheindorf et al., 1981) was chosen to evaluate its applicability in predicting the quality of treated water in this study. The model assumptions were the same as those in the single-element Freundlich isotherm model. Some of the required parameters (n_i and k_i) of the SRS model were similar to the predetermined parameters from the single-element Freundlich adsorption model.

Other parameters in the SRS model were obtained from the multi-element adsorption experiments. The assumptions behind the application of this model were: (i) each element follows the Freundlich isotherm model; (ii) each element in the multi-element adsorption present as an exponential distribution of site adsorption energies (Sheindorf et al., 1981).

A general SRS model (Sheindorf et al., 1981) is given by Equation 3.6:

$$q_i = k_i C_i \Sigma (a_{ij} C_j)^{n_i - 1}$$

Equation 3.6

where, q_i is the adsorption of element i per gram (μmol/g); C_i and C_j are the concentrations of elements i and j in the equilibrium solution in (μmol/L); $k_i$and n_i are the Freundlich constants obtained for i in single-element system; and a_{ij} is the competition coefficient for the adsorption of element i in the existence of element j. The three-component isotherm (Sağ et al., 2001) can be written as:

$$q_1 = k_1 C_1 (a_{11} C_1 + a_{12} C_2 + a_{13} C_3)^{n_1 - 1}$$

Equation 3.7

$$q_2 = k_2 C_2 (a_{21} C_1 + a_{22} C_2 + a_{23} C_3)^{n_2 - 1}$$

Equation 3.8

$$q_3 = k_3 C_3 (a_{31} C_1 + a_{32} C_2 + a_{33} C_3)^{n_3 - 1}$$

Equation 3.9

The competition coefficients of the first of three elements can be obtained from the following equations:

$$\frac{C_1}{C_2} = \frac{\beta_1}{C_2} - a_{12} \text{ and } \frac{C_2}{C_1} = \frac{\beta_2}{C_1} - a_{21}$$

Equation 3.10

where $\beta_1 = (\frac{k_1 C_1}{q_1})^{1/(1-n_1)}$ *and* $\beta_2 = (\frac{k_2 C_2}{q_2})^{1/(1-n_2)}$

Equation 3.11

The competition coefficients can be obtained from the intercept of the straight line in the plotting of $\frac{C_1}{C_2}$ against $\frac{\beta_1}{C_2}$. The experimentally determined competitive coefficient can be verified using a_{ij}=$\frac{1}{a_{ji}}$. However, only one of the coefficient (a_{ij} or a_{ji}) is required (Sheindorf et al., 1981).

3.6.3 Verification of adsorption model output

Results from two independent data sets from each tested biomass together with derived Langmuir, Freundlich and SRS model constants were used to verify the model constants obtained in this study from the previous section. The percentage (%) error allowed between the concentrations obtained from experimental and model calculated were used to evaluate the applicability of the selected model as given in Equation 3.12.

$$\% \, Error = \left(\frac{C_{e_{experiment}} - C_{e_{model}}}{C_{e_{experiment}}} \right) x100$$

Equation 3.12

3.7 Predicting treated groundwater quality and assessment of WHO standards exceedance and compliance probabilities

In a laboratory, it was not possible to conduct experiments with a large number of samples while varying concentrations in order to determine the treatment levels using the predetermine biomass dosage. A large number of raw groundwater quality input combinations were generated using Monte Carlo random number generation procedure using Microsoft Excel library. It was assumed that the random numbers generated followed the standard normal distribution (mean zero and a standard deviation of one) as it is widely used in modeling quantitative phenomena in natural sciences (Khan, 2010).

From the adsorption batch tests and the modelling of adsorption isotherms, Freundlich equation (Equation 3.3 and Equation 3.4) performed best in estimating the treatment levels. The Equation 3.13 was obtained by substituting Equation 3.2 into Equation 3.4.

$$\frac{(C_0-C_e)V}{m} = K_F {C_e}^{1/n_F}$$

Equation 3.13

Equation 3.13 could be rewritten as Equation 3.14.

$$0 = K_F {C_e}^{1/n_F} + C_e\left(\frac{V}{m}\right) - C_o\left(\frac{V}{m}\right)$$

Equation 3.14

To obtain the treated groundwater quality (C_e), the above non-linear equation (Equation 3.14) was solved by using Solver tool in Excel. 1000 random concentration values were generated for each of target contaminant. An example of the written Macro Visual Basic program is depicted in Figure 3.3.

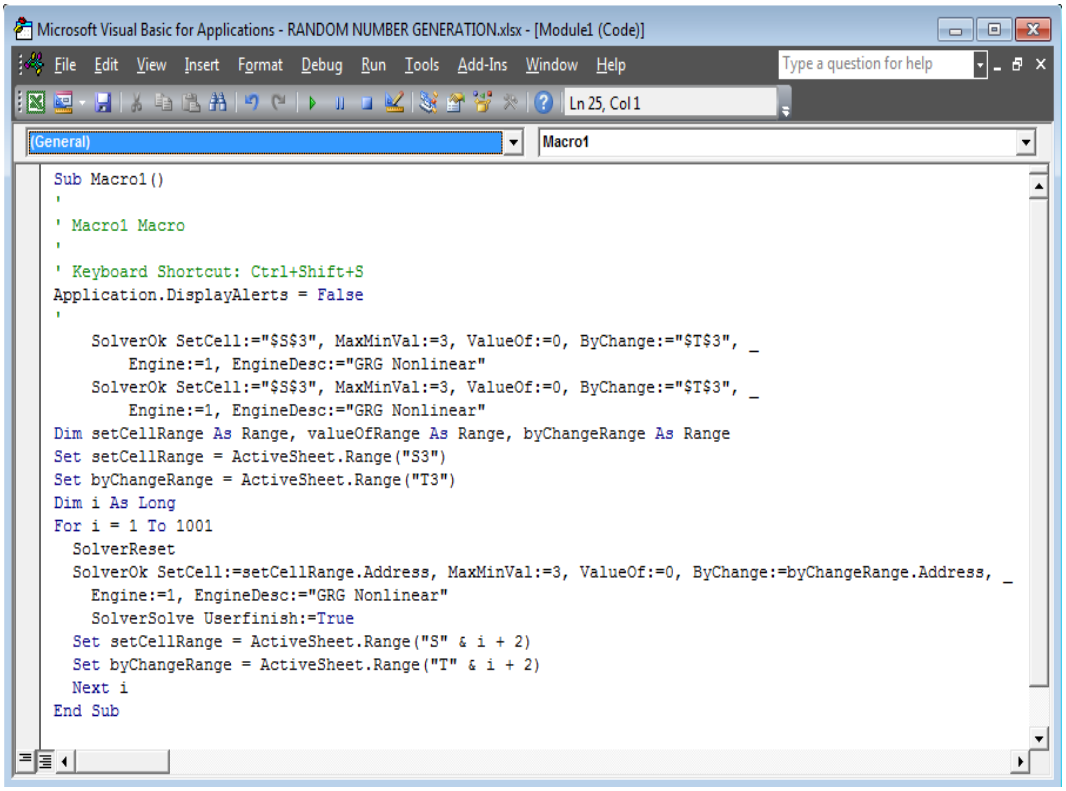

Figure 3.3 Example of Macro Visual Basic Editor for solving non-linear equation

The Solver application was incorporated into the Macro Visual Basic Editor tool in Microsoft Excel. Schmidt et al. (2013) also adopted this method for quantitative microbial risk assessment.

3.7.1 Random number generation for simulating input groundwater quality

It was a time-consuming process to predict the final concentration of target contaminants for a large number of samples (i.e. 1000 samples) after being treated by specific biomass. Therefore, a large number of raw groundwater quality input was generated using the Microsoft Excel. Mean and standard deviation were required to generate the random numbers. Normal-type distribution was selected for the samples distribution in this study because it is widely used in modeling quantitative phenomena in natural sciences (Khan, 2010).

The generated data set was presented by using probability density function (PDF) and cumulative density functions. Both functions were generated directly using Microsoft Excel. The n^{th} percentile of the treated samples was calculated by sorting the values in the data set from smallest to largest. The n^{th} percentile was determined using the function of [=PERCENTILE (array, n^{th} percentile)] in Microsoft Excel. Array was a range from which the n^{th} percentile intended to be calculated and n^{th} percentile was the percentile value which can be a value between zero and one.

3.7.2 Uncertainty analysis

Uncertainty analysis was carried out to measure the level of precision and random error. Uncertainty range was defined as the ratio between the 95% percentiles of the upper and lower limit of the target concentrations (Smeets & Medema, 2006). Therefore, the mean (μ), variance (σ^2), standard deviation (σ), count (N, number of sample), degree of freedom ($d.f.$), confidence level (α), critical-t (t_c =1.962 for α = 95%) standard error, lower limit and upper limit were required prior to the determination of the uncertainty range.

3.7.3 Probabilities of exceedance and compliance of WHO drinking water quality standards

The C_e value obtained by solving Equation 3.14 provided the final treated groundwater quality with the predetermined biomass dosage. Probability of exceeding WHO standards can be defined by the percentage of samples that fail to be treated adequately by the proposed treatment as to meet the recommended standard limit. In this study, WHO drinking water quality standard was referred as a standard value for the probability of exceedance calculations. To calculate the specific probability of exceedance, the output of 1000 predicted treated heavy metal-contaminated

groundwater was sorted from the highest to the lowest in a single column using the Microsoft Excel. The largest value was then ranked as one, the second largest value as two and so on, until each of the value has a rank. Then, the rank of WHO standard limit value associated with the specific contaminant was determined as the value for which the exceedance probability desired to be calculated. After that, the rank of the standard value was plugged into the formula as shown in Equation 3.15 to yield the exceedance probability (expressed in percentage). Alternatively, the understanding associated with the treatment efficiency was also represented by the WHO drinking water quality standard compliance probability. It is the inverse form of exceedance probability.

$$Exceedance\ probability = \frac{rank\ of\ the\ standard\ value}{total\ number\ of\ values + 1} x100$$

Equation 3.15

3.8 Cost estimation

Cost estimation was carried out to provide an understanding of the potential costs involved in the proposed treatment process. Thus, affordability of the proposed treatment process was confirmed as it was proposed to be used by rural communities in developing countries. Cost estimation was carried out by collecting related information regarding the cost of the materials used in this study from relevant sources. In this study, the costs of treatment with MO, MC, MO+MC, and alum were evaluated and compared.

CHAPTER 4 Application of plant-based materials in removing heavy metals, fluoride and turbidity from synthetic and actual groundwater samples

This chapter investigates the effectiveness of plant-based materials in removing heavy metals, fluoride and turbidity from contaminated groundwater. It is claimed by Nguyen et al. (2013) that the removal efficiency by different types of plant-based material may vary significantly. It means that plant-based material tends to remove some contaminants more effectively than others. For example, cadmium removed by banana peel and lemon peel at 87% and 57% removal efficiency, respectively (Kelly-Vargas et al., 2012). This effectiveness could be attributed to the variation in functional groups on the biomass' surface. Specific functional groups of atoms or bonds within molecules are responsible for the distinctive chemical reactions of those molecules. Different biomass types have different active functional groups which correspond to the affinity of one contaminant to another (Nguyen et al., 2013). Thus, it is important to investigate the variation of the treatment performance of each selected material in treating various target contaminants and their specific mechanism of removal. As discussed in Chapter 2, arsenic (As), lead (Pb), nickel (Ni), cadmium (Cd) and fluoride were selected as the target contaminants in the current study. Also, treatment efficacy of plant-based materials in treating turbidity was investigated to discover whether the selected biomass could treat the groundwater samples that might contain organic matters especially for the groundwater that is not properly withdrawn from its source. The best treatment was chosen by taking into account the capability of the materials in meeting the WHO drinking water quality standards for all target contaminants. *Moringa oleifera* (Moringa seeds, MO), *Cicer arietinum* (chickpeas, CA), *Musa cavendish* (banana peel, MC), *Cocos nucifera* (coconut's solid endosperm,

CN) and *Lentinus edodes* (Shiitake mushroom, LE) were chosen to be tested in this study as they have been reported to have a promising capability in removing target contaminants (as described in Chapter 2). In this chapter, the effectiveness of plant-based materials in treating target contaminants was investigated at preselected target contaminant concentrations. Effect of treatment by the selected biomass on pH of the samples after the treatment process was also investigated followed by determination of optimum dose of biomass and biomass dosing method for the removal of target contaminants. Furthermore, the performance of the selected biomass/dosing method at optimum conditions on actual groundwater samples to ensure its applicability in real field conditions was also investigated. Final part of this chapter reports the investigation on the pre-treatment of biomass with acid, base and thermal treatment to assist removal of problematic contaminants such as As and fluoride. Besides, the use of alum with considerably low dosage also has been investigated to ensure that these problematic contaminants can be removed from the drinking water in cases where contaminants had exceeded the World Health Organisation (WHO) standards.

4.1 Effectiveness of plant-based materials in removing heavy metals, fluoride, and turbidity from multi-element synthetic groundwater samples

Initially, the experiments were carried out to examine the performance efficiency of *Moringa oleifera* (MO), *Cicer arietinum* (CA), *Musa cavendish* (MC), *Cocos nucifera* (CN) and *Lentinus edodes* (LE) in treating synthetic groundwater samples. Experiments were conducted to determine the treatment efficiency of plant-based materials at preselected initial target contaminants concentrations (Table 3.1). The initial concentrations of target contaminants in the synthetic groundwater samples

were selected based on their range of concentrations detected in groundwater as reported in the literature (Table 2.1).

Initially, MO, CA, MC, CN and LE were tested and the most effective biomass from these five selected biomass types were chosen for further study. The biomass dose varied between 10 to 100 mg/L. Each experiment was triplicated and the average values were reported with the error bars representing the standard deviations (<10%). Based on the obtained experimental results, initial concentrations of the contaminants were reduced to the lower values within the range of concentrations of contaminants as reported in the literature (Table 2.1). Later in the study, biomass were limited only to MO, MC and CN. Experiments were also conducted by dosing with MO and MC together and dosing sequentially. The dose of biomass was increased to 200 mg/L for single biomass and 400 mg/L (200:200 mg/L) for combined biomass.

4.1.1 Experimental results from the multi-element solution

4.1.1.1 Lead (Pb) removal

Figure 4.1a shows that there was a significant reduction in Pb concentration when treated with all selected biomass when the biomass dose was increased from 50 to 100 mg/L. However, none of the biomass were successful in removing pollutants meeting the WHO standard recommended for Pb (10 µg/L). The lowest final concentration for Pb (53.6 µg/L) was recorded for treatment with 100 mg/L of MC.

Figure 4.1b demonstrates that the range of Pb percentage removal was increased as the biomass dose increased from 10 mg/L (removal efficiency: 5% to 9%) to 100 mg/L (removal efficiency: 50% to 57%). It is encouraging to see that the selected biomass had the potential of reducing Pb concentration up to 57% from its initial concentration

of 125.0 µg/L. This finding suggests that the removal efficiency of target contaminants may be further improved by increasing the biomass dosage.

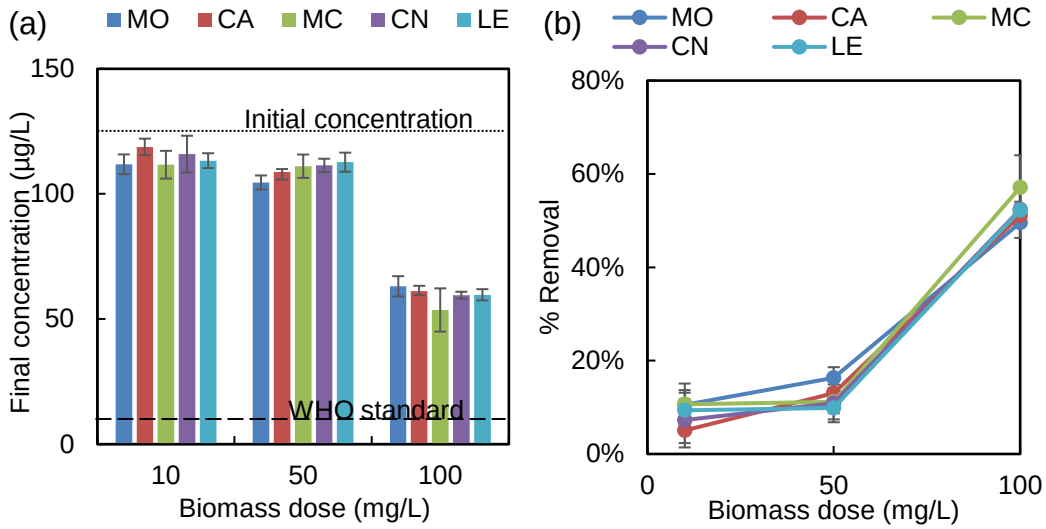

Figure 4.1 (a) Pb final concentrations and (b) Pb removal efficiencies achieved by MO, CA, MC, CN and LE at initial high Pb concentration of 125.0 µg/L (multi-element solutions)

Anwar et al. (2010) used 40 g/L of MC biomass to successfully achieve 85% of Pb removal at pH of 5 with an initial concentration of 50 µg/L. 40 g/L is a relatively high dose compared to the maximum biomass dose deployed for the current study (100 mg/L). A high biomass dose could generate more sludge at the end of the treatment process which needs to be avoided if possible. Furthermore, the pH value of 5 could be another reason for the success in Pb removal from the aqueous solution. In the present study, pH was maintained at natural conditions to minimise the additional cost associated with chemicals for pH adjustment.

4.1.1.2 Nickel (Ni) removal

Figure 4.2 (a&b) present the final concentrations of Ni after being treated with MO, CA, MC, CN, and LE. The following figures exhibit no significant difference of Ni removal efficiency when the biomass dose was increased from 10 to 50 mg/L. Similar

to Pb, removal efficiency of Ni was increased markedly when the dose of biomass was increased from 50 to 100 mg/L for MO, CA, MC and CN. It is interesting to see that Ni removal has declined dramatically when increasing the dose of LE from 50 to 100 mg/L (Figure 4.2b). The reason could be due to the saturation of available binding sites on the biomass (Kumar et al., 2012). This finding suggests that MO, CA, MC and CN had the potential of removing Ni concentration up to 45% from its initial concentration of 112.0 µg/L.

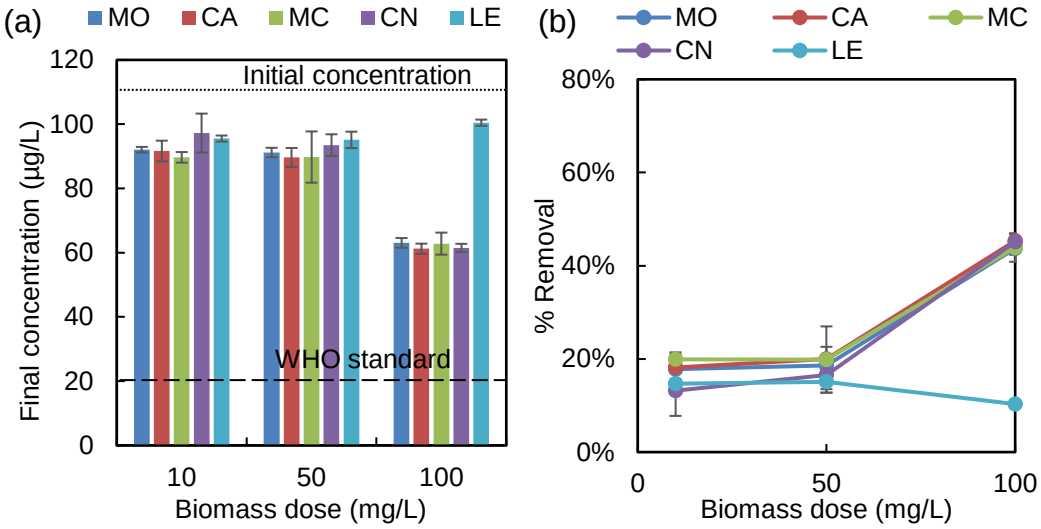

Figure 4.2 (a) Ni final concentrations and (b) Ni removal efficiencies achieved by MO, CA, MC, CN and LE at initial high Ni concentration of 112.0 µg/L (multi-element solutions)

4.1.1.3 Cadmium (Cd) removal

Figure 4.3 (a&b) depict that the slight reduction in final concentrations and removal efficiencies of Cd for all tested biomass as the biomass dose was increased from 10 to 100 mg/L. The lowest final concentration of 9.5 µg/L was achieved with MC from its initial concentration level of 11.7 µg/L. The range of removal efficiencies of Cd was increased with the increase of biomass dose from 10 mg/L (2% to 9%) to 100 mg/L (11% to 18%). MC and CN showed the highest removal of Cd (18%). None of the

biomass with a dose of up to 100 mg/L can meet the WHO standard recommended for Cd, that is 3 µg/L.

Sharma et al. (2006) reported that 85% removal of Cd from a high initial concentration of Cd (25 mg/L) with MO as the biomass. However, the dose of MO was 20 g/L and the study was conducted at pH of 6.5. Furthermore, Anwar et al. (2010) removed 89% of Cd from its initial concentration of 50 µg/L by using MC with a dose of 30 g/L and at a lower pH of 3. Both of the studies above applied much higher biomass doses compared to the one applied in the current study, and the latter was conducted at much lower pH values. The purpose of this research is to reduce the cost involve in the treatment process. High dose of biomass that usually applied in the treatment created high volume of sludge at the end of treatment process. Also, high dose of biomass also does not necessarily promise the improvement of the removal contaminants in some cases due to saturation of binding sites on the biomass surface. As mentioned earlier in the current study section, the pH adjustment was avoided to minimise the additional costs required for chemicals used for pH adjustments.

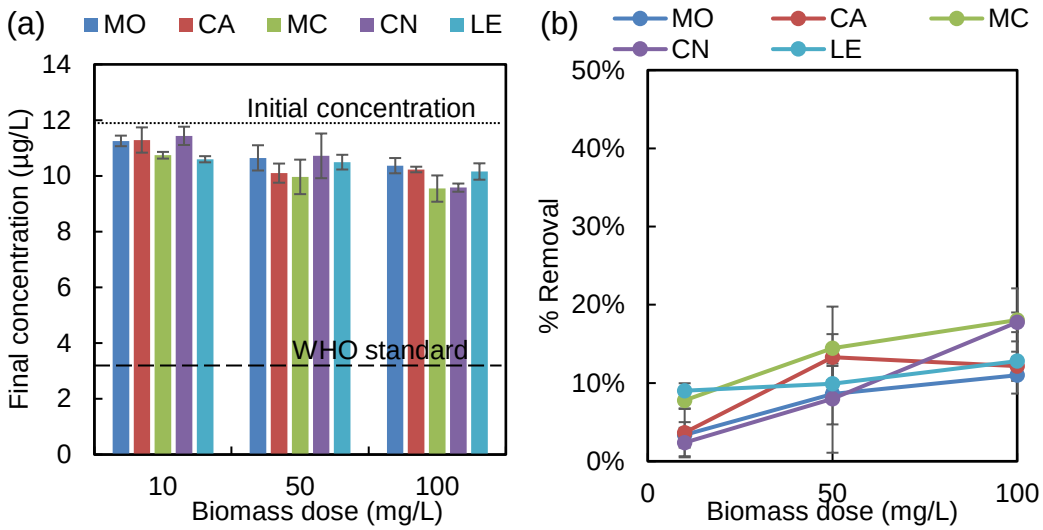

Figure 4.3 (a) Cd final concentrations and (b) Cd removal efficiencies achieved by MO, CA, MC, CN and LE at initial high Cd concentration of 11.7 µg/L (multi-element solutions)

4.1.1.4 Arsenic (As) removal

Figure 4.4a presents the final concentrations of As after being treated with MO, CA, MC, CN and LE. Surprisingly, no significant reduction in As concentration was found for all biomass. The results indicate that the biomass were not capable of meeting the WHO standard for As of 10 µg/L with the tested biomass dosage range (10 to 100 mg/L).

Furthermore, Figure 4.4b shows that there were insignificant variations of treatment efficiency achieved by all biomass in treating As. It can also be seen from the figure that the As reductions were slightly increased with the increase of biomass dose from 10 to 100 mg/L. The highest removal was achieved by all biomass at 100 mg/L. Nonetheless, there was only a slight difference between the maximum and minimum removal efficiencies demonstrated by MC (13%) and LE (10%) respectively. These results suggest that the biomass used were ineffective in removing As or the biomass dosage was too low compared to the As initial concentration of 656 µg/L.

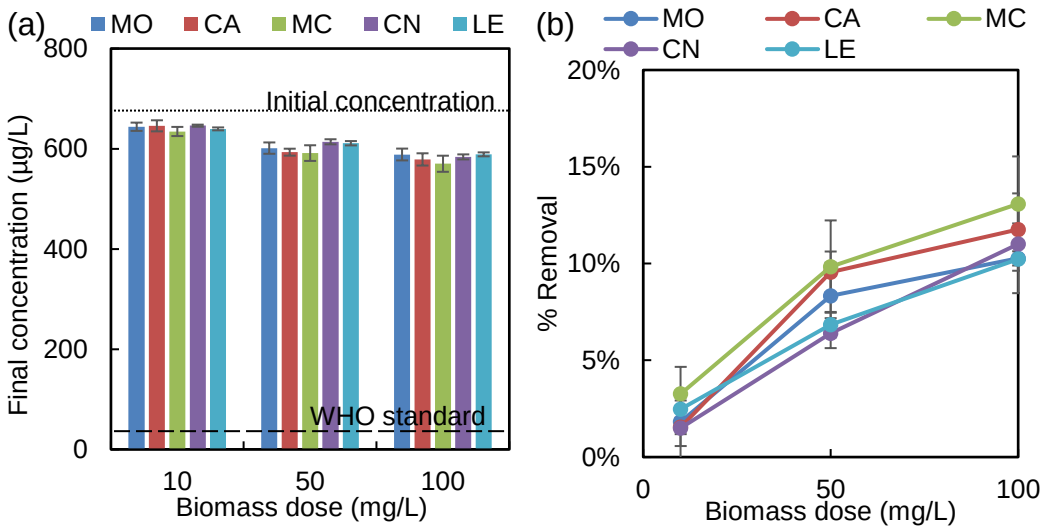

Figure 4.4 (a) As final concentrations and (b) As removal efficiencies obtained by MO, CA, MC, CN and LE at initial high As concentration of 655.9 µg/L (multi-element solutions)

According to the author's knowledge, there were no similar studies carried out to treat As with a similar initial concentration as conducted in this study except for the study reported in Kumari et al. (2006). This study had been carried out for As with the initial concentration of 1 mg/L; which is greater than that applied in the present study and it has achieved a 32% of arsenic removal with 2.5 g/L of MO at pH of 7.5 (Kumari et al., 2006). The result proved that even with a higher MO dose of 2.5 g/L, the As removal efficiency achieved was quite low.

4.1.1.5 Fluoride removal

Figure 4.5 (a & b) depicts the final concentrations and removal efficiencies of fluoride with all tested biomass. As the biomass dose increased from 10 to 100 mg/L, the reduction of fluoride remained almost unchanged except with MO. The final concentration of fluoride was reduced from 14.0 mg/L to 10.6 mg/L with 100 mg/L of MO. However, this concentration was still higher than the recommended WHO standard of 1.5 mg/L for fluoride.

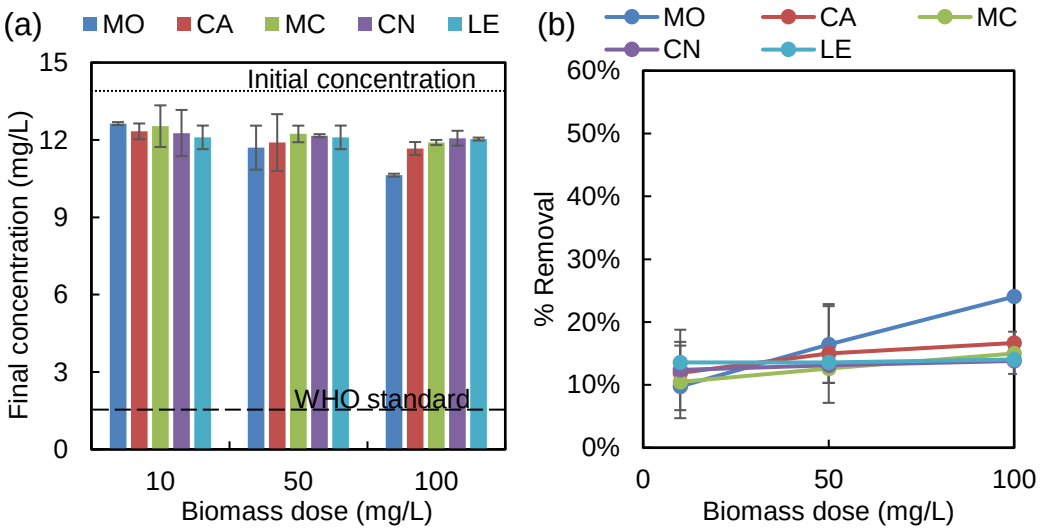

Figure 4.5 (a) Fluoride final concentrations and (b) fluoride removal efficiencies achieved by MO, CA, MC, CN and LE at initial high fluoride concentration of 14.0 mg/L (multi-element solutions)

Figure 4.5b exhibits that the removal efficiencies of fluoride achieved by all tested biomass were below 30%. Unlike other biomass, MO showed the potential of reducing fluoride as the biomass dose increased. This result indicates that there is potential to improve removal efficiency of fluoride by increasing the dose of biomass.

Bazanella et al. (2012) reported that MO achieved 91% removal of fluoride with a biomass dose of 2.5 g/L at pH of 5.5. A high removal efficiency was achieved due to very high dose of biomass at a low pH value. This condition results in higher volume of sludge at the end of the treatment process and additional costs related to pH adjustment. It is important to re-iterate the overall objective of this study to come up with a low-cost drinking water treatment solution to be used by the rural community in developing countries, hence, avoiding the use of chemicals to correct pH.

4.1.1.6 Turbidity removal

Compared to the other contaminants, the behaviour of turbidity removal varies with the type biomass used. It can be seen from Figure 4.6a that there was a variation in the final concentrations of turbidity after its treatment with the tested biomass. It is evident that 100 mg/L of MO dose can successfully removed the turbidity to meet the recommended WHO standard of 5 NTU with a final turbidity concentration of 2.7 NTU. The removal efficiency of MO improved markedly from 45% to 93% with the increase of biomass dose from 10 to 100 mg/L. The findings of the current study are consistent with those reported in the literature (Pritchard et al., 2010; Sengupta et al., 2012). The authors above have claimed that MO is effective in the removal of turbidity from water. The biomass MC, CN and LE also acted positively by improving the removal efficiency with the increase in biomass dose from 10 to 100 mg/L. On the other hand, CA showed its limited ability in removing turbidity at an optimum biomass

dose of 50 mg/L (Figure 4.6b). In the case of CA, it is inferred that biomass such as CA can also be referred as organic matter. Therefore, there is possibility if it is introduced to the water with a substantial amount (i.e., more than 100 mg/L), it could create extra turbidity to the water. The other reason could also be due to the lower availability of number of active functional groups which affects affinity of CA towards kaolin (turbidity).

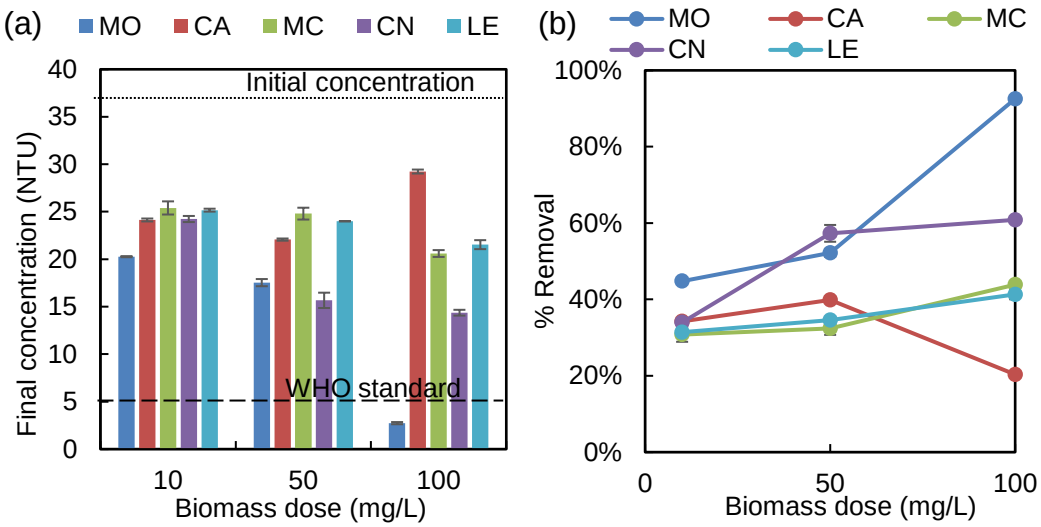

Figure 4.6 (a) Turbidity final concentrations and (b) turbidity removal efficiencies achieved by MO, CA, MC, CN and LE at initial high turbidity concentration of 36.7 NTU (multi-element solutions)

4.1.2 Preliminary selection of effective plant-based materials for further investigations

Based on the above-mentioned initial experimental results, the removal rate of pollutants were still improving at the maximum biomass dose of 100 mg/L. In most of the experiments, the optimum biomass dose for pollutant removed had not been reached. Figure 4.7 depicts the removal efficiencies of all contaminants with tested biomass dose at 100 mg/L.

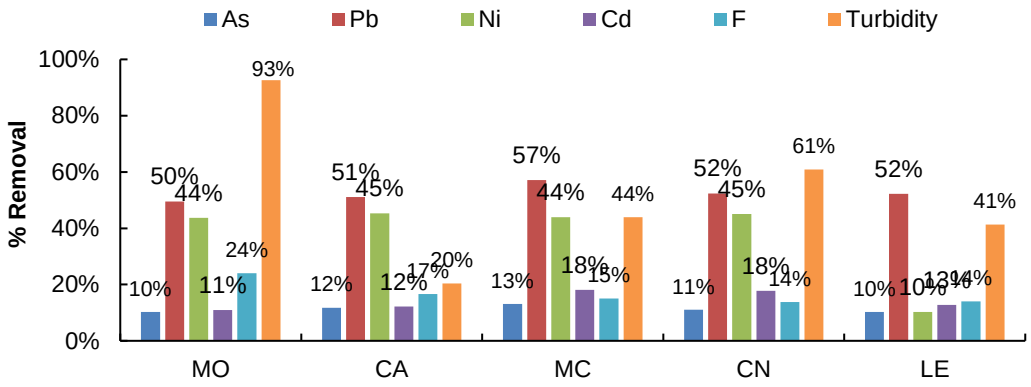

Figure 4.7 Removal efficiency of selected biomass for the removal of As, Pb, Ni, Cd, F and turbidity at the highest tested biomass dose of 100 mg/L

From the figure, MO showed the highest removal efficiency of 93% for turbidity. Apart from that, MO also removed 50% and 44% of Pb and Ni respectively. Similarly, relatively high removal rates for Pb, Ni and turbidity were obtained from MC and CN as well. It has been decided that CA and LE were to be excluded from further experiments due to their limited capability in removing turbidity and Ni, respectively, as their removal efficiencies were incrementally reduced when the biomass dose increased. This behaviour could be attributed to the saturation of binding sites on the biomass surface for the retention of the above contaminants (turbidity and Ni).

The removal of turbidity and Ni by CA and LE, respectively achieved their limitations due to the competition of these contaminants with other contaminants that were present in the same sample (multi-element solution).

The findings from the initial set of experiments demonstrated that all selected biomass with predetermined doses were ineffective (except for turbidity when MO dose was 100 mg/L) to remove pollutants to meet WHO standards from the synthetic groundwater samples. The concentrations of the above synthetic groundwater samples

were obtained from the literature, where the highest was recorded in different countries.

Therefore, it was decided to redo a batch of experiments with a synthetic groundwater sample containing lower concentrations of contaminants with an expectation that the selected biomass will be effective in treating the water to reduce concentrations of contaminants to WHO recommended standards.

It was also decided to exclude CA and LE from further testing as these biomass demonstrated limited capacity in removing target contaminants, especially for As, Ni and turbidity. Furthermore, it was also decided to increase the biomass doses up to 200 mg/L, as the maximum biomass dose used (100 mg/L) did not reach the optimum removal.

4.1.3 Experimental results from a multi-element solution with lower initial concentrations of target contaminants

The concentrations of target contaminants in the synthetic groundwater sample were reduced to lower levels as it was demonstrated that the selected biomass with predetermined dosages were ineffective at earlier initial concentrations of contaminants. The earlier initial concentrations of contaminants (As: 656 µg/L, Pb: 125 µg/L, Ni: 112 µg/L, Cd: 12 µg/L, fluoride: 14 mg/L and turbidity: 37 NTU) were selected based on the high recorded values in the literature (within the range of the reported concentrations of contaminants) as reported in the literature (Table 2.1).

However, in this batch of experiments, the concentrations of target contaminants were reduced to the lower concentrations (As: 40 µg/L, Pb: 40 µg/L, Ni: 29 µg/L, Cd: 5

µg/L, fluoride: 3.5 mg/L and turbidity: 15 NTU) (within the range of the reported concentrations of contaminants) as reported in the literature (Table 2.1).

As mentioned earlier in Chapter 3, a combination of MO and MC was introduced at this stage of the study, intending to improve the treatment efficiency. In addition to that, the biomass dose was also increased up to 200 mg/L to determine the optimum dose of biomass. It is noteworthy that the dose applied for combined biomass (MO+MC) was used in the ratio of 1:1. For example, 200 mg/L dose of MO+MC means that 100 mg/L of MO was dosed concurrently with 100 mg/L of MC. Thus, the combined total dose for MO+MC is 200 mg/L.

4.1.3.1 Lead (Pb) removal

Figure 4.8 (a&b) depicts the final concentrations and removal efficiencies of Pb after being treated with the selected biomass. Treatment with MC and combined biomass (MO+MC) were quite different when compared to the treatment with MO and CN as they showed a steady increase in the removal of Pb when the biomass dose was increased from 10 to 200 mg/L.

On the other hand, MO and CN showed a significant removal of Pb when the biomass dose was increased from 50 to 100 mg/L and had further improved at biomass dose of 200 mg/L. However, none of the biomass could reduce the Pb concentration to meet the recommended WHO standard of 10 µg/L although the initial concentration of Pb was reduced from 125 µg/L (previous batch) to 39.6 µg/L (recent batch).

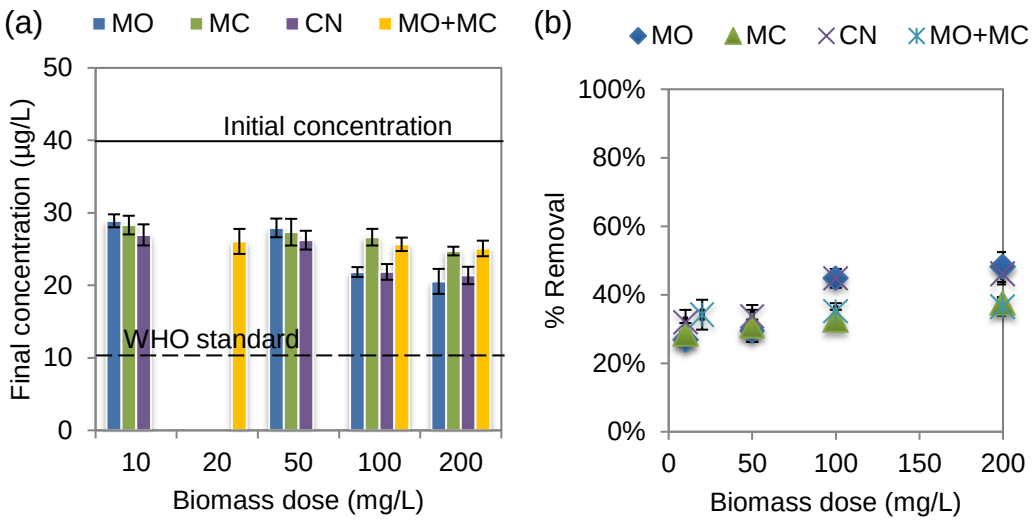

Figure 4.8 (a) Pb final concentrations and (b) Pb removal efficiencies achieved by MO, MC, CN and MO+MC at initial low Pb concentration of 39.6 µg/L (multi-element solutions)

This finding revealed that MO+MC was ineffective to improve the Pb treatment efficiency as it produced results almost similar to that of the individual MC's. The removal of Pb by MO+MC was less than that achieved by single MO. This could be due to the overlapping of binding sites between MO and MC when they were combined, thus, reducing the number of available binding sites for the retention of Pb.

4.1.3.2 Nickel (Ni) removal

It can be seen in Figure 4.9a that MO has successfully reduced the Ni concentration to below 20 µg/L (recommended WHO standard for Ni) at the biomass dose of beyond 100 mg/L. Furthermore, CN was also capable of meeting the recommended WHO standard at a biomass dose of 200 mg/L. On the other hand, MC and MO+MC were unsuccessful in meeting the standard across the tested biomass doses.

Figure 4.9b shows a significant improve in Ni removal from 19% to 34% when the MO biomass dose was increased from 50 mg/L to 100 mg/L. However, there was no further increase in the removal of Ni when the biomass dose was increased to 200

mg/L. Other biomass showed improvement in Ni removal as the biomass dose was increased from 10 to 200 mg/L for individual biomass (i.e. MC and CN) and from 100 to 200 mg/L for combined biomass (MO+MC). The optimum dose of MO for removal of Ni was 100 mg/L, while for MC, CN and MO+MC, the optimum biomass doses were still not achieved.

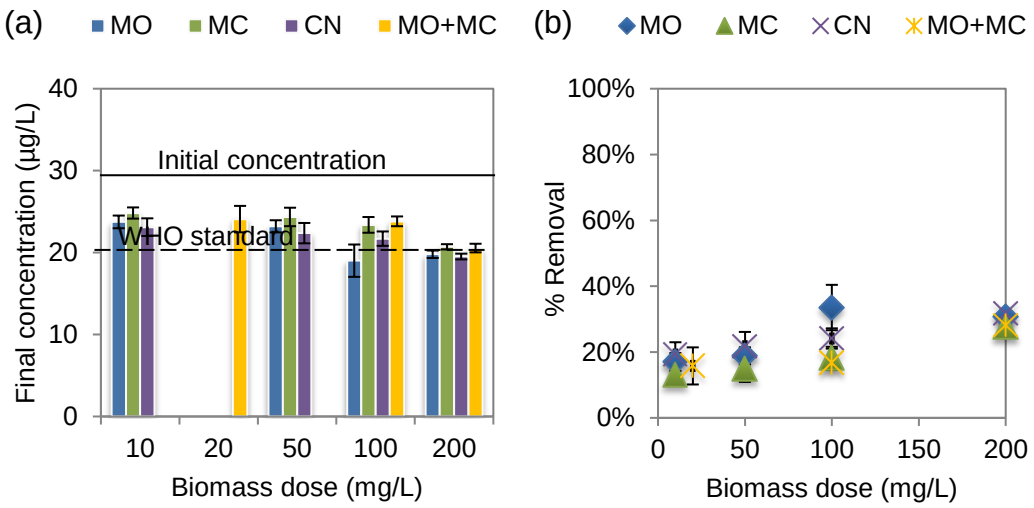

Figure 4.9 (a) Ni final concentrations and (b) Ni removal efficiencies obtained by MO, MC, CN and MO+MC at initial low Ni concentration of 28.6 µg/L (multi-element solutions)

4.1.3.3 Cadmium (Cd) removal

Figure 4.10a shows that MO+MC is capable of reducing Cd concentrations to just above the recommended WHO standard of 3 µg/L for Cd at the biomass dose of 100 mg/L and above. On the other hand, Cd concentrations were reduced steadily by MO and MC when the biomass dose was increased from 10 to 200 mg/L. Cd did not reduce to the recommended WHO standard when the CN dose was increased from 10 to 200 mg/L. Furthermore, the reduction levels were the same when the CN doses were 100 and 200 mg/L respectively. This finding concludes that CN has reached its optimum

dose and is not an effective material for Cd removal at the initial Cd concentration of 5.1 µg/L.

It can be observed from Figure 4.10b that MO+MC possesses the highest removal of 39% at the biomass doses of 100 mg/L (50:50 mg/L) and 200 mg/L (100:100 mg/L) respectively. MO showed a significant improvement (24% to 34%) of Cd removal when the biomass dose was increased from 10 to 50 mg/L. However, the removal rate had increased only by 2% when the MO dose was increased to 200 mg/L. It is evident from Figure 4.10 that the Cd removal remained unchanged across the tested CN doses.

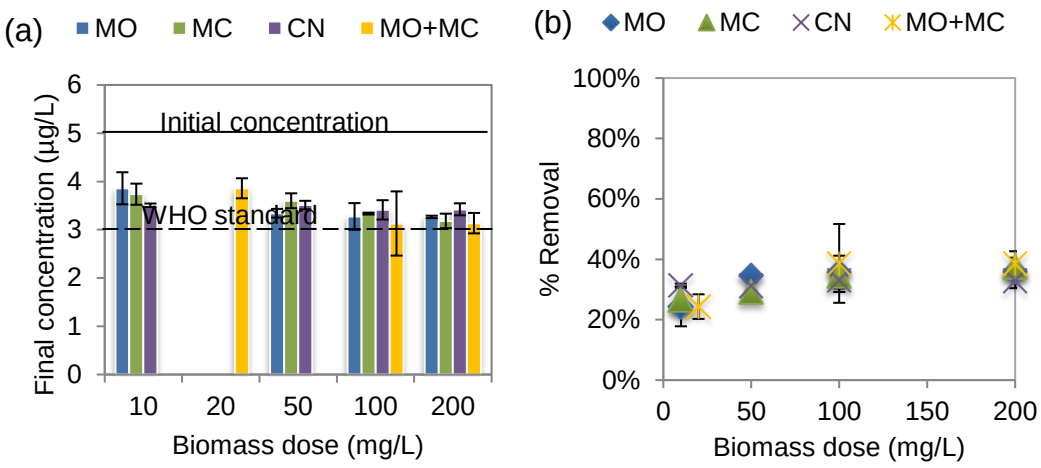

Figure 4.10 (a) Cd final concentrations and (b) Cd removal efficiencies achieved by MO, MC, CN and MO+MC at initial low Cd concentration of 5.1 µg/L (multi-element solutions)

4.1.3.4 Arsenic (As) removal

Figure 4.11 (a&b) depicts the final concentrations and the removal efficiencies of As after being treated with MO, MC, CN and MO+MC. It can be seen from the figure that the As concentrations reduced gradually as the biomass dose was increased from 10 to 200 mg/L. However, it was not possible to achieve the WHO standard of 10 µg/L recommended for As with the selected biomass range.

Based on above results, it is inferred that the initial As concentration in the synthetic groundwater sample could still be too high for these biomass to effectively treat the water or the maximum biomass dose applied at this stage of the study could be insufficient to reduce the As concentration below the As WHO drinking water standard of 10 µg/L.

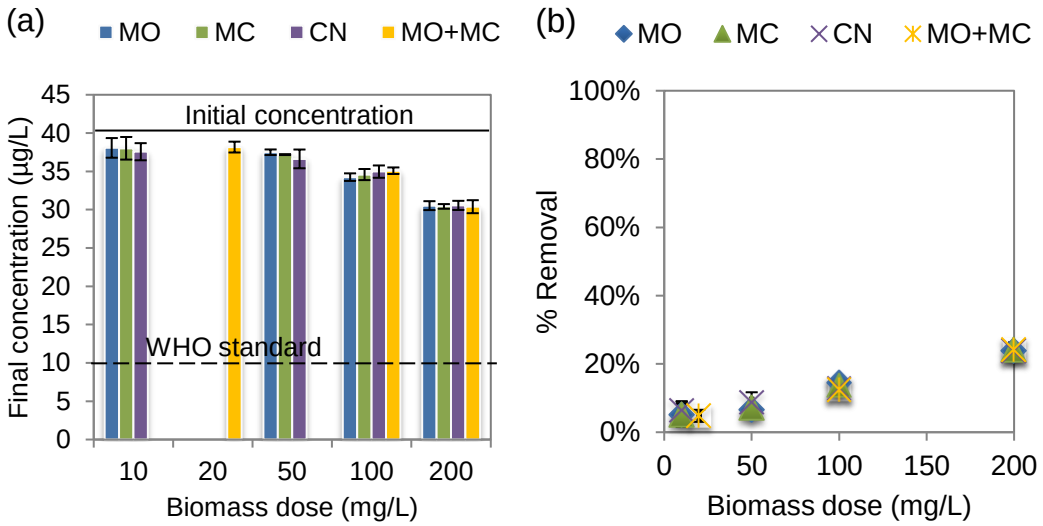

Figure 4.11 (a) As final concentrations and (b) As removal efficiencies achieved by MO, MC, CN and MO+MC at initial low As concentration of 40.1 µg/L (multi-element solutions)

4.1.3.5 Fluoride removal

Figure 4.12a shows that none of the biomass were successful in reducing fluoride concentrations to meet the WHO standard recommended for fluoride of 1.5 mg/L. However, combined biomass (MO+MC) showed a potential for fluoride removal as the removal efficiency increased from 21% to 48% when biomass dose was increased from 100 mg/L to 200 mg/L respectively.

Figure 4.12b demonstrates similar fluoride removal trends by using MO and MC with both biomass showing effectiveness (26 % to 35%) but not meeting the recommended WHO standard for fluoride. The optimum MO and MC doses were between 50 to 100

mg/L. On the other hand, fluoride removal had drastically increased when the CN biomass dose was increased from 50 to 100 mg/L. However, the fluoride removal had reduced when the biomass dose further increased to 200 mg/L, maintaining the optimum conditions at 100 mg/L.

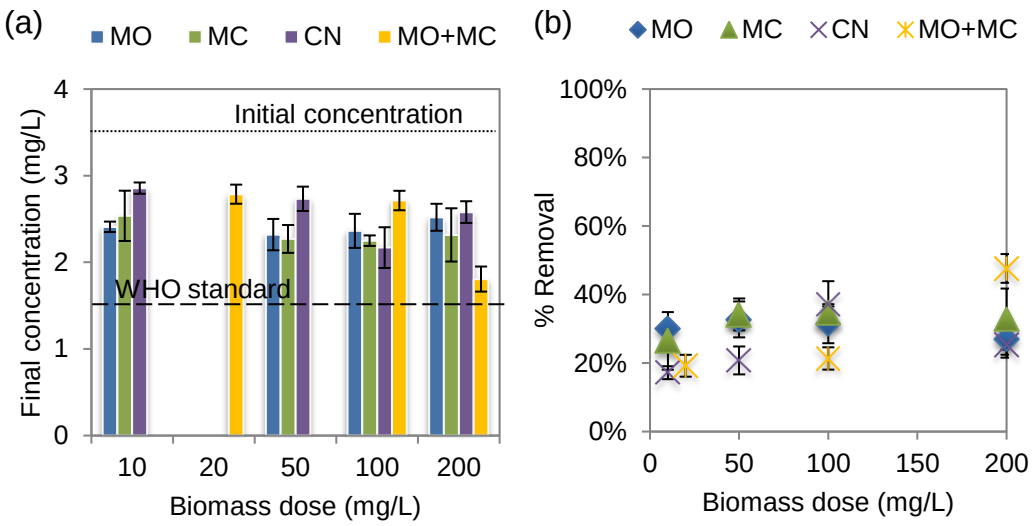

Figure 4.12 (a) Fluoride final concentrations and (b) fluoride removal efficiencies achieved by MO, MC, CN and MO+MC at initial low fluoride concentration of 3.5 mg/L (multi-element solutions)

4.1.3.6 Turbidity removal

The most striking results to emerge from Figure 4.13a is that the MO showed an excellent turbidity removal at the biomass doses of 100 mg/L and 200 mg/L with final turbidity concentrations of 0.6 and 0.5 NTU, respectively. These concentrations were below the recommended WHO standard of 5 NTU for turbidity. On the other hand, although MC, CN and MO+MC decreased turbidity levels as the biomass dose was increased from 10 to 200 mg/L, the efforts were unsuccessful in meeting the turbidity standard recommended by the WHO.

Figure 4.13b shows that turbidity removal by MO boosted from 53% to 96% when the MO dose was increased from 50 mg/L to 100 mg/L. However, the turbidity removal

increased only by 1% when the MO dose was further increased to 200 mg/L. Similar to MO, CN also showed a significant increase of turbidity removal (36% to 56%) when the CN dose was increased from 10 to 50 mg/L. However, the removal of turbidity remained unchanged when the CN dose was further increased to 200 mg/L. Kumar et al. (2012) attributed this behavior to the saturation of adsorption sites on biomass surface. MC and MO+MC showed an almost similar trend of turbidity removal at the biomass doses of 100 mg/L and 200 mg/L.

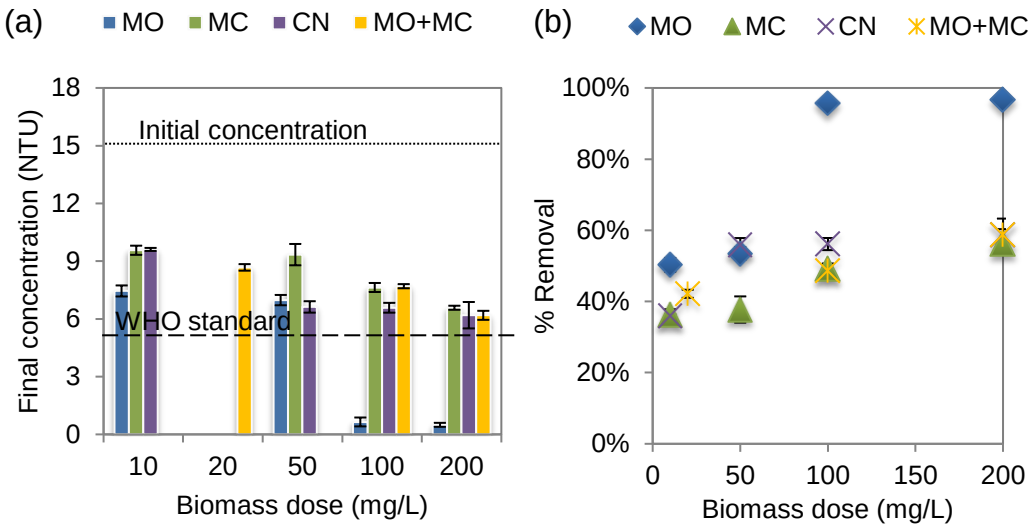

Figure 4.13 (a) Turbidity final concentrations and (b) turbidity removal efficiencies achieved by MO, MC, CN and MO+MC at initial low turbidity concentration of 15.0 NTU (multi-element solutions)

4.1.4 Effect on pH

Figure 4.14 shows the impact of treatment with MO, MC, CN and MO+MC on the pH of treated multi-element synthetic groundwater samples. It can be seen from the figure that the pH of the treated samples varied only between 6.4 and 7.0 from their initial pH of 7.0 (before treatment).

The recommended pH range of the WHO drinking water quality standard is between 6.5 and 8.5. The pH values of the synthetic groundwater samples that were treated

with MO at a dose of 50 mg/L was 6.4. The rest of the treated samples were within the WHO standards. Unlike typical chemical agents in water treatment, plant-based materials did not significantly affect the pH of the treated water. This result highlights that the use of chemicals for pH adjustments after treatment can be avoided. Furthermore, the overall treatment cost can be reduced by not using expensive chemicals. This finding is an added benefit to the people living in remote areas in developing countries that are economically disadvantaged.

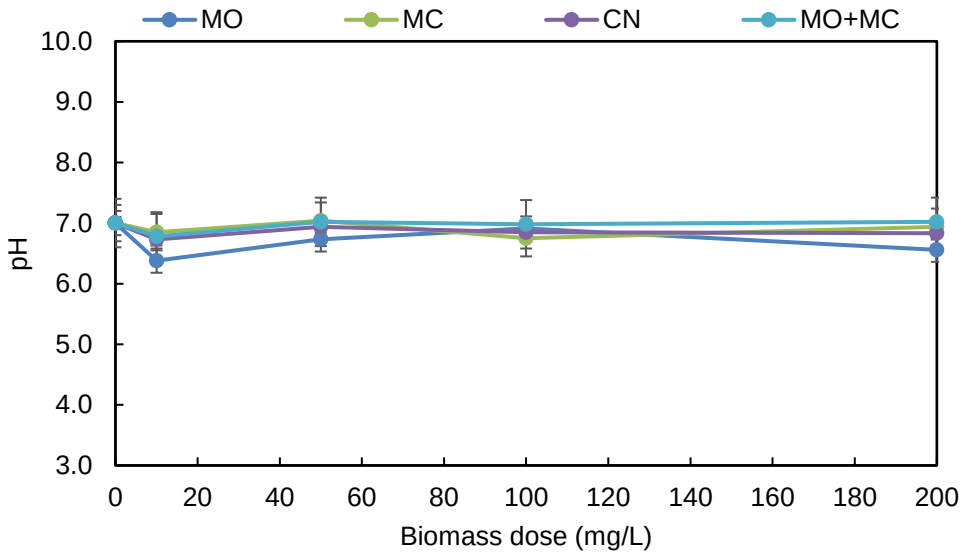

Figure 4.14 Effect of treatment with MO, MC, CN and MO+MC on the pH of treated samples in multi-element solutions

Based on the results from this section, it was shown that CN is ineffective in removing Cd, F and turbidity at selected initial concentrations to meet the WHO standards from multi-element solutions. Also, the interaction between contaminants in the multi-element solutions might have an influence on the removal of some contaminants by the selected biomass. The interactions could be (i) mutual interference between the contaminants which could lead to the improvement of removal rate or (ii) competition between the contaminants which could lead to the reduction in the removal rate. From

the findings, it was also found that As and fluoride were unable to be reduced to meet the WHO standards by the tested biomass.

4.2 Determination of optimum dose and biomass dosing method for heavy metals, fluoride and turbidity from single-element synthetic groundwater samples

It was decided to conduct the experiments in single-element solutions to eliminate the possible interactions between the multiple elements present in the same system. All experiments were performed with synthetic groundwater samples containing As, Pb, Ni, Cd, fluoride and turbidity individually (single-element solutions). This condition will enable the determination of optimum biomass dose to treat separate elements from groundwater. The initial concentration of As and Pb were reduced from 40.1 and 39.6 μg/L respectively, to lower concentrations of 20.7 and 19.3 μg/L, respectively (Table 3.1 and Table 3.2) for this batch of experiments. In the earlier batches of tests, none of the tested biomass were successful in reducing As and Pb concentrations needed to comply with the WHO standards of As (10 μg/L) and Pb (10 μg/L) respectively. CN was excluded for further experiments due to its limited capability in removing Cd, fluoride and turbidity.

Sequential dosing methods (i.e., MO→MC and MC→MO) were also introduced in this batch of experiments to investigate their possibilities in improving treatment efficiency of individual MO and MC in treating single target contaminant. The biomass dose was further increased up to 400 mg/L for single biomass dosing method and up to 600 mg/L for combined and sequential biomass dosing methods to determine the overall optimum biomass dose.

4.2.1 Lead (Pb) removal

Unlike in previously reported multi-element solutions, the treatment methods were successful in meeting the recommended WHO standard of 10 µg/L for Pb except with MC at lower biomass doses of 100 mg/L and 200 mg/L. It is important to note that the concentration of Pb was 19.3 µg/L, lower than what was used in the multi-element solution. The biomass worked more efficiently with the lower initial Pb concentration of 19.3 µg/L compared to the higher initial Pb concentrations of 125.0 µg/L and 39.6 µg/L as conducted in the previous batches of experiments (See Figure 4.1 and Figure 4.8).

Among all biomass, MO showed the best potential with a small biomass dose of 100 mg/L for removal of Pb to meet the WHO standard. It can be seen from Figure 4.15b that the optimum MO dose is 300 mg/L with a removal efficiency of 87%. The second highest removal efficiency was achieved by MO→MC (78%) with an optimum dose of 400 mg/L (200:200 mg/L). The optimum dose of MC was at 300 mg/L with removal efficiency of 63% while MC→MO showed gradual improvement in Pb removal as the biomass dose was increased up to 600 mg/L (300:300 mg/L). After 600 mg/L, there was no further increase in biomass dose that was attempted. There was a concern that the higher the amounts of biomass dosed into the system, the harder the process of sludge removal at the end of treatment process.

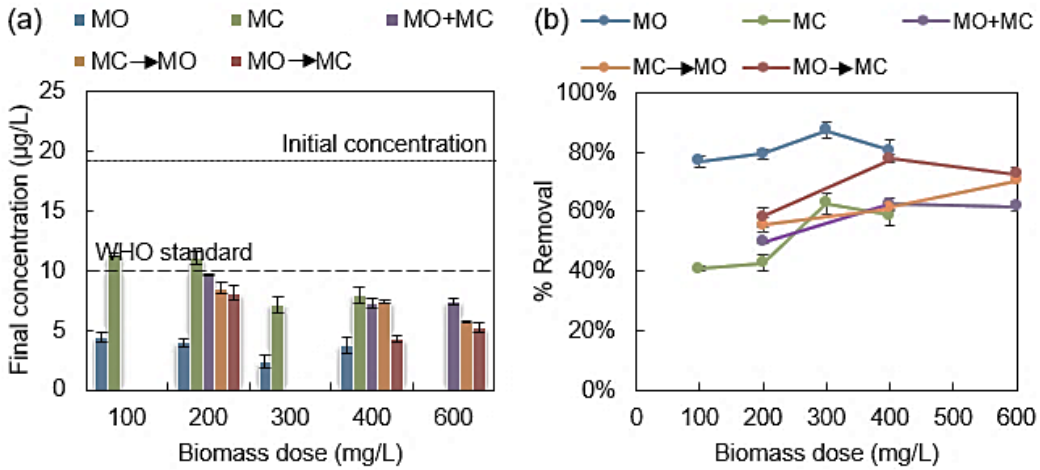

Figure 4.15 (a) Pb final concentrations and (b) Pb removal efficiencies achieved by MO, MC, MO+MC, MC→MO and MO→MC at Pb initial concentration of 19.3 µg/L (single-element solutions)

4.2.2 Nickel (Ni) removal

It is apparent from Figure 4.16a that most of the treatment methods were successful in meeting the WHO standard of 20 µg/L for Ni except for MC at the lowest biomass dose of 100 mg/L and MO+MC at the highest attempted biomass dose of 600 mg/L (300:300 mg/L). On the other hand, Figure 4.16b showed that individual biomass of MO (65% removal) and MC (59% removal) was optimised at the biomass dose of 200 mg/L respectively. However, MO+MC and MC→MO showed similar Ni removal trends when the biomass dose was increased from 200 mg/L (100:100 mg/L) to 400 mg/L (200:200 mg/L).

The optimum dose for combined and sequential biomass dosing methods was found to be at 400 mg/L (200:200 mg/L), respectively. MO+MC and MC→MO showed rapid reductions beyond the biomass dose of 400 mg/L (200:200 mg/L), respectively. This finding indicated that the biomass were applied in excess to the system, to which it could have caused an overlapping of binding sites on biomass surfaces, thus reduced metal binding on the biomass surface (Boota et al., 2009).

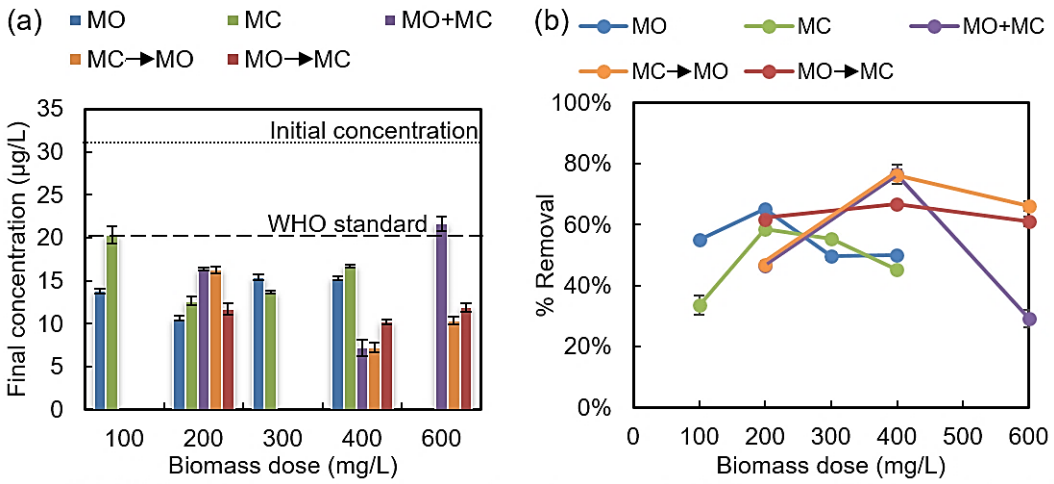

Figure 4.16 (a) Ni final concentrations and (b) Ni removal efficiencies achieved by MO, MC, MO+MC, MC→MO and MO→MC at Ni initial concentration of 30.6 µg/L (single-element solutions)

4.2.3 Cadmium (Cd) removal

As an individual biomass, MC showed a greater potential for Cd reduction than MO did, as shown in Figure 4.17a. MC was able to meet the standard at a wider dosage range of 100 to 300 mg/L (residual concentrations ranging from 2.0 to 2.7 µg/L), whereas MO could meet the WHO standard only at the dose of 200 mg/L (residual concentration of 3.0 µg/L).

Similar to Ni, Figure 4.17b shows that MO+MC exhibited the greatest removal of Cd (67%) at the dose of 400 mg/L (200:200 mg/L). The residual concentration was 1.6 µg/L, which met the WHO standard of 3 µg/L. The performance of MO and MC was improved when introduced to the mixing or sequential dosing method. However, at a dose of higher than 300 mg/L for individual biomass and 400 mg/L for combined biomass, the removal efficiencies were reduced markedly. The reason was likely due to the overlapping of binding sites of the biomass when they were applied in excess.

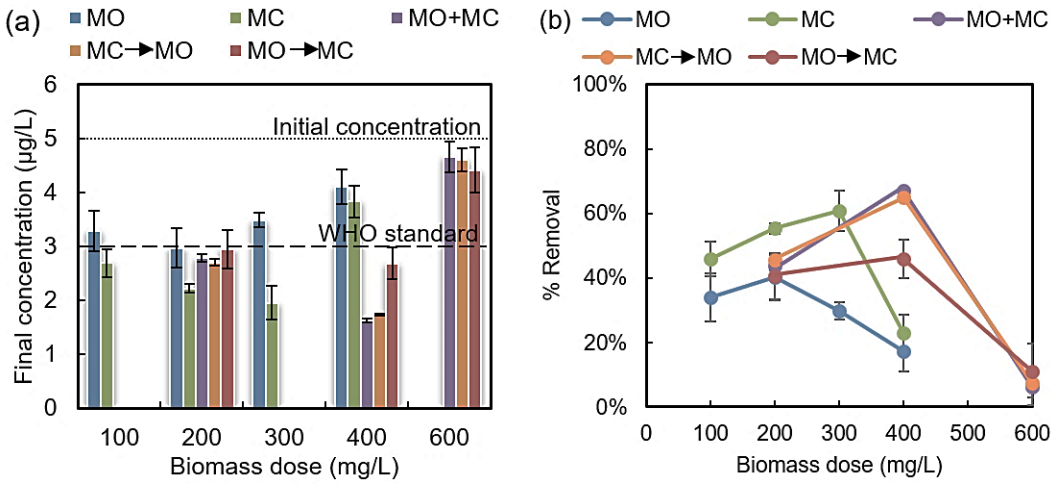

Figure 4.17 (a) Cd final concentrations and (b) Cd removal efficiencies achieved by MO, MC, MO+MC, MC→MO and MO→MC at Cd initial concentration of 5.0 µg/L (single-element solutions)

4.2.4 Arsenic (As) removal

Figure 4.18a demonstrates that the biomass worked more efficiently at lower initial concentration of As (20.7 µg/L) compared to higher initial concentrations As (655.9 µg/L and 40.1 µg/L) as conducted in the previous batches of experiments (Figure 4.4 and Figure 4.11). As seen from Figure 4.18a, the individual biomass of MO and MC cannot reduce the concentration of As to meet the WHO standard.

MO+MC with 400 mg/L (200:200 mg/L) biomass dose showed the lowest residual concentration of As (13.3 µg/L), which is slightly above the As WHO standard of 10 µg/L. It is noteworthy to find out from Figure 4.18b that the combination (MO+MC) and both sequential methods (MC→MO and MO→MC) performed better than that of treatment with individual MO and MC. The highest removal efficiencies were achieved by using MO+MC (40%) followed by MC→MO (36%) and MO→MC (27%) at the biomass dose of 400 mg/L (200:200 mg/L). The optimum doses of biomass for individual MO and MC were found to be at 200 mg/L. However, at this

biomass dose, the final concentration of As was much higher than the WHO recommended values for drinking water.

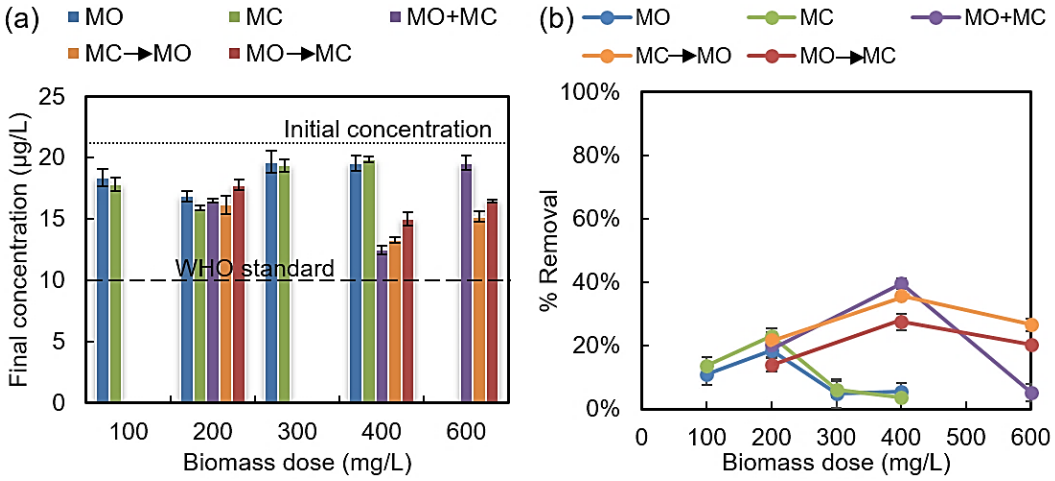

Figure 4.18 (a) As final concentrations and (b) As removal efficiencies achieved by MO, MC, MO+MC, MC→MO and MO→MC at As initial concentration of 20.7 µg/L (single-element solutions)

4.2.5 Fluoride removal

Similar to As, Figure 4.19a shows that none of the treatment methods was successful in meeting WHO drinking water quality standard of 1.5 mg/L for fluoride. MO+MC achieved the least fluoride residual concentration of 1.7 mg/L at biomass dose of 400 mg/L (200:200 mg/L). This concentration was slightly above the WHO standard. MC→MO also showed a comparable performance to the MO+MC since it is capable of reducing fluoride concentration to 1.9 mg/L at the same biomass dose applied for MO+MC. Figure 4.19b exhibits the highest removal of fluoride was achieved by MO+MC (42%) followed by MC→MO (38%) at the optimum dose of 400 mg/L (200:200 mg/L). MO→MC showed gradual improvement in fluoride removal as the biomass dose was increased up to 600 mg/L (300:300 mg/L). After 600 mg/L, no further increase in biomass dose was attempted as it is of concern that the higher the amount of biomass dosed into the system, the harder the process of handling the sludge

at the end of the treatment process. However, the optimum dose for individual biomass (MO and MC) was determined at 200 mg/L, respectively.

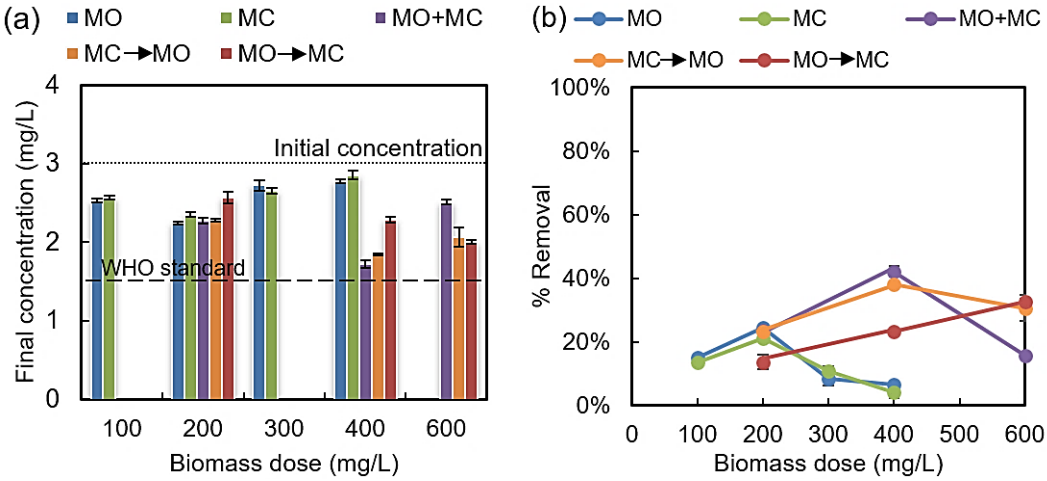

Figure 4.19 (a) Fluoride final concentrations and (b) fluoride removal efficiencies achieved by MO, MC, MO+MC, MC→MO and MO→MC at fluoride initial concentration of 3.0 mg/L (single-element solutions)

4.2.6 Turbidity removal

As seen in Figure 4.20a, MO proved that it has a high capability in removing turbidity as reported in the earlier experiments. The WHO standard of 5 NTU for turbidity was met (with residual turbidity of 4.5 NTU) with a low dose of 100 mg/L of MO. Further turbidity reductions were shown when the biomass dose increased up to 400 mg/L. Similar to MO, MO→MC was also successful in meeting the WHO standard of turbidity for all attempted biomass doses. Figure 4.20b shows that MO was optimised with 97% removal at a biomass dose of 300 mg/L followed by MC→MO, which optimised with 94% removal at a biomass dose of 400 mg/L (200:200 mg/L). At biomass dose of 300 mg/L, MC was optimised with 70% turbidity removal. All treatment methods in the above were successful in meeting the WHO standards at their respective optimum dose. On the contrary, MO+MC and MO→MC showed limited ability in removing turbidity to meet the WHO standards.

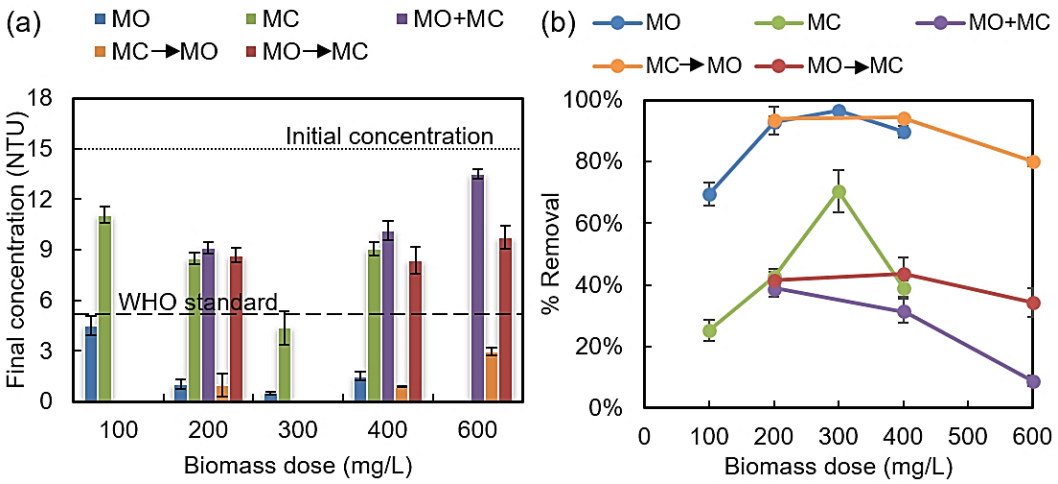

Figure 4.20 (a) Turbidity final concentrations and (b) turbidity removal efficiencies achieved by MO, MC, MO+MC, MC→MO and MO→MC at initial turbidity concentration of 14.8 NTU (single-element solutions)

Based on the results in Section 4.2, MO+MC with the dose of 400 mg/L (200:200 mg/L) was selected as the best treatment method considering its highest removal efficiency and capability of treating water to meet the WHO standards for most the target contaminants. The best removals were obtained at the dose of 200 mg/L for most of the individual biomass (MO and MC) as shown in Table 4.1. However, MO showed an excellent capability in removing Pb and turbidity with as low as 100 mg/L of MO dose. Besides, the results also revealed that MO and MC were quite biased towards the removal of some contaminants (Pb, Ni, Cd and turbidity), which is in agreement with the findings reported by Nguyen et al. (2013).

The sequential biomass dosing, MC→MO showed better removal of contaminants compared to MO→MC especially for Ni, Cd, fluoride and turbidity (Figure 4.16b, Figure 4.17b, Figure 4.19b, Figure 4.20b). Sequential dosing methods showed a comparable performance to the combined biomass dosing method (MO+MC). MO+MC performed better for the majority of target contaminants such as As, Ni, Cd and fluoride (Figure 4.18b, Figure 4.16b, Figure 4.17b, and Figure 4.19b).

In the combined biomass dosing method, MO and MC were dosed into the samples concurrently, while in the sequential biomass dosing method, the first sequent was subjected treatment by the first biomass. Then, the treated samples from the first biomass was subjected for a second sequent with the second biomass. Thus, sequential methods required almost double the treatment duration compared to MO+MC to achieve similar treatment performance. Therefore, MO+MC with a dose of 400 mg/L (200+200 mg/L) was selected for further testing to investigate the treatment efficiency of multi-element actual groundwater samples, as the combined biomass showed greater potential to treat source of water to meet the WHO standards, compared to that of individual biomass. Overall, optimum doses were found at 200 mg/L (single biomass) and 200:200 mg/L (combined biomass) for most of the tested treatments (Table 4.1).

Table 4.1 Optimum doses of different tested methods of treatment for the removal of Pb, Ni, Cd, As, fluoride and turbidity from single-element synthetic groundwater samples and their compliance with the WHO standards

Biomass	Optimum biomass dose (mg/L)					
	Pb (C_o=20 µg/L)	Ni (C_o=30 µg/L)	Cd (C_o=5 µg/L)	As (C_o=20 µg/L)	Fluoride (C_o=3 mg/L)	Turbidity (C_o=15 NTU)
MO	300 (Yes)	200 (Yes)	200 (Yes)	200 (No)	200 (No)	300 (Yes)
MC	300 (Yes)	200 (Yes)	300 (Yes)	200 (No)	200 (No)	300 (Yes)
MO+MC	200+200 (Yes)	200+200 (Yes)	200+200 (Yes)	200+200 (No)	200+200 (No)	200+200 (No)
MC→MO	300→300 (Yes)	200→200 (Yes)	200→200 (Yes)	200→200 (No)	200→200 (No)	200→200 (Yes)
MO→MC	200→200 (Yes)	200→200 (Yes)	200→200 (Yes)	200→200 (No)	300→300 (No)	200→200 (No)

C_o: Initial concentration
Yes: Complied with WHO standards
No: Not complied with WHO standards

4.3 Effects of solution matrix in multi-element solutions

The effects of single and multi-element solution matrices were studied using MO+MC (200:200 mg/L) as the best treatment process. The experiments were conducted with initial concentrations of As (20 µg/L), Pb (20 µg/L), Ni (30 µg/L), Cd (5 µg/L), fluoride (3 mg/L) and turbidity (15 NTU) in single and multi-element solution matrices. The effect of solution matrix to the selected treatment performance was evaluated in this study as shown in Figure 4.21.

The presence of Pb, Ni, As, Cd, fluoride and turbidity in the multi-element solution was compared with the single-element solution during the treatment process. As seen in Figure 4.21a, the presence of Pb, Ni, Cd, fluoride and turbidity in multi-element solution had no significant effects, whereas the final concentrations of As in the multi-element solution (12.0 µg/L) was almost the same as in the single-element solution (12.5 µg/L). This result suggested that As showed no interactions with the other elements present in the same system. On the other hand, the residual concentrations of Pb and turbidity (Figure 4.21f) in the multi-element solutions (5.8 µg/L and 4.6 NTU, respectively) were lower than that of in the single-element solutions (7.2 µg/L and 10.1 NTU, respectively). This finding indicated that there could be mutual interactions between Pb and kaolin (represented as turbidity) with the other elements present in the same solution.

In other cases, residual concentrations of Ni, Cd and fluoride (Figure 4.21c, Figure 4.21d and Figure 4.21e) were higher in the multi-element solutions (10.0 µg/L, 2.1 µg/L and 2.2 mg/L, respectively) than that of in the single-element solutions (7.2 µg/L, 1.6 µg/L and 1.7 µg/L, respectively). This finding indicated that Ni, Cd and fluoride

were probably competing with the other elements that were present in the multi-element system for binding sites on the biomass' surface.

Based on the results, MO+MC (200:200 mg/L) was seen to have successfully removed pollutants needed to meet the WHO standards for Pb, Ni and Cd in both solution systems. In the case of turbidity, WHO standard was only met in the multi-element solution matrix. It is assumed that the kaolin (represented as turbidity) bound with the other metals through electrostatic interactions as they possess opposite charges, leading to the better removal of turbidity in multi-element solutions. Other than that, MO+MC (200:200 mg/L) was unsuccessful in meeting the WHO standards of As and fluoride.

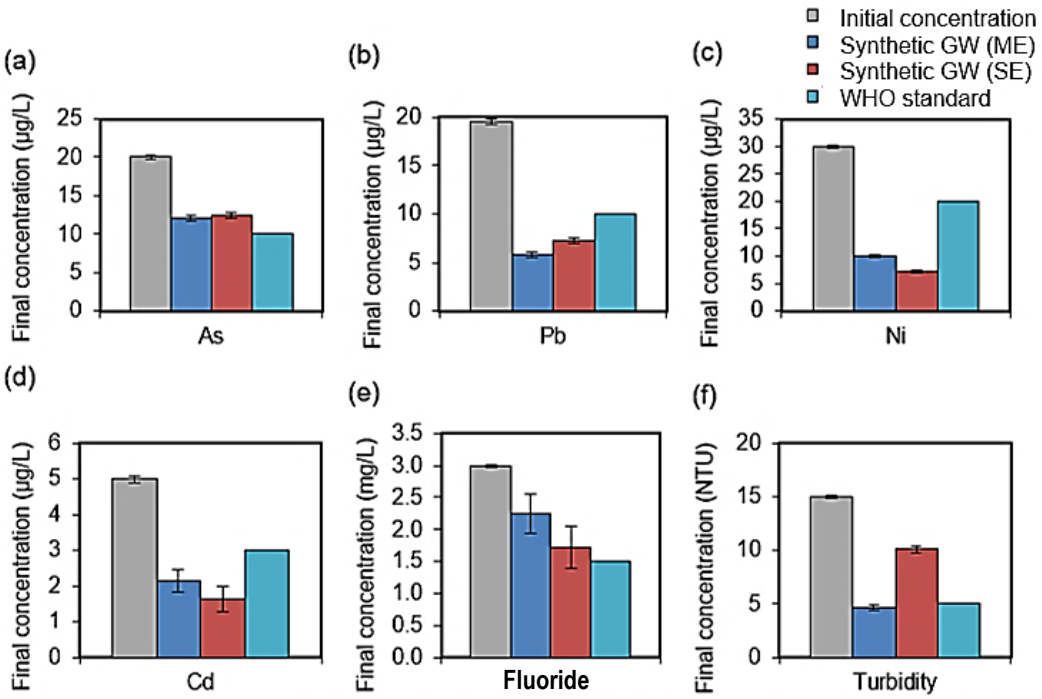

Figure 4.21 Comparison of treatment performance of 200:200 mg/L (MO+MC) on multi-element (ME) and single-element (SE) synthetic groundwater (GW) samples

Overall, it can be observed that the final concentrations of target contaminants had only slight differences when they were tested in multi-element and single-element

solutions except for fluoride and turbidity. This finding indicated that the presence of other elements in the same system interfered strongly on the removal behaviour of fluoride and turbidity.

4.4 Testing with real groundwater samples using the selected treatment conditions

Treatment tests were conducted on groundwater samples taken from three different sites around Victoria, Australia to evaluate the applicability of the chosen treatment process (i.e., MO+MC with 200:200 mg/L). The characteristics of the samples are given in Table 3.3. The actual groundwater samples consist of dissolved organic carbon (DOC), salinity (measured by EC) and organic micropollutants (measured by UVA_{254}) in addition to the parameters of interest. The concentrations of target contaminants in real groundwater samples were all below their individual WHO standards except for Ni (24.4 µg/L) in the sample taken from Cranbourne, Victoria, Australia. The samples were spiked with desired concentrations of target contaminants to make the concentration of the target contaminants in the samples consistent with the previous experiments (synthetic groundwater sample) (Table 3.4). Thus, the comparison between them can be made accordingly.

The final concentrations of the treated actual groundwater samples were compared with the results from multi-element synthetic groundwater samples as shown in Figure 4.22. The final concentration of As, Pb, Cd and turbidity was lower in actual groundwater samples (9.9 µg/L, 1.4 µg/L, 1.3 µg/L and 3.0 NTU respectively) when compared with the treated synthetic groundwater samples (12.0 µg/L, 5.8 µg/L, 2.1 µg/L and 4.6 NTU respectively) in the multi-element solution matrix.

The variation of reduction could be attributed to the presence of other substances (e.g., organic matter) in the actual groundwater samples and these could have potentially influenced the reduction of As, Pb, Cd and turbidity in the samples. The reason can be referred to the high level of dissolved organic carbon (DOC) ranging from 8.6 to 11.1 mg/L (Table 3.1). Meanwhile, in another study conducted by Wu et al. (2011), it is reported that the mechanism of complexation between humic acid-like substances in the DOC and the heavy metals played a significant role in the binding process during treatment. Humic acid represents a major component of DOC occurring naturally. DOC has great binding properties and electrostatic interactions with heavy metals, thus leading to the metal-organic complexation (Chen, 2012; Sounthararajah et al., 2015). A study conducted by Mlakar et al. (2015) also exhibited that dissolved trace metals such as copper (Cu), lead (Pb) and zinc (Zn) are mostly bound to organic matter.

In terms of compliance with the WHO standards, it can be seen from Figure 4.22(b,c,d&f) that the residual concentrations of Pb, Ni, Cd and turbidity were below their respective WHO recommended standards when the real groundwater samples were treated with MO+MC (200:200 mg/L). On the other hand, the final concentrations (after treatment) of As and fluoride were greater than their respective recommended WHO standards in both actual and synthetic groundwater samples. Based on the experimental results, it was clear that the tested biomass and treatment methods were ineffective in the removal of As and fluoride and its compliance with the WHO standards for drinking water.

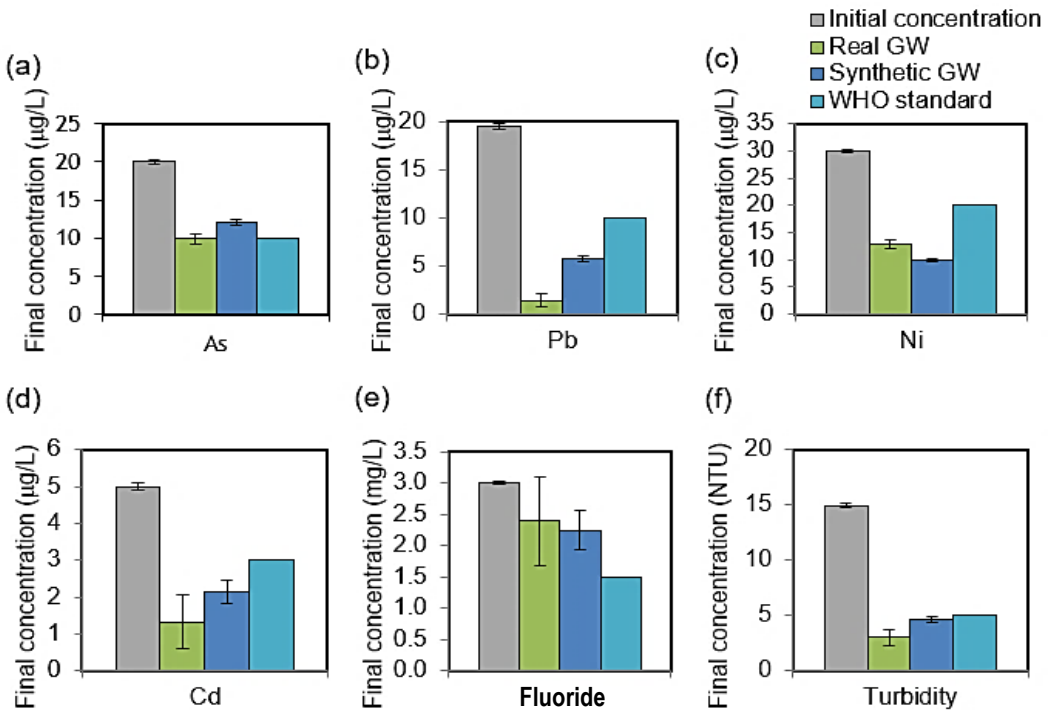

Figure 4.22 Comparison of treatment performance of 200:200 mg/L (MO+MC) on multi-element real and synthetic groundwater (GW) samples (Average concentrations of all three sites)

Overall, it is understood that the presence of one element may hinder or enhance the binding process of the target contaminants in the removal process. MO+MC with the dose of 400 mg/L (200:200 mg/L) showed the potential in removing Pb, Ni, Cd and turbidity from real groundwater samples to meet WHO standards. Based on the experimental results, MO+MC is an effective biomass with the potential to remove Pb, Ni, Cd and turbidity from groundwater and comply with the WHO standards.

4.5 Pre-treatment of biomass and treatment with alum for the removal of problematic arsenic and fluoride from drinking water

As revealed in the previous batch of experiments, residual concentrations of arsenic (As) and fluoride did not comply with their respective WHO drinking water standards of 10 µg/L and 1.5 mg/L respectively. For this reason, modification or pre-treatment of biomass was attempted intending to improve the treatment efficiency for As and

fluoride removal. A similar study was conducted by Feng et al. (2011), whereby the above-mentioned authors chemically modified the orange peel for biosorption of lead (Pb), cadmium (Cd) and nickel (Ni) from aqueous solutions. For the current study, *Moringa oleifera* (MO) and *Musa cavendish* (MC) were pre-treated with the following three methods:

1. Basic pre-treatment - The biomass was mixed with 1 Molar (M) of NaOH
2. Acidic pre-treatment - The biomass was mixed 1 M of H_2SO_4
3. Thermal pre-treatment - The biomass was placed at 300°C for 1 hour in the oven.

Majority of adsorption studies have used biomass for testing in single-element solutions (Nguyen et al., 2013). Therefore, it is suggested that further research need to be carried out with multi-element solutions to enable a more convincing use of biomass in the future. 200 mg/L each of pre-treated biomass dose of MO and MC was applied to single-element and multi-element solutions of As and fluoride as shown in Table 4.2, Table 4.3 and Table 4.4.

Table 4.2 Characteristics of synthetic groundwater samples (single-element) of arsenic (As)

Parameter	Average initial concentration	WHO drinking water quality guideline permissible limit
As	20.7 μg/L	10 μg/L
pH	7.0	6.5-8.5

Table 4.3 Characteristics of synthetic groundwater samples (single-element) of fluoride

Parameter	Average initial concentration	WHO drinking water quality guideline permissible limit
Fluoride	3.0 mg/L	1.5 mg/L
pH	7.0	6.5-8.5

Table 4.4 Characteristics of synthetic groundwater samples (multi-element)

Parameter	Average initial concentration	WHO drinking water quality guideline permissible limit
As	20.7 μg/L	10 μg/L
Pb	19.3 μg/L	10 μg/L

Table 4.4 (Continued)

Parameter	Average initial concentration	WHO drinking water quality guideline permissible limit
Ni	30.6 μg/L	20 μg/L
Cd	5.0 μg/L	3 μg/L
Fluoride	3.0 mg/L	1.5 mg/L
Turbidity	14.8 NTU	5 NTU
pH	7.00	6.5-8.5

Furthermore, treatment with a considerably low dosage of conventional water purification agent, alum (0.5 to 50 mg/L of Al^{3+}) was also attempted. According to Crittenden et al. (2012), typical doses for alum are 10 to 50 mg/L when pH is between 6 to 7.

4.6 Arsenic removal using pre-treated biomass

4.6.1 Moringa oleifera (MO)

Figure 4.23 depicts the residual concentration's removal rates of As with pre-treated (acidic, base and thermal) MO from single and multi-element solutions. The above figure indicated that the removal efficiencies from the three pre-treatment methods (acidic, basic and thermal) are almost the same for both solution conditions (i.e., single-element or multi-element solutions). As anticipated, removal of As has improved with the pre-treated MO.

The removal rates of As were improved by almost double from 18% (untreated MO) to 42% when MO seeds were pre-treated with 1 M of NaOH, 1 M of H_2SO_4 and thermal (300°C for 1 hour), respectively in single-element solutions. Furthermore, there was a slight improvement in the removal rates of As in multi-element solutions. The results showed that the removal efficiencies of As by the pre-treated MO were around 44% to 45% compared to the untreated MO of 41%. Although the pre-treated MO was able to reduce the As levels considerably, the treatment level was insufficient to meet the stringent WHO standards.

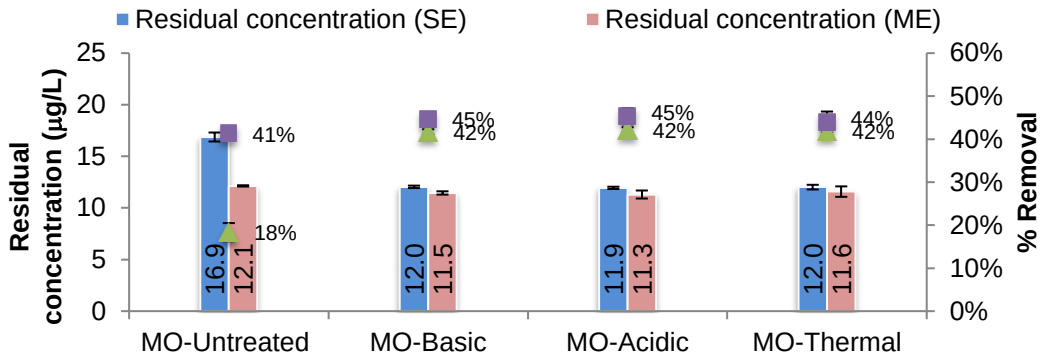

Figure 4.23 As residual concentrations and removal efficiencies after being treated with untreated MO and pre-treated MO with base (MO-basic), acid (MO-acidic) and thermal (MO-thermal) in single-element (SE) and multi-element (ME) solutions with initial As concentration of 20.7 µg/L with 200 mg/L of pre-treated biomass, respectively

The lowest residual concentrations of As (11.5 µg/L and 11.3 µg/L) were achieved by MO pre-treated with 1 M of NaOH and 1 M of H_2SO_4 in single-element and multi-element solutions respectively. The results demonstrated that none of the tested pre-treatment methods were successful in reducing the residual As concentration to satisfy the WHO drinking water standard recommended level of 10 µg/L.

4.6.2 *Musa cavendish* (MC)

The pre-treated MC with 1 M of NaOH, 1 M of H_2SO_4 and thermal temperature (300°C) performed almost similar to those produced by the pre-treated MO in both solution conditions (single and multi-element solutions). The removal efficiencies of As were improved by almost double from 23% (untreated MO) to around 42%, 41% and 41% when MC was pre-treated with 1 M of NaOH, 1 M of H_2SO_4 and thermal (300°C) respectively in single-element solutions (Figure 4.24). Similar to the performance shown by the pre-treated MO, there were only slight improvements in the removal rates of As from 41% (untreated MC) to around 44% to 45% (pre-treated MC) in multi-element solutions.

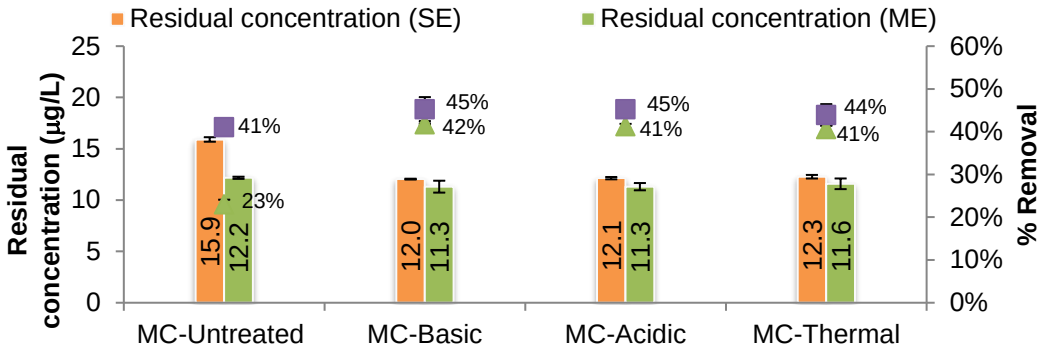

Figure 4.24 As residual concentrations and removal efficiencies after being treated with untreated MC and pre-treated MC with base (MC-basic), acid (MC-acidic) and thermal (MC-thermal) in single-element (SE) and multi-element (ME) solutions with initial As concentration of 20.7 µg/L with 200 mg/L of pre-treated biomass, respectively

The lowest residual concentration of As (12.0 µg/L) was achieved by MC pre-treated with 1 M of NaOH in single-element. Surprisingly, in multi-element solutions, MC-basic and MC-acidic showed similar final concentrations for As (11.3 µg/L), which is also lower than that achieved with the MC-thermal (11.6 µg/L). Similar to the performance of pre-treated MO for As removal, the results revealed that none of the pre-treatment methods adopted on MC were successful in reducing the residual As concentration to satisfy the WHO drinking water standard recommended level of 10 µg/L.

From results reported on for As removal, it is observed that the removal efficiencies were higher in multi-element solutions than from single-element solutions for both untreated and pre-treated biomass. In the multi-element situation, the improvement of As removal efficiencies could be due to the mutual interactions between As and other elements present (i.e. Pb, Ni, Cd, fluoride and turbidity) in the same solution than the effects of pre-treatments on MO and MC respectively.

4.7 Fluoride removal using pre-treated biomass

4.7.1 *Moringa oleifera* (MO)

The variation in the removal rates of fluoride with pre-treated MO are depicted in Figure 4.25. In the single-element solutions, MO pre-treated with 1 M of H_2SO_4 improved the removal rate of fluoride from 25% (untreated MO) to 28%. However, the removal rates of fluoride were observed to have been reduced after being treated with the MO-NaOH (23%) and MO-thermal (21%).

In multi-element solutions, unlike in As, there were only slight improvements in the removal rates of fluoride with the pre-treated MO. The removal rates improved from 29% (untreated MO) to about 34% to 36% with the pre-treated MO.

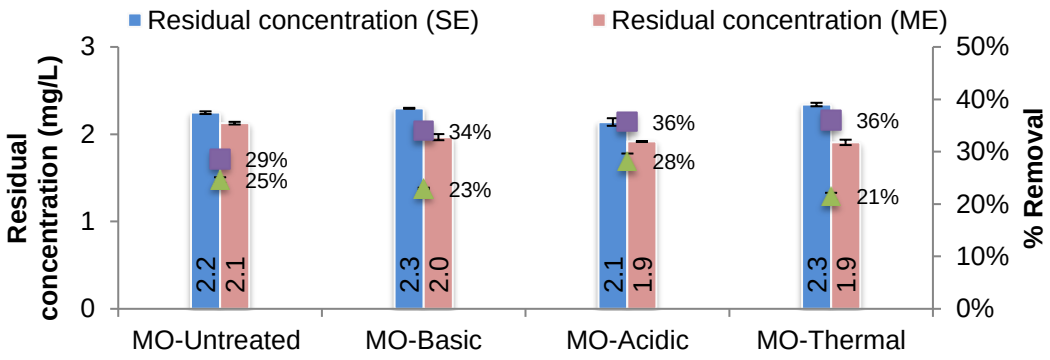

Figure 4.25 Fluoride residual concentrations and removal efficiencies after being treated with untreated MO and pre-treated MO with basic (MO-Basic), acid (MO-Acidic) and thermal (MO-Thermal) in single- and multi-element solutions with initial fluoride concentration of 3.0 mg/L with 200 mg/L of pre-treated biomass, respectively

For both solution conditions, MO treated with acid (1 M of H_2SO_4) showed better removals compared to MO treated with base and thermal treatment. The reason could be due to the binding sites on the MO surface that was chemically modified when dissolved with H_2SO_4. The introduction of more H^+ ions on the MO surface may contribute a significant role in attracting the anion such as fluoride onto the acidic

modified MO surface. Unfortunately, for fluoride removal, the results revealed that none of the pre-treatment methods adopted on MO were successful in reducing the residual fluoride concentration to satisfy the recommended WHO drinking water standard of 1.5 mg/L.

4.7.2 *Musa cavendish* (MC)

Pre-treated MC enhanced the removal rate of fluoride from 21% (untreated MC) to about 23% to 25% (Figure 4.26). In multi-element solutions, there were only slight improvements in the removal rates of fluoride from 30% (untreated MO) to about 31% to 32% with MC-basic and MC-acidic. However, MC-thermal showed an improvement from 30% (untreated MC) to 40%. For both solution conditions, MO treated with acid (H_2SO_4) showed better removals compared to MO treated with a base (NaOH). The reason could be due to binding sites on the MO surface being chemically modified when dissolved in H_2SO_4. The availability of H^+ ions on the MO surface could play a significant role in attracting the anion such as fluoride for attachment. The results also discovered that none of the pre-treatment methods adopted on MC were successful in reducing the residual fluoride concentration to satisfy the recommended WHO drinking water standard of 1.5 mg/L.

Overall, removal efficiencies of fluoride were higher in multi-element solutions compared to single-element solutions for the untreated biomass and pre-treated biomass. In multi-element condition, it is more likely that the improvement of fluoride removal efficiencies was caused by the mutual interactions between the fluoride and other presented elements (i.e., Pb, Ni, Cd, fluoride, and turbidity) in the same solution rather than the effects of pre-treatments on the MO and MC, respectively.

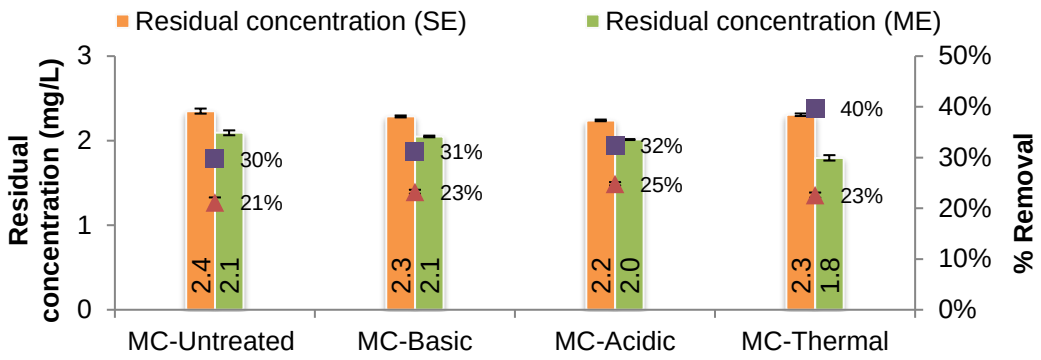

Figure 4.26 Fluoride residual concentrations and removal efficiencies after being treated with untreated MC and pre-treated MC with base (MC-Basic), acid (MC-Acidic) and thermal (MC-Thermal) in single- and multi-element solutions with initial fluoride concentration of 3.0 mg/L with 200 mg/L of pre-treated biomass respectively

4.8 Treatment using a conventional water purification agent (alum)

Based on previous experiments, it was found that the pre-treatment of biomass by the base, acid or thermal was unsuccessful in satisfying the WHO recommended levels of As and fluoride. Therefore, the use of alum (low dose) was attempted for the removal of these problematic As and fluoride from the synthetic single-element groundwater samples. The aim of this experiment is to evaluate the removal of As and fluoride from the synthetic groundwater by using alum to get the residual pollutant levels to comply with the WHO recommended levels of As and fluoride.

4.8.1 Arsenic removal

Figure 4.27 depicts that the removal rates of As increased rapidly (55% to 99%) with the increasing alum dose from 0.5 to 5.0 mg/L. The removal rate remained unchanged (99%) when the dose was further increased to 50 mg/L of Al^{3+}. It was also shown that the highest removal of As (99%) was achieved with a dose of 5 mg/L of Al^{3+}. WHO standard recommended for As of 10 µg/L was satisfied with a low dose of 0.5 mg/L of Al^{3+}. This finding has proved that As can be removed to a concentration of 9.2 µg/L,

which fell just below the recommended WHO standard of 10 µg/L with a very minimum dose of 0.5 mg/L of Al^{3+}. Hence, it is proved that a very minimal dose of alum (0.5 mg/L of Al^{3+}) can be applied in the case of groundwater contaminated with As particularly with an initial concentration of 20 µg/L. Furthermore, it is also expected that the amount of dose is considered to have less effect on the pH of the treated water and the amount of sludge produced at the end of the treatment process.

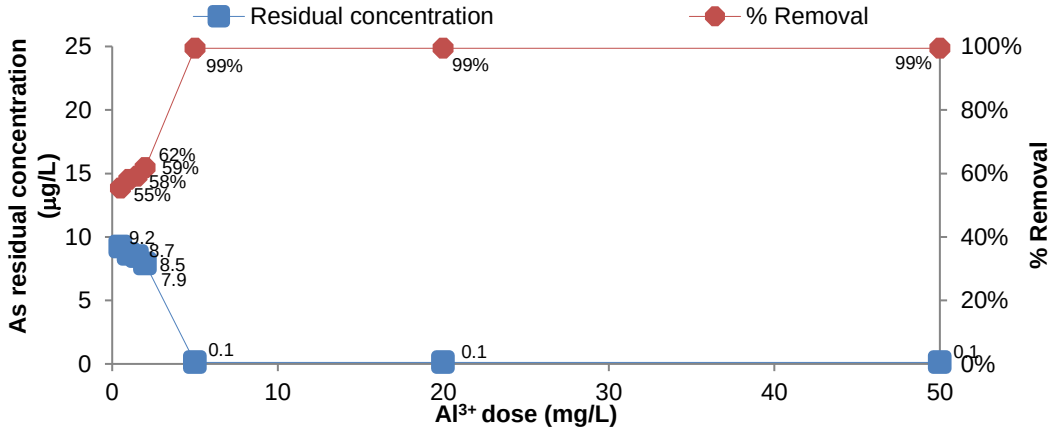

Figure 4.27 Residual concentration and removal efficiency of As after being treated with alum

4.8.2 Fluoride removal

The removal of fluoride required an alum dose of 20 mg/L of Al^{3+} to reduce the fluoride concentration from 3.0 mg/L to 1.14 mg/L which satisfies the WHO standard for fluoride (1.5 mg/L). This amount of alum was higher compared to the dose of alum (0.5 mg/L) to reduce the As concentration to a level that meets the WHO standard for As (10 µg/L).

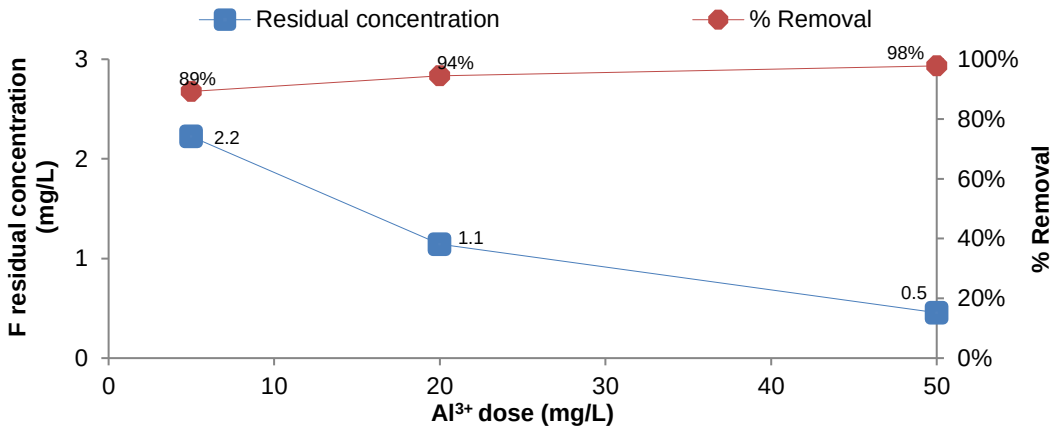

Figure 4.28 Residual concentration and removal efficiency of fluoride after being treated with alum

4.9 Summary and Conclusions

The effectiveness of plant-based materials *Moringa oleifera* (MO), *Cicer arietinum* (CA), *Musa cavendish* (MC), *Cocos nucifera* (CN) and *Lentinus edodes* (LE) for the removal of heavy metals arsenic (As), lead (Pb), nickel (Ni), cadmium (Cd), flouride and turbidity from synthetic and real groundwater samples has been investigated. In the initial stage of the study, it was found that most of the selected plant-based materials at their optimum doses (200 mg/L: single biomass, 200+200 mg/L: combined biomass) were more effective when treating the synthetic groundwater containing low concentrations (within the range of typical concentrations of contaminants in the literature) of contaminants compared to when treated with the high concentrations (maximum recorded concentrations of contaminants in the literature) of contaminants. This condition could be a result of the saturation of binding sites on the biomass surface when the initial concentrations of contaminants are high.

From the preliminary screening, MO and MC were selected as the potential plant-based materials to be used as water purification agents as they exhibited potential in

removing target contaminants. Combined and sequential methods of biomass dosing were also introduced with a view to improve the treatment efficiency.

MO alone, with the dose as low as 100 mg/L, was able to reduce the initial Pb and turbidity concentrations of 19.3 μg/L and 14.8 NTU, respectively, to the residual concentration of 4.5 μg/L and 4.5 NTU, respectively, to meet their respective WHO standard of 10 μg/L and 5 NTU for single-element synthetic groundwater samples. However, the removal of turbidity was lower for combined biomass (MO+MC) compared to the single biomass (MO) with the same biomass dose. The reason could be due to the different of chemical properties possesses by MO and MC which one might have affinity towards the turbidity while another one might hinder the attachment of kaolin (turbidity) onto the surface of biomass. In this study, it was proven that MO has a great ability to treat turbidity while MC was not effective for turbidity removal. However, MO+MC showed the highest removal efficiencies of 77% and 67% for nickel and cadmium, respectively, with the coagulant dose at 400 mg/L (200+200 mg/L), with the treated water successfully meeting the WHO drinking water standards.

MO+MC with the biomass dose set at 400 mg/L (200+200 mg/L) resulted in the highest removal of the target contaminants in the single-element synthetic groundwater samples compared to the same dose applied for single biomass (which mostly showed reductions in removal efficiencies when the biomass doses were increased from 200 or 300 to 400 mg/L). This finding suggests that single biomass has limited ability in treating a specific contaminant when the dose beyond the optimum point was applied. It is also hypothesised that when MO and MC are applied in combination, interactions between different functional groups possessed by MO and

MC, respectively, may facilitate the attachment of target contaminants on the biomass, which consequently improved the treatment efficiency (as explained beforehand in Chapter 5). Therefore, MO+MC with the selected dose was selected for the testing of the real groundwater samples spiked with the target contaminants.

Testing of the selected treatment method on the actual groundwater samples showed that the removal efficiency of As, Pb, Cd and turbidity was higher in real groundwater samples. This condition was likely due to the interactions between the target contaminants and other substances present (e.g., organic substances) in the real groundwater samples.

As and fluoride appeared to be problematic contaminants as none of the biomass or methods of biomass dosing were capable of reducing above contaminants to meet their respective WHO standards. The findings indicated that MO, MC or the combinations were not fully effective for As and fluoride removals from the synthetic and real groundwater samples. Further investigations were attempted on the biomass (i.e. pre-treatment of biomass) to see the possible improvement on As and fluoride removals using the pre-treated biomass. Based on the earlier attempts with pre-treated biomass, none of these methods were successful in meeting the recommended WHO standards for As and fluoride of 10 μg/L and 1.5 mg/L, respectively. Therefore, treatment with conventional alum appeared to be another option as it is also low-cost and widely available in the market. However, precautions regarding the dose of alum need to be considered as the excessive amount of alum could produce harmful sludge at the end of the treatment process due to its non-biodegradable and toxic characteristics. The present study demonstrated that As and fluoride with initial concentrations of 20 μg/L and 3 mg/L, respectively can be reduced to the concentrations of 9.2 μg/L and 1.1

mg/L with the dose of 0.5 mg/L of Al^{3+} (for As removal) and 20 mg/L of Al^{3+} (for fluoride removal), respectively. These doses are within the typical range of alum as reported by Crittenden et al. (2012), which is between 10 to 50 mg/L. Thus, in the case of removal of problematic arsenic (As) and fluoride, alum demonstrated a superior performance to those pre-treated biomass at similar initial contaminant concentration and initial pH levels.

CHAPTER 5 Characterisation of unloaded and contaminant-loaded Moringa oleifera seeds (MO), Musa cavendish (MC) and their combination (MO+MC)

This chapter examines the possible mechanisms involved in the treatment process by characterising the unloaded and contaminant loaded-biomass using Attenuated Total Reflectance-Fourier Transform Infrared spectroscopy spectrum (ATR-FTIR) 100 (Perkin Elmer), Scanning Electron Microscope (SEM Quanta FEI 200) and Energy Dispersive X-Ray (EDX) instruments. The combination of *Moringa oleifera* (MO) seeds and *Musa cavendish* (MC) was found to be more effective in the treatment compared to the other tested biomass. For optimising the treatment, it is important to understand the mechanism(s) behind the treatment process through the detailed characterisation of the unloaded and contaminant-loaded biomass. For a comparison purpose, the characterisation was carried out for not only the combined MO and MC (MO+MC) but also the individual MO and MC.

The first characterisation was to determine the main functional groups available on the unloaded biomass surface and compared them with the contaminant-loaded biomass by studying the alterations of the infrared spectra using ATR-FTIR 100.

The surface profile of the biomass before and after the treatment process characterised by SEM may provide further information regarding the possible mechanism of the contaminant removal process by using the selected biomass.

The elemental composition of the unloaded and contaminant-loaded biomass was also examined by using the SEM facility integrated with EDX function. The detection of contaminants on the loaded biomass could indicate the adsorption of the contaminants

occurred. At the end of this chapter, the likely mechanism(s) that is responsible for the removal of target contaminants are proposed.

5.1 Results of Fourier Transform Infrared spectroscopy spectrum (FTIR)

FTIR spectroscopy is a valuable tool in examining the presence of certain functional groups in a molecule, since each particular chemical bond shows a unique energy absorption band (Zhu et al., 2012). Therefore, functional groups responsible for the removal of a contaminant could be determined by analysing the variation on the spectra of the biomass before and after the treatment process. According to Beer-Lambert law, the percentage of transmittance is opposite to that of percentage of absorbance. The percentage of transmittance which presented on the FTIR spectrum indicates that the amount of the light beam absorbed by the biomass signifies characteristic peaks of specific functional groups that exist on the biomass surface (Lykos, 1992).

5.1.1 *Moringa oleifera* seeds (MO)

Spectral analyses were conducted for both the unloaded and contaminant-loaded MO to identify any changes occurred on the spectrum profile of the contaminant-loaded biomass which might indicate possible interactions between the target contaminants and MO.

5.1.1.1 Unloaded MO

FTIR spectra of MO displayed significant peaks in the region between 3400 cm^{-1} to 800 cm^{-1} (Figure 5.1).

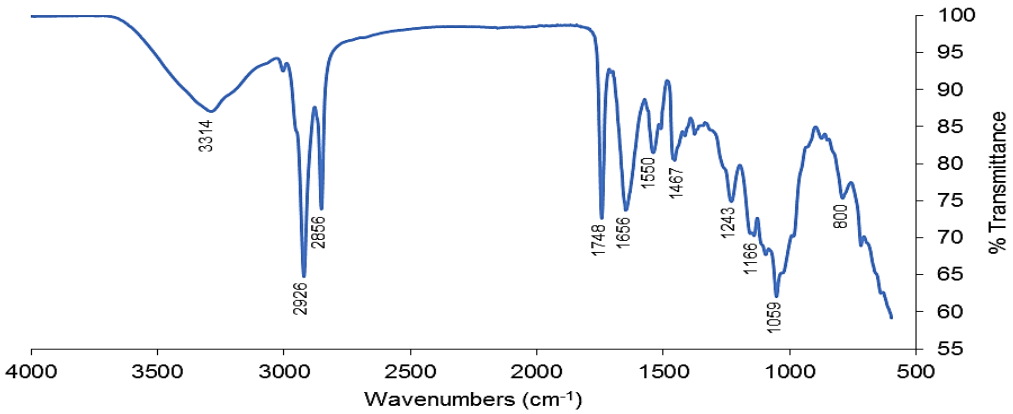

Figure 5.1 FTIR spectra of unloaded MO

A broad band centered at 3314 cm^{-1} (O-H stretch of carboxylic acids) and N-H stretch of secondary amines also are contibuting in this region due to the high content of proteins present in the seeds. These groups appears to be dominant in the proteins and fatty acids of MO seeds (Araújo et al., 2010). The strong peaks which appeared at 2926 cm^{-1} and 2856 cm^{-1} are assigned to C-H asymmetric and symmetric stretch of alkanes, respectively. Whereas another significant peaks at 1748 cm^{-1} and 1656 cm^{-1} are assigned to C=O stretch of carbonyl groups of esters and amide, respectively while peak at 1059 cm^{-1} is assigned to C-O stretch of ethers. Weak to medium peaks observed at 1550 cm^{-1} (N-H bend of primary amines and amides), 1467 cm^{-1} (C-H bend of alkanes), 1243 cm^{-1} (C-O stretch of carboxylic acids and C-N stretch of amines), 1166 cm^{-1} (C-N stretch of amines) and 800 cm^{-1} (N-H wag of amines).

This result indicates that the MO seeds consists of various functional groups which mainly coming from proteins that could play important role in the adsorption of target contaminants. The profile of FTIR spectrum for the unloaded MO was comparable to those exhibited by the previous studies reported elsewhere (Reddy et al., 2012; Araujo et al., 2013; Bhutada et al., 2016). The nature of the functional groups of the unloaded MO was considered as a basis for further comparison with the contaminant-loaded

MO. Thus, the functional groups responsible for the removal of individual target contaminant could be elucidated.

5.1.1.2 Contaminant-loaded MO

Generally, FTIR spectra for both unloaded and contaminant-loaded biomass were found to be nearly identical for cases involving target contaminants (Figure 5.2).

For cases involving As, Cd, fluoride, and kaolin, for instance, the changes in the peak intensities together with the slight shift of wavenumbers were observed, especially between 1700 to 600 cm^{-1}. Slight alterations of peak intensities were noticed on the FTIR spectra profile of As-, Cd- fluoride-, and kaolin- loaded MO compared with the spectra of the unloaded MO along the studied wavenumbers (Figure 5.2a,d,e&f). The notable changes of the transmittance intensities were detected at 1656 cm^{-1} (C=O stretch of carbonyl amides), 1550 cm^{-1} (N-H bend of primary amines and amides) and 1059 cm^{-1} (C-O stretch of ethers), when As, Cd, fluoride and kaolin were loaded onto the unloaded MO, respectively.

Interestingly, peak at 800 cm^{-1} which corresponds to N-H wag of amines was absent when As, Cd, fluoride and kaolin was in contact with MO, respectively. The disappearance of the peak at 800 cm^{-1} indicates amine's role in the complexation with As, Cd, fluoride and kaolin. Based on this result, it is suggested that specific functional groups such as C=O stretch of carbonyl amides, N-H bend of primary amines and amides, C-O stretch of ethers and N-H wag of amines might involve in the removal of As, Cd, fluoride and kaolin from the synthetic groundwater samples when MO seeds was used as a biomass in the treatment process. Pagnanelli et al. (2003) has demonstrated that these groups have the ability to adsorb heavy metals (lead, copper and cadmium) to form complexes with ions in solution.

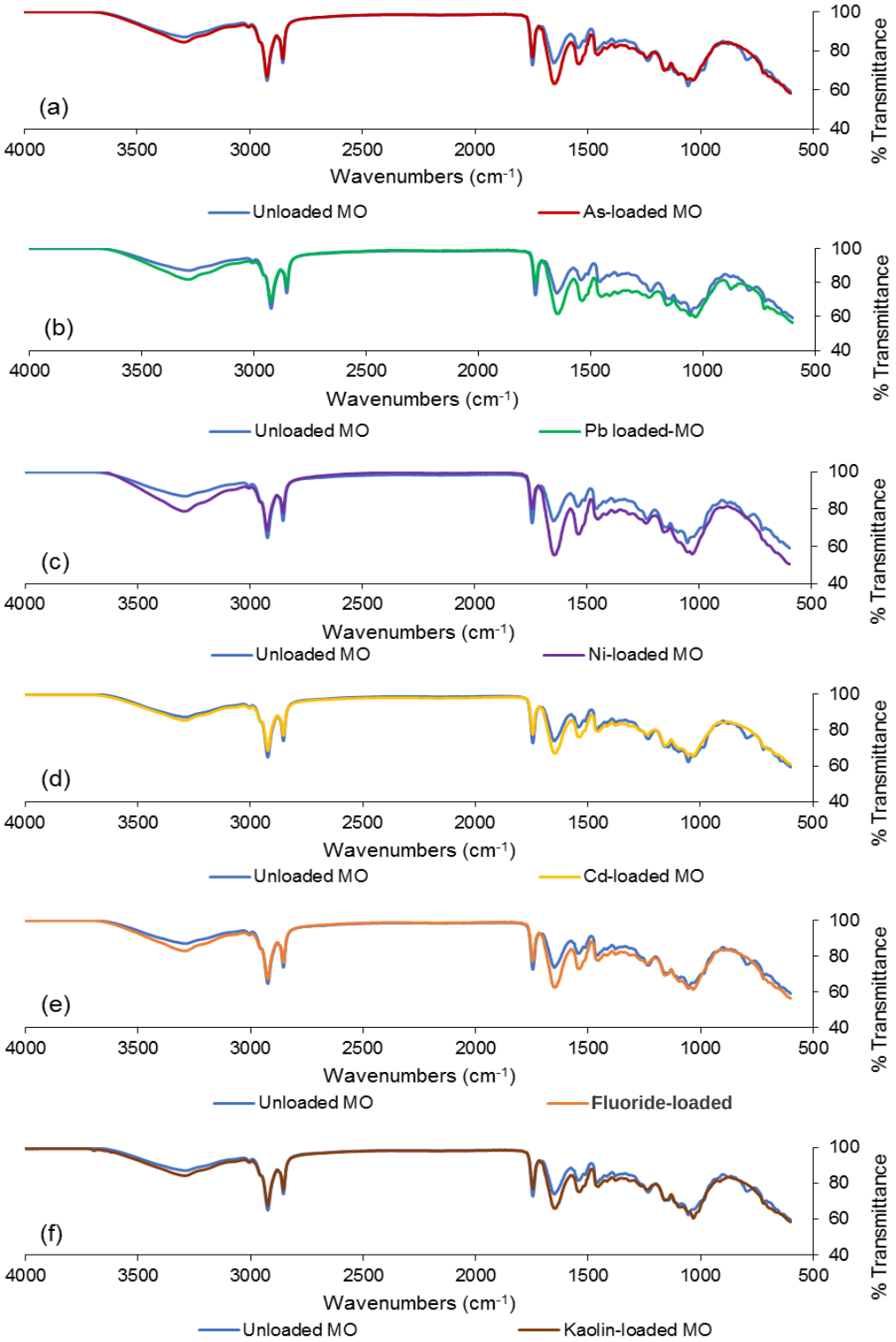

Figure 5.2 FTIR spectra of unloaded MO and (a) As-, (b) Pb-, (c) Ni-, (d) Cd-, (e) fluoride- and (f) kaolin-loaded MO

Bhende & Jadhav (2012) reported that interaction of proton donors with carbonyl oxygen through hydrogen bonding could reduce the frequency of the C=O because of

the weakening of C=O bond. In the present study, this phenomenon can be seen through the shift of the peak at 1656 cm^{-1} (unloaded MO) to a lower wavenumber of 1654 cm^{-1}, respectively (As-, Cd- fluoride-, and kaolin-loaded MO, respectively).

From the previous findings in Chapter 4 (Section 4.2), MO shows a very promising removal efficiency for turbidity (represented by kaolin in this chapter) with 93% removal compared to As (18%), Cd (40%) and fluoride (25%) at an optimum dose of MO (200 mg/L). In contrast to the findings with As, Cd and fluoride, it was inferred that the removal of turbidity by MO seeds was assisted dominantly by the coagulation activity and other mechanisms such as adsorption and charge neutralisation (Sengupta et al., 2012). Several researchers have also reported that the cationic proteins of MO seeds, which were with high in molecular weight, that is between 6 to 16 kDa, contributed to the destabilisation of particles in water (Ndabigengesere K. & Narasiah, 1998).

On the other hand, significant alterations of transmittance intensity for Pb- and Ni-loaded MO were observed in these two regions; 3500 to 3000 cm^{-1} and 1700 to 600 cm^{-1} (Figure 5.2b and Figure 5.2c). In the first region, the peak of transmittance intensity centered at 3314 cm^{-1} (O-H stretch of carboxylic acids and N-H stretch of secondary amines) changed slightly, indicating the role of these two groups in adsorbing Pb and Ni on the MO seeds, respectively. Furthermore, the broad band between 3500 and 2500 cm^{-1} confirms the presence of carboxylic acids (Reddy et al., 2012). Whereas in the second region (1700 to 600 cm^{-1}) the change in the peak intensities are noticeable, especially at 1656 cm^{-1} (C=O stretch of carbonyl amides), 1550 cm^{-1} (N-H bend of primary amines and amides), 1467 cm^{-1} (C-H bend of alkanes), 1243 cm^{-1} (C-O strecth of carboxyic acids and C-N stretch of amines), and

1059 cm^{-1} (C-O stretch of ethers). Thus, it was presumed that there were interactions between these above functional groups with Pb and Ni. Similar to the previous cases (As, Cd, fluoride and kaolin), the disappearance of peak 800 cm^{-1} (C-H bend of alkenes) indicates the role of alkenes in the complexation with Pb and Ni ions. Meanwhile, it is worth to note that a new peak appeared at the wavenumber of 879 cm^{-1} (N-H wag of amines) shows that the Pb removal was also assisted by the presence of this additional group. The finding indicates that carboxylic acids and secondary amines, carbonyl amides, amides or aromatic compounds, alkanes, ethers and alkenes were the contributing functional groups for the removal Pb and Ni by MO seeds. Therefore, it is worth to note that the number of reactive groups is higher when Pb and Ni was in contact with the MO seeds compared to As, Cd, fluoride and kaolin adsorption on the MO. Table 5.1 summarises the significant peaks detected for the unloaded and the contaminant-loaded MO.

Table 5.1 Summary of significant peaks detected for unloaded MO (before treatment) and contaminant-loaded MO (after treatment)

Bond	Region (cm^{-1})	Functional group	Wavenumbers (cm^{-1})						
			UB*	LB*					
				As	Pb	Ni	Cd	Fluoride	Turbidity
O-H stretch, N-H stretch	3500-2500 3400-3300	Carboxylic acids Secondary amines	3314	3314	3313	3315	3314	3313	3314
C-H asymmetric stretch	3000-2850	Alkanes	2926	2926	2926	2927	2927	2926	2927
C-H symmetric stretch	3000-2850	Alkanes	2856	2855	2856	2856	2856	2856	2856
C=O stretch	1750-1720	Carbonyl (Esters)	1748	1747	1747	1748	1747	1748	1747
C=O stretch	1690-1640	Carbonyl Amides)	1656	1654	1653	1653	1654	1654	1654
N-H bend N-H bend	1640-1550 1560-1500	Primary amines Amides	1550	1547	1545	1546	1548	1548	1548
C-H bend	1480-1350	Alkanes	1467	1466	1458	1461	1466	1465	1466
C-O stretch C-N stretch	1320-1210 1250-1000	Carboxlylic acids Amines	1243	1247	1248	1248	1248	1247	1247
C-N stretch	1250-1000	Amines	1166	1165	1165	1165	1165	1164	1164
C-O stretch	1300-1000	Ethers	1059	1052	1039	1039	1052	1055	1036
N-H wag	1000-675	Amines	-	-	879	-	-	-	-
N-H wag	1000-675	Amines	800	-	-	-	-	-	-

*UB (unloaded biomass), LB (loaded biomass)
References: Silverstein et al. (1981), Kwaambwa & Maikokera (2008), Reddy et al. (2012), Bhende & Jadhav (2012), Sharma & Paliwal (2013) and Bhutada et al. (2016)

5.1.2 *Musa cavendish* (MC)

FTIR spectral analyses were also conducted for both unloaded and contaminant-loaded MC to identify any changes in the spectrum profile of the contaminant-loaded biomass, which might indicate the possibility of interactions between the target contaminants and MC.

5.1.2.1 Unloaded MC

The vibration displayed by the FTIR spectrum of the unloaded MC was less intense compared to the unloaded MO (Figure 5.2 and Figure 5.3). This is due to different biomass might contain different functional groups.

In the spectrum of the unloaded MC, a broad band was shown at 3305 cm^{-1} (O-H stretch of carboxylic acids and N-H stretch of secondary amines). This was in agreement with the previous studies which related the apperance of broad band in the region between 3500 and 2500 cm^{-1} which shows the presence of carboxylic acids and association of secondary amines from proteins (Reddy et al., 2012; Bhutada et al., 2016).

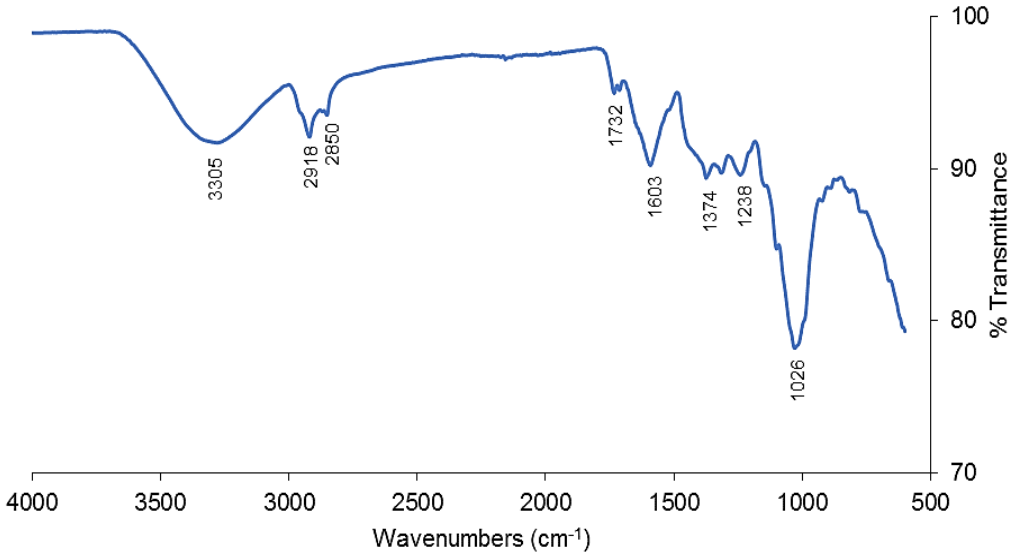

Figure 5.3 FTIR spectra of unloaded MC

The appearance of double peaks at 2918 cm^{-1} and 2850 cm^{-1} were assigned to C-H asymmetric and symmetric stretch of alkanes. Other peaks were also observed at 1732 cm^{-1} (C=O stretch of carbonyl esters), 1603 cm^{-1} (N-H bend of amides), 1374 cm^{-1} (C-H bend of alkanes), 1238 cm^{-1} and 1026 cm^{-1} (C-O stretch of ethers, respectively) (Figure 5.3). The identification of these groups was considered as a basis for the subsequent comparison with the contaminant-loaded MC. Furthermore, this allows the determination of the functional groups that is responsible for the removal of individual target contaminants by examining the significant alterations on the FTIR spectra of contaminant-loaded MC. The FTIR spectrum of the unloaded MC found in the present study are comparable to that reported by other researchers (Gopi et al., 2014; Rajoriya & Kaur, 2014).

5.1.2.2 Contaminant-loaded MC

Generally, the FTIR spectra profiles for most contaminant-loaded MC are nearly identical to the unloaded MC, except for Cd-loaded MC (Figure 5.4d). It was inferred that Cd are prone to interact with the functional groups, which are represented by the smoothen peaks as observed in the region between 1800 and 600 cm^{-1}. There were significant changes of peak intensities for most of the target contaminants except for Ni- and fluoride-loaded MC as shown in Figure 5.4c&e. The FTIR spectra of Ni and fluoride remained unchanged, suggesting that the possible mechanism of adsorption of these elements might be through a physisorption rather than a chemisorption process.

For the other contaminants, most of the peak intensities were altered in the region between 1750 to 800 cm^{-1} which corresponded to the presence of carbonyl (esters), amides, alkanes, ethers and amines. Table 5.2 presents the significant peaks for the

unloaded MC and the contaminant-loaded MC, while Figure 5.4 displays FTIR spectra of the unloaded and contaminant-loaded MC.

Table 5.2 Summary of significant peaks for unloaded MC (before treatment) and contaminant-loaded MC (after treatment)

Bond	Region (cm^{-1})	Functional group	Wavenumbers (cm^{-1})						
			UB	LB					
				As	Pb	Ni	Cd	Fluoride	Turbidity
O-H stretch, N-H stretch	3500-3300 3400-3300	Carboxylic acids Secondary amines	3305	3334	3299	3325	3328	3325	3322
C-H asymmetric stretch	3000-2850	Alkanes	2918	2919	2918	2913	2913	2915	2914
C-H symmetric stretch	3000-2850	Alkanes	2850	2855	2850	2851	2850	2855	2850
C=O stretch	1750-1720	Carbonyl (Esters)	1732	1734	1740	1728	1724	1727	1728
N-H bend	1650-1590	Amides	1603	1629	1621	1627	1631	1623	1622
C-H bend	1480-1350	Alkanes	-	1453	1430	1455	1448	1449	1435
C-H bend	1390-1370	Alkanes	1374	1375	1388	1381	1361	1359	1366
C-O stretch	1300-1000	Ethers	1238	1241	1242	1250	1243	1242	1262
C-O stretch	1300-1000	Ethers	1026	1026	1024	1034	1034	1032	1034
N-H wag	1000-675	Amines	-	888	886	880	880	881	880

*UB (unloaded biomass), LB (loaded biomass)
References: (Bhende & Jadhav, 2012; Bhutada et al., 2016; Kwaambwa & Maikokera, 2008; Reddy et al., 2012; Sharma & Paliwal, 2013; Silverstein et al., 1981)

According to Table 5.2, the new peaks observed in the region between 1430 cm^{-1} to 1455 cm^{-1} and 880 cm^{-1} to 888 cm^{-1} on all contaminant-loaded MC corresponded to the presence of C-H bend of alkanes and N-H wag of amines. This may indicate the interaction of these contaminants with alkanes and amines groups. The presence of the peaks between 880 cm^{-1} to 888 cm^{-1} suggested that the deformation of N-H (amines) might occurred during the removal of contaminants process (Zheng & Wang, 2013). Zheng & Wang (2013) also reported that bands appearing at 889 cm^{-1} which represent the same functional group was retained through the adsorption of gold (Au) ion with hydroxyl group (-OH) on MC biomass. According to the authors, peaks observed from 1600 to 950 cm^{-1} are assigned to esters and polysaccharides. These groups have strong affinity towards Au ion and base metal ions such as Cu, Fe, Ni and Pb, which may also be the case for the heavy metals (As, Pb, Ni and Cd) in the present study.

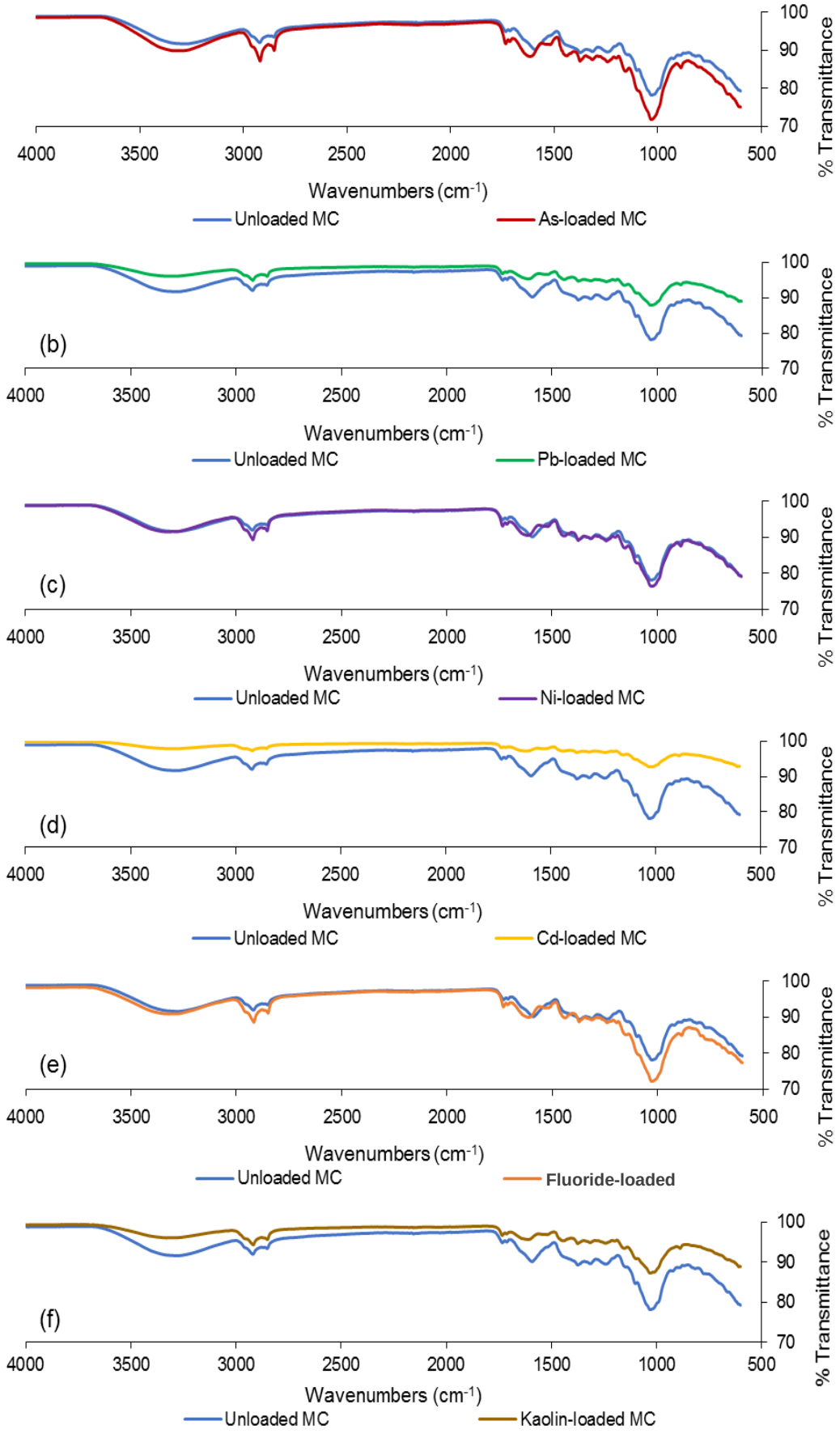

Figure 5.4 FTIR spectra of the unloaded MC and (a) As-, (b) Pb-, (c) Ni-, (d) Cd-, (e) fluoride- and (f) kaolin-loaded MC

5.1.3 Combined biomass (MO+MC)

5.1.3.1 Unloaded MO+MC

Prominent peaks for combined biomass are presented in Figure 5.5 were observed at wavenumbers of 3375 cm^{-1} (O-H stretch of carboxylic acids and N-H stretch of secondary amines), 2920 cm^{-1} and 2854 cm^{-1} (C-H asymmetric and symmetric stretch of alkanes, respectively), 1745 cm^{-1} (C=O stretch of carbonyl esters), 1650 cm^{-1} (C=O stretch of carbonyl amides and carboxylic acids), 1516 cm^{-1} (N-H bend of primary amines and amides), 1452 and 1375 cm^{-1} (C-H bend of alkanes, respectively), 1323 cm^{-1} (N=O bend of nitro compounds), 1286, 1233, 1154 and 1022 cm^{-1} (C-O stretch of ethers), and 884, 808 and 717 cm^{-1} (N-H wag of amines).

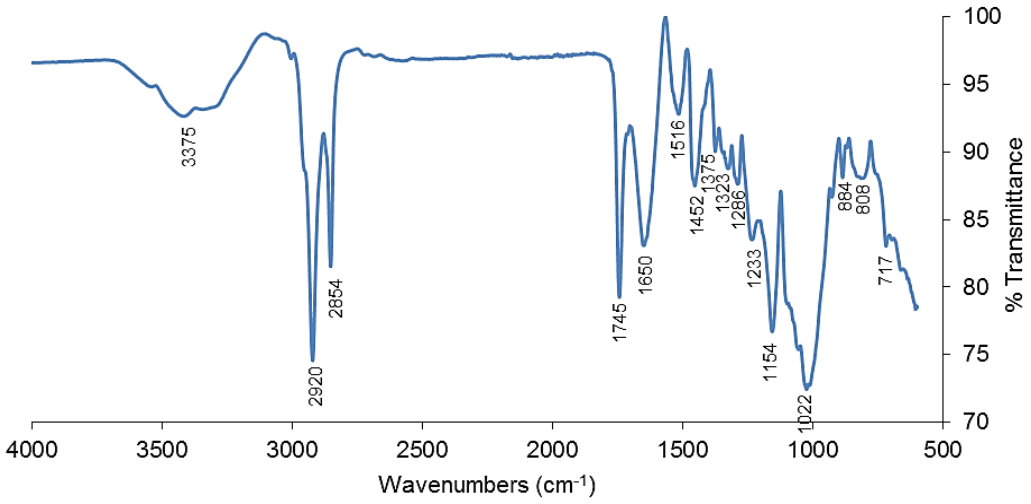

Figure 5.5 FTIR spectra of the unloaded MO+MC

Interestingly, the combination of MO and MC (MO+MC) exhibited additional groups as indicated at 1323 cm^{-1} (N=O bend of nitro compounds), 1286 cm^{-1} (C-O stretch of ethers), 884 and 717 cm^{-1} (N-H wag of amines, respectively) when their functional groups are compared to the individual MO and MC. The additional groups of the MO+MC might have led to a better performance when compared with the individual MO and MC on most of the target contaminants except Pb and turbidity as reported in

Chapter 4 (Section 4.2). The additional functional groups might result from the possible chemical interactions between the existing functional groups of MO and MC.

This finding has not been previously reported elsewhere. Further FTIR spectral analyses on the contaminant-loaded MO+MC were expected to confirm the involvement of these additional groups in assisting the adsorption of target contaminants on the mixed biomass (MO+MC).

5.1.3.2 Contaminant-loaded MO+MC

In general, the profile of the FTIR spectra for all target contaminants are almost identical to that of displayed for the unloaded MO+MC. However, the FTIR spectra of As- and fluoride-loaded MO+MC were remained unchanged, respectively along the studied wavenumbers (Figure 5.6a&e). This finding suggests that the removal mechanism of these two contaminants might be through physisorption rather than chemisorption since there were insignificant alterations on the FTIR spectra of the As- and fluoride-loaded MO+MC as compared to the spectrum of the unloaded MO+MC. Besides, the result also indicates that As and F might not have significant chemical interactions with the available functional groups of the MO+MC.

As shown in Figure 5.6b,c,d&f, the peak at 3375 cm^{-1} were significantly shifted to the lower wavenumbers, that is between 3284 to 3293 cm^{-1} (Table 5.3). This indicates that the functional group such as carboxylic acids, secondary amines and alcohol (phenol) might have interact with Pb, Ni, Cd and kaolin during the treatment process. Table 5.3 presents the significant peaks detected for the unloaded MC and contaminant-loaded MC.

Table 5.3 Summary of significant peaks detected for unloaded MO+MC (before treatment) and contaminant-loaded MO+MC (after treatment)

Bond	Region (cm^{-1})	Functional group	Wavenumbers (cm^{-1})						
			UB*	LB*					
				As	Pb	Ni	Cd	Fluoride	Turbidity
O-H stretch, N-H stretch O-H stretch	3500-3300 3400-3300 3550-3200	Carboxylic acids Secondary amines Alcohol, phenols	3375	3366	3284	3284	3290	3286	3293
C-H asymmetric stretch	3000-2850	Alkanes	2920	2919	2922	2919	2920	2917	2918
C-H symmetric stretch	3000-2850	Alkanes	2854	2854	2854	2851	2851	2852	2858
C=O stretch	1750-1720	Carbonyl (Esters)	1745	1745	1743	1745	1742	1748	1740
C=O stretch C=O stretch	1690-1640 1700-1650	Carbonyl (Amides) Carboxylic acids	1650	1647	1640	1654	1642	1650	1640
N-H bend N-H bend	1640-1550 1560-1500	Primary amines Amides	1516	1517	1531	1532	1534	1532	1530
C-H bend	1480-1350	Alkanes	1452	1454	1465	1449	1448	1458	1457
C-H bend	1480-1350	Alkanes	1375	1370	1377	1372	1374	1374	1371
N=O bend	1400-1300	Nitro compound	1323	1320	1315	1327	1310	1308	1310
C-O stretch	1300-1000	Ethers	1286	1285	-	-	-	-	-
C-O stretch	1300-1000	Ethers	1233	1231	1232	1249	1234	1230	1235
C-O stretch	1300-1000	Ethers	1154	1158	1154	1151	1146	1149	1146
C-O stretch	1300-1000	Ethers	1022	1022	1026	1027	1022	1019	1025
N-H wag	1000-675	Amines	884	884	885	887	886	883	887
N-H wag	1000-675	Amines	808	809	-	-	-	-	-
N-H wag	1000-675	Amines	717	717	724	720	717	708	698

*UB (unloaded biomass), LB (loaded biomass)
References: Silverstein et al. (1981), Kwaambwa & Maikokera (2008), Reddy et al. (2012), Bhende & Jadhav (2012), Sharma & Paliwal (2013) and Bhutada et al. (2016)

As for Pb, Ni, Cd and kaolin, FTIR spectra for loaded-MO+MC found to be altered in the region between 1700 to 600 cm^{-1} (Figure 5.6b,c,d,f). These alterations indicate that there were possible interactions between the contaminants with the functional groups in this region which are assigned to carbonyl (amides), carboxylic acids, primary amines, amides, alkanes, nitro compounds, ethers and amines during the treatment process.

On the other hand, peaks at 1286 cm^{-1} (ethers) and 808 cm^{-1} (amines) disappeared when MO+MC were loaded with Pb, Ni, Cd, fluoride and kaolin. The disappeared peaks may be related to the chemical activities occurred between these two active groups with the target contaminants during the adsorption process.

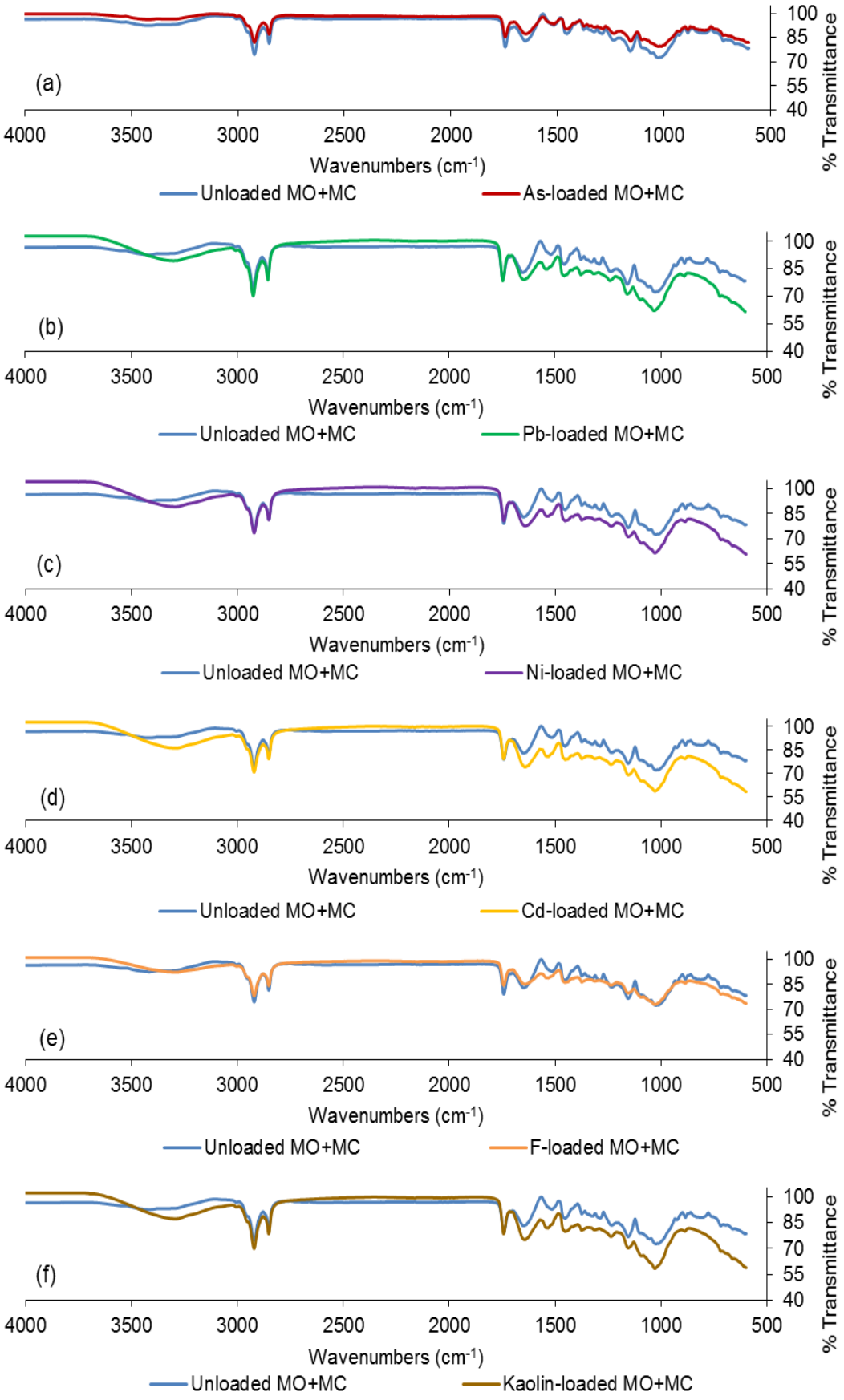

Figure 5.6 FTIR spectra of the unloaded MO+MC and (a) As-, (b) Pb-, (c) Ni-, (d) Cd-, (e) fluoride- and (f) kaolin-loaded MO+MC

Overall, the characterisation of the unloaded and contaminant-loaded biomass by FTIR spectroscopy revealed that there were various functional groups present on the biomass surface. The results indicate that there were likely interactions between heavy metals, fluoride and kaolin and the biomass (MO, MC and MO+MC).

Moreover, as revealed by the significant peaks on FTIR spectra of the unloaded MO, MC and MO+MC, possible active functional groups mainly carboxylic acids, amines and amides from protein that might responsible for the binding process of the specific contaminant which could be dependent on the type of contaminant and biomass. This phenomenon was proved by the results shown on the FTIR spectra for the unloaded biomass which exhibited some of the functional groups on MO, which were different to those of MC.

Furthermore, additional functional groups such as nitro compounds (1323 cm^{-1}), ethers (1286 cm^{-1}) and amines (884 and 717 cm^{-1}) were identified on the FTIR spectrum of the unloaded MO+MC, which might have improved the removal of some of contaminants such as Ni, Cd and Pb, compared with the individual MO and MC. Putra et al. (2014) reported that carbonates, carbonyls, hydroxyls, and amines are the main adsorption sites found in coconut tree sawdust, eggshell and sugarcane bagasse, indicating that these are the most active groups exist in many of plant-based materials. Yi et al. (2003) also suggests that the amine groups in chitosan are responsible for the binding with silver (Ag) through chelation mechanism. This explanation is in consistent with the identification of amines groups on MO, MC and MO+MC in the present study.

5.2 Scanning Electron Microscopy (SEM)

Surface morphology of the biomass before and after contaminant loading was examined using SEM instrument at 400 to 1200x magnifications. The SEM images of the unloaded biomass before and after the treatment tests are shown in Figure 5.7 to Figure 5.12. The unloaded MO and MC exhibited a porous and sponge-like surface texture (Figure 5.7 and Figure 5.9). Furthermore, the interaction occurs between the unloaded MO with the target contaminants could have resulted in the formation of fibrous texture on the surface of the MO biomass (Figure 5.8), whereas the surface structure of MC became more porous and rough after the contaminants were loaded (Figure 5.10).

On the other hand, the unloaded combined biomass (MO+ MC) shows a complex aggregated surface due to the mixing of different type of contaminants (MO and MC) as shown in Figure 5.11. Similar to the individual contaminant-loaded MO and MC, the surface of the contaminant-loaded MO+MC became porous and fibrous (Figure 5.12). The deformation of the biomass surface structure suggests interactions between the contaminants and the active sites of the biomass. For example, the development of porosity on the surface of bituminous coal was observed when potassium hydrochloride (KOH) was used for the pre-treatment of coal (Hsu & Teng, 2000). In their study, dehydrogenation and oxidation reactions were suggested to occurred between KOH and existing carbon atoms on the coal's surface. This phenomenon can be related to the finding from the current study which the attachment of the contaminants on the biomass (which contains various functional groups, particularly carboxylic acids and amines) suggests the occurrence of chemical interactions leading to such deformations on the biomass surface.

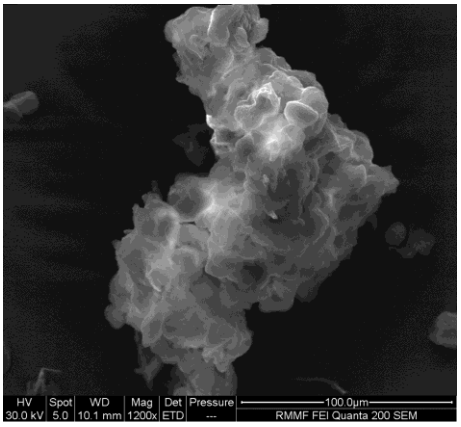

Figure 5.7 Morphological surface of unloaded MO

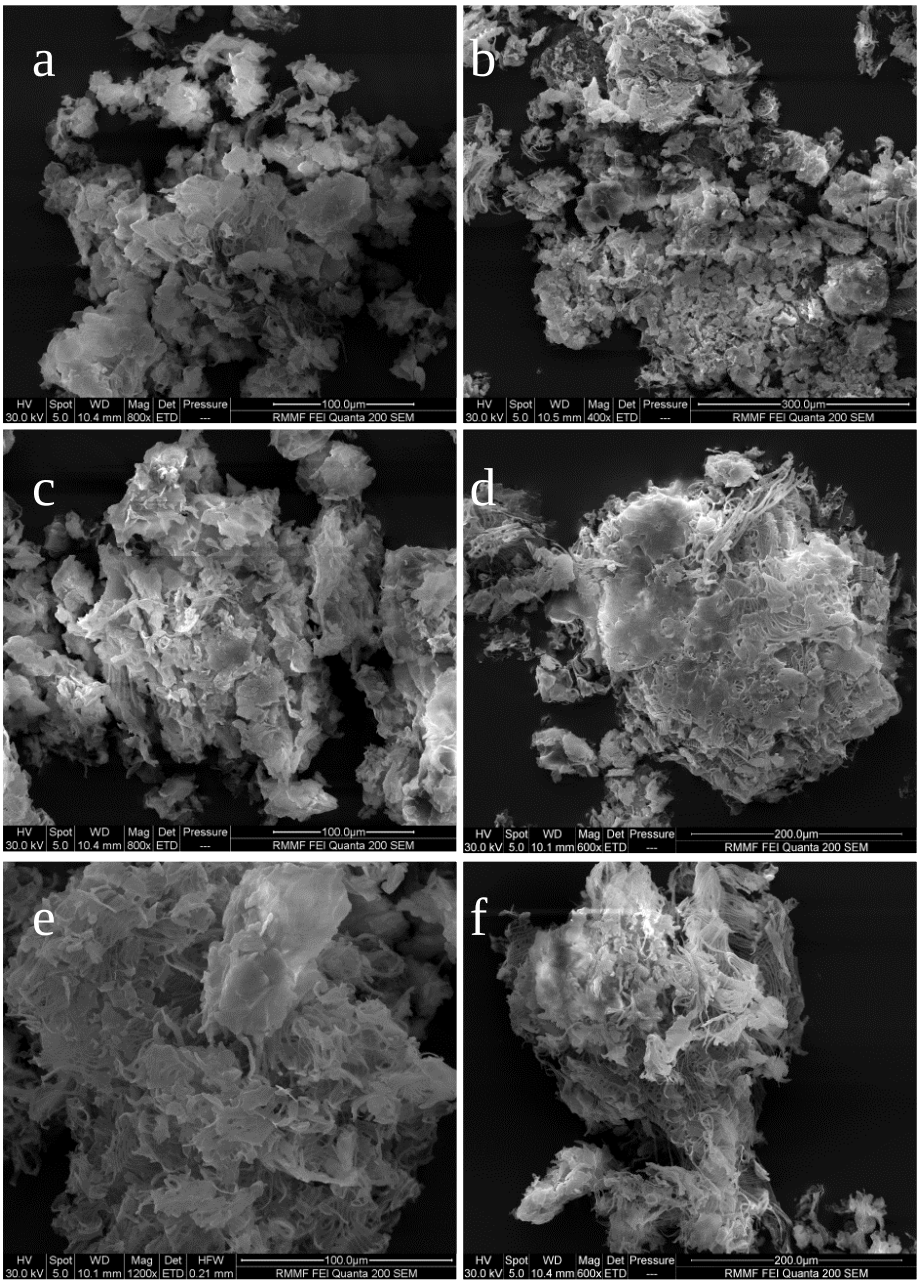

Figure 5.8 Morphological surfaces of MO loaded with (a) As, (b) Pb, (c) Ni, (d) Cd, (e) fluoride, and (f) kaolin (turbidity)

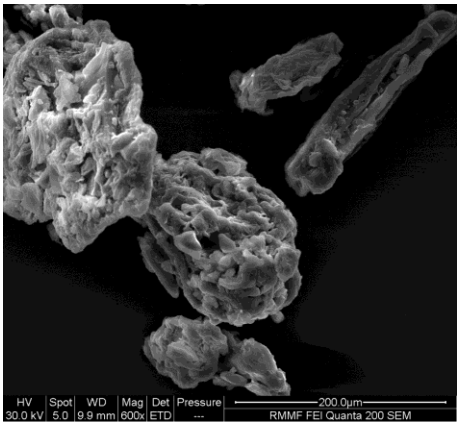

Figure 5.9 Morphological surface of unloaded MC

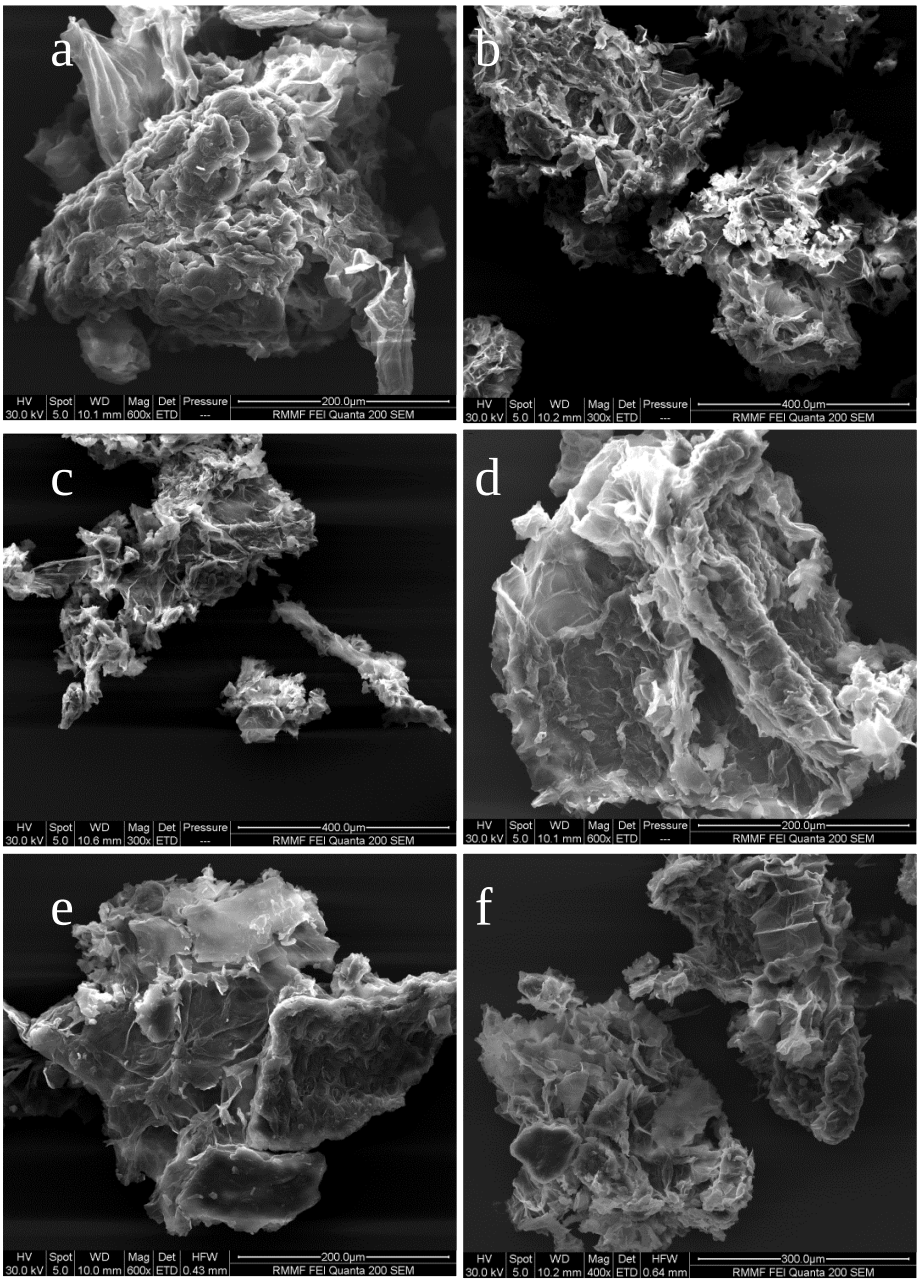

Figure 5.10 Morphological surfaces of loaded MC with (a) As, (b) Pb, (c) Ni, (d) Cd, (e) fluoride, and (f) kaolin (turbidity) after treatment

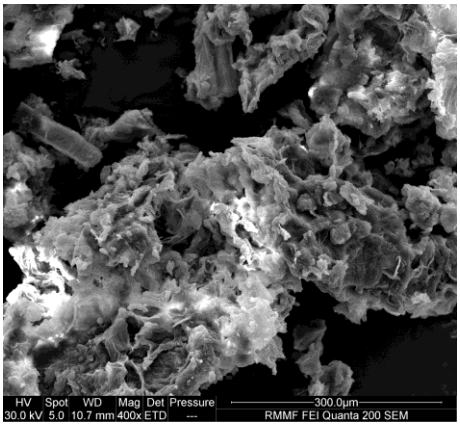

Figure 5.11 Morphological surface of unloaded MO+MC (before treatment)

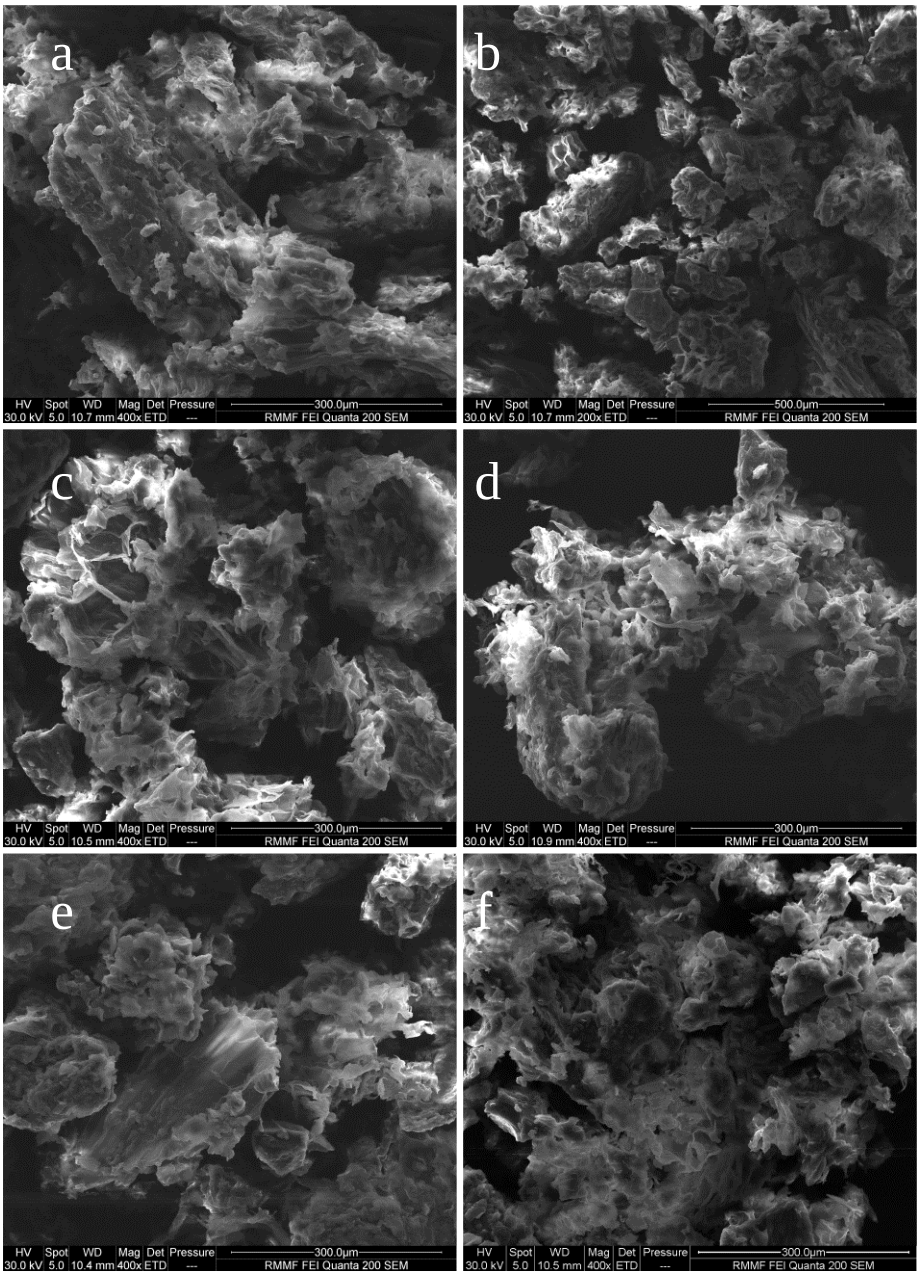

Figure 5.12 Morphological surfaces of loaded MO+MC with (a) As, (b) Pb, (c) Ni, (d) Cd, (e) fluoride, and (f) kaolin (turbidity) after treatment

It can be observed from Figure 5.8, Figure 5.10 and Figure 5.12 that there were significant changes in the surface morphology of the biomass, as well as the formation of discrete deposits on their surfaces following contaminants' attachment. The SEM analyses confirmed that the porous structure of the natural materials provide abundant binding sites for accumulating contaminants and hence leading to their removal from the solution.

Previous studies reported that the average pore size and pore area of MO seeds are 43.63 nm^2 and 8.66 μm^2, respectively (Kumari et al., 2006; Agnihotri et al., 2013). Whereas the Brunauer-Emmett-Teller (BET) surface area and pore volume of MC were reported to be 1.79 to 5 m^2/g and 0.003 m^3/g, respectively (Palma et al., 2011; Zheng & Wang, 2013). Work by Zheng & Wang (2013) also emphasised that due to high specific areas and pore volume may have contributed a role in the adsorption of gold as conducted in their study, by introducing abundant sites for contaminant binding. These findings appear to be in agreement with the results obtained from the present study.

Further EDX analyses were conducted to reveal a more detailed information on the chemical composition of the accumulants found on the surfaces of the biomass, by gaining better insights into the mechanisms involved during the contaminant removal process.

5.3 Energy Dispersive X-ray (EDX)

The chemical compositions of the unloaded biomass and contaminant-loaded biomass were analysed using the EDX instrument. The results are presented with the characteristic peaks of the elements and the percentage weight (%Wt). However, it is

important to take note that there is an aspect that has been modified due to experimental limitations such as energy of the identical beam and the composition of the sample, and hence is only used as a semi-quantitative characterisation technique (Solomon et al., 2015).

5.3.1 Elemental composition

The EDX analyses present the percentage weight of the chemical composition present on the surfaces of both the unloaded and contaminant-loaded biomass (see Appendix A2). Even though the Au element was detected on the micrographs, it has not been analysed, as it is not a nature element of the biomass. Both MO and MC showed a higher content in carbon (0.277 keV), oxygen (0.525 keV) and nitrogen (0.392 keV) than in the other elements, which may suggest the functional groups contained significant amounts of these components, hence, play a major role in the removal process of target contaminants (Figure 5.13).

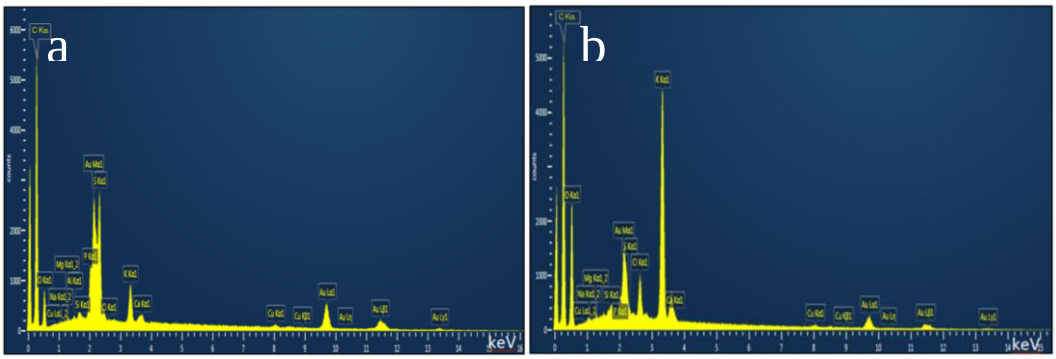

Figure 5.13 EDX spectra of unloaded (a) MO and (b) MC

It has been noted in the previous section (FTIR analysis, Section 5.1) that these key elements confirm on the existence of carbonyls (C=O), carboxylic acids (-COOH), hydroxyls (-OH) and amines (N-H) groups which present in MO, MC and MO+MC. Meanwhile, the elemental composition of the unloaded MC is consistent with several

other studies especially on the high content in potassium (K), a similar element found on the MC surface with 3.312 keV were observed (Memon et al., 2008; Zheng & Wang, 2013).

On the other hand, the adsorption of As, Pb, Ni, Cd, fluoride and kaolin (represented by the silica (Si)) have resulted in the presence of EDX, which features at 10.530, 10.550, 7.471, 3.133, 0.677 and 1.739 keV, as shown in Figure 5.14 and Appendix A2.

Tables A3.1 to A3.3 (Appendix A3) summarised the elemental compositions for the unloaded and target contaminant-loaded MO, MC and MO+MC. The major constituents of the unloaded MO (Table A3.1) are carbon (C) and oxygen (O) with percentage weight of 74.21 and 18.21%, respectively, followed by sulphur (S) and nitrogen (N) with percentage weight of 2.65 and 2.54%, respectively. Other elements were also detected, such as sodium (Na), magnesium (Mg), Aluminium (Al), silica (Si), phosphorus (P), chlorine (Cl), potassium (K), calcium (Ca) and copper (Cu) with percentage weight of 0.06, 0.28, 0.08, 0.03, 0.93, 0.04, 0.57, 0.19 and 0.21%, respectively. For the unloaded MO, the percentage weight of As, Pb, Ni, Cd and fluoride were not detected.

Similar to the unloaded MO, C and O were detected for the unloaded MC as major constituents with percentage weight of 57.22 and 34.40%, respectively. However, for the unloaded MC, K obtained the highest percentage weight of 5.63%, followed by the other elements such as N (0.29%), Na (0.14%), Mg (0.11%), Si (0.08%), P (0.15%), S (0.08%), Cl (0.93%), Ca (0.67%) and Cu (0.30%). Similar to the unloaded MO, the percentage weight of As, Pb, Ni, Cd and fluoride were not detected (Table A3.2)

For MO+MC, C and O were also found to be major constituents with percentage weight of 65.67 and 29.21%, respectively. Other elements presented were N (2.84%), Na (0.10%), Mg (0.32%), Al (0.08%), Si (0.22%), P (0.26%), S (0.30%), Cl (0.02%), K (0.33%), Ca (0.37%) and Cu (0.28%). For the unloaded MO+MC, the percentage weight of As, Pb, Ni, Cd and fluoride were also not detected (Table A3.3).

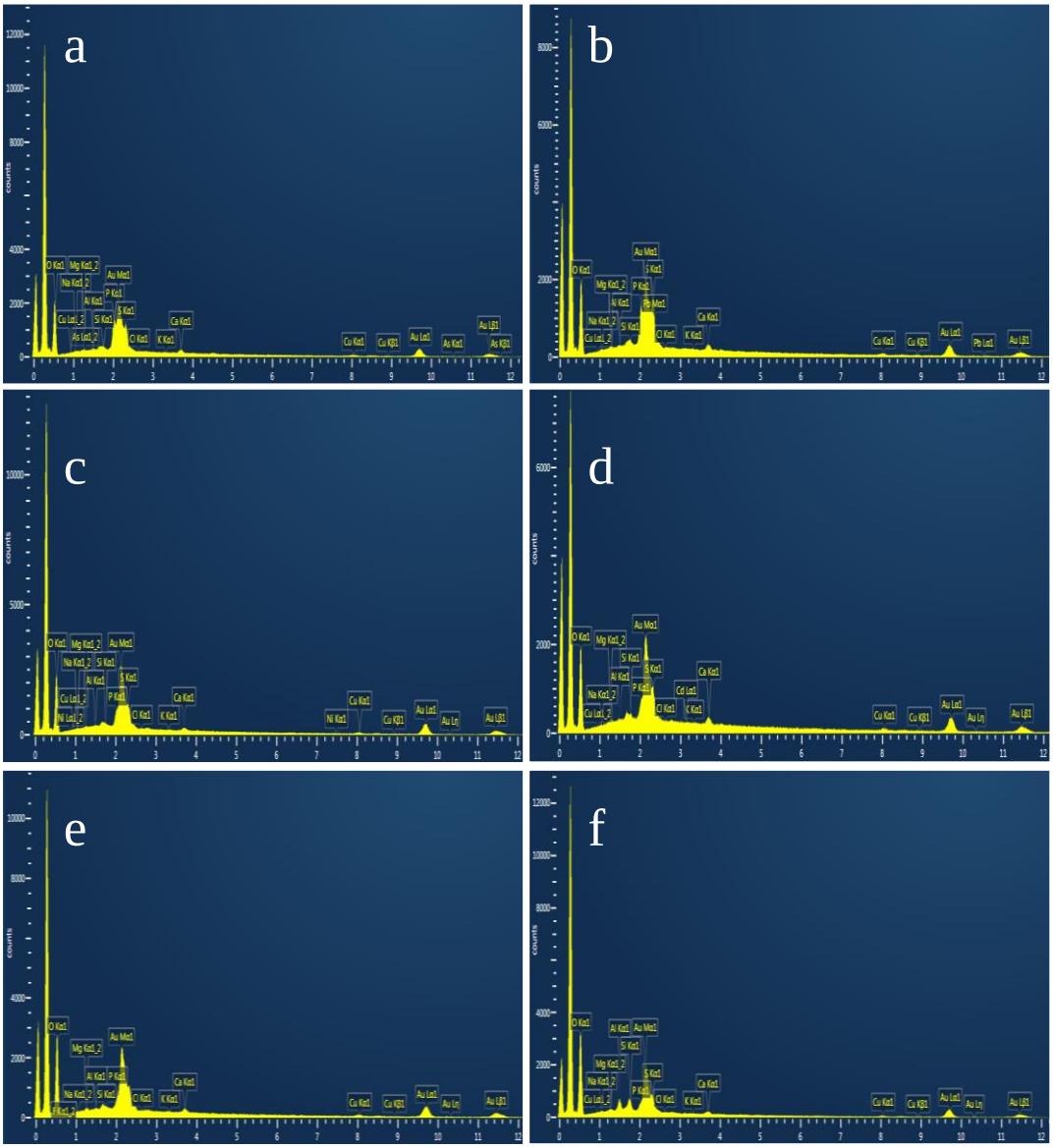

Figure 5.14 EDX spectra of MO loaded with (a) As, (b) Pb, (c) Ni, (d) Cd, (e) fluoride and kaolin (turbidity)

The elemental compositions of EDX showed a considerable amount of target contaminants on the heavy contaminant-loaded biomass, verifying the adsorption of

contaminants on their surfaces. Furthermore, there were only small amount (0.01 to 0.05%) of contaminants (i.e., As, Pb, Ni, and Cd) found in the analyses. The reason could be due to the initial concentrations of heavy metals were set relatively very low (in µg/L level) compared with the other nature elements present on the biomass surface. Moreover, x-rays released by particular element present in a sample has a proportional relationship with the concentration of that element (Heath, 2015). Nevertheless, the results might confirm their adsorption on the biomass surface.

In the case of fluoride, the fluoride-loaded MO+MC shows the highest amount of fluoride detected with 0.17% compared to the fluoride-loaded MO (0.03%) and fluoride-loaded MC. This finding also supports the earlier experimental results (Chapter 4, Section 4.2) which demonstrated that MO+MC had better performance compared to MO and MC alone in terms of fluoride removal, even though none of them could meet the WHO standard for fluoride (1.5 mg/L).

For turbidity, the kaolin-loaded MO showed an increment of Si percentage weight from 0.03% (unloaded MO) to 0.28% compared to kaolin-loaded MC from 0.08% (unloaded MC) to 0.17%. This finding supported the earlier experimental results (Chapter 4, Section 4.2) which shows that the MO gave excellent performance for turbidity removal compared to MC and MO+MC. However, for the combined MO+MC, the Si percentage weight was reduced from 0.22% to 0.08%, suggesting that the Si from kaolin might compete with the Si that exist naturally on the MO and MC for binding sites. Overall, the appearance of EDX features of As, Pb, Ni, Cd, fluoride and Si on the surface of biomass implies that the adsorption of the target contaminants on the MO, MC, and MO+MC surfaces.

5.3.2 Elemental mapping

Additional analyses were carried out using EDX elemental mapping which demonstrate the detection of target elements on the electron images of contaminant-loaded MO, MC and MO+MC. The purposes of conducting these analyses were to confirm the adsorption of target contaminant and its distribution on the biomass surface. It is important to note that the data presented may have only been interpreted qualitatively due to the elastic and thermal scattering of the electron probe through quantitative analysis (Kothleitner et al., 2014).

For this study, the analysis was done by scanning the contaminant-loaded biomass via EDX instrument which result in the detecting the elemental distribution on the biomass surface. The distribution of the target element is indicated by the colour dots which are assigned to a specific element. As can be seen in Figure 5.15, the electron images show random distribution of various nature elements of the biomass along with the adsorbed contaminants. The small box, placed at the top right of each figure signifies the magnified adsorption of an element which are (a) As, (b) Pb, (c) Ni, (d) Cd, (e) fluoride and (f) Si (kaolin). For example, Figure 5.15f shows the most obvious detection of an element (represented by the intense purple dots) which corresponds to the presence of silica (Si) or kaolin on the surface of MO. These findings indicate that the adsorption of Si was occurred during the treatment process. Although the other contaminants such as As, Pb, Ni, Cd and fluoride weredetected as shown in the electron images, they are not adsorbed as much as Si on MO surface. This might be due to the initial concentrations of these elements, which are lower than the other nature elements of the biomass (in µg/L level) or the low adsorption of these elements (i.e. As and fluoride) on MO.

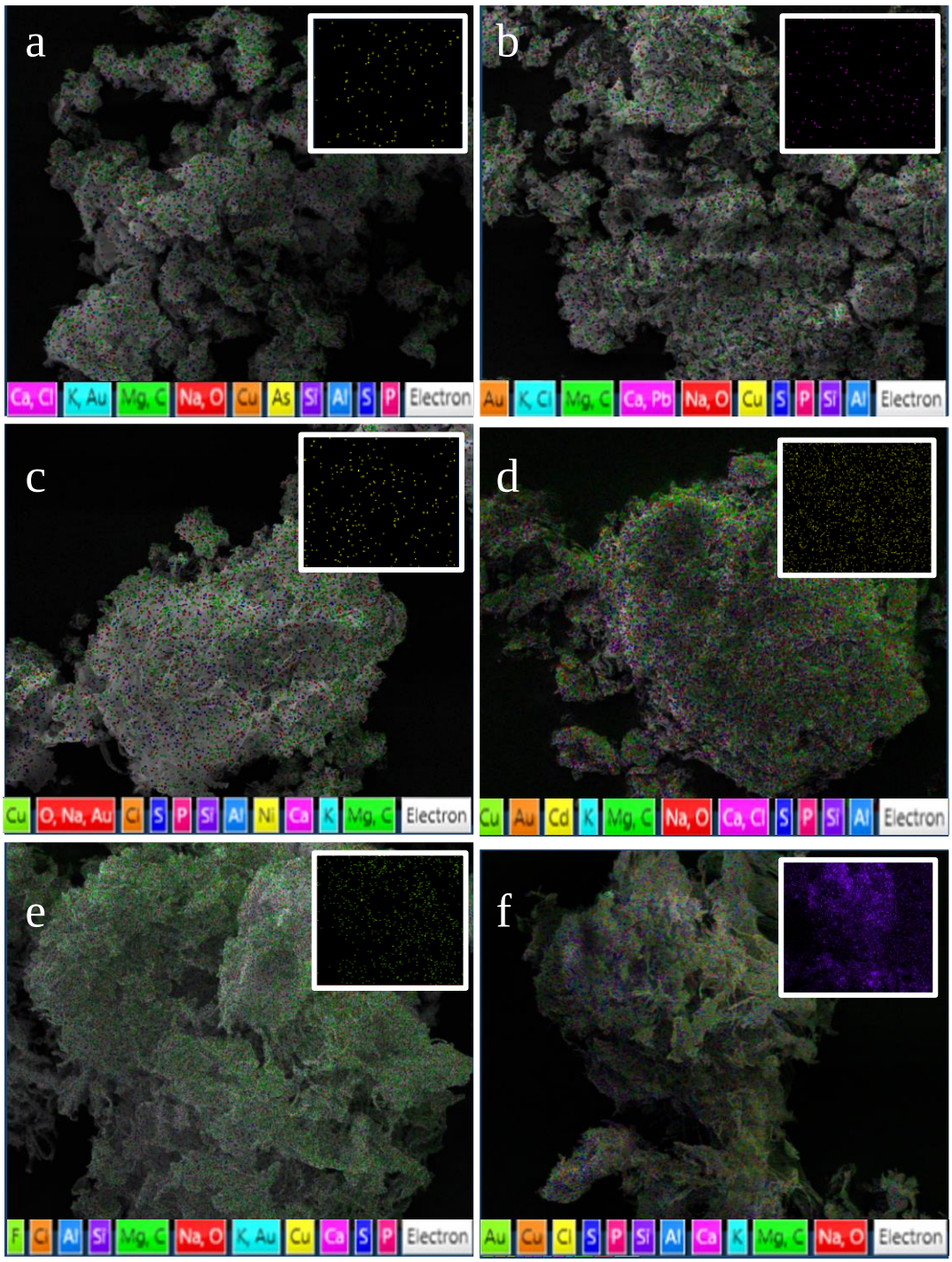

Figure 5.15 EDX elemental mapping images of MO loaded with (a) As, (b) Pb, (c) Ni, (d) Cd, (e) fluoride and (f) kaolin (turbidity)

The same observations were done on MC and MO+MC as documented in Appendix A4. The electron images confirmed the adsorption of target contaminants on MC and MO+MC (Figures A4.1 and A4.2, respectively). The difference in the distribution of the adsorbed elements on the biomass surface indicates that the adsorption capacity

for different contaminants may be due to their atomic properties (Moreno-Tovar et al., 2014).

It was also suggested that the adsorption is not the only mechanism involved in removing contaminant when using a plant-based biomass. There are other mechanisms that in the process of contaminant removal by using natural materials. Prior studies conducted by Jahn (1988) and Poumayen et al. (2012) found that the cationic peptides and polyelectrolytes located at the side chain of proteins in MO present when the pH of water is less than 10. This also could be the reason for the adsorption of anion such as fluoride (F) and turbidity on the biomass surface. Such characteristics suggests that through adsorption for other metal ions (i.e., Pb, Ni, Cd and As) could be facilitated by the chemical interactions occurred between the active functional groups such as amine and carboxylic acids with the metal ions as found in the present study.

The detection of oxygen (O) and nitrogen (N) by the EDX instrument on the biomass surfaces suggest electron pair sharing might occurred between these electron donor atoms (O and nitrogen N) with the contaminants which consequently result in a complex formation on the biomass surface. This phenomenon is called surface complexation mechanism. Another study reported by Zhu et al. (2012) suggested that electrostatic attraction could also play a role between the target contaminants and the specific functional group such as of carbonyl group (C-O stretch). In addition to that, a slight decrease in pH which was recorded whenever the biomass was in contact with the target contaminants particularly heavy metals (as discussed in Chapter 4, Section 4.1.4), may be an indication of the occurrence of ion exchange between the functional groups and the contaminants.

5.4 Conclusions

The results from this study highlight on the possible mechanism(s) of the removals of arsenic (As), lead (Pb), nickel (Ni), cadmium (Cd), fluoride and turbidity from synthetic groundwater by *Moringa oleifera* seeds (MO), *Musa cavendish* peel (MC) and the combination of both (MO+MC) as an alternative low-cost biomass.

The combination of different characterisation methods such as Attenuated Total Reflectance-Fourier Transform Infrared spectroscopy spectrum (ATR-FTIR) 100 (Perkin Elmer), Scanning Electron Microscope (SEM Quanta FEI 200) and Energy Dispersive X-Ray (EDX) indicated that the biomass interacted with target contaminants in different ways.

The FTIR analyses showed carboxylic acids, primary and secondary amines and carbonyl (amides) were the dominant functional groups in MO, MC and MO+MC, which would favour the adsorption of the studied contaminants. Additional functional groups (nitro compounds, ethers and amines) that appeared on the FTIR spectrum of the unloaded MO+MC, indicates possible additional contributing factors for contaminant removal compared to the individual MO and MC. Thus, it is suggested that the combination of two different biomass has the potential to improve the treatment efficiency of the biomass.

The SEM images exhibited the abundant availability of porous and irregular surfaces which could provide binding sites that facilitate the accumulation (adsorption) of target contaminants on the biomass.

The EDX analysis demonstrated the existence of oxygen (O) and nitrogen (N) on the biomass surface. This could suggest that electron sharing had occured between donor

atoms (O and nitrogen N) and the contaminants, resulting in the formation of contaminant-biomass complexes. Furthermore, the detection of a specific feature (element) on the EDX spectrum of the contaminant-loaded biomass (i.e., after treatment) confirmed the adsorption of the contaminant by the biomass. In addition to that, a slight decrease in pH of the treated water indicated the occurrence of ion exchange between the functional groups and the contaminants.

Overall, adsorption was suggested as a key mechanism for the removal of the target contaminant due to the abundant availability of porous and irregular surfaces which provide binding sites to facilitate the accumulation of target contaminants on the biomass. Adsorption by the biomass may be considered as physisorption and/or chemisorption depending on the nature of the contaminants. However, it was suspected that other mechanisms might also involve in the removal processes, such as surface complexation, electrostatic attraction and ion exchange.

The understanding on the mechanism of the treatment using the studied biomass should be taken into account in the future development and design considerations. For example, a suitable pre-treatment method which intending to improve the treatment efficiency of biomass can be selected knowing the chemical and physical properties of the tested biomass.

CHAPTER 6 Selection of an adsorption model to predict treated groundwater with natural biomass

In the previous chapter, possible mechanisms involved in the treatment process were examined by characterising the unloaded and contaminant loaded-biomass using Attenuated Total Reflectance-Fourier Transform Infrared spectroscopy (ATR-FTIR) spectrum 100 (Perkin Elmer), Scanning Electron Microscope (SEM Quanta FEI 200) and Energy Dispersive X-Ray (EDX) instruments. From the characterisation study, adsorption was identified as the main mechanism for the target contaminant removal process mainly due to the abundant availability of porous and irregular surfaces which provide binding sites for target contaminants accumulation. Additionally, detection of specific features on EDX spectra of contaminant-loaded biomass (after treatment) that correspond to the existence of target contaminants demonstrated that the adsorption of these elements had occurred (Chapter 5). The mode of adsorption operation for this study was explained in Chapter 3 (Section 3.5). In this chapter, adsorption batch experiments were carried out for MO, MC and combination of the two biomass (MO+MC) for the removal of lead (Pb), nickel (Ni) and cadmium (Cd). The experiment was performed by applying the coagulation processes as reported in Chapter 4. Pb, Ni and Cd were the contaminants chosen for this study (present chapter) based on the findings from Chapter 4 which demonstrated that the selected biomass did not remove arsenic (As) and fluoride to meet the WHO standards. In this chapter, Langmuir, Freundlich and Sheindorf-Rebhun-Sheintuch (SRS) adsorption models were evaluated to describe the behaviour of the adsorption process (Freundlich, 1906; Langmuir, 1916; Sheindorf et al., 1981) as described in detail in Chapter 3. Langmuir and Freundlich adsorption models were assessed for the single and multi-element systems while the SRS model was assessed for the multi-element system. The final part of this chapter investigates whether the optimum doses of biomass/es (MO: 200

mg/L, MC: 200 mg/L and MO+MC: 200+200 mg/L) that have been determined in the previous experiments can treat the incoming target contaminant concentrations to bring the parameters to be within WHO standards with a certain reliability using the selected model.

Overall, this chapter presents the effect of initial concentration of heavy metal on the performance of the selected biomass. The experiment was followed by investigation on the applicability of the selected adsorption models for single and multi-element adsorptions and verifications of the models. Prediction of treated water quality using the selected adsorption was also carried out. Presentation of the results involved generation of random number and probability plots for the groundwater quality input, followed by the estimation of heavy metals in treated water by MO, MC and MO+MC; presented as probability and cumulative density functions. Furthermore, uncertainty analysis, exceedance probabilities of WHO drinking water quality standards and concluding remarks are also presented.

6.1 Effect of the initial heavy metal concentrations

Table 3.5 and Table 3.6 present the initial concentrations (in molarity unit) of the contaminants in single-element and multi-element synthetic groundwater samples, respectively. The samples were prepared as reported in Chapter 3 (Section 3.2.1). The initial concentration values of heavy metals were chosen based on the mean groundwater quality values reported in the literature (Midrar-Ul-Haq et al., 2005; Bandara et al., 2010; Buragohain et al., 2010).

The initial concentrations of Pb, Ni, and Cd of the single-element synthetic groundwater samples were varied as shown in Table 3.5. Figure 6.1a depicts the relationship between initial Pb concentration and removal efficiency at fixed dosages

of 200 mg/L for each of MO and MC, and 200+200 mg/L for MO+MC. The above doses were the selected optimum biomass doses as reported in Chapter 4. For MO, the increase of initial Pb concentration from 0.024 µmol/L to 0.097 µmol/L increased the Pb removal from 65% to 81%. However, Pb removal remained unchanged (around 79% to 81%) for concentrations between 0.097 to 0.483 µmol/L. Similar to MO, the removal percentage increased from 32% to 61% with MC until the Pb concentration is 0.290 µmol/L. The removal of Pb was slightly reduced from 61% to 58% with the increase of Pb initial concentration beyond 0.290 µmol/L. The combined biomass gave similar removal rates to MO alone. For the removal of Pb, MC showed the least removal efficiency compared to MO and MO+MC.

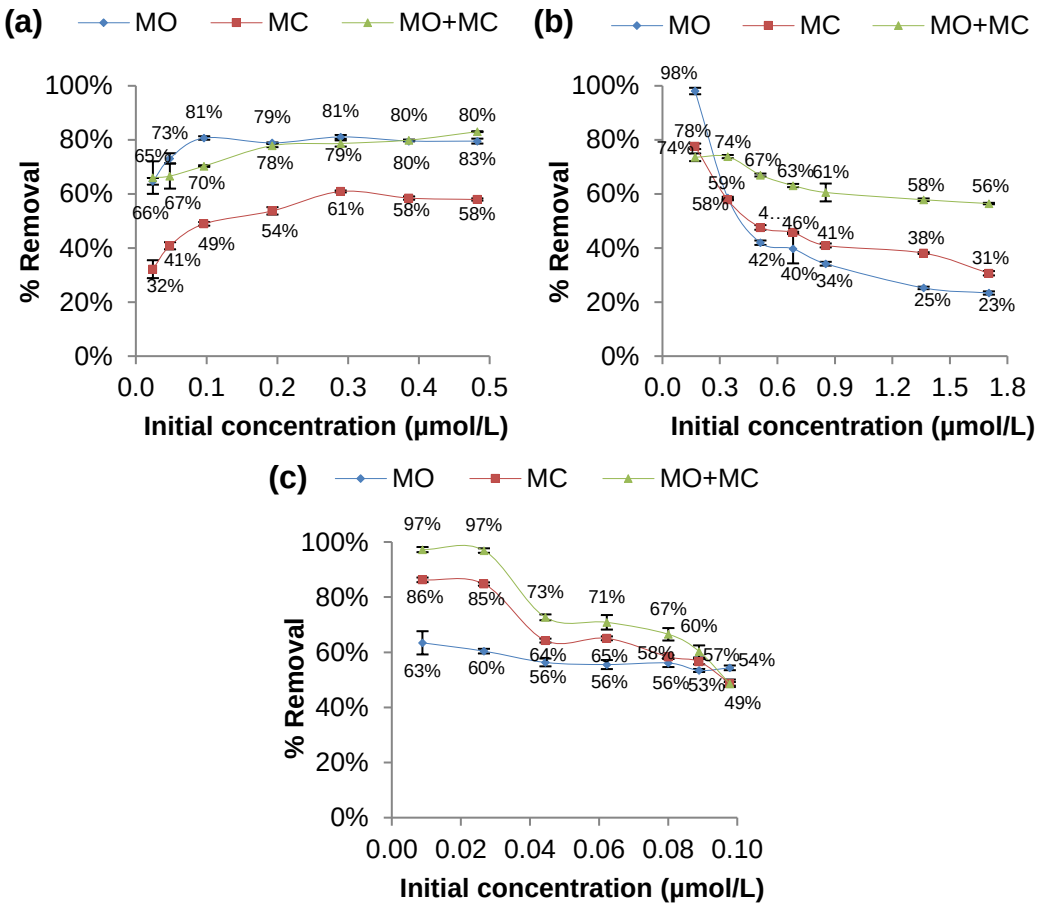

Figure 6.1 The relationship between removal efficiency of plant-based biomass and initial concentrations of (a) Pb (b) Ni (c) Cd

In contrast to Pb, removal efficiencies with MO, MC and MO+MC were decreased with the increase of Ni and Cd concentrations. Figure 6.1b shows that the removal efficiency decreased rapidly from 98% to 42% with MO when Ni concentration was increased from 0.170 to 0.511 μmol/L. The rate of decrease in removal efficiency was lower with MC and MO+MC when the initial Ni concentrations were gradually increased. As depicted in Figure 6.1b the removal efficiency of Ni was improved by combining MO and MC.

Similar to Ni, MO+MC showed a better removal efficiency of Cd compared to MO and MC alone. There was a sudden drop in removal efficiency when the Cd concentration was increased from 0.009 to 0.044 μmol/L and further reductions were shown when Cd concentration was increased beyond 0.080 μmol/L for MC and MO+MC (Figure 6.1c). Kumar et al. (2012) attributed this behaviour to the saturation of adsorption sites on biomass surface. The reduction rate of Cd with MO did not vary much (63% to 54%) when the initial concentration of Cd was increased from 0.009 to 0.098 μmol/L.

Overall, MO showed the highest removal efficiency for Pb while MO+MC showed the highest removal for Ni and Cd compared to MO and MC alone. Furthermore, it would be worth noting that the trend of Pb removals by MO, MC and MO+MC was different compared to the trend of Ni and Cd removals (Figure 6.1). The reasons underlying this phenomenon would be elucidated by further evaluating these experimental data using the Langmuir and Freundlich models.

6.2 Single-element adsorption

Langmuir and Freundlich models were presented in Chapter 3 (Equation 3.1 to Equation 3.3) and are also discussed below. Based on the Langmuir model, a plot of $\frac{C_e}{Q_e}$ vs C_e is a straight line. The Langmuir constant, Q_m (monolayer adsorption capacity, µmol/g) and K_L (binding energy, L/µmol) can be obtained from the gradient and intercept of the linear graph between $\frac{C_e}{Q_e}$ and C_e. Similarly, based on the Freundlich model, a plot of ln Q_e vs. ln C_e is a straight line. The Freundlich adsorption constants K_F (L/mmol) and n_F (dimensionless) can be obtained from the gradient and intercept of the linear graph between ln Q_e and ln C_e. C_e and Q_e are the final concentration of the heavy metal (µmol/L) and Q_e is the amount of heavy metal adsorbed (µmol/g). Results from the treatment of the first five samples in Table 3.6 were used to obtain the above parameters in Langmuir and Freundlich models while results from the treatment of the last two samples were kept to verify the above parameters.

Figure 6.2 to Figure 6.4 depict the linearisation of single-element adsorption experimental data using Langmuir and Freundlich isotherm models, respectively. Table 6.1 presents the model parameters and the coefficient of determination (R^2) obtained by fitting Langmuir and Freundlich models (Equation 3.1 and Equation 3.2) to the experimental data. Negative values have been observed for Q_m (adsorption capacity) and K_L (binding energy) by fitting the Langmuir linearisation model with MO, MC and MO+MC biomass for Pb adsorption. This condition was due to the negative gradients on the linear graph as shown in Figure 6.2a. This result indicates that the adsorption behavior of the treatment did not follow the assumptions behind the Langmuir isotherm theory (Igwe & Abia, 2007).

Negative Q_m and K_L for Pb adsorption (Figure 6.2a and Table 6.1), suggest that the adsorption behavior do not agree to assumptions in Langmuir's theory (surface of biomass is energetically homogeneous). The experimental plots of Pb adsorption by MO, MC, and MO+MC (Figure 6.2) were best fitted with Freundlich model for all three biomass with R^2 values of 0.99 (Figure 6.2b and Table 6.1). Junior et al. (2013) also reported that Freundlich model showed a better fit than the Langmuir model for Pb adsorption experimental data with MO as biomass.

Heterogenous profile of MO seeds from SEM images reported (Chapter 5) that multilayer surface of MO may facilitate the adsorption of the metal. As described in Chapter 3 (Section 3.6.1), the Freundlich model isotherm accounts for multisite adsorption of heterogeneous surfaces, whereas Langmuir theory assumes that the multilayer surface of MO may facilitate the metal adsorption. Good agreement of data with Freundlich model indicates that the Pb was interacting with the biomass multilayer sites for adsorption.

In nature, MO and MC may have heterogeneous adsorption sites. This is due to their abundant availability of functional groups, considering that they originate from plant-based materials (Okoro & Okoro, 2011). Therefore, Pb in this case might have chemical interactions with specific functional groups present on the biomass surface. Such interactions could lead to the generation of new chemical bonds that could improve the adsorption capacity of the biomass.

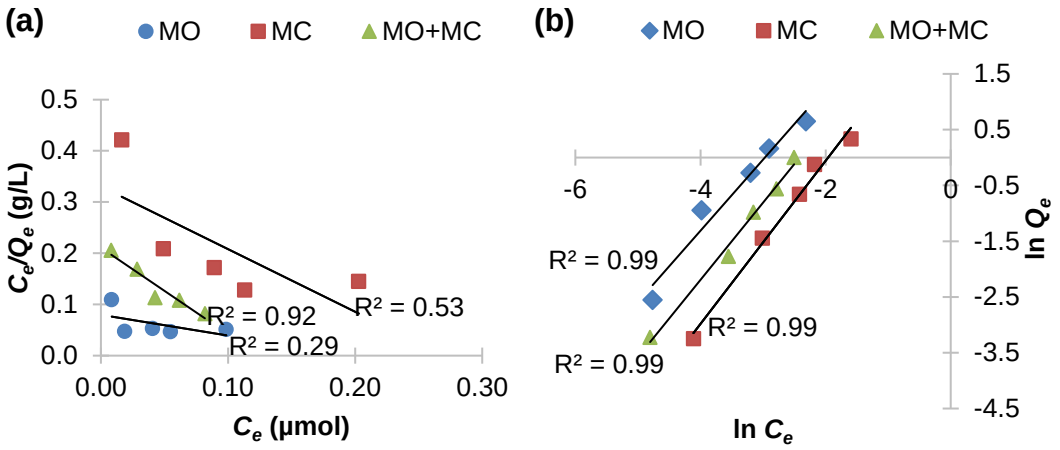

Figure 6.2 Linearisation of single-element experimental data of Pb on MO, MC, and MO+MC using (a) Langmuir and (b) Freundlich isotherm models

The experimental results of Ni adsorption on the MC and MO+MC were best fitted with Freundlich model with R^2 values of 0.98 and 1.00, respectively (Figure 6.3b and Table 6.1). On the other hand, MO exhibited a better fitness with the Langmuir model (R^2 = 0.94) as shown in Figure 6.3a and Table 6.1 compared to the Freundlich model (R^2 = 0.76). These indicate an occurrence of a greater monolayer adsorption instead of multilayer adsorption.

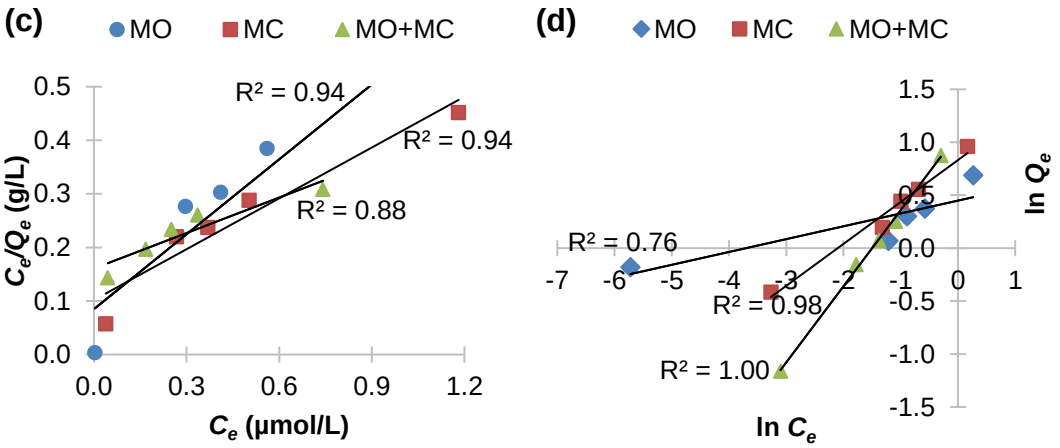

Figure 6.3 Linearisation of single-element experimental data of Ni on MO, MC, and MO+MC using (c) Langmuir and (d) Freundlich isotherm models

Based on Figure 6.4a and Figure 6.4b, the Freundlich model (R^2=1.00) demonstrated a better fit than the Langmuir model (R^2=0.81) for Cd adsorption with MO. A similar

finding was reported by Mataka et al. (2010) who found that Freundlich model (R^2=0.97) has a better fit than the Langmuir model (R^2=0.95) for Cd adsorption using MO. However, the above study was conducted at a temperature of 30°C while the current study was performed at a temperature of 20°C. The difference between the R^2 values from both models (Langmuir: R^2=0.97 and Freundlich: R^2=0.98) was insignificant when adsorption by MC was considered. This suggests that there is a possibility for Cd to undertake the multilayer and monolayer adsorption on the MC surface. This finding reinforces the conclusions made by Junior et al. (2013) that the insignificant difference between R^2 values obtained for both models, indicate a possible existence of more than one type of adsorption site interacting with Cd.

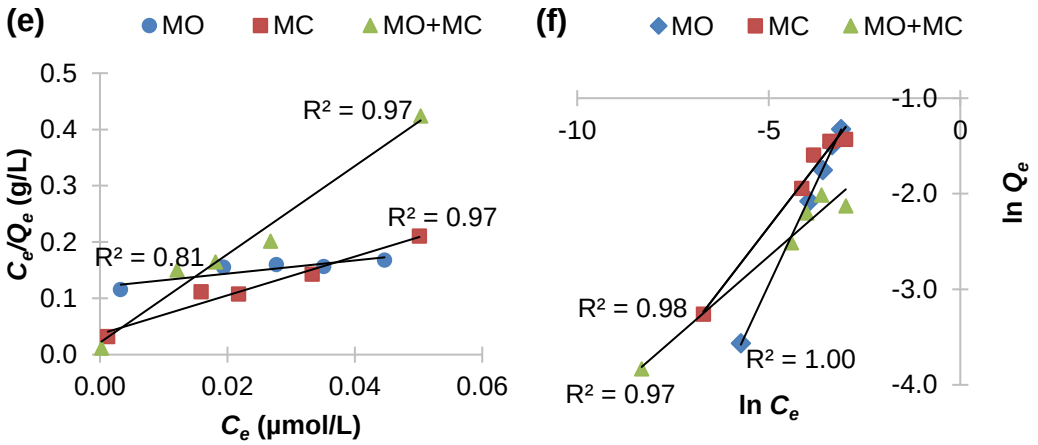

Figure 6.4 Linearisation of single-element experimental data of Cd on MO, MC and MO+MC using (e) Langmuir and (f) Freundlich isotherm models

As mentioned before, Pb did not agree to Langmuir adsorption model assumptions. The reason could be due to the specific adsorption mechanism (i.e. chemisorption) because the behavior of Pb removal was different when compared to Ni and Cd (Figure 6.3 and Figure 6.4).

In the Langmuir linearisation of MO, MC and MO+MC for Ni adsorption, it was verified that MO+MC had a higher adsorption capacity of Ni (Q_m) compared to MO

and MC alone. However, MO had the highest binding energy (K_L) with Ni. The binding energy (K_L) of Cd by MO+MC was significantly greater in the Langmuir linearisation compared with MO and MC. This result was likely the reason that the Cd removal efficiency was better achieved by MO+MC compared to MO and MC alone (Figure 6.1c).

In the Freundlich linearisation, the K_F constants (adsorption capacity) obtained for Pb by all biomass were much higher than those of Ni and Cd. This result was consistent with the increase of Pb removal with the increase in initial Pb concentration (Figure 6.1a).

The n_F value in the Freundlich model represents the reactivity of biomass active sites. According to Bhatt et al. (2012), if a value of $n_F = 1$, the adsorption is linear; for $n_F < 1$, the adsorption is chemisorption, and for $n_F > 1$ the adsorption is a favorable physical adsorption. Thus, analysing the n_F values (Table 6.1), adsorption of Pb onto MO, MC and MO+MC was found to be through chemisorption.

Table 6.1 Parameters of equilibrium of Langmuir and Freundlich models for single-element adsorption of Pb, Ni, and Cd on MO, MC and MO+MC

Heavy metal	Biomass	Langmuir isotherm coefficients			Freundlich isotherm coefficients		
		Q_m (µmol/g)	k_L (L/µmol)	R^2	n_F	k_F (L/mmol)	R^2
Pb	MO	-2.47	-5.06	0.29	0.78	44.17	0.99
	MC	-0.82	-3.71	0.53	0.68	17.55	0.99
	MO+MC	-0.59	-8.00	0.92	0.72	28.33	0.99
Ni	MO	2.15	5.50	0.94	8.25	1.57	0.76
	MC	3.16	3.10	0.94	2.53	2.30	0.98
	MO+MC	4.53	1.38	0.88	1.39	2.94	1.00
Cd	MO	0.85	9.68	0.81	1.16	3.84	1.00
	MC	0.29	95.58	0.97	1.92	1.29	0.98
	MO+MC	0.13	373.33	0.97	2.87	0.40	0.97

In this case, adsorption of Pb on MO, MC and MO+MC was likely to generate new chemical bonds at the biomass surface which could lead to the improvement of the biomass adsorption capacity. This phenomenon could explain the reason for the

increase in removal efficiency with the increase of initial Pb concentration and the higher values of K_F (adsorption capacity) compared to Ni and Cd. On the other hand, physical adsorption was shown to be favorable for adsorption of Ni and Cd on MO, MC and MO+MC. The findings made in Pb adsorption can also be elucidated by the physicochemical of the metal ions as shown in Table 6.2.

Table 6.2 Physicochemical properties of heavy metal

Properties	Pb	Ni	Cd
Atomic weight	207.2	58.693	112.411
Electronegativity	2.33	1.91	1.69
Ionic radius (Å)	1.19	0.69	0.97
Charge	2^+	2^+	2^+

Pb has a higher atomic number (207.2 g/mol) and electronegativity (2.33) compared to Ni and Cd. The high atomic number may lead to the probability of high collision occurred between the metal and biomass surface. The high negativity of Pb atom allows easy adsorption onto the biomass surface. However, ionic radius of Pb did not play a significant role in the adsorption process since the Pb ionic radius is higher than that of Ni and Cd. According to Sağ et al. (2001), the preference of metal ions adsorption does not essentially follow the general trends explained above since the observed behaviour could be attributed to the combination of the above factors.

Overall, it could be concluded that the Freundlich model gave a better agreement than the Langmuir model for single element adsorption. Evaluations of the adsorption of Pb, Ni and Cd on MO, MC and MO+MC in the multi-element system using Langmuir and Freundlich models are reported in the next section.

6.3 Multi-element adsorption

For multi-element or competitive adsorption, the original Langmuir and Freundlich models were used to determine the existence effect of other elements on the model

performance. Zhu et al. (2012) also used the original Langmuir and Freundlich isotherm models to evaluate the fitness of multi-element experimental data of Pb, copper (Cu) and zinc (Zn) on xanthate-modified magnetic chitosan. The study found that the adsorption data of Pb and Cu in the multi-element system were in good agreement with the Langmuir model while Zn had a good fit with the Freundlich model.

Initial concentrations of metals in the multi-element solutions are given in Table 3.6. Similar to the analysis of single-element solutions, Langmuir and Freundlich models were applied to obtain Q_m, K_L, n_F and K_F. The model constants obtained from the multi-element solutions are presented in Table 6.3. These constants were compared with the constants obtained from the single-element solutions (Table 6.1).

Similar to single-element adsorption, experimental data of multi-element adsorption also showed a good agreement with Freundlich model compared to the Langmuir model, except for Ni adsorption on MC with the R^2 value of 0.20. The results also indicated that both models are not suitable to be used to describe the adsorption behaviour of Ni adsorption on MC for the multi-element system.

Table 6.3 Parameters of equilibrium of Langmuir and Freundlich models for Pb, Ni and Cd adsorption on MO, MC and MO+MC

Heavy metal	Biomass	Langmuir isotherm coefficients			Freundlich isotherm coefficients		
		Q_m (µmol/g)	k_L (L/µmol)	R^2	n_F	k_F (L/mmol)	R^2
Pb	MO	-0.53	-11.27	0.67	0.55	222.07	0.99
	MC	-0.07	-10.32	0.96	0.37	609.72	0.90
	MO+MC	-0.12	-11.47	0.28	0.44	325.71	0.80
Ni	MO	3.03	4.18	0.89	4.81	2.10	0.84
	MC	8.62	0.39	0.04	5.18	1.45	0.20
	MO+MC	1.21	6.55	0.94	5.59	1.04	0.92
Cd	MO	1.35	4.16	0.06	1.12	3.41	0.94
	MC	0.28	114.61	0.97	1.86	1.45	0.96
	MO+MC	0.14	184.18	0.96	2.80	0.40	0.99

On the contrary, Ni adsorption on MC in a single-element system showed a good agreement with both Langmuir and Freundlich models. This could be attributed to the inconsistency of variations in the composition and structure of the biomass surface by changing physicochemical parameters of the solutions (Sağ et al., 2001).

Overall, the adsorption of target contaminants showed a better agreement with Freundlich model than the Langmuir model. Therefore, a comparison between Freundlich isotherm constants was made between single-element and multi-element adsorptions. Table 6.1 and Table 6.3 tabulates the model parameters obtained from both models. The adsorption constants (Q_m, $k_{L,}$ n_F and k_F) obtained for both systems were different to each other, and it could be attributed to the presence of multi-elements with various concentrations in the same system. In the next stage, existing competitive adsorption model known as the Sheindorf-Rebhun-Sheintuch (SRS) model was evaluated to determine the degree of competition between the present elements in the competitive regimes.

6.4 Application of modified Freundlich (Sheindorf-Rebhun-Sheintuch, SRS) model for competitive adsorption

The SRS model which is a multi-element adsorption model (Sheindorf et al., 1981), was chosen to evaluate its applicability in predicting treated water quality for this study. Some of the required parameters (n_i and k_i) of SRS model are similar to the predetermined parameters from the single-element adsorption experiments. Other parameters can be obtained from the multi-element adsorption experiments. The assumptions behind the application of this model are: (i) each element followed the Freundlich isotherm model; (ii) each element in multi-element adsorption, presents an exponential distribution of site adsorption energies (Sheindorf et al., 1981).

Experimental results from the multi-element samples were used to evaluate the applicability of the SRS model. It is worth noting that the SRS model does not suggest certain reaction mechanisms, but it can be used to assess the degree of competition and selectivity of the elements under certain experimental conditions (Roy et al., 1985; Selim & Zhang, 2013). However, the selectivity of heavy metal adsorption could not be evaluated for this study since the concentrations for each element in the samples were not set in equimolar. Thus, it is impossible to determine the preference of biomass towards element in this kind of adsorption (competitive) when the concentration of each heavy metal was not consistent with each other.

The competition coefficients of the SRS model ($a_{i1}, a_{i2}$and a_{i3}) are predicted from multi-element adsorption data using Equations 3.10 and 3.11 as described under Section 3.6.2 (Chapter 3). A good agreement of adsorption data with the SRS model can be demonstrated if the product of competition coefficients $a_{ij}.a_{jk}.a_{ki}$, is close to unity for the three-metal systems (Sağ et al., 2001). The product of competition coefficients for MO, MC and MO+MC were found to be 1.21, 1.20 and 1.14, respectively. These results are slightly higher than unity (Table 6.4). The reason could be due to variation in concentration of an individual metal ion in each sample. Furthermore, a good agreement between the data and the model can be supported if $a_{12} = 0.102$ can be replaced by $\frac{1}{a_{21}} = \frac{1}{12.163} = 0.082$ without introducing a large error.

It is observed that Ni was significantly affected by the presence of Pb and Cd for MO, MC and MO+MC as most of the competition coefficients were more than 10 (Table 6.4). On the other hand, Cd was almost unaffected by the presence of Pb and Ni as the competition coefficients were less than one. The reason could be that the molar

concentrations of Pb and Ni in the solutions were relatively higher than Cd. Therefore, these two metal ions must have competed to bind to the biomass surface.

Table 6.4 Parameters of multi-element adsorption estimated from SRS model

Biomass	i	Heavy metal	k_i	n_i	a_{i1}	a_{i2}	a_{i3}	$a_{12}.a_{23}.a_{31}$
MO	1	Pb	44.168	0.784	1	0.102	1.42	
	2	Ni	1.566	8.251	12.163	1	15.892	1.21
	3	Cd	3.842	1.163	0.747	0.073	1	
MC	1	Pb	17.549	0.684	1	0.186	3.305	
	2	Ni	2.297	2.527	6.267	1	18.083	1.20
	3	Cd	1.290	1.919	0.358	0.055	1	
MO+MC	1	Pb	28.332	0.722	1	0.101	1.944	
	2	Ni	2.939	1.390	10.207	1	19.761	1.14
	3	Cd	0.402	2.865	0.572	0.052	1	

Table 6.5 summarises the predicted C_e for multi-element adsorption of Pb, Ni and Cd on MO, MC and MO+MC. For MO, large deviations are shown especially in the first two samples (lower concentrations) and the deviation becomes smaller for the remaining samples (at higher concentrations).

For MC, SRS model did not perform well in predicting the C_e values for Cd and for Pb and Ni at lower concentrations. Similarly, the model did not perform well for MO+MC, except for Ni when initial concentration was 0.511 µmol/L. Results in Table 6.5, show that SRS model does not give satisfactory results in predicting the adsorption of Pb, Ni and Cd on MO, MC or MO+MC.

Furthermore, verifications on the single and multi-element adsorption using Langmuir, Freundlich and SRS models were also carried out in the next section. The following section will present the verification of Langmuir and Freundlich model parameters obtained from the above mentioned single and multi-element solutions.

Table 6.5 Summary of the predicted C_e using SRS model for multi-element adsorption of Pb, Ni, and Cd on MO, MC and MO+MC

Biomass	C_0 (µmol/L)			C_e calculated (µmol/L)			C_e experiment (µmol/L)			Percentage error (%)		
Heavy metal	Pb	Ni	Cd	Pb	Ni	Cd	Pb	Ni	Cd	Pb	Ni	Cd
MO	0.024	0.170	0.009	0.001	0.170	0.006	0.012	0.007	0.004	92	-2329	-50
	0.097	0.511	0.044	0.005	0.492	0.019	0.030	0.265	0.026	83	-86	27
	0.193	0.682	0.062	0.039	0.395	0.041	0.041	0.366	0.031	5	-8	-32
	0.290	0.852	0.080	0.058	0.536	0.057	0.054	0.481	0.035	-7	-11	-63
	0.483	1.704	0.098	0.097	1.016	0.077	0.084	1.167	0.050	-15	13	-54
MC	0.024	0.170	0.009	0.003	0.157	0.009	0.020	0.008	0.001	85	-1863	-800
	0.097	0.511	0.044	0.014	0.320	0.043	0.068	0.250	0.014	79	-28	-207
	0.193	0.682	0.062	0.031	0.345	0.061	0.079	0.379	0.023	61	9	-165
	0.290	0.852	0.080	0.050	0.361	0.076	0.086	0.493	0.029	42	27	-162
	0.483	1.704	0.098	0.088	0.576	0.081	0.101	1.039	0.051	13	45	-59
MO+MC	0.024	0.170	0.009	0.001	0.099	0.009	0.018	0.007	0.000	-94	-1314	3261
	0.097	0.511	0.044	0.004	0.229	0.044	0.027	0.211	0.012	85	-9	-267
	0.193	0.682	0.062	0.010	0.281	0.063	0.037	0.390	0.022	73	28	-186
	0.290	0.852	0.080	0.016	0.330	0.083	0.055	0.541	0.030	71	39	-177
	0.483	1.704	0.098	0.029	0.610	0.104	0.098	1.241	0.047	70	51	-121

6.5 Verification of the adsorption models

6.5.1 Single-element adsorption using Langmuir and Freundlich models

The common application of Langmuir and Freundlich model is predicting the adsorption capacity, Q_e, of a heavy metal on a biomass. However, the current study was planned to predict the final concentrations (C_e) of the metal after the adsorption process using these models.

Two independent sets of test results were used for each of the tested biomass to verify the adsorption parameters using Langmuir, Freundlich and SRS models. For this test, initial concentrations were set to 0.048 and 0.386 µmol/L (equivalent to 10 and 80 µg/L, respectively) for Pb, 0.341 and 1.363 µmol/L (equivalent to 20 and 80 µg/L, respectively) for Ni and 0.027 and 0.089 µmol/L (equivalent to 3 and 10 µg/L, respectively) for Cd. The percentage (%) errors of final concentrations between the experimental and calculated values from Langmuir and Freundlich models were obtained using Equation 3.12 and are presented in Table 6.6. The negative sign

indicates that the calculated values from the models are higher than the experimental value.

It was found that the prediction of C_e values from these two models is rather more complex and requires basic mathematical knowledge as it involves solving non-linear equations. The values of C_e were calculated using the Solver tool in the Microsoft Excel for the independent test data points.

Table 6.6 shows that the calculated percentage errors for Pb (all less than 10%) were comparatively lower than that of Ni and Cd. On the other hand, the percentage errors for Ni and Cd vary depending on the initial concentrations. For instance, the percentage error for Ni adsorption on MO was higher (27%) at lower concentrations (in this case is of 0.341 µmol/L) compared to -3% at higher concentrations (in this case 1.363 µmol/L).

Table 6.6 Verification of K_F and n_F parameters in the Freundlich model using two independent data sets

Heavy metal	Biomass	C_0 (µmol/L)	C_e experiment (µmol /L)	C_e calculated (µmol/L)		Percentage Error (%)	
				Langmuir	Freundlich	Langmuir	Freundlich
Pb	MO	0.048	0.013	0.013	0.013	0	0
		0.386	0.079	0.076	0.073	4	6
	MC	0.048	0.029	0.029	0.029	0	0
		0.386	0.160	0.157	0.157	2	2
	MO+MC	0.048	0.016	0.015	0.015	6	6
		0.386	0.077	0.071	0.075	0	3
Ni	MO	0.341	0.141	0.148	0.103	-5	27
		1.363	1.019	0.999	1.047	2	-3
	MC	0.341	0.144	0.145	0.133	-1	8
		1.363	0.843	0.898	0.918	-7	-9
	MO+MC	0.341	0.089	0.107	0.106	-20	-19
		1.363	0.574	0.567	0.574	1	0
Cd	MO	0.027	0.011	0.011	0.011	0	0
		0.089	0.041	0.041	0.041	0	0
	MC	0.027	0.004	0.006	0.007	-50	-75
		0.089	0.039	0.000	0.040	100	-3
	MO+MC	0.027	0.001	0.002	0.004	-100	-300
		0.089	0.035	0.000	0.038	100	-9

C_0: Initial concentration of heavy metal, C_e: Final concentration of heavy metal

In the context of modelling in the current study, it is preferable to underestimate simulated values rather than overestimate which subsequently result in values exceeding the treatment targets (i.e., WHO standards). Based on Table 6.6, most of the percentage errors are ±20% except for the removal of Ni with MO and Cd with MC and MO+MC. The reason underlying the large deviations in Cd adsorption on MC (Langmuir: 100% [C_o: 0.089 µmol /L]; Freundlich: -75% [C_o: 0.027 µmol /L] and MO+MC (Langmuir: ±100% [C_o: 0.027, 0.089 µmol /L]; Freundlich: -300% [C_o: 0.027 µmol /L]) could be due to the low Cd concentrations (0.027 and 0.089 µmol/L) which consequently resulted in higher sensitivity while calculating the percentage error.

This demonstrates that the parameters obtained for both models show a good agreement between observed and simulated concentrations for single element solutions. However, considering the coefficient of determination (R^2) determined earlier, Freundlich was seen to be a better model for the prediction of treated water quality (C_e) as most of the data showed a better agreement with this model compared to the Langmuir model. For comparison purposes, verifications of multi-element adsorption using Langmuir and Freundlich models are also presented in the next section.

6.5.2 Multi-element adsorption using Langmuir and Freundlich models

Similar to verification of single-element adsorption, the data from the two independent tests were applied to selected models to validate the parameters obtained from the earlier results. The percentage errors (%) were calculated using Equation 3.12. Table 6.7 compares the experimental and simulated final concentrations from the two independent data sets of multi-element adsorption data. For the Langmuir model, large deviations (more than ±20%) were observed for some data points (i.e., adsorption of

Pb on MO+MC: -35%, adsorption of Ni on MO, MC and MO+MC: -30%, -57% and -31%, respectively, adsorption of Cd on MC: 100% [C_o: 0.089 µmol /L], MO+MC: -300% [C_o: 0.027 µmol /L] and 100 [C_o: 0.089 µmol /L]).

On the other hand, the Freundlich model showed that most of the calculated percentage errors were less than +20% for all adsorption of heavy metals on the selected biomass, except for the adsorption of Ni on MC (-29% [C_o: 1.363 µmol /L]) and adsorption of Cd on MC and MO+MC: -40% µmol /L and -300%, respectively (C_o: 0.027). Large deviations observed for some data points could be due to the irregularity of adsorption sites thus impacting distribution of metal ions on the biomass surface (Sağ et al., 2001). However, for almost all samples (except for three samples) the percentage errors calculated with Freundlich model were less than 20%.

Table 6.7 Verification of Freundlich model parameters using two independent tests of multi-element adsorption data.

Heavy metal	Biomass	C_0 (µmol/L)	C_e experiment (µmol /L)	C_e calculated (µmol/L)		Percentage error (%)	
				Langmuir	Freundlich	Langmuir	Freundlich
Pb	MO	0.048	0.018	0.019	0.018	-6	0
		0.386	0.064	0.067	0.066	-5	-3
	MC	0.048	0.039	0.039	0.034	0	13
		0.386	0.090	0.092	0.106	-2	-18
	MO+MC	0.048	0.020	0.027	0.023	-35	-15
		0.386	0.075	0.076	0.071	-1	5
Ni	MO	0.341	0.099	0.129	0.088	-30	11
		1.363	0.910	0.886	0.948	3	-4
	MC	0.341	0.134	0.210	0.142	-57	-6
		1.363	0.830	0.911	1.069	-10	-29
	MO+MC	0.341	0.095	0.124	0.078	-31	18
		1.363	0.938	0.946	0.951	-1	-1
Cd	MO	0.027	0.011	0.013	0.013	-18	-18
		0.089	0.042	0.046	0.046	-10	-10
	MC	0.027	0.005	0.005	0.007	0	-40
		0.089	0.039	0.000	0.039	100	0
	MO+MC	0.027	0.001	0.004	0.004	-300	-300
		0.089	0.037	0.000	0.039	100	-5

C_0: Initial concentration of heavy metal, C_e: Final concentration of heavy metal

Similar to results obtained from single-element solutions, it can be stated that the calculated percentage errors were acceptable (less than ±20%) with Freundlich model application. Considering the coefficient of determination (R^2) and values of error percentages, the Freundlich model has the potential for predicting adsorption of heavy metals on the selected biomass compared to Langmuir model for multi-element system. The next section reports the verification of SRS model parameters in the multi-element solution.

Considering the coefficient of determination (R^2) and percentage error values, Freundlich model showed more potential in predicting each heavy metal adsorption on the selected biomass, compared to the Langmuir model for the multi-element system. The next sub-section reports the verification of SRS model parameters in the multi-element solution.

6.5.3 Multi-element adsorption using the SRS model

Although the SRS model did not perform well with multi-element solution, that is similar to the Langmuir and Freundlich models, the obtained model parameters were verified on a set of independent data. As can be seen in Table 6.8, the calculated percentage error was high in almost each of the samples. This could be due to the irregularity of adsorption sites on the biomass thus impacting the distribution of the metal ions (Sağ et al., 2001). The varied concentration of each metal ion in a sample could also become another reason for the poor performance of the model.

Overall, results from this study has highlighted the applicability of the existing adsorption models for single-element and multi-element systems to represent adsorption of Pb, Ni and Cd on MO, MC and MO+MC. Goodness-of-fit parameters were used to test the applicability of Langmuir, Freundlich, and Sheindorf-Rebhun-

Sheintuch (SRS) models. Freundlich model performed best (percentage error within 20%) in predicting treated water quality concentrations (C_e) from single-element systems compared to the Langmuir model.

Table 6.8 Verification of SRS model parameters using two independent tests of multi-element adsorption data

Biomass	C_0 (µmol/L)			*Ce* calculated (µmol/L)			*Ce* experiment (µmol/L)			Percentage error (%)		
	Pb	Ni	Cd	Pb	Ni	Cd	Pb	Ni	Cd	Pb	Ni	Cd
MO	0.048	0.341	0.027	0.003	0.336	0.018	0.018	0.099	0.011	83	-239	-64
	0.386	1.363	0.089	0.077	0.807	0.068	0.064	0.91	0.042	-20	11	-62
MC	0.048	0.341	0.027	0.006	0.259	0.027	0.039	0.134	0.005	85	-93	-440
	0.386	1.363	0.089	0.069	0.493	0.082	0.09	0.83	0.039	23	41	-110
MO+MC	0.048	0.341	0.027	0.002	0.167	0.027	0.02	0.095	0.001	90	-76	-2600
	0.386	1.363	0.089	0.022	0.507	0.091	0.075	0.938	0.037	71	46	-146

C_0: Initial concentration of heavy metal, C_e: Final concentration of heavy metal

Although the Freundlich model could satisfactorily estimate the adsorption of most of the targeted contaminants in the multi-element system, it failed to predict Ni adsorption with MC. The SRS model also could not successfully estimate the final metal concentrations in the treated water. Therefore, the original Freundlich model will be used in the following investigation to estimate heavy metal concentrations on treated water quality.

Even though, the Freundlich model is commonly used in determining the adsorption capacity of a contaminant onto a biomass or adsorbent (Junior et al., 2013; Mataka et al., 2010; Sumathi & Alagumuthu, 2014), literature reporting its usage to estimate final concentration of contaminant is rarely found. From this current study, Freundlich model was proven successful for estimating the final concentration of contaminants treated with the predetermined biomass concentration.

6.6 Predicting treated groundwater quality using Freundlich model for single-element contaminated groundwater

Based on the findings from the previous sections, the Freundlich model is the most favourable to predict the heavy metals (Pb, Ni, and Cd) removal rate using the predetermined MO, MC, and MO+MC dosages. The experimental results in Chapter 4 had reported MO+MC (200+200 mg/L) as the best biomass dosage for the removal of Pb, Ni and Cd, to meet WHO drinking water quality standards. For comparison purposes, prediction of final water quality was also assessed from using the individual MO and MC.

6.6.1 Random number generation

Input water quality could vary inherently with time and location. Therefore, the selected biomass doses must be adequate to treat contaminated water with certain reliability. Raw groundwater quality input was generated using random number generator (mode: normal distribution) in Microsoft Excel. The required means, standard deviations and concentration ranges to generate the individual heavy metal-contaminated groundwater inputs for each of the heavy metals are tabulated in Table 6.9. These values were generated by referring to the concentrations of target contaminants (within the range of contaminants' concentrations) as reported in the literature (Table 2.1).

Table 6.9 Mean, standard deviation and concentration ranges (in μmol/L) of Pb, Ni, and Cd to generate groundwater quality inputs using random number generation on Excel

Target metal	Mean	Standard deviation	Minimum	Maximum	WHO standard
Pb	0.145 (30 μg/L)	0.050 (10 μg/L)	0.004 (1 μg/L)	0.283 (60 μg/L)	0.048 (10 μg/L)
Ni	0.682 (40 μg/L)	0.100 (6 μg/L)	0.343 (20 μg/L)	0.997 (60 μg/L)	0.341 (20 μg/L)
Cd	0.058 (7 μg/L)	0.015 (2 μg/L)	0.012 (1 μg/L)	0.096 (11 μg/L)	0.027 (3 μg/L)

It was assumed that the heavy metal concentrations of the groundwater samples are normally distributed, and is widely used in modelling quantitative phenomena in natural sciences (Khan, 2010). Moreover, it holds the hypothesis of data normality that can be evaluated through a number of statistical goodness-of-fit tests (Nielsen, 2006). Monte Carlo random number generation procedure was selected to represent different combinations of target contaminants in groundwater quality.

6.6.2 Probability plots for groundwater quality input

The plots (Figure 6.5 to Figure 6.7) indicate the normally distributed target contaminants (i.e. Pb, Ni and Cd) in randomly generated raw groundwater samples. The inputs were generated using random number generator function in Microsoft Excel. Probability (scatter) plots, cumulative frequency plots, and frequency distribution of each initial target heavy metal (Pb, Ni, and Cd) are presented in Figure 6.5 to Figure 6.7 to demonstrate the random distribution of the generated data.

The plots as shown in Figure 6.5a, Figure 6.6a and Figure 6.7a display the distributions of each contaminant of water quality obtained from 1000 random samples. The vertical axis indicates the concentration of contaminant (μmol/L) and the horizontal axis shows the sample number. The generated concentration ranges are approximately 0 to 0.300 μmol/L for Pb, 0.300 to 1.000 μmol/L for Ni and 0 to 0.100 μmol/L for Cd. The means values for Pb (0.145 μmol/L), Ni (0.682 μmol/L) and Cd (0.058 μmol/L) were set higher than their respective WHO drinking quality standards of 0.048, 0.341 and 0.027 μmol/L, respectively (Table 6.9).

Figure 6.5b, Figure 6.6b and Figure 6.7b show the cumulative density function of Pb, Ni and Cd concentrations in randomly generated groundwater input samples. The curve shape displayed for each target contaminant represents the characteristic of

normally distributed data. In this case, the values corresponding to the 5th and 95th percentiles of the frequency are 0.015 and 0.049 µmol/L respectively for Pb, 0.250 and 0.555 µmol/L respectively for Ni and 0.014 and 0.037 µmol/L respectively for Cd. Frequency distribution of the generated initial concentrations of Pb, Ni and Cd, are shown in Figure 6.5c, Figure 6.6c, and Figure 6.7c, respectively. As can be seen, the frequency distribution for each of the initial concentration of Pb, Ni and Cd showed a bell-shaped curve, respectively. These indicate that the data are normally distributed.

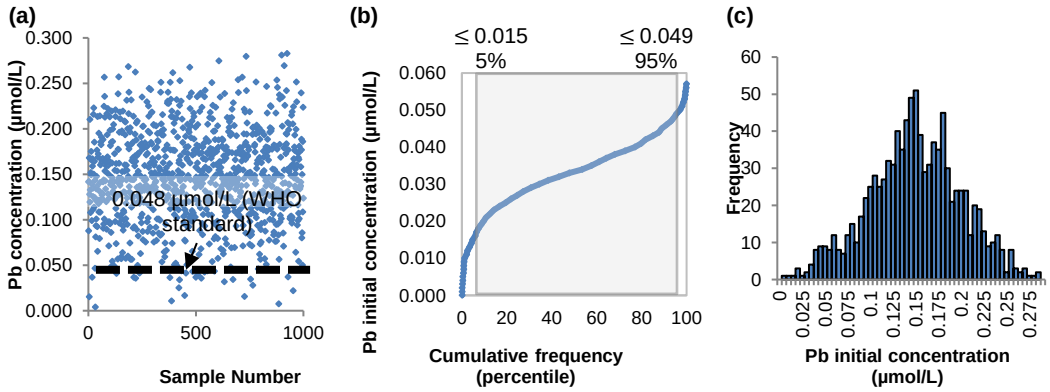

Figure 6.5 (a) Scatter plot (b) cumulative density function (c) frequency distribution of randomly generated hypothetical Pb initial concentrations in groundwater samples

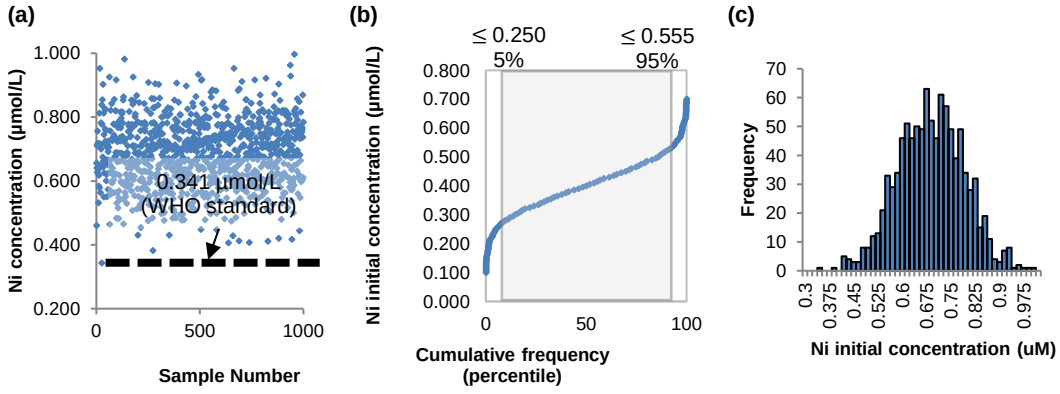

Figure 6.6 (a) Scatter plot (b) cumulative density function (c) frequency distribution of randomly generated hypothetical Ni initial concentrations in groundwater samples

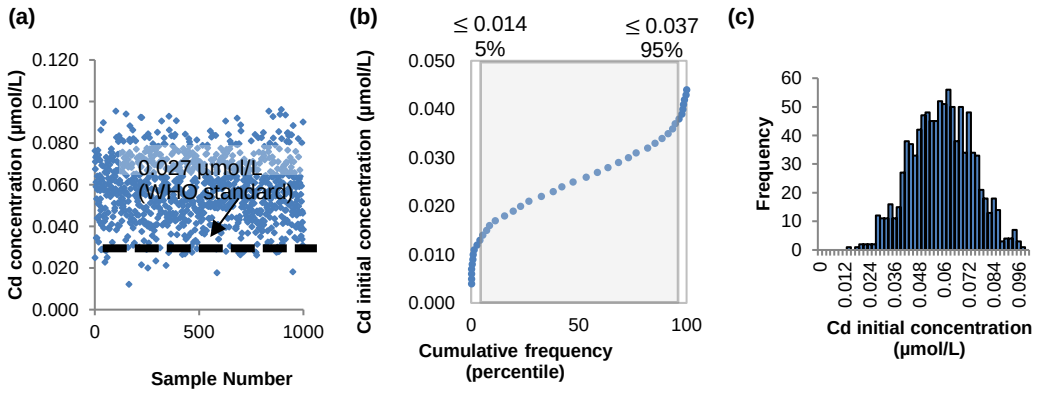

Figure 6.7 (a) Scatter plot (b) cumulative density function (c) frequency distribution of randomly generated hypothetical Cd initial concentrations in groundwater samples

A simple technique was applied to check whether the generated data are normally distributed. The test was carried out by changing the scale of both axes from linear to $\log_{10}$ probability scale. Then, the characteristic of the plots can be observed as shown in Figure 6.8.

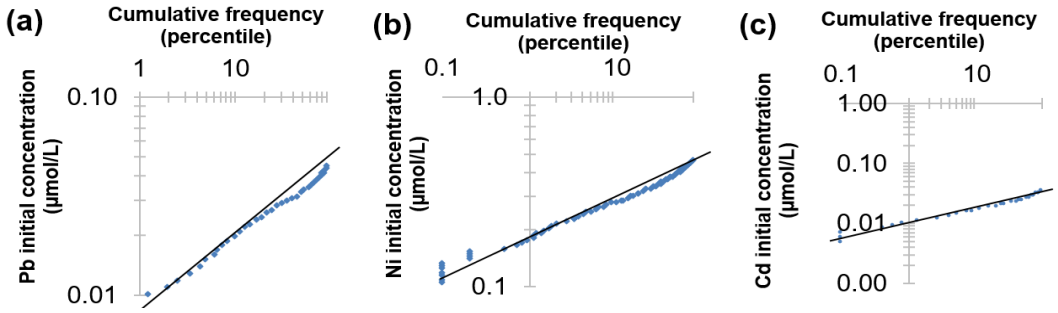

Figure 6.8 Probability scale charts for normally distributed target contaminants data for (a) Pb, (b) Ni and (c) Cd in groundwater quality input for normally distributed data testing

Most of the data points for each of target contaminants are in a straight line. These mean the data are normally distributed. The calculated skewness for generated data that have been plotted in Figure 6.8 are 0.093, 0.020 and 0.030, respectively. These also indicate that the data are normally distributed as the skewness values are close to zero. The normally distributed groundwater quality input for Pb, Ni and Cd data were

processed using the Freundlich model by the aid of the Solver and Macro Visual Basic Editor tool in Microsoft Excel to predict the treated groundwater quality output.

6.7 Probability of Exceedance of heavy metals in treated water by *Moringa oleifera* seeds (MO), *Musa cavendish* (MC) and combined MO+MC

6.7.1 Probability plots

The generated data together with the Freundlich model was used to estimate the final concentrations of Pb, Ni and Cd when treated with MO, MC or MO+MC. Figure 6.9a depicts the final concentrations of Pb (initial concentration of Pb between 0.004 to 0.283 µmol/L) treated with MO, MC and MO+MC for 1000 normally distributed random samples. Figure 6.9a-i shows that the concentrations of Pb reduced significantly from the maximum initial concentrations of Pb (0.283 µmol/L) to the maximum final concentrations of Pb (0.057 µmol/L). The value is slightly above the WHO standard for Pb (0.048 µmol/L) as shown in Table 6.10. Figure 6.9a-ii shows that most of the predicted treated Pb-contaminated samples by MC were reduced to the concentrations between 0.003 to 0.123 µmol/L. Figure 6.9a-iii indicates that the Pb concentrations were reduced significantly by MO+MC from the maximum initial concentrations of Pb of 0.283 µmol/L to the maximum final concentrations of Pb of 0.059 µmol/L. This result indicates that MO+MC performance is almost similar and comparable to the MO performance. Therefore, it is concluded that MC did not have a significant role in improving treatment efficiency.

On the other hand, Ni-contaminated groundwater inputs were generated from 0.343 to 0.997 µmol/L. The probability plots of Ni concentrations before and after treatment using MO, MC and MO+MC can be seen in Figure 6.9b. Figure 6.9b-i shows that the concentration of Ni was reduced by MO from the maximum initial concentration of

Ni (0.997 μmol/L) to the maximum final concentration of Ni (approximately 0.697 μmol/L). Figure 6.9b-ii displays the concentrations of Ni were reduced by MC from the maximum concentration of Ni (0.997 μmol/L) to the maximum concentration of Ni (0.617 μmol/L). It can be observed from Figure 6.9b-iii that there is an apparent gap between the range of initial and final concentrations of Ni after treatment with MO+MC. Most of the samples met the WHO standard for Ni (0.341 μmol/L). This finding demonstrates the advantage of combining MO and MC together to improve the treatment efficacy for removing Ni.

Cd-contaminated groundwater qualities were generated between 0.012 to 0.096 μmol/L. Figure 6.9c-i to Figure 6.9c-iii display the probability plots of normally distributed samples of Cd concentrations before (C_0) and after (C_e) treatment. The performance of MO seeds in treating Cd-contaminated groundwater was comparable to its performance in treating Pb-contaminated groundwater. It can be observed that the concentrations of Cd were reduced markedly to the maximum final Cd concentration (0.044 μmol/L) from the maximum initial Cd concentration (0.096 μmol/L). Figure 6.9c-ii displays the reduction of Cd occurred from the maximum Cd concentration (0.096 μmol/L) in the groundwater input to the concentration ranging from 0.002 to 0.045 μmol/L (after treatment with MC). Figure 6.9c-iii displays the reduction of Cd occurred from the maximum Cd concentration (0.096 μmol/L) in the groundwater input to the maximum final Cd concentration (0.043 μmol/L) after treatment with MO+MC.

Overall, the probability plots exhibited that MO was performing better for the adsorption of Pb compared to Ni and Cd. Meanwhile MC showed a better removal for Cd compared to Pb and Ni. Interestingly, when the MO and MC were combined

(MO+MC), most of the concentrations of heavy metals were reduced to the levels that comply with the WHO standards. Next section presents the plots of predicted and experimental water quality results of Pb, Ni and Cd after treatment with MO, MC and MO+MC.

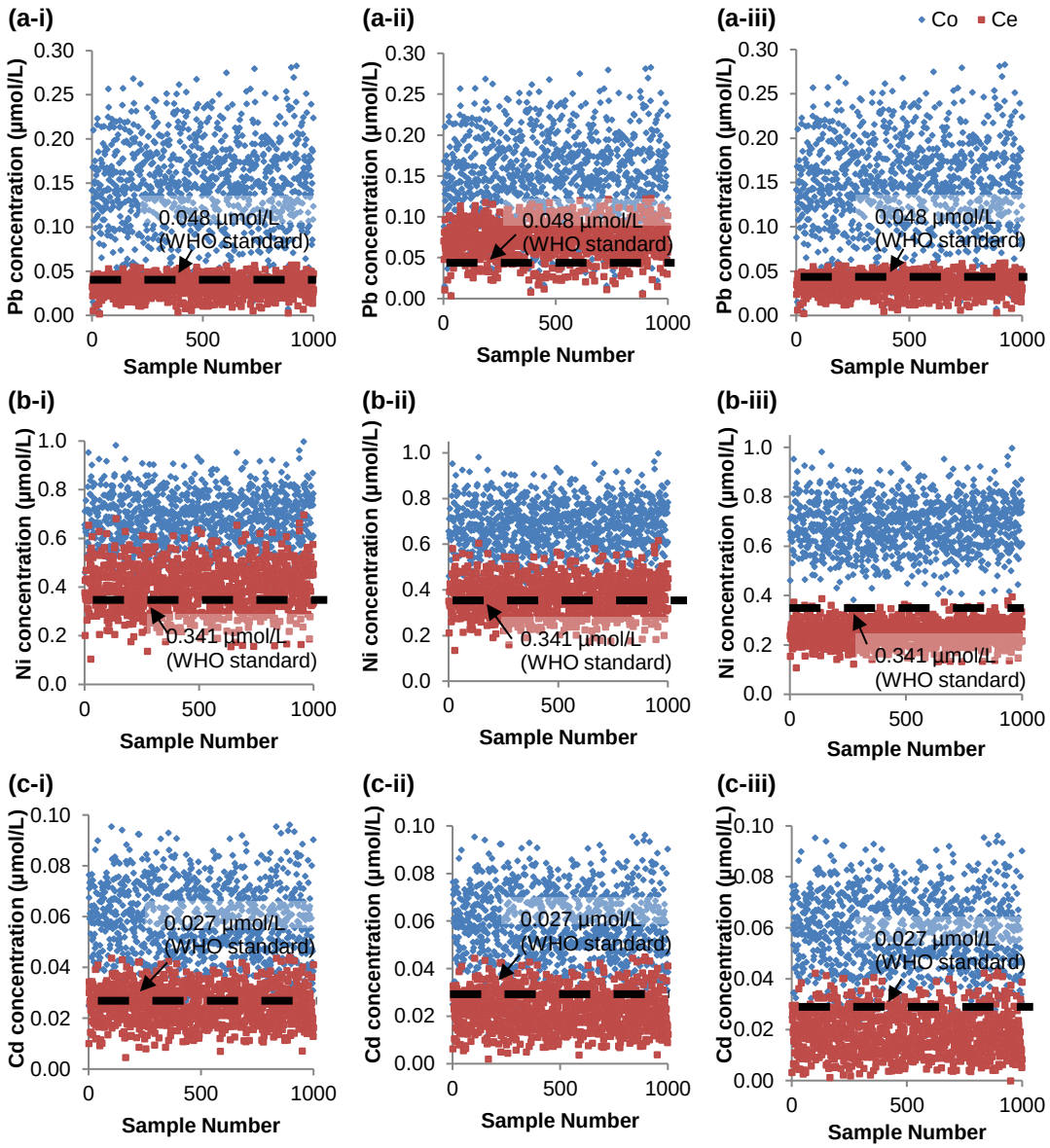

Figure 6.9 (a) Probability plots of (a) Pb (b) Ni (c) Cd concentrations before (C_0) and after (C_e) treatment using (i) MO (200 mg/L) (ii) MC (200 mg/L) and (iii) MO+MC (200+200mg/L)

6.7.2 Prediction of maximum possible initial concentrations of heavy metals to comply with WHO standards

It is essential to determine the maximum possible initial concentrations of the target contaminants (Pb, Ni and Cd) that MO, MC and MO+MC with predetermined optimum dosages could treat to meet their respective WHO standards. Table 6.10 presents the summary of maximum final concentrations and possible maximum initial concentrations of heavy metals that could meet WHO standards after the treatment with MO (200 mg/L), MC (200 mg/L) and MO+MC (200+200 mg/L).

Table 6.10 Possible maximum initial concentrations of heavy metals that could meet WHO standards after the treatment with MO (200 mg/L), MC (200 mg/L) and MO+MC (200+200 mg/L)

Heavy metal	Biomass	Possible maximum initial concentration of heavy metal that could meet the WHO standard (μmol/L)	WHO standard
Pb	MO	0.236	0.048
	MC	0.088	
	MO+MC	0.216	
Ni	MO	0.615	0.341
	MC	0.641	
	MO+MC	0.884	
Cd	MO	0.060	0.027
	MC	0.066	
	MO+MC	0.072	

It is demonstrated for Pb that MO and MO+MC could reduce the concentration of Pb to meet the WHO standard of 0.048 μmol/L with the maximum possible initial concentration of 0.236 and 0.216 μmol/L, respectively. On the other hand, MC showed the least ability to treat the groundwater containing Pb. The maximum possible initial concentration of Pb that could comply with the WHO standard is only 0.088 μmol/L. Overall, it was clear that MO+MC showed a better performance in treating most of the target contaminants (Pb, Ni, and Cd) compared to MO and MC alone.

6.7.3 Probability density function (PDF) and cumulative density function

Probability density function (PDF) was used to ensure that the treated water quality data that have been analysed were normally distributed while cumulative density function was used to determine the probability of treated water quality complied with the WHO standards. The methods used to generate PDF cumulative density functions and calculation of the n^{th} percentile from simulated data sets can be referred to in Chapter 3 (Section 3.7.1).

The PDFs of the treated groundwater contaminated with Pb by MO, MC, and MO+MC, respectively are shown in Figure 6.10a. In this case, the data were fitted to a normal distribution. The means and standard deviations of the treated data sets are given in Table 6.11. The predicted final Pb concentrations corresponding to the 5th and 95th percentiles are 0.015 μmol/L and 0.048 μmol/L, respectively for MO; 0.033 μmol/L and 0.104 μmol/L, respectively for MC; and 0.017 μmol/L and 0.051 μmol/L, respectively for MO+MC.

Figure 6.10a shows that 94% and 91% of the 1000 treated groundwater samples contaminated with Pb were complied with the WHO standard (0.048 μmol/L) when MO and MO+MC, respectively, were used as the treatment agents. These percentages are higher than that obtained by MC (13%). Although MO and MO+MC showed comparable percentages in terms of their compliance with the WHO standard, MO by itself possesses a great potential to effectively treat the Pb-contaminated groundwater.

The PDFs of the treated groundwater contaminated with Ni by MO, MC, and MO+MC are illustrated in Figure 6.10b. The data were fitted to a normal distribution function for Ni as well (mean and standard deviation in Table 6.11). The predicted final concentrations of Ni corresponding to the 5th and 95th percentiles are 0.250 μmol/L

and 0.553 μmol/L for MO, 0.250 μmol/L and 0.497 μmol/L for MC, and 0.177 μmol/L and 0.323 μmol/L for MO+MC, respectively.

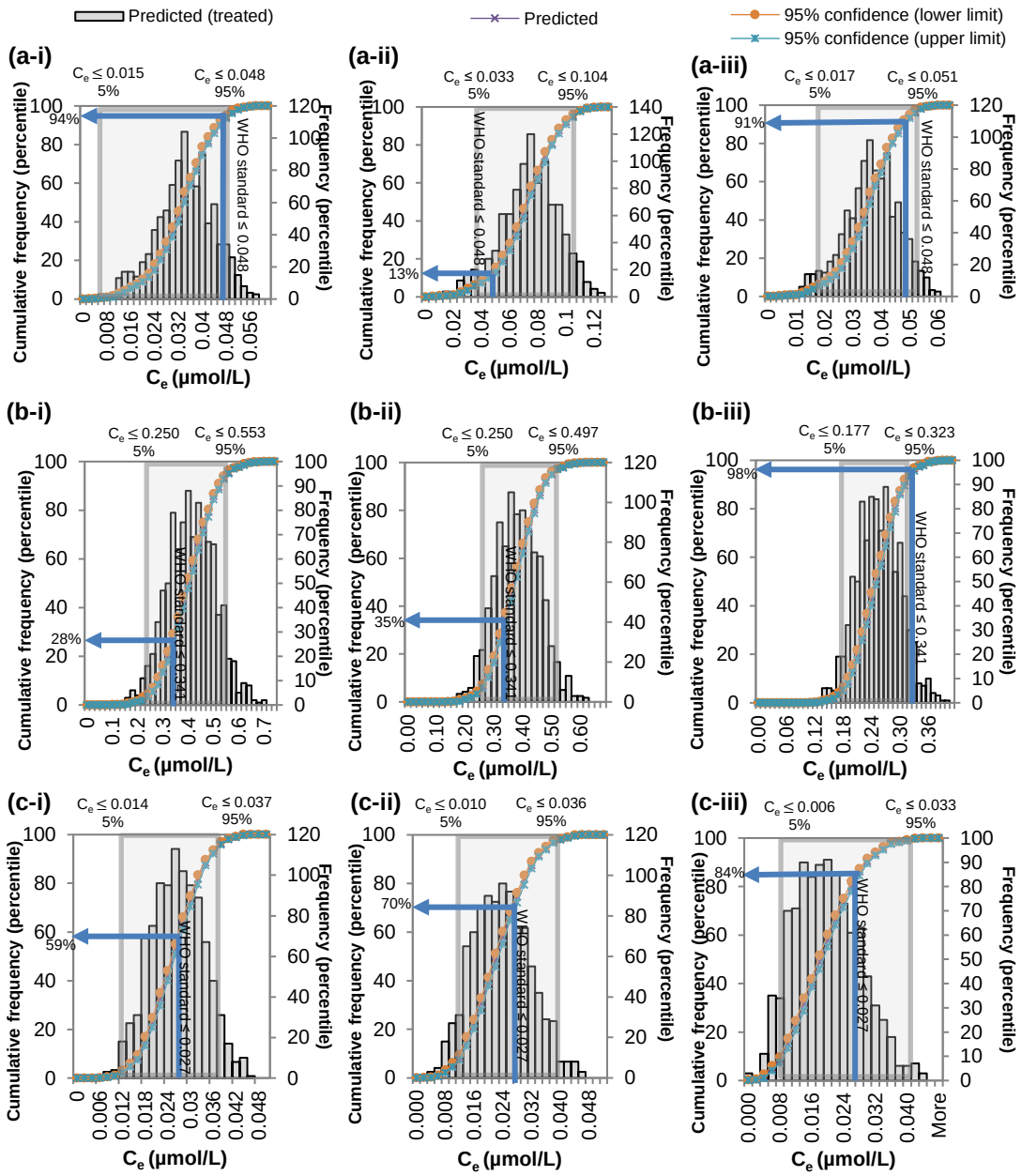

Figure 6.10 Probability density function and cumulative density function of predicted (a) Pb, (b) Ni (c) Cd after treatment with (i) MO (200 mg/L), (ii) MC (200 mg/L) (iii) MO+MC (200+200 mg/L)

Unlike MO seeds that have superior performance in treating Pb, only 28% of the 1000 treated groundwater samples contaminated with Ni were complied with the WHO standard (0.341 μmol/L) as can be seen in Figure 6.10b-i. It is clear that MO is not as

effective as for Pb in treating the Ni-contaminated groundwater. However, the effectiveness of treating Ni with MC to comply with WHO standards was also low (35%). As anticipated MO+MC demonstrated that the treatment is highly effective for removal of Ni. It is shown that 98% of the treated samples successfully met the WHO standard of 0.341 μmol/L for Ni treatment (Figure 6.10b-iii).Figure 6.10c shows the PDFs of treated Cd-contaminated groundwater by MO, MC and MO+MC (mean and standard deviation in Table 6.11). The values of the predicted final concentrations of Cd corresponding to the 5^{th} and 95^{th} percentiles are 0.014 μmol/L and 0.037 μmol/L, respectively for MO; 0.010 μmol/L and 0.036 μmol/L, respectively for MC; and 0.006 μmol/L and 0.033 μmol/L, respectively for MO+MC. Figure 6.10c-i illustrates the cumulative density function for the respective PDF of the predicted final concentrations of Cd after treatment with MO. It can be observed that more than half (59%) of the 1000 samples could meet the recommended WHO permissible limit for Cd (0.027 μmol/L).

Table 6.11 Summary of PDF and cumulative density function of the predicted heavy metal concentration after the treatment with MO (200 mg/L), MC (200 mg/L) and MO+MC (200+200 mg/L)

Heavy metal	Biomass	Mean (μmol/L)	Standard deviation (μmol/L)	Final concentration of heavy metal (μmol/L)		WHO standard (μmol/L)	% of samples complied with the WHO standard
				5^{th} percentile	95th percentile		
Pb	MO	0.033	0.010	0.015	0.048	0.048	94%
	MC	0.072	0.021	0.033	0.104		13%
	MO+MC	0.035	0.010	0.017	0.051		91%
Ni	MO	0.401	0.094	0.250	0.553	0.341	28%
	MC	0.372	0.077	0.250	0.497		35%
	MO+MC	0.249	0.045	0.177	0.323		98%
Cd	MO	0.025	0.007	0.014	0.037	0.027	59%
	MC	0.023	0.008	0.010	0.036		70%
	MO+MC	0.019	0.008	0.006	0.033		84%

On the other hand, 70% of the 1000 treated groundwater samples were able to successfully meet the recommended WHO standard for Cd using MC. The percentage

of compliance with the WHO standard is higher than that achieved by treatment with MO seed (59%). Thus, it suggests that MC has a better affinity towards Cd compared to MO. As anticipated, treatment with MO+MC showed that 84% of the 1000 treated Cd-contaminated groundwater samples succeeded in meeting the WHO standard for Cd. Table 6.11 summarises the data obtained from PDF and cumulative density function of the predicted heavy metal concentration after the treatment with MO, MC and MO+MC.

Overall, the findings suggest that MO+MC had the highest probabilities of compliance in meeting the WHO standards of Pb, Ni and Cd compared to MO and MC alone. The results show that 94% of the treated Pb-contaminated groundwater samples complied with the WHO standard after treatment with MO. The result was comparable with MO+MC (91%). This suggests that MO by itself is proficient for Pb removal. To further evaluate the reliability of this model in predicting treated water quality, an uncertainty analysis needs to be carried out for each of the treatment options.

On the other hand, MC showed the lowest ability to treat most of the targeted heavy metals especially for Pb and Ni as the compliance with WHO standards were only 13% and 35% respectively. It is also worth to note that the probability of the treated groundwater in meeting the WHO standard for Ni and Cd were improved up to 98% and 84%, respectively, when MO+MC was applied compared to the MO and MC, individually. This finding supports the earlier findings which suggested that the combination of MO and MC has obviously improved the treatment efficiency (to meet the WHO standard) that could not be achieved by MO and MC alone.

6.8 Uncertainty analysis

Uncertainty analysis was carried out to evaluate the level of precision and random error. The uncertainty ranges were calculated (as described in Chapter 3, Section 3.7.2) for all tested biomass. Table 6.12 presents the statistical analysis data for MO, MC, and MO+MC to predict the Pb, No, and Cd of treated water quality using the Freundlich model in the single-element system. The uncertainty values obtained from the present study varied between 1.023 and 1.056.

Table 6.12 Results of statistical analysis of predicted treated water quality of Pb, Ni and Cd using MO, MC and MO+MC (single-element adsorption: Freundlich model)

Biomass	MO			MC			MO+MC		
Heavy metal	Pb	Ni	Cd	Pb	Ni	Cd	Pb	Ni	Cd
Min	0.002	0.104	0.005	0.003	0.135	0.002	0.002	0.107	0.000
Max	0.057	0.697	0.044	0.123	0.617	0.045	0.059	0.395	0.043
Range	0.056	0.592	0.039	0.119	0.482	0.043	0.057	0.287	0.043
Mean (μ)	0.033	0.401	0.025	0.072	0.372	0.023	0.035	0.249	0.019
Variance (σ^2)	0.000	0.009	0.000	0.000	0.006	0.000	0.000	0.002	0.000
Standard deviation (σ)	0.010	0.094	0.007	0.021	0.077	0.008	0.010	0.045	0.008
Count (N)	1000	1000	1000	1000	1000	1000	1000	1000	1000
Degree of freedom ($d.f.$)	999	999	999	999	999	999	999	999	999
Confidence level (α)	95%	95%	95%	95%	95%	95%	95%	95%	95%
Critical-t (t_c)	1.962	1.962	1.962	1.962	1.962	1.962	1.962	1.962	1.962
Standard error	0.000	0.003	0.000	0.001	0.002	0.000	0.000	0.001	0.000
Lower limit	0.032	0.395	0.025	0.070	0.367	0.022	0.035	0.247	0.018
Upper limit	0.034	0.407	0.026	0.073	0.376	0.023	0.036	0.252	0.019
Uncertainty	1.037	1.030	1.035	1.037	1.026	1.045	1.035	1.023	1.056
Skewness	0.311	0.033	0.024	0.352	0.074	0.181	0.380	0.063	0.344

Smeets & Medema (2006) recorded uncertainty up to 64 on microbiological treatment which was higher than the uncertainty values obtained from the current study. The reason could be due to the variations in the concentration of the microorganisms. These are often much higher compared to the concentration level of heavy metals in the present study. According to Smeets & Medema (2006), uncertainty value for a system is considered to be minimal when the values are closer to one.

Therefore, it can be concluded that the proposed model (Freundlich model) could predict the treated water quality with small uncertainties. The following section presents the evaluation of exceedance probabilities of WHO drinking water quality standards.

6.9 Probability of the treated water quality exceeds the WHO drinking water quality standards

Comparison of WHO drinking water quality standard exceedance probabilities between MO, MC and MO+MC is presented in Figure 6.11. Treatment with the lowest exceedance probability means that the treatment has a high efficacy in minimising the risk of treated groundwater quality exceeding the recommended concentrations. Exceedance probability can be determined using Equation 3.15 as described in Chapter 3 (Section 3.7.3).

It is clear from the graph (Figure 6.11) that MO+MC demonstrated the lowest exceedance probabilities (2% to 16%) for all target contaminants compared to the single biomass (i.e. MO and MC). On the other hand, MC showed a relatively high exceedance probability for Pb and Ni (87% and 65%, respectively), followed by MO for Ni (72%).

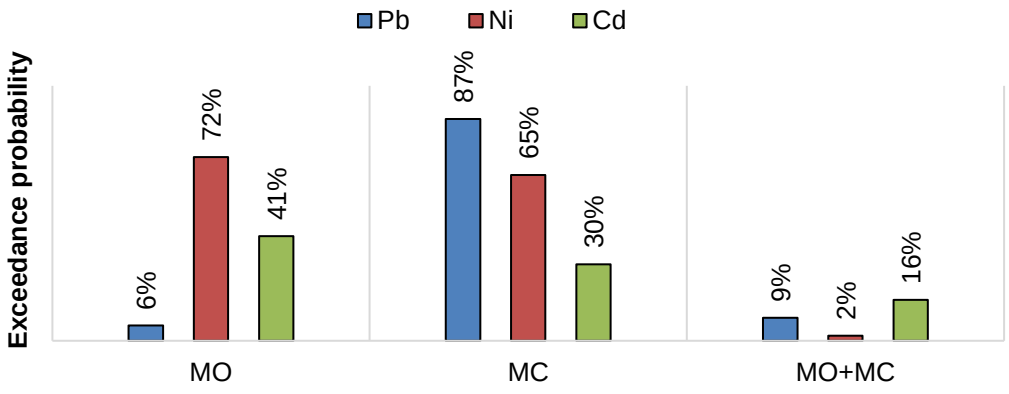

Figure 6.11 Probability of WHO drinking water quality standards exceedance achieved by MO, MC, and MO+MC for individual treatment of Pb, Ni, and Cd

Thus, it can be concluded that treatment of Pb-, Ni- and Cd- contaminated groundwater with combined biomass (MO+MC) has lower risk factor for the treated water quality to exceed the recommended WHO standards.

6.10 Summary and Conclusions

There is limited information in the literature regarding the prediction of heavy metals in treated groundwater using adsorption models. According to literature, the application of the existing adsorption models such as the Langmuir and Freundlich models are usually used to determine the adsorption capacity of contaminants onto a particular adsorbent (Anwar et al., 2010; Mataka et al., 2010; Sivakumar, 2012). Based on the findings from this chapter, it was demonstrated that the Freundlich model gave the best performance in predicting the final concentration of lead (Pb), nickel (Ni), and cadmium(Cd) after treatment with 200 mg/L of *Moringa oleifera* (MO) seeds and *Musa cavendish* (MC, banana peel), respectively, and 200:200 mg/L of combined MO and MC (MO+MC). The results obtained from the adsorption experiments for the specific types and doses of biomass (as mentioned above) were compatible to the previous experimental results as presented in Chapter 4. Monte Carlo random number generation procedure was selected to represent different combinations of target contaminants in the ground water quality.

It is predicted that 0.236 μmol/L, 0.615 μmol/L, and 0.060 μmol/L is the maximum possible initial concentration of Pb, Ni and Cd that could meet with the WHO standard of respective parameters when treated with 200 mg/L MO seeds. For treatment with 200 mg/L of MC, it was predicted that 0.088 μmol/L, 0.641 μmol/L and 0.066 μmol/L was the maximum possible initial concentrations of Pb, Ni and Cd that could meet the WHO standard of respective parameters. For treatment with 200+200 mg/L of

MO+MC, it is predicted that 0.216 μmol/L, 0.884 μmol/L, and 0.072 μmol/L are the maximum possible initial concentration of Pb, Ni and Cd that could meet the WHO standard of respective parameters. This finding demonstrated that MO+MC could treat a higher maximum possible initial concentration of Pb, Ni and Cd and meet their respective WHO standard compared to the individual MO and MC.

WHO compliance or exceedance probability of WHO standard was used to describe the effectiveness of the treatment options rather than the removal efficiency as they represent how well the treatment method is capable of reducing the contaminant concentration to meet the WHO drinking water quality standard for the individual metal. MO+MC combination was found to give the lowest probability to exceed WHO standards (Pb: 9%, Ni: 2% and Cd: 16%). The probability of the WHO standard compliance for Pb was comparable for MO (94%) and MO+MC (91%). On the other hand, the probabilities of WHO standard compliance were markedly improved for Ni and Cd when MO and MC were applied in combination, compared to MO and MC individually. This indicates the feasibility of using MO+MC as a treatment method for Pb, Ni and Cd removal from groundwater.

Determination of the uncertainty range of the predicted values is essential to ensure that the predicted values are varied within an acceptable range. The value is considered as minimal when it approaches one (Smeets & Medema, 2006). According to Khan, (2010), uncertainty could be sourced from the limitations in analytical precisions of the instruments. The uncertainty ranges calculated for all treatment methods in this study were ranging from 1.023 to 1.056. The ranges are considered as minimal when the values are close to one. Therefore, the selected biomass with the predetermined doses were proved to be capable of predicting a large number of treated groundwater quality with a small uncertainty range using the Freundlich model.

WHO standard compliances and exceedance probabilities for each treatment method has given valuable information in terms of maximum possible heavy metal concentration that could be treated by the selected biomass to meet the WHO standard. This information is necessary for future selection of the best treatment method especially for the removal of Pb, Ni and Cd from the contaminated drinking water sources.

CHAPTER 7 Cost estimation for a small drinking water treatment system

This chapter provides an overview of the cost estimation for drinking water treatment system involving heavy metal contaminants (i.e., lead, nickel and cadmium) removal using the combination of *Moringa oleifera* seed and *Musa cavendish* (MO+MC) as water purification agents. Combined MO and MC (MO+MC) was selected as the optimum biomass dosing method compared to using MO and MC individually as reported in the previous chapter. The effectiveness of MO+MC resulted in the highest reduction of the contaminants mentioned above, complying with WHO standards for drinking water. It is important to evaluate and estimate the cost involved in the proposed treatment system to compare the effectiveness of biomass used. However, limited numbers of peer-reviewed articles that report on low-cost drinking water treatment systems only referred to retail prices. The cost differs depending on the method of processing specific materials and local accessibility. Usually, an inexpensive treatment agent only needs simple processing and is widely available or gathered from waste material originated from agricultural and industry. It offers an understanding into simple and effective costing that a specialist would use and a non-specialist at national as well as local level would understand (Višekruna et al., 2011). The cost estimation presented in this study focused only on the treatment unit in which the selected plant-based materials (MO+MC) are intended to be applied.

This chapter consists of six parts, starting with an overview of the proposed treatment process, followed by a description of its installation at the residential areas of remote communities. Following that, the operation and maintenance of the proposed treatment unit, as well as all the steps required in the preparation of the selected biomass, is fully explained together with the proposed sludge management. Finally, the total cost of the

treatment unit is presented in a table, thus concluding the affordability of the proposed treatment unit to be installed at the residential area of remote communities, especially in developing countries. Based on the estimated costs of the proposed treatment system, the costs of other similar treatment systems with different water purification agents (materials) could also be estimated.

7.1 Description for the proposed treatment unit

It was proposed that coagulation method will be implemented in the simple water treatment system with the intention to provide safe drinking water to remote communities. Considering the average amount of drinking water intake per person per day is between 2.5 L to 3 L (Howard & Bartram, 2003), for a house consisting four to five members, the system is expected to be able to supply around 15 L to 20 L of treated drinking water per day. However, the demand changes depending on the number of occupants per house.

In remote areas, drinking water is usually sourced from groundwater as discussed in Chapter 2. The groundwater, which complied with WHO standards, is safe to be supplied to the end users without treatment. Normally, groundwater is chosen as drinking water supply since a centralised abstraction process only requires small costs. Cost estimation in this study does not include the costs involved in the abstraction of groundwater from the available wells or bore holes and also transportation from groundwater to the water storage of a house. It only covers the cost estimation for the proposed treatment unit for a house with four to five members.

7.2 Installation of the proposed treatment unit at a household level

The proposed treatment unit consists of:

1. Raw groundwater storage container with volume of 50 L
2. Reactor of 20 L for mixing the prepared biomass stock solution of (MO+MC) with the untreated groundwater. The optimum dose for these mixed biomass is 400 mg/L (200:200 mg/L in ratio). The optimum dose was selected based on the effectiveness to remove target contaminants particularly heavy metals to meet the WHO standards as conducted in the previous experiments (Chapter 4).
3. Sand filter container. A brief diagram (not to scale) of the proposed treatment system set up for point-of-use drinking water is illustrated in Figure 7.1.

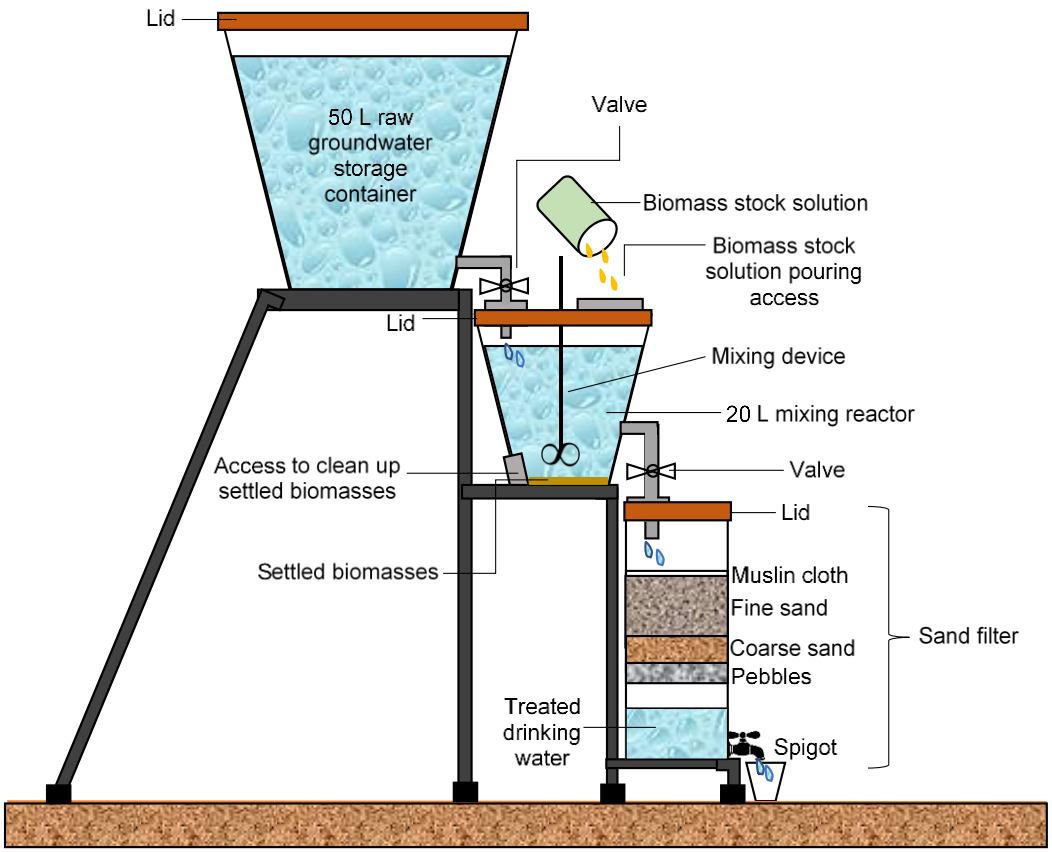

Figure 7.1 Proposed drinking water treatment units (point-of-use) for Pb, Ni and Cd removal using combined MO and MC (MO+MC) as water purification agents (not to scale)

It is proposed that the raw groundwater storage container should be connected to the coagulation reactor using a PVC pipe equipped with a valve to control the volume of water flows into the reactor. Similar connection using PVC pipe with a valve should also be connected from the coagulation reactor to the sand filter container. The sand filter is proposed in the treatment system since filter paper (micron size of pores) was used at the end of each treatment process to mimic the function of the sand filter. A piece of muslin cloth should be placed on the top layer of the sand. The purpose of placing the muslin cloth on the top of the fine sand layer is to retain the unsettled biomass from the coagulation reactor when the valve is open to let the water flow. Beneath the muslin cloth would be layers of fine sands, coarse sands and pebbles.

7.3 Operation and maintenance of the proposed treatment unit

Considering the purpose of this research which intends to minimise the cost of operation, there would be no electrical power needed to operate the proposed water treatment system. The agitation of prepared biomass stock solution with the untreated water can be performed by anyone in the house using a mixing tool such as a long wooden stick. According to Jagals & Rietveld (2011), small systems requires only one hour of operation per day. In this system, the only task that needs to be carried out by a person is the mixing process. Similar to the proposed treatment system, the mixing would require less than one hour (3 minutes of rapid mixing and 30 minutes of slow mixing) and settlement time of 30 minutes as conducted in the previous experiments reported in Chapter 4. Therefore, costs incurred during the installation, operation and maintenance can be minimised.

To avoid the use of an electrical pump, the raw groundwater storage container should be placed higher than the position of the coagulation reactor to allow the water to flow under the force of gravity when the valve is open. A similar situation also applies to the coagulation reactor which should be placed higher than the sand filter.

7.4 Preparation of biomass

One of the advantages of using natively available materials as water purification agents is that it bears no costs and widely available in the local region. In this study, a combination of MO with MC (MO+MC) was chosen as the biomass dosing method to be applied in the proposed treatment system.

In tropical countries, such as India, Sri Lanka, Pakistan and Bangladesh, MO seeds are widely found. This plant is commonly used in cooking and for medicinal purposes due to its high content of nutritional ingredients.

On the other hand, banana peels (MC) can also be obtained freely since it was considered as waste material. The use of MC as water treatment agent is suitable to the concept of being eco-friendly which encourages people to reuse and reduce the amount of waste materials that usually ends up in a landfill.

Raw MO and MC need to be processed to ensure the ‘treatment efficiency’ using these biomass was ‘maintained’ throughout the treatment process. Preparation of MO and MC was explained in detail as in Chapter 3 (Section 3.1.2).

The steps involved during the preparation of MO and MC were selection, cleaning, drying, grinding and sieving of biomass. Out of the steps mentioned, the cost was incurred only during the sieving process, which used stainless-steel mesh. The ground

biomass needs to be sieved to a homogenous size before being used in the treatment process. Figure 7.2 shows step by step process in preparing MO and MC biomass for the proposed water treatment system.

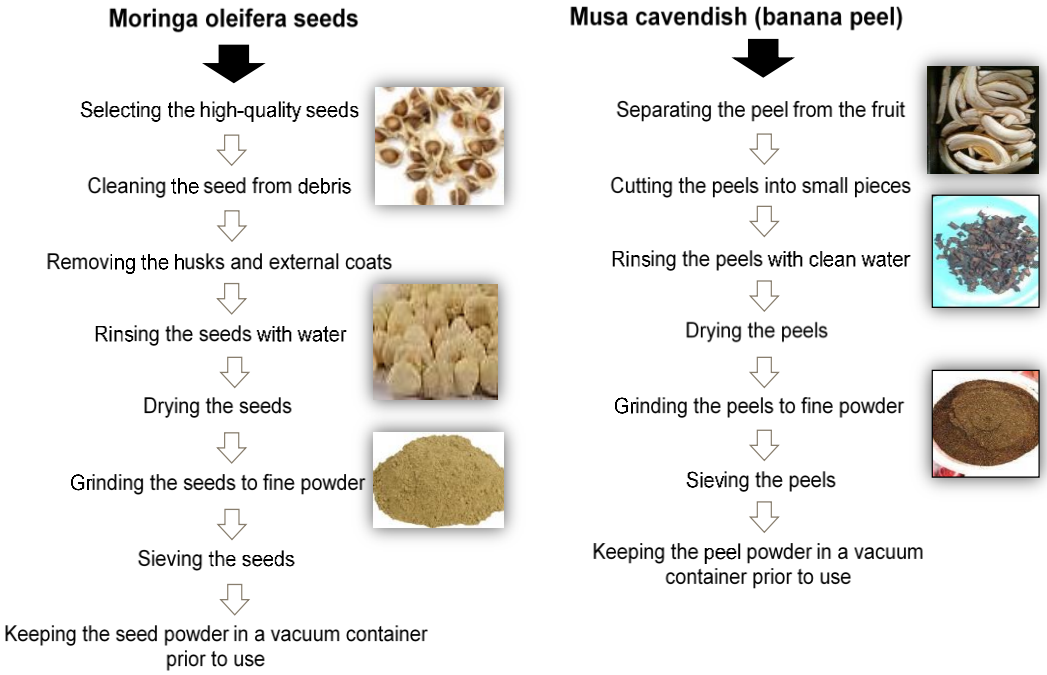

Figure 7.2 Preparation steps of MO and MC

7.5 Sludge management

The cleaning of the filter needs to be carried out by taking out the muslin cloth from the filter and remove the sludge (contaminant loaded-biomass) retained on the cloth. This step is more practical and easier to clean. The quantity of filtered solids or sludge from the system was found to be the same to that of amount introduced into the system. For example, if 200 mg of biomass was added for the treatment process, then was 200 mg of filtered solids will be collected at the end of treatment process. The contaminant-loaded biomass can be managed by using native earthworms namely *Perionyx excavatus* (Chakravarty et al., 2002). Native earthworms convert arsenic from plant

available to plant unavailable form. This method may be applicable to manage the sludge produced at the end of the proposed water treatment system.

7.6 Cost estimates for the proposed treatment systems

The costs of the proposed water treatment system were estimated based on the market price of the required materials (presented in Indian Rupees for the year of 2017) and are briefly presented in Table 7.1.

Table 7.1 Cost estimation for the proposed treatment unit at household level (according to the 2017 prices in India Rupees)

Description		Unit	Quantity	Rate (Rs)	Cost (Rs)	Cost (AUD)	Cost (USD)
Raw groundwater storage container (50 L)		piece	1	300	300	5.94	4.71
Coagulation reactor container (20 L)		piece	1	120	120	2.38	1.89
Sand filter container with spigot (20 L-transparent)		piece	1	120	120	2.38	1.89
L-shaped pipe connector (PVC)		piece	2	5	10	0.20	0.16
PVC pipe		m	6	1	6	0.12	0.10
Valve (PVC)		piece	2	25	50	0.99	0.78
Timber woods (stands to place the water containers)		kg	NA	0	0	0.00	0.00
Stainless steel sieve (for the preparation of biomass)		piece	1	80	80	1.58	1.25
Muslin cloth (to be used in the sand filter)		m	1	120	120	2.38	1.89
Fine sand, coarse sand, pebbles		NA	NA	0	0	0.00	0.00
Biomass* (optimum dose x 20 L capacity of water)	A. MO (optimum dose: 0.2 g/L)	g	4	0	0	0.00	0.00
	B. MC (optimum dose: 0.2 g/L)	g	4	0	0	0.00	0.00
	C. MO+MC (optimum dose: 0.4 g/L)	g	8	0	0	0.00	0.00
	D. Alum (optimum dose: 0.05 g/L)	g	1	0.05	0.05	0.00	0.00
Sub-total (Rs)					A. 806.00	15.96	12.65
					B. 806.00	15.96	12.65
					C. 806.00	15.96	12.65
					D. 806.05	15.96	12.65
10% contigency (Rs)					A. 80.60	1.60	1.27
					B. 80.60	1.60	1.27
					C. 80.60	1.60	1.27
					D. 80.60	1.60	1.27
Total (Rs)					A. 886.60	17.56	13.92
					B. 886.60	17.56	13.92
					C. 886.60	17.56	13.92
					D. 886.60	17.56	13.92

NA: not applicable; *: g x 20 L; MO (freely available in South Asian coutries but in Australia the price is AUD 30/kg where AUD 1 equivalent to ~Rs 50.46 (Indian Rupees)

The prices of medium to heavy duty 20 L PVC container varies between Rs 50 to Rs 300 (depending on the material and the required size). It was assumed that the

container for the proposed treatment system was made of heavy duty PVC material to ensure long-term durability. The retail prices of these containers vary from Rs 120 to Rs 300 for volume of 20 L to 50 L, respectively. The market prices of muslin cloth is in the range of Rs 8 to Rs 120 per meter (depending on the quality of the fabric). Alternatively, other available pieces of clean cloth can be used. According to Table 7.1, a good quality of muslin cloth priced at Rs 120 per meter was selected. The market price of L-shaped pipe connector (PVC) varies from Rs 1 to Rs 5 per piece while PVC pipe can be purchased at a price of Rs 1 per meter. Timber or reusable steel was suggested to be used as a stand, where the water containers and the sand filter will be placed. Stainless steel sieve that will be used in the preparation of biomass can be purchased at a price between Rs 60 to Rs 80 per piece while sands (fine and coarse) and pebbles can be collected from the surroundings. However, sands and pebbles need to be cleaned before they were placed in the filter container. In comparison to the conventional water purification agent (alum), the biomass (MO and MC) was expected to be found freely in the targeted countries as they were located in tropical climate region. Thus, no costs relating to these biomass were incurred. The retail price of alum per kg ranged between Rs 30 to Rs 45 per kg. According to Crittenden et al. (2012), typical doses for alum are 10 to 50 mg/L with pH between 6 to 7. Even though the cost of alum is considered inexpensive, the use of alum should be avoided due to harmful sludge production to reduce the environmental impact.

7.7 Conclusions

The estimated total cost for the proposed treatment system (based on the current market prices) is Rs 886.60 (equivalent to ~AUD 17.56 or ~USD 13.92). Therefore, it can be concluded that the proposed drinking water treatment system is affordable to be installed and applied at residential area of remote communities in developing countries.

CHAPTER 8 Conclusions and recommendations

The final chapter summarises the main findings of the research and relates the implications of this research for treating polluted groundwater using indigenous material in developing countries supplying rural communities. Recommendations are also included in this chapter to guide future research.

8.1 Conclusions

The major findings presented throughout this study are highlighted as follows:

8.1.1 Capability of plant-based material (biomass) in removing lead, nickel, cadmium, arsenic, fluoride and turbidity from drinking water to meet the WHO drinking water quality standards

- *Cicer arietinum* (chickpeas), *Cocos nucifera* (coconut's solid endosperm) and *Lentinus edodes* (Shiitake mushroom) did not show any potential in removing the target contaminants from the synthetic groundwater samples efficiently.
- *Moringa oleifera* (MO) and *Musa Cavendish* (MC) have the potential to be used as water purification agents. The optimum MO and MC doses of 200 mg/L gave the maximum removal of nickel, cadmium, arsenic, and fluoride from drinking water to meet the WHO drinking water quality standards (except arsenic and fluoride). However, 400 mg/L (200:200mg/L in the ratio) of combined MO and MC (MO+MC) gave a better removal efficiency (for most of target contaminants except turbidity) than 400 mg/L of individual biomass with the treated water successfully meeting the WHO drinking water standards (for most of target contaminants except arsenic and fluoride).
- The treatment of target contaminants using MO, MC and MO+MC did not significantly affect the pH of the water after treatment. It was able to maintain

the pH around the initial pH value of 7.0. This result highlights that the use of chemicals for pH adjustments after treatment can be minimised which consequently can reduce the overall treatment costs. This finding is another added benefit to the people living in remote areas in developing countries who are mostly economically disadvantaged.

- Testing of the selected treatment method (MO+MC at the optimum dose of 200:200 mg/L) on the actual groundwater samples showed that the removal efficiency of As, Pb, Cd and turbidity was higher in real groundwater samples. Overall, the results suggested that the combined biomass (MO+MC) was capable of treating the real groundwater samples to meet the stringent WHO standards.
- Arsenic (As) and fluoride appeared to be problematic contaminants as none of the untreated or pre-treated biomass were capable of reducing above contaminants to meet their respective WHO standards. However, 0.5 and 20 mg/L of alum (Al^{3+}) were able to remove As and fluoride concentrations, respectively to meet the respective WHO standards. Although it is not an indigenous material, the use of alum is an economical option to treat As and fluoride as it is also a low-cost material and widely available in the market.

8.1.2 Suggested contaminant removal mechanisms of plant-based biomass

The combination of different characterisation methods such as Attenuated Total Reflectance-Fourier Transform Infrared spectroscopy spectrum (ATR-FTIR) 100 (Perkin Elmer), Scanning Electron Microscope (SEM Quanta FEI 200) and Energy Dispersive X-Ray (EDX) indicated that the biomass interacted with target contaminants in different ways.

- The FTIR analyses showed carboxylic acids, primary and secondary amines and carbonyl (amides) were the dominant functional groups in MO, MC and MO+MC, which would favour the adsorption of the studied contaminants.
- The SEM images exhibited the abundant availability of porous and irregular surfaces which could provide binding sites that facilitate the accumulation (adsorption) of target contaminants on the biomass.
- The EDX analysis demonstrated the existence of oxygen (O) and nitrogen (N) on the biomass surface. This could suggest that electron sharing had occured between donor atoms (O and nitrogen N) and the contaminants, resulting in the formation of contaminant-biomass complexes. Furthermore, the detection of a specific feature (element) on the EDX spectrum of the contaminant-loaded biomass (i.e., after treatment) confirmed the adsorption of the contaminant by the biomass. In addition to that, a slight decrease in pH of the treated water indicated the occurrence of ion exchange between the functional groups and the contaminants.
- Overall, adsorption was suggested as a key mechanism for the removal of the target contaminant due to the abundant availability of porous and irregular surfaces which provide binding sites to facilitate the accumulation of target contaminants on the biomass. Adsorption by the biomass may be considered as physisorption and/or chemisorption depending on the nature of the contaminants. However, it was suspected that other mechanisms might also involve in the removal processes, such as surface complexation, electrostatic attraction and ion exchange.

The understanding on the mechanism of the treatment using the studied biomass should be taken into account in the future development and design considerations.

For example, a suitable pre-treatment method which intending to improve the treatment efficiency of biomass can be selected knowing the chemical and physical properties of the tested biomass.

8.1.3 Prediction of water quality output using an existing adsorption model

- The Freundlich model performed the best compared to Langmuir model in predicting the final concentration of lead (Pb), nickel (Ni) and cadmium (Cd) after treatment their with 200 mg/L of *Moringa oleifera* (MO) seeds and *Musa cavendish* (MC, banana peel), respectively and 200:200 mg/L of combined MO and MC (MO+MC).
- The maximum permissible concentrations of Pb (0.236, 0.088, 0.216 μmol/L), Ni (0.615, 0.641, 0.884 μmol/L), and Cd (0.060, 0.066, 0.072 μmol/L), were identified could be treated with optimum doses of MO, MC and MO+MC, respectively. Overall, MO+MC combination was found to give the highest probabilities to comply with the WHO standards (Pb: 91%, Ni: 98% and Cd: 84%) of 1000 simulated groundwater quality samples.

This intelligence is required to ensure that the selected treatment dose of the biomass is treating the groundwater to safe drinking water standards.

8.1.4 Cost estimation for a small drinking water treatment system

- The estimated total cost for the proposed treatment system/unit (based on the Indian current market prices) is Rs 886.60 (equivalent to ~USD 13.92 or ~AUD 17.56). Therefore, it is confirmed that the proposed household scale drinking water treatment system is affordable to be installed and applied at a household level by communities in remote areas in developing countries.

Conclusively, this research demonstrated that tropical plant-based materials have the potential for the removal of target contaminants from contaminated groundwater to meet the WHO drinking water standards. The understanding of the whole treatment process is essential for developing an operational scale decentralised treatment system in the future.

8.2 Recommendations for future works

The following recommendations are suggested to guide future research:

- Investigations on the effectiveness of MO and MC could be extended to other types of water quality contaminants such as biological contaminants as it was documented in literature that MO biomass can act as antimicrobial agent in water treatment.
- In this research, the applicability of the proposed treatment method using real groundwater samples from three different sites in Australia has shown to be promising. However, the characteristics of groundwater samples taken from these sites could be different to that of groundwater samples collected from the targeted South Asian countries. Thus, it is suggested that tests should also be performed with the real groundwater samples taken from the countries such as Sri Lanka, Bangladesh Pakistan and India to validate the applicability of the proposed treatment methods.
- The adsorption studies on MO+MC with the optimum dose of 200:200 mg/L (400 mg/L) for the removal of Pb, Ni and Cd were carried out according to the concept of static adsorption, which is normally applied for powdered activated carbon (PAC) in a closed system. This concept was expected to mimic the coagulation process as conducted in the preliminary experiments. It is

suggested that studies with the adsorption kinetic models (i.e. pseudo-first order and pseudo-second order models) should also be carried out on MO+MC to understand the rate controlling steps (Matouq et al., 2015).

- It is revealed that adsorption was identified to be the principal mechanism in the treatment of target contaminants (Pb, Ni, Cd, As, F and kaolin) using MO, MC and MO+MC as water treatment agents. However, the results from characterisation studies also suggested that there are other mechanisms (i.e., ion exchange and surface complexation) that could be working simultaneously along with the adsorption. Therefore, it is suggested that studies on the models that can reveal the mechanism of ion exchange and surface complexation should be carried out on the proposed biomass.
- It is important to evaluate the use of other multi-element adsorption models such as competitive Langmuir model, competitive multi-reaction model, ion exchange model and surface complexation model for the prediction of treated groundwater quality with predetermined biomass doses.
- The use of MO and MC in the treatment process could be further improved by coupling them with the other low-cost treatment units such as sand filtration or solar disinfection as these treatment methods are typically applied in remote areas.
- Further investigations on the low-cost sludge management methods should be carried out to minimise the impact of storing untreated sludge on the environment.

References

Adhikary, S. K., Manjur-A-Elahi, M., & A.M. Iqbal Hossain. (2012). Assessment of shallow groundwater quality from six wards of Khulna City Corporation, Bangladesh. International Journal of Applied Sciences and Engineering Research, 1(3), 488–498.

Afzal, S., Ahmad, I., Younas, M., Zahid, M. D., Khan, M. H. A., Ijaz, A., & Ali, K. (2000). Study of water quality of Hudiara drain, India-Pakistan. Environment International, 26, 87–96.

Agnihotri, N., Pathak, V. K., Khatoon, N., & Rahman, M. (2013). Removal of fluoride from water by Moringa oleifera seed residue after oil extraction. International Journal of Scientific & Engineering Research, 4(10), 106–110.

Ahluwalia, S. S., & Goyal, D. (2007). Microbial and plant derived biomass for removal of heavy metals from wastewater. Bioresource Technology, 98(12), 2243–2257.

Akhtar, M., Moosa Hasany, S., Bhanger, M. I., & Iqbal, S. (2007). Sorption potential of Moringa oleifera pods for the removal of organic pollutants from aqueous solutions. Journal of Hazardous Materials, 141, 546–556.

Akter, A., & Ahmed, S. (2015). Potentiality of rainwater harvesting for an urban community in Bangladesh. Journal of Hydrology, 528, 84–93.

Ali, E. N., Muyibi, S. A., Salleh, H. M., Alam, M. Z., & Salleh, M. R. M. (2010). Production of natural coagulant from Moringa Oleifera seed for application in treatment of low turbidity water. Journal of Water Resource and Protection, 2, 259–266.

Anawar, H. M., Akai, J., Komaki, K., Terao, H., Yoshioka, T., Ishizuka, T., Safiullah, S., Kato, K. (2003). Geochemical occurrence of arsenic in groundwater of Bangladesh: sources and mobilization processes. Journal of Geochemical Exploration, 77, 109–131.

Anwar, J., Shafique, U., Waheed-uz-Zaman, Salman, M., Dar, A., & Anwar, S. (2010). Removal of Pb(II) and Cd(II) from water by adsorption on peels of banana. Bioresource Technology, 101, 1752–1755.

Arain, M. B., Kazi, T. G., Baig, J. A., Jamali, M. K., Afridi, H. I., Shah, A. Q., Jalbani, N. Sarfraz, R. A. (2009). Determination of arsenic levels in lake water, sediment, and foodstuff from selected area of Sindh, Pakistan: estimation of daily dietary intake. Food and Chemical Toxicology, 47, 242–248.

Araújo, C. S. T., Alves, V. N., Rezende, H. C., Almeida, I. L. S., De Assunção, R. M. N., Tarley, C. R. T., Segatelli, M. G., Coelho, N. M. M. (2010). Characterization and use of Moringa oleifera seeds as biosorbent for removing metal ions from aqueous effluents. Water Science and Technology, 62(9), 2198–2203.

Araujo, C. S. T., Carvalho, D. C., Rezende, H. C., Almeida, I. L. S., Coelho, L. M., Coelho, N. M. M., Marques, T. L., Alves, V. N. (2013). Bioremediation of waters contaminated with heavy metals using Moringa oleifera seeds as biosorbent. Applied Bioremediation - Active and Passive Approaches, 227–255.

Arif, M., Hussain, I., Hussain, J., Sharma, S., & Kumar, S. (2012). Fluoride in the drinking water of Nagaur Tehsil of Nagaur district, Rajasthan, India. Bulletin of Environmental Contamination and Toxicology, 88(6), 870–875.

Asrafuzzaman, M., Fakhruddin, A. N. M., & Hossain, M. A. (2011). Reduction of Turbidity of Water Using Locally Available Natural Coagulants. International Scholarly Research Network (ISRN) Microbiology. New York: Hindawi Publishing Corporation.

Aturaliya, T. N. C., Abeysekera, D. T. D. J., Amerasinghe, P. H., Kumarasiri, P. V., & P. Bandara. (2006). Towards understanding of chronic kidney disease of North Central Province. Proc of Annual Scientific Sessions of Sri Lanka Medical Association.

Aziz, N.A.A., Jayasuriya, N. & Fan, L. (2014). Effectiveness of plant-based indigenous materials for the removal of heavy metals and fluoride from drinking water. In 5th International Conference on Sustainable Built Environment Proceedings. Kandy, Sri Lanka, 3, 34-41.

Aziz, N.A.A., Jayasuriya, N. and Fan, L (2015). Application of Moringa oleifera seeds and Musa cavendish as coagulants for lead, nickel and cadmium removal from drinking water. In: Asia Pacific Confederation of Chemical Engineering Congress 2015: APCChE 2015, incorporating CHEMECA 2015. Melbourne: Engineers Australia, 2015: 1774-1781.

Aziz, N. A. A., Jayasuriya, N., & Fan, L. (2016). Adsorption study on Moringa oleifera seeds and Musa cavendish as natural water purification agents for removal of lead, nickel and cadmium from drinking water. IOP Conference Series: Materials Science and Engineering, 136, 12044.

Bakken, T. H., Ruden, F., & Mangset, L. E. (2012). Submarine groundwater: A new concept for the supply of drinking water. Water Resources Management, 26(4), 1015–1026.

Bandara, J. M. R. S., Wijewardena, H. V. P., Liyanege, J., Upul, M. A., & Bandara, J. M. U. A. (2010). Chronic renal failure in Sri Lanka caused by elevated dietary cadmium: Trojan horse of the green revolution. Toxicology Letters, 198(1), 33–39.

Basu, N. B., & Van Meter, K. (2013). Sustainability of Groundwater Resources. In Comprehensive Water Quality and Purification (Vol. 4, pp. 57–75).

Bazanella, G. C. S., Silva, G. F., Vieira, A. M. S., & Bergamasco, R. (2012). Fluoride Removal from Water Using Combined Moringa oleifera/Ultrafiltration Process. Water, Air, & Soil Pollution, 223(9), 6083–6093.

Beltrán-Heredia, J., & Sánchez-Martín, J. (2009). Improvement of water treatment pilot plant with Moringa oleifera extract as flocculant agent. Environmental Technology, 30(6), 525–34.

Berger, P. S., Clark, R. M., Reasoner, D. J., Rice, E. W., & Santo Domingo, J. W. (2009). Water, Drinking. Encyclopedia of Microbiology (Third Edition) (pp. 121–137). Oxford: Academic Press.

Beyene, H. D. (2014). The potential of dyes removal from textile wastewater by using different treatment technology. A review. Int. J. Environ. Monit. Anal., 2(6), 347–353.

BGS, & DPHE. (2001). Arsenic contamination of groundwater in Bangladesh (Vol. 1). Department for International Development.

Bhatt, A. S., Sakaria, P. L., Vasudevan, M., Pawar, R. R., Sudheesh, N., Bajaj, H. C., & Mody, H. M. (2012). Adsorption of an anionic dye from aqueous medium by organoclays: equilibrium modeling, kinetic and thermodynamic exploration. RSC Advances, 2, 8663–8671.

Bhatti, H. N., Mumtaz, B., Hanif, M. A., & Nadeem, R. (2007). Removal of Zn(II) ions from aqueous solution using Moringa oleifera Lam. (horseradish tree) biomass. Process Biochemistry, 42(4), 547–553.

Bhende, S., & Jadhav, N. (2012). Moringa coagulant as a stabilizer for amorphous solids: Part I. American Association of Pharmaceutical Scientist, 13(2), 400-410.

Bhutada, P. R., Jadhav, A. J., Pinjari, D. V., Nemade, P. R., & Jain, R. D. (2016). Solvent assisted extraction of oil from Moringa oleifera Lam. seeds. Industrial Crops and Products, 82, 74–80.

BIS. (2012). Indian Standard-Drinking water Specification. New Delhi, India.

Boota, R., Bhatti, H. N., & Hanif, M. A. (2009). Removal of Cu(II) and Zn(II) using lignocellulosic fiber derived from Citrus reticulata (Kinnow) waste biomass. Separation and Purification Technology, 16(44), 4000–4022.

Bruanuer, S., Emmett, P. H., & Teller, E. (1938). Adsorption of gases in multimolecular layers. J. Am. Chem. Soc., (60), 309–316.

Buragohain, M., Bhuyan, B., & Sarma, H. P. (2010). Seasonal variations of lead, arsenic, cadmium and aluminium contamination of groundwater in Dhemaji district, Assam, India. Environmental Monitoring and Assessment, 170(1–4), 345–51.

Castro, R. S. D., Caetano, L. L., Ferreira, G., Padilha, P. M., Saeki, M. J., Zara, L. F., Martines, M. A. U., Castro, G. R. (2011). Banana Peel Applied to the Solid Phase Extraction of Copper and Lead from River Water: Preconcentration of Metal Ions with a Fruit Waste. Industrial & Engineering Chemistry Research, 50(6), 3446–3451.

Cempel, M., & Nikel, G. (2006). Nickel: A review of its sources and environmental toxicology. Polish Journal of Environmental Studies, 15(3), 375-382.

Chakraborti, D., Rahman, M. M., Das, B., Murrill, M., Dey, S., Chandra Mukherjee, S., Dhar, R. K., Biswas, B. K., Chowdhury, U. K., Roy, S., Sorif, S., Selim, M., Rahman, M., Quamruzzaman, Q. (2010). Status of groundwater arsenic contamination in Bangladesh: a 14-year study report. Water Research, 44(19), 5789–5802.

Chakravarty, S., Dureja, V., Bhattacharyya, G., Maity, S., & Bhattacharjee, S. (2002). Removal of arsenic from groundwater using low cost ferruginous manganese ore. Water Research, 36(3), 625–632.

Chandrajith, R., Dissanayake, C. B., Ariyarathna, T., Herath, H. M. J. M. K., & Padmasiri, J. P. (2011). Dose-dependent Na and Ca in fluoride-rich drinking water -Another major cause of chronic renal failure in tropical arid regions. Science of The Total Environment, 409(4), 671–675.

Chau, N. D. G., Sebesvari, Z., Amelung, W., & Renaud, F. G. (2015). Pesticide pollution of multiple drinking water sources in the Mekong Delta, Vietnam: evidence from two provinces. Environmental Science and Pollution Research, 22(12), 9042–9058.

Chaudhary, V., Kumar, M., Sharma, M., & Yadav, B. S. (2010). Fluoride, boron and nitrate toxicity in ground water of northwest Rajasthan, India. Environmental Monitoring and Assessment, 161(1–4), 343–348.

Chen, G., Zeng, G., Tang, L., Du, C., Jiang, X., Huang, G., Liu, H., Shen, G. (2008). Cadmium removal from simulated wastewater to biomass byproduct of Lentinus edodes. Bioresource Technology, 99(15), 7034–40.

Chen, G., Zeng, G., Tu, X., Niu, C.-G., Huang, G.-H., & Jiang, W. (2006). Application of a by-product of Lentinus edodes to the bioremediation of chromate contaminated water. Journal of Hazardous Materials, 135(1–3), 249–55.

Chen, J. P. (2012). Decontamination of heavy metals, processes, mechanisms, and applications. Boca Raton, London, New York: CRC Press.

Chowdhury, S., Mazumder, M. A. J. A. J., Al-Attas, O., & Husain, T. (2016). Heavy metals in drinking water: Occurrences, implications, and future needs in developing countries. Science of the Total Environment, 569–570, 476–488.

Choy, S. Y., Prasad, K. M. N., Wu, T. Y., & Ramanan, R. N. (2015). A review on common vegetables and legumes as promising plant-based natural coagulants in water clarification. International Journal of Environmental Science and Technology, 12(1), 367–390.

Chung, Y.-L., Liaw, Y.-P., Hwang, B.-F., Cheng, Y.-Y., Lin, M.-S., Kuo, Y.-C., & Guo, H.-R. (2013). Arsenic in drinking and lung cancer mortality in Taiwan. Journal of Asian Earth Sciences, 77, 327-331.

Coates, J. (2000). Interpretation of Infrared Spectra, A Practical Approach. Encyclopedia of Analytical Chemistry, 10815–10837.

Crittenden, J. C., Rhodes, T. R., David W Hand, J, H. K., & Tchobanoglous, G. (2012). MWH's Water Treatment: Principles and Design (3rd Edition). Wiley.

Dauphiné, D. C., Ferreccio, C., Guntur, S., Yuan, Y., Hammond, S. K., Balmes, J., Smith, A. H., Steinmaus, C. (2011). Lung function in adults following in utero and childhood exposure to arsenic in drinking water: Preliminary findings. International Archives of Occupational and Environmental Health, 84(6), 591–600.

Delpla, I., Jung, A. V., Baures, E., Clement, M., & Thomas, O. (2009). Impacts of climate change on surface water quality in relation to drinking water production. Environment International, 35(8), 1225-1233.

Dubinin, M. M., & Radushkevich, L. V. (1947). The equation of the characteristic curve of the activated charcoal. Proc. Acad. Sci. USSR Phys. Chem., (55), 331–337.

FAO. (2015). AQUASTAT database: Food and Agriculture Organization of the United Nations (FAO).

Farooqi, A., Masuda, H., & Firdous, N. (2007). Toxic fluoride and arsenic contaminated groundwater in the Lahore and Kasur districts, Punjab, Pakistan and possible contaminant sources. Environ Pollut, (145), 839–849.

Farooqi A., Masuda, H., Kusakabe, M., Naseem, M., & Firdous, N. (2007). Distribution of highly arsenic and fluoride contaminated groundwater from East Punjab, Pakistan, and the controlling role of anthropogenic pollutants in the natural hydrological cycle. Geochem J, (41), 213–234.

Fatombi, J. K., Lartiges, B., Aminou, T., Barres, O., & Caillet, C. (2013). A natural coagulant protein from copra (Cocos nucifera): Isolation, characterization, and potential for water purification. Separation and Purification Technology, 116, 35–40.

Feng, N., Guo, X., Liang, S., Zhu, Y., & Liu, J. (2011). Biosorption of heavy metals from aqueous solutions by chemically modified orange peel. Journal of Hazardous Materials, 185(1), 49–54.

Fewtrell, L., Smith, S., Kay, D., & Bartram, J. (2006). An attempt to estimate the global burden of disease due to fluoride in drinking water. Journal of Water and Health, 4(4), 533–542.

Flaten, T. P. (2001). Aluminium as a risk factor in Alzheimer's disease, with emphasis on drinking water. Brain Research Bulletin, 55(2), 187–196.

Freundlich, H. M. F. (1906). Over the adsorption in solution. J. Phys. Chem., 57, 385–471.

Gao, W., Majumder, M., Alemany, L. B., Narayanan, T. N., Ibarra, M. A., Pradhan, B. K., & Ajayan, P. M. (2011). Engineered Graphite Oxide Materials for Application in Water Purification. ACS Applied Materials & Interfaces, 3(6), 1821–1826.

Gautam, R. K., Mudhoo, A., Lofrano, G., & Chattopadhyaya, M. C. (2014). Biomass-derived biosorbents for metal ions sequestration: Adsorbent modification and activation methods and adsorbent regeneration. Journal of Environmental Chemical Engineering, 2(1), 239-259.

Ghoraba, S. M., & Khan, A. D. (2013). Hydrochemistry and groundwater quality assessment in Balochistan province, Pakistan. International Journal of Research and Reviews in Applied Sciences, 17(2), 185–199.

Gibson, K. E., & Schwab, K. J. (2011). Detection of bacterial indicators and human and bovine enteric viruses in surface water and groundwater sources potentially impacted by animal and human wastes in Lower Yakima Valley, Washington. Applied and Environmental Microbiology, 77(1), 355–362.

Gleick, P. H., & IWRA, M. (1996). Basic Water Requirements for Human Activities: Meeting Basic Needs. Water International, (21), 83–92.

Gopi, D., Kanimozhi, K., Bhuvaneshwari, N., Indira, J., & Kavitha, L. (2014). Novel banana peel pectin mediated green route for the synthesis of hydroxyapatite nanoparticles and their spectral characterization. Spectrochimica Acta - Part A: Molecular and Biomolecular Spectroscopy, 118, 589–597.

Gupta, D. A. (2008). Implication of environmental flows in river basin management. Physics and Chemistry of the Earth, 33(5), 298–303.

Halder, D., Bhowmick, S., Biswas, A., Chatterjee, D., Nriagu, J., Guha Mazumder, D. N., Lejkovec, Z., Jacks, G., Bhattacharya, P. (2013). Risk of arsenic exposure from drinking water and dietary components: Implications for risk management in rural Bengal. Environmental Science and Technology, 47(2), 1120–1127.

Hashim, M. A. a, Mukhopadhyay, S., Sahu, J. N., & Sengupta, B. (2011). Remediation technologies for heavy metal contaminated groundwater. Journal of Environmental Management, 92(10), 2355–2388.

Heath, J. (2015). Energy Dispersive Spectroscopy. Essential Knowledge Briefings, Second edition. West Sussex : John Wiley and Sons.

Hosono, T., Siringan, F., Yamanaka, T., Umezawa, Y., Onodera, S., Nakano, T., & Taniguchi, M. (2010). Application of multi-isotope ratios to study the source and quality of urban groundwater in Metro Manila, Philippines. Applied Geochemistry, 25(6), 900–909.

Hossain, M. A., Kumita, M., & Mori, S. (2010). SEM Characterization of the mass transfer of Cr (VI) during the adsorption on used black tea leaves. African Journal of Pure and Applied Chemistry, 4(7), 135–141.

Hossain, M. A., Ngo, H. H., Guo, W. S., & Nguyen, T. V. (2012). Biosorption of Cu (II) from water by banana peel based biosorbent : experiments and models of adsorption and desorption, 2(1), 87–104.

Hsu, L.-Y., & Teng, H. (2000). Influence of different chemical reagents on the preparation of activated carbons from bituminous coal. Fuel Processing Technology, 64(1), 155–166.

Howard, G., & Bartram, J. (2003). Domestic Water Quantity, Service, Level and Health.

Hu, C., Chen, Q., Chen, G., Liu, H., & Qu, J. (2015). Removal of Se(IV) and Se(VI) from drinking water by coagulation. Separation and Purification Technology, 142, 65–70.

Hussain, S., Mane, V., Pradhan, V., & Farooqui, M. (2012). Efficiency of seeds of Moringa Oleifera in estimation of water turbidity. International Journal of Research in Pharmaceutical and Biomedical Sciences, 3(3), 1334–1337.

Igwe, J. C., & Abia, A. A. (2007). Adsorption isotherm studies of Cd (II), Pb (II) and Zn (II) ions bioremediation from aqueous solution using unmodified and EDTA-modified maize cob. Ecletica Quimica, 32(1), 33–42.

Inglezakis, V. J., & Loizidou, M. D. (2007). Ion exchange of some heavy metal ions from polar organicsolvents into zeolite. Desalination, 211(1–3), 238–248.

Jagals, P., & Rietveld, L. (2011). Valuing water, valuing livelihoods: Guidance on social cost-benefit analysis of drinking-water interventions, with special reference to small community water supplies. In J. Cameron, P. Hunter, P. Jagals, & K. Pond (Eds.), Water Supply (pp. 149–166). London, United Kingdom: IWA Publishing.

Jayawardana, D. T., Pitawala, H. M. T. G. A., & Ishiga, H. (2012). Geochemical assessment of soils in districts of fluoride-rich and fluoride-poor groundwater, north-central Sri Lanka. Journal of Geochemical Exploration, (114), 118–125.

Jayawardanaa, D., Pitawala, H., & Ishigaa, H. (2010). Groundwater quality in different climatic zones of Sri Lanka: focus on the occurrence of fluoride. International Journal of Environmental Science and Development, 1(3), 244–250.

Jiang, J. Q. (2015). The role of coagulation in water treatment. Current Opinion in Chemical Engineering.

Joshi, J., & Sahu, O. (2014). Adsorption of Heavy Metals by Biomass. Journal of Applied & Environmental Microbiology, 2(1), 23–27.

Junior, A. C. G., Meneghel, A. P., Rubio, F., Strey, L., Dragunski, D. C., & Coelho, G. F. (2013). Applicability of Moringa oleifera Lam. pie as an adsorbent for removal of heavy metals from waters. Revista Brasileira de Engenharia Agrícola E Ambiental, 17(1), 94–99.

Kadirvelu, K., Thamaraiselvi, K., & Namasivayam, C. (2001). Adsorption of nickel(II) from aqueous solution onto activated carbon prepared from almond husk. Separation and Purification Technology, 24, 497–505.

Kaewsarn, P., Saikaew, W., & Wongcharee, S. (2008). Dried biosorbent derived from banana peel : a potential biosorbent for removal of cadmium ions from aqueous solution. In The 18th Thailand Chemical Engineering and Applied Chemistry Conference, 1–7.

Kalavathy, M. H., & Miranda, L. R. (2010). Moringa oleifera—A solid phase extractant for the removal of copper, nickel and zinc from aqueous solutions. Chemical Engineering Journal, 158(2), 188–199.

Kale, A. A. (2013). Uptake capacity of Pb2+ by sulphonated biomass of Cicer arietinum : batch studies. ISRN Environmental Chemistry, 1–6.

Kamsonlian, S., Balomajumder, C., & Chand, S. (2012). A Potential of biosorbent derived from banana peel for removal of As (III) from contaminated water. International Journal of Chemical Sciences and Applications, 3(2), 269–275.

Kannan, N., & Veemaraj, T. (2010). Batch adsorption dynamics and equilibrium studies for the removal of Cd(II) ions from aqueous solution using jack fruit seed and commercial activated carbons - a comparative study. Electronic J Environ. Agric. Food Chem., (9), 327–336.

Karnib, M., Kabbani, A., Holail, H., & Olama, Z. (2014). Heavy metals removal using activated carbon, silica and silica activated carbon composite. In Energy Procedia, 50, 113–120.

Katayon, S., Noor, M. J. M. M., Asma, M., Ghani, L. A. A., Thamer, A. M., Azni, I., Ahmad, J., Khor, B. C., Suleyman, A. M. (2006). Effects of storage conditions of Moringa oleifera seeds on its performance in coagulation. Bioresource Technology, 97(13), 1455–1460.

Kelly-Vargas, K., Cerro Lopez, M., Reyna-Tellez, S., Bandala, E. R., & Sanchez-Salas, J. L. (2012). Biosorption of heavy metals in polluted water , using different waste waste fruit cortex. Phys. Chem. Earth, (37–39), 26–29.

Khan, S. J. (2010). Quantitative chemical exposure assessment for water recycling schemes. Canberra.

Khan, S., Shahnaz, M., Jehan, N., Rehman, S., Shah, M. T., & Din, I. (2013). Drinking water quality and human health risk in Charsadda district, Pakistan. Journal of Cleaner Production, 60, 93–101.

Kiliç, M., Kirbiyik, Ç., Çepelioğullar, Ö., & Pütün, A. E. (2013). Adsorption of heavy metal ions from aqueous solutions by bio-char, a by-product of pyrolysis. Applied Surface Science, 283, 856–862.

Kim, D., Amy, G. L., & Karanfil, T. (2015). Disinfection by-product formation during seawater desalination: A review. Water Research, 81, 343–355.

Kothleitner, G., Neish, M. J., Lugg, N. R., Findlay, S. D., Grogger, W., Hofer, F., & Allen, L. J. (2014). Quantitative elemental mapping at atomic resolution using X-ray spectroscopy. Physical Review Letters, 112, 1–5.

Kumar, P., Barrett, D. M., Delwiche, M. J., & Stroeve, P. (2009). Methods for pretreatment of lignocellulosic biomass for efficient hydrolysis and biofuel production. Industrial and Engineering Chemistry Research, 48(8), 3713-3729.

Kumar, P. S., Ramalingam, S., Sathyaselvabala, V., Kirupha, S. D., Murugesan, A., & Sivanesan, S. (2012). Removal of Cd(II) from aqueous solution by agricultural waste cashew nut shell. Korean J. Chem. Eng., (29), 756-768.

Kumari, P., Sharma, P., Srivastava, S., & Srivastava, M. M. (2006). Biosorption studies on shelled Moringa oleifera Lamarck seed powder: Removal and recovery of arsenic from aqueous system. International Journal of Mineral Processing, 78(3), 131-139.

Kwaambwa, H. M., & Maikokera, R. (2008). Infrared and circular dichroism spectroscopic characterisation of secondary structure components of a water treatment coagulant protein extracted from Moringa oleifera seeds. Colloids and Surfaces B: Biointerfaces, 64(1), 118-125.

Langmuir, I. (1916). The constitution and fundamental properties of solids and liquids. J. Am. Chem. Soc., 38(11), 2221–2295.

Lantagne, D., Quick, R., & Mintz, E. (2006). Household water treatment and safe storage options in developing countries: a review of current implementation practices. Woodrow Wilson Quarterly, 17–38.

Leiknes, T., Ødegaard, H., & Myklebust, H. (2004). Removal of natural organic matter (NOM) in drinking water treatment by coagulation-microfiltration using metal membranes. Journal of Membrane Science, 242(1–2), 47–55.

Levantesi, C., Bonadonna, L., Briancesco, R., Grohmann, E., Toze, S., & Tandoi, V. (2012). Salmonella in surface and drinking water: Occurrence and water-mediated transmission. Food Research International, 45(2), 587–602.

Liu, C., Ngo, H. H., Guo, W., & Tung, K.-L. (2012). Optimal conditions for preparation of banana peels, sugarcane bagasse and watermelon rind in removing copper from water. Bioresource Technology, 119, 349–54.

Lombardo, A. W., & Brigano, F. A. (2014). Designing Filtration Systems to Remove Heavy Metals from Water. International Journal of High Speed Electronics and Systems, 23(1&2), 1-7.

Lürling, M., & Beekman, W. (2010). Anti-cyanobacterial activity of Moringa oleifera seeds. Journal of Applied Phycology, 22(4), 503–510.

Lykos, P. (1992). The Beer-Lambert law revisited: A development without calculus. Journal of Chemical Education, 69(9), 730–732.

Maher, A., Sadeghi, M., & Moheb, A. (2014). Heavy metal elimination from drinking water using nanofiltration membrane technology and process optimization using response surface methodology. Desalination, 352, 166–173.

Majumdar, K. K., & Guha Mazumder, D. N. (2012). Effect of drinking arsenic-contaminated water in children. Indian Journal of Public Health, 56(3), 223–226.

Mandinic, Z., Curcic, M., Antonijevic, B., Carevic, M., Mandic, J., Djukic-Cosic, D., & Lekic, C. P. (2010). Fluoride in drinking water and dental fluorosis. Science of the Total Environment, 408(17), 3507–3512.

Mann, A. G., Tam, C. C., Higgins, C. D., & Rodrigues, L. C. (2007). The association between drinking water turbidity and gastrointestinal illness: a systematic review. BMC Public Health, 7, 256.

Mansour, M. S., Ossman, M. E., & Farag, H. A. (2011). Removal of Cd (II) ion from waste water by adsorption onto polyaniline coated on sawdust. Desalination, 272(1–3), 301–305.

Mataka, L. M., Sajidu, S. M. I., Masamba, W. R. L., & Mwatseteza, J. F. (2010). Cadmium sorption by Moringa stenopetala and Moringa oleifera seed powders : Batch , time , temperature , pH and adsorption isotherm studies. International Journal of Water Resources and Environmental Engineering, 2(3), 50–59.

Matouq, M., Jildeh, N., Qtaishat, M., Hindiyeh, M., & Al Syouf, M. Q. (2015). The adsorption kinetics and modeling for heavy metals removal from wastewater by Moringa pods. Journal of Environmental Chemical Engineering, 3(2), 775–784.

Mayilswami, C., Thangarajan, M., Kulkarni, P. S., & Singh, V. P. (2012). Proceedings of the Fifth International Groundwater Conference Proceedings of the Fifth International Groundwater Conference. Water and Environment (Vol. 5).

Meenakshi, V., Meenakshi, Garg, V. K., Kavita, Renuka, & Malik, A. (2004). Groundwater quality in some villages of Haryana, India: focus on fluoride and fluorosis. Journal of Hazardous Materials, 106(1), 85–97.

Memon, J. R., Memon, S. Q., Bhanger, M. I. I., Memon, G. Z., El-Turki, A., & Allen, G. C. (2008). Characterization of banana peel by scanning electron microscopy and FT-IR spectroscopy and its use for cadmium removal. Colloids and Surfaces. B, Biointerfaces, 66(2), 260–5.

Memon, M., Soomro, M. S., Akhtar, M. S., & Memon, K. S. (2011). Drinking water quality assessment in Southern Sindh (Pakistan). Environmental Monitoring and Assessment, 177(1–4), 39–50.

Midrar-Ul-Haq, Khattak, R. A., Puno, H. K., Saif, M. S., & Memon, K. S. (2005). Surface and groundwater contamination in NWFP and Sindh provinces with respect to trace elements. Int J Agri Biol, 7, 214–217.

Mlakar, M., Fiket, Ž., Geček, S., Cukrov, N., & Cuculić, V. (2015). Marine lake as in situ laboratory for studies of organic matter influence on speciation and distribution of trace metals. Continental Shelf Research, 103, 1–11.

Mohammed, R. R., & Chong, M. F. (2014). Treatment and decolorization of biologically treated Palm Oil Mill Effluent (POME) using banana peel as novel biosorbent. Journal of Environmental Management, 132, 237–249.

Mondal, P., Balomajumder, C., & Mohanty, B. (2007). A laboratory study for the treatment of arsenic, iron, and manganese bearing ground water using Fe3+ impregnated activated carbon: Effects of shaking time, pH and temperature. Journal of Hazardous Materials, 144(1–2), 420–426.

Moreno-Tovar, R., Terrés, E., & Rangel-Mendez, J. R. (2014). Oxidation and EDX elemental mapping characterization of an ordered mesoporous carbon: Pb(II) and Cd(II) removal. Applied Surface Science, 303, 373–380.

Muhammad, S., Shah, M. T., & Khan, S. (2011). Health risk assessment of heavy metals and their source apportionment in drinking water of Kohistan region, northern Pakistan. Microchemical Journal, 98(2), 334–343.

Murali, V., & Aylmore, L. A. G. (1983). Competitive adsorption during solute transport in soils: A review of experimental evidence of competitive adsorption and an evaluation of simple competition models. Soil Science, 136(5), 279–290.

Naddeo, V., Scannapieco, D., & Belgiorno, V. (2013). Enhanced drinking water supply through harvested rainwater treatment. Journal of Hydrology, 498, 287–291.

Nagarajan, R., Rajmohan, N., Mahendran, U., & Senthamilkumar, S. (2010). Evaluation of groundwater quality and its suitability for drinking and agricultural use in Thanjavur city, Tamil Nadu, India. Environmental Monitoring and Assessment, 171(1–4), 289–308.

Najm, I. N. (1996). Mathematical modeling of PAC adsorption process. American Water Works Association, (October), 79–89.

Nasrullah, R., Naz, H., Bibi, M., Qbal, M. I., & Durrani. (2006). Pollution load in industrial effluent and ground water of Gadoon Amazai Induatrial Estate (GAIE) Swabi, NWFP. J Agri Biol Sci, 1, 18–24.

Ndabigengesere, A., Narasiah, K. S., & Talbot, B. G. (1995). Active agents and mechanism of coagulation of turbid waters using Moringa oleifera. Water Research, 29(2), 703–710.

Ndabigengesere, A., & Subba Narasiah, K. (1998). Quality of water treated by coagulation using Moringa oleifera seeds. Water Research, 32(3), 781–791.

Ndabigengesere K., & Narasiah, S. (1998). Use of Moringa Oleifera Seeds as a Primary Coagulant in Wastewater Treatment. Environmental Technology, 19(8), 789–800.

Ndibewu, P. P., Mnisi, R. L., Mokgalaka, S. N., & Mccrindle, R. I. (2011). Heavy Metal Removal in Aqueous Systems Using Moringa oleifera: A Review. Journal of Materials Science and Engineering, 1, 843–853.

NDWQS. (2011). Bangladesh national drinking water quality survey. Bangladesh.

Nguyen, T. A. H., Ngo, H. H., Guo, W. S., Zhang, J., Liang, S., Yue, Q. Y., Li, Q., Nguyen, T. V. (2013). Applicability of agricultural waste and by-products for adsorptive removal of heavy metals from wastewater. Bioresource Technology, 148, 574–85.

Nielsen, D. (2006). The Science Behind Ground-Water Sampling. In The Essential Handbook of Ground-Water Sampling (pp. 1–34). CRC Press.

NSDWQ. (2008). National Standards for Drinking Water Quality of Pakistan. Pakistan.

Oehmen, A., Valerio, R., Llanos, J., Fradinho, J., Serra, S., Reis, M. A. M. M., Crespo, J. G., Velizarov, S. (2011). Arsenic removal from drinking water through a hybrid ion exchange membrane - Coagulation process. Separation and Purification Technology, 83(1), 137–143.

Okoro, I. A., & Okoro, S. O. (2011). Agricultural by Products as Green Chemistry Absorbents for the Removal and Recovery of Metal Ions from Waste-Water Environments. Continental J. Water, Air and Soil Pollution, 2(1), 15–22.

Okuda, T., Baes, A. U., Nishijima, W., & Okada, M. (2001). Coagulation Mechanism of Salt Solution-Extracted Active Component in Moringa oleifera Seeds. Water Research, 35(3), 830–834.

Pagnanelli, F., Mainelli, S., Vegliò, F., & Toro, L. (2003). Heavy metal removal by olive pomace: Biosorbent characterisation and equilibrium modelling. Chemical Engineering Science, 58(20), 4709–4717.

Palma, C., Contreras, E., Urra, J., & Martínez, M. J. (2011). Eco-friendly technologies based on banana peel use for the decolourization of the dyeing process wastewater. Waste and Biomass Valorization, 2(1), 77–86.

Pandey, P. K., Verma, Y., Choubey, S., Pandey, M., & Chandrasekhar, K. (2008). Biosorptive removal of cadmium from contaminated groundwater and industrial effluents. Bioresource Technology, 99(10), 4420–4427.

Pandey, V. P., Shrestha, S., & Thatikonda, S. (2016). Water Environment in South Asia : An Introduction. In Groundwater Environment in Asian Cities (pp. 41–46). Elsevier Inc.

Pang, F. M., Teng, S. P., Teng, T. T., & Mohd Omar, A. K. (2009). Heavy metals removal by hydroxide precipitation and coagulation-flocculation methods from aqueous solutions. Water Quality Research Journal of Canada, 44(2), 174–182.

Pritchard, M., Craven, T., Mkandawire, T., Edmondson, A. S., O'Neill, J. G., & O'Neill, J. G. (2010). A study of the parameters affecting the effectiveness of Moringa oleifera in drinking water purification. Physics and Chemistry of the Earth, 35, 798–805.

Pritchard, M., Mkandawire, T., Edmondson, A., O'Neill, J. G., Kululanga, G., O'Neill, J. G., & Kululanga, G. (2009). Potential of using plant extracts for purification of shallow well water in Malawi. Physics and Chemistry of the Earth, 34(13–16), 799–805.

Putra, W. P., Kamari, A., Najiah, S., Yusoff, M., & Ishak, C. F. (2014). Biosorption of Cu (II), Pb (II) and Zn (II) Ions from Aqueous Solutions Using Selected Waste Materials : Adsorption and Characterisation Studies. Journal of Encapsulation and Adsorption Sciences, 4, 25–35.

Rafique, A., Awan, M. A., Wasti, A., Qazi, I. A., & Arshad, M. (2013). Removal of fluoride from drinking water using modified immobilized activated alumina. Journal of Chemistry, 1-7.

Rahman, M. M., Asaduzzaman, M., & Naidu, R. (2013). Consumption of arsenic and other elements from vegetables and drinking water from an arsenic-contaminated area of Bangladesh. Journal of Hazardous Materials, 262, 1056–1063.

Rajapakse, J., Waterman, P., Millar, G., & Sumanaweera, S. (2014). Emerging water treatment technologies for decentralised systems : and very remote regions of Australia and vulnerable and lagging rural regions in Sri Lanka. In Sustainable Economic Growth for Regional Australia (SEGRA) 2014 Conference Proceedings (pp. 1–28). Northern Territory, Australia, Australia.

Rajasooriyar, L. D., Boelee, E., Prado, M. C. C. M., & Hiscock, K. M. (2013). Mapping the potential human health implications of groundwater pollution in southern Sri Lanka. Water Resources and Rural Development, 1, 27–42.

Rajoriya, S., & Kaur, B. (2014). Adsorptive removal of zinc from waste water by natural biosorbents. International Journal of Engineering Science Invention, 3(6), 60–80.

Reddy, D. H. K., Harinath, Y., Seshaiah, K., & Reddy, A. V. R. (2010). Biosorption of Pb(II) from aqueous solutions using chemically modified Moringa oleifera tree leaves. Chemical Engineering Journal, 162(2), 626–634.

Reddy, D. H. K., Seshaiah, K., Reddy, A. V. R., & Lee, S. M. (2012). Optimization of Cd(II), Cu(II) and Ni(II) biosorption by chemically modified Moringa oleifera leaves powder. Carbohydrate Polymers, 88(3), 1077–1086.

Redlich, O., & Peterson, D. L. (1959). A useful adsorption isotherm. J. Phys. Chem., (63), 1024–1026.

Regmi, P., Garcia Moscoso, J. L., Kumar, S., Cao, X., Mao, J., & Schafran, G. (2012). Removal of copper and cadmium from aqueous solution using switchgrass biochar produced via hydrothermal carbonization process. Journal of Environmental Management, 109, 61–69.

Rinta-Kanto, J. M., Lehtola, M. J., Vartiainen, T., & Martikainen, P. J. (2004). Rapid enumeration of virus-like particles in drinking water samples using SYBR green I-staining. Water Research, 38(10), 2614–2618.

Roy, W. R., Hassett, J. J., & Griffin, R. A. (1985). Competitive Coefficients for the Adsorption of Arsenate, Molybdate, and Phosphate Mixtures by Soils. Soil Science Society of America Journal, 50(5), 1176–1182.

Ryan, P. B., Huet, N., & MacIntosh, D. L. (2000). Longitudinal investigation of exposure to arsenic, cadmium, and lead in drinking water. Environmental Health Perspectives, 108(8), 731–735.

Sağ, Y., Akçael, B., & Kutsal, T. (2001). Evaluation, interpretation, and representation of three-metal biosorption equilibria using a fungal biosorbent. Process Biochemistry, 37(1), 35–50.

Sánchez-Martín, J., Ghebremichael, K., & Beltrán-Heredia, J. (2010). Comparison of single-step and two-step purified coagulants from Moringa oleifera seed for turbidity and DOC removal. Bioresource Technology, 101(15), 6259–6261.

Sang, Y., Li, F., Gu, Q., Liang, C., & Chen, J. (2008). Heavy metal-contaminated groundwater treatment by a novel nanofiber membrane. Desalination, 223(1–3), 349–360.

Saqib, A. N. S., Waseem, A., Khan, A. F., Mahmood, Q., Khan, A., Habib, A., & Khan, A. R. (2013). Arsenic bioremediation by low cost materials derived from Blue Pine (Pinus wallichiana) and Walnut (Juglans regia). Ecological Engineering, 51(0), 88–94.

Saraswat, S., & Rai, J. P. N. (2010). Heavy metal adsorption from aqueous solution using Eichhornia crassipes dead biomass. International Journal of Mineral Processing, 94(3–4), 203–206.

Sarker, M. M. R. (2012). Spatial modeling of households' knowledge about arsenic pollution in Bangladesh. Social Science & Medicine, 74(8), 1232–1239.

Sarparastzadeh, H., Saeedi, M., Naeimpoor, F., & Aminzadeh, B. (2007). Pretreatment of municipal wastewater by enhanced chemical coagulation. International Journal of Environmental Research, 1(2), 104–113.

Sasikala, G., & Muthuraman, G. (2016). A Laboratory Study for the Treatment of Turbidity and Total Hardness Bearing Synthetic Wastewater/Ground Water Using Moringa oleifera. Industrial Chemistry, 2, 112.

Schmidt, P. J., Emelko, M. B., & Thompson, M. E. (2013). Analytical recovery of protozoan enumeration methods: have drinking water QMRA models corrected or created bias? Water Research, 47(7), 2399–408.

Schneider, I. A. H., Rubio, J., & Smith, R. W. (2001). Biosorption of metals onto plant biomass: Exchange adsorption or surface precipitation? International Journal of Mineral Processing, 62(1–4), 111–120.

Schoeters, G., Den Hond, E., Zuurbier, M., Naginiene, R., Van Den Hazel, P., Stilianakis, N., Ronchetti, R., Koppe, J. (2006). Cadmium and children: Exposure and health effects. Acta Paediatrica, 95(453), 50–54.

Sekar, M., Sakthi, V., & Rengaraj, S. (2004). Kinetics and equilibrium adsorption study of lead(II) onto activated carbon prepared from coconut shell. Journal of Colloid and Interface Science, 279(2), 307–13.

Selim, H. M., & Zhang, H. (2013). Modeling approaches of competitive sorption and transport of trace metals and metalloids in soils: a review. Journal of Environmental Quality, 42(3), 640–653.

Sengupta, M. E., Keraita, B., Olsen, A., Boateng, O. K., Thamsborg, S. M., Pálsdóttir, G. R., & Dalsgaard, A. (2012). Use of Moringa oleifera seed extracts to reduce helminth egg numbers and turbidity in irrigation water. Water Research, 46(11), 3646–3656.

Sethi, V., & Clark, R. M. (1998). Cost estimation models for drinking water treatment unit processes. Indian Journal of Engineeering & Materials Sciences, 5(August), 223–235.

Sharma, P., Kumari, P., Srivastava, M. M., & Srivastava, S. (2006). Removal of cadmium from aqueous system by shelled Moringa oleifera Lam. seed powder. Bioresource Technology, 97(2), 299–305.

Sharma, V., & Paliwal, R. (2013). Isolation and characterization of saponins from Moringa oleifera (moringaeceae) pods. International Journal of Pharmacy and Pharmaceutical Sciences, 5(1), 179–183.

Sheindorf, C., Rebhun, M., & Sheintuch, M. (1981). A Freundlich-type multicomponent isotherm. Journal of Colloid And Interface Science, 79(1), 136–142.

Silverstein, R. M., Bassler, G. C., & Morill, T. C. (1981). Spectrometric Identification of Organic Compounds. (N. Y. J. W. and Sons, Ed.) (4th ed.). New York: John Wiley and Sons.

Singh, B., Gaur, S., & Garg, V. K. (2007). Fluoride in drinking water and human urine in Southern Haryana, India. Journal of Hazardous Materials, 144(1–2), 147–151.

Singh, B., Singh, K., Rejeshwar Rao, G., Chikara, J., Kumar, D., Mishra, D. K., Saikia, S. P., Pathre, U. V., Raghuvanshi, N., Rahi, T. S., Tuli, R. (2013). Agro-technology of Jatropha curcas for diverse environmental conditions in India. Biomass and Bioenergy, 48(0), 191–202.

Singh, S. P., Ma, L. Q., & Hendry, M. J. (2006). Characterization of aqueous lead removal by phosphatic clay: equilibrium and kinetic studies. Journal of Hazardous Materials, 136(3), 654–62.

Sivakumar, D. (2012). Adsorption study on municipal solid waste leachate using Moringa oleifera seed. International Journal of Environmental Science and Technology, 10(1), 113–124.

Sivapriya, M., & Leela, S. (2007). Isolation and purification of a novel antioxidant protein from the water extract of Sundakai (Solanum torvum) seeds. Food Chemistry, 104(2), 510–517.

SLS. (2013). Drinking water standard - First Revision (Sri Lanka Standards for potable water – SLS 614: 2013). Sri Lanka.

Smeets, P. W. M. H., & Medema, G. J. (2006). Combined use of microbiological and non-microbiological data to assess treatment efficacy. Water Science and Technology, 54(3), 35–40.

Smith, A. H., & Steinmaus, C. M. (2009). Health effects of arsenic and chromium in drinking water: recent human findings. Annual Review of Public Health, 30, 107–122.

Sultana, S., & Ahmed, K. M. (2016). Assessing risk of clogging in community scale managed aquifer recharge sites for drinking water in the coastal plain of south-west Bangladesh. Bangladesh Journal of Scientific Research, 27(1), 75.

Sounthararajah, D., Loganathan, P., Kandasamy, J., & Vigneswaran, S. (2015). Effects of humic acid and suspended solids on the removal of heavy metals from water by adsorption onto granular activated carbon. International Journal of Environmental Research and Public Health, 12(9), 10475–10489.

Sumathi, T., & Alagumuthu, G. (2014). Adsorption studies for arsenic removal using activated Moringa oleifera, 1–7.

Tariq, M., Ali, M., & Shah, Z. (2006). Characteristics of industrial effluents and their possible impacts on quality of underground water. Soil Environ, (25), 64–69.

Tariq, S. R., Shah, M. H., Shaheen, N., Jaffar, M., & Khalique, A. (2008). Statistical source identification of metals in groundwater exposed to industrial contamination. Environmental Monitoring and Assessment, 138(1–3), 159–165.

Tempkin, M. I., & Pyzhev, V. (1940). Kinetics of ammonia synthesis on promoted iron catalyst. Acta Phys. Chim., (12), 327–356.

Tibolla, H., Pelissari, F. M., & Menegalli, F. C. (2014). Cellulose nanofibers produced from banana peel by chemical and enzymatic treatment. LWT - Food Science and Technology, 59(2P2), 1311–1318.

Tomar, G., Thareja, A., & Sarkar, S. (2015). Enhanced fluoride removal by hydroxyapatite-modified activated alumina. International Journal of Environmental Science and Technology, 12(9), 2809–2818.

Ul-Haq, N., Arain, M. a, Badar, N., Rasheed, M., & Haque, Z. (2011). Drinking water: a major source of lead exposure in Karachi, Pakistan. Eastern Mediterranean Health Journal, 17(11), 882–886.

Ullah, R., Malik, R. N., & Qadir, A. (2009). Assessment of groundwater contamination in an industrial city, Sialkot, Pakistan. Afr J Environ Sci Technol, 3, 429–446.

USEPA. (2002). Short-term Methods for Estimating the Chronic Toxicity of Effluents and Receiving Waters to Freshwater Organisms Fourth Edition October 2002 (4th Edition) (Vol. 4). Washington, DC.

USGS. (2013). Quality of Ground Water. U.S. Department of the Interior U.S. Geological Survey

van Halem, D., Bakker, S. a., Amy, G. L., & van Dijk, J. C. (2009). Arsenic in drinking water: a worldwide water quality concern for water supply companies. Drinking Water Engineering and Science, 2(1), 29–34.

Vardhan, C. M. V., & Karthikeyan, J. (2011). Removal of fluoride from water using low-cost materials. In Fifteenth International Water Technology Conference, IWTC-15 2011, Alexandria, Egypt (pp. 1–14).

Verma, V. K., Tewari, S., & Rai, J. P. N. (2008). Ion exchange during heavy metal bio-sorption from aqueous solution by dried biomass of macrophytes. Bioresource Technology, 99(6), 1932–1938.

Višekruna, A., Štrkalj, A., & Pajc, L. M. (2011). The use of low Cost adsorbents for purification Wastewater. The Holistic Approach to Environment, 1, 29–37.

Viswanathan, G., Jaswanth, A., Gopalakrishnan, S., Siva ilango, S., & Aditya, G. (2009). Determining the optimal fluoride concentration in drinking water for fluoride endemic regions in South India. Science of The Total Environment, 407(20), 5298–5307.

WHO. (2004). Fluoride in Drinking Water. WHO Guidelines for Drinking-water Quality.

WHO. (2005). Nickel in Drinking Water. WHO Guidelines for Drinking-water Quality.

WHO. (2006). Guidelines for conducting cost–benefit analysis of household energy and health interventions.

WHO. (2011a). Arsenic in drinking-water. WHO Guidelines for Drinking-water Quality.

WHO. (2011b). Cadmium in Drinking-water. WHO Guidelines for Drinking-Water Quality.

WHO. (2011c). Guidelines for drinking-water Quality. WHO, pp. 5–6.

WHO. (2011d). Lead in Drinking Water-Background document for development of WHO Guidelines for Drinking Water Quality. WHO Guidelines for Drinking-water Quality. Geneva.

WHO, & UNICEF. (2015). 25 YEARS Progress on Sanitation and Drinking Water: 2015 Update and MDG Assessment. New York, NY: UNICEF and World Health Organisation, 4.

WQPBS. (2012). Water Quality Parameters Bangladesh Standards & WHO Guide Lines. Bangladesh.

Wu, J., Zhang, H., He, P. J., & Shao, L. M. (2011). Insight into the heavy metal binding potential of dissolved organic matter in MSW leachate using EEM quenching combined with PARAFAC analysis. Water Research, 45(4), 1711–1719.

Xu, P., Huang, S., Wang, Z., & Lagos, G. (2006). Daily intakes of copper, zinc and arsenic in drinking water by population of Shanghai, China. Science of The Total Environment, 362(1–3), 50–55.

Xu, Z., Cai, J.-G., & Pan, B.-C. (2013). Mathematically modeling fixed-bed adsorption in aqueous systems. Journal of Zhejiang University-SCIENCE A (Applied Physics & Engineering), 14(3), 155–176.

Yi, Y., Wang, Y., & Liu, H. (2003). Preparation of new crosslinked chitosan with crown ether and their adsorption for silver ion for antibacterial activities. Carbohydrate Polymers, 53(4), 425–430.

Yin, C.-Y. (2010). Emerging usage of plant-based coagulants for water and wastewater treatment. Process Biochemistry, 45(9), 1437–1444.

Zheng, H., & Wang, L. (2013). Banana Peel Carbon Containing Functional Groups Applied to the Selective Adsorption of Au (III) from Waste Printed Circuit Boards. Soft Nanoscience Letters, 3, 29–36.

Zheng, Y., van Geen, A., Stute, M., Dhar, R., Mo, Z., Cheng, Z., Horneman, A., Gavrieli, I., Simpson, H. J., Versteeg, R., Steckler, M., Grazioli-Venier, A., Goodbred, S., Shahnewaz, M., Shamsudduha, M., Hoque, M A., Ahmed, K. M. (2005). Geochemical and hydrogeological contrasts between shallow and deeper aquifers in two villages of Araihazar, Bangladesh: Implications for deeper aquifers as drinking water sources. Geochimica et Cosmochimica Acta, 69(22), 5203–5218.

Zhou, H., Chen, W., Gao, Z. Y., & Chen, D. (2014). Removal of fluoride from aqueous media by zirconium modified zeolite. Asian Journal of Chemistry, 26(23), 8062–8068.

Zhu, K., Zhang, L., Hart, W., Liu, M., & Chen, H. (2004). Quality issues in harvested rainwater in arid and semi-arid Loess Plateau of northern China. Journal of Arid Environments, 57(4), 487–505.

Zhu, Y., Hu, J., & Wang, J. (2012). Competitive adsorption of Pb(II), Cu(II) and Zn(II) onto xanthate-modified magnetic chitosan. Journal of Hazardous Materials, 221–222, 155–161.

List of appendices

Appendix A1 Results of standard calibrations for ICP-MS analyses

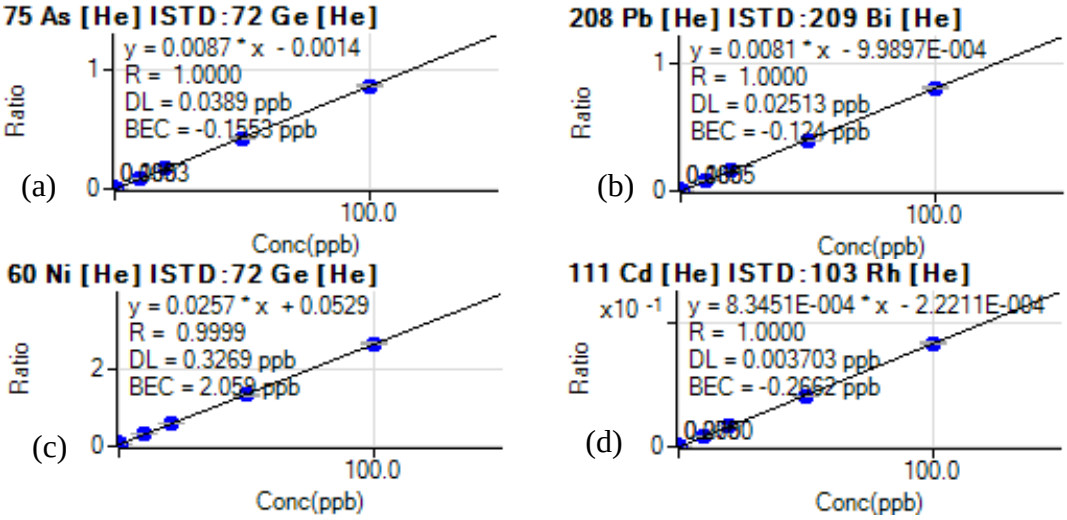

Figure A1.1 Standard calibration of ICP-MS analyses for (a) arsenic (As), (b) lead (Pb), (c) nickel (Ni) and (d) cadmium (Cd)

*Standard solutions of 10, 20, 50, 80 and 100 ppb @ µg/L for As, Pb, Ni and Cd, respectively were prepared prior to the ICP-MS standard calibration

Appendix A2 EDX spectra of contaminant loaded MC and MO+MC

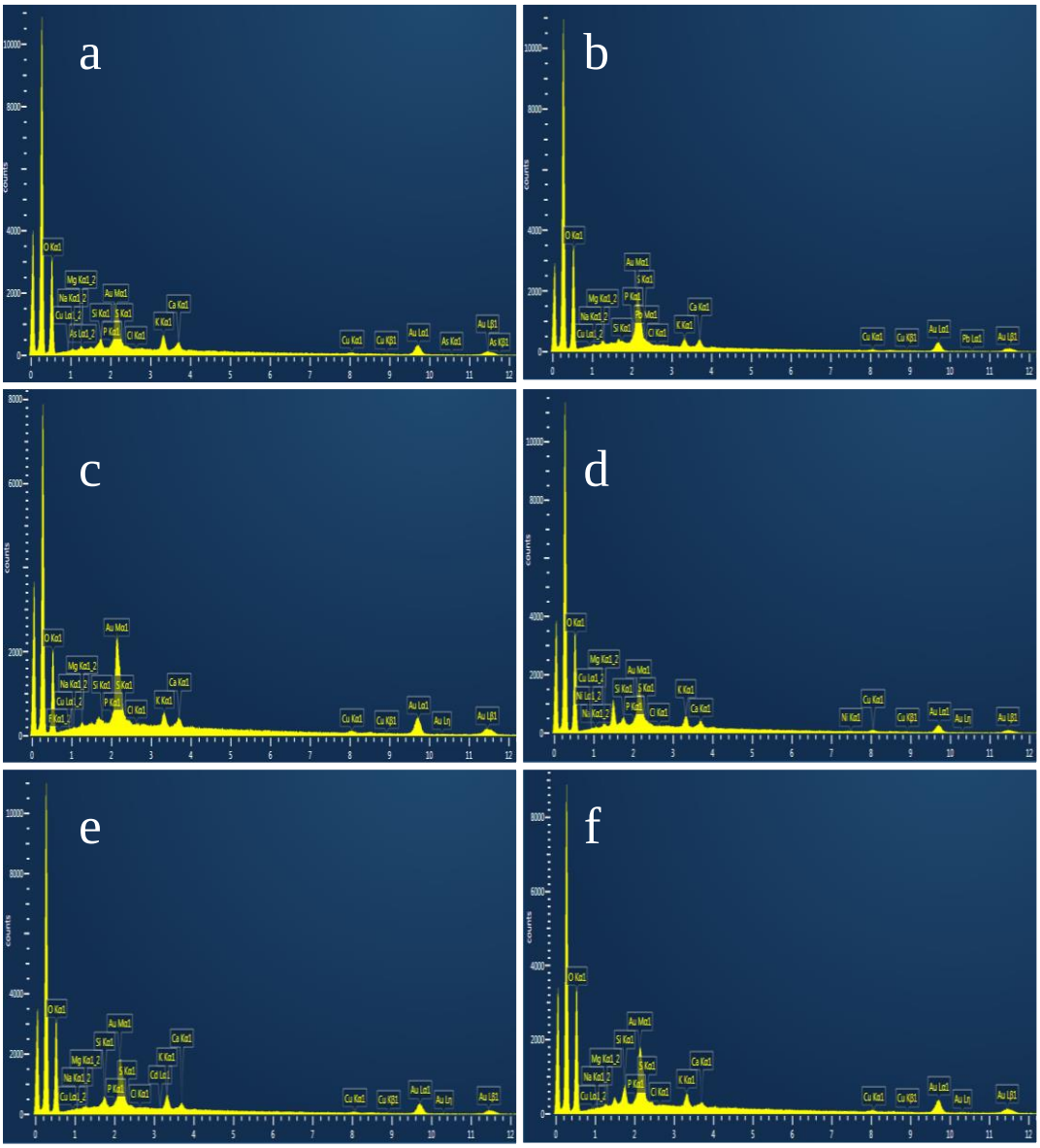

Figure A2.1 EDX spectra of MC loaded with (a) As, (b) Pb, (c) Ni, (d) Cd, (e) fluoride and kaolin (turbidity)

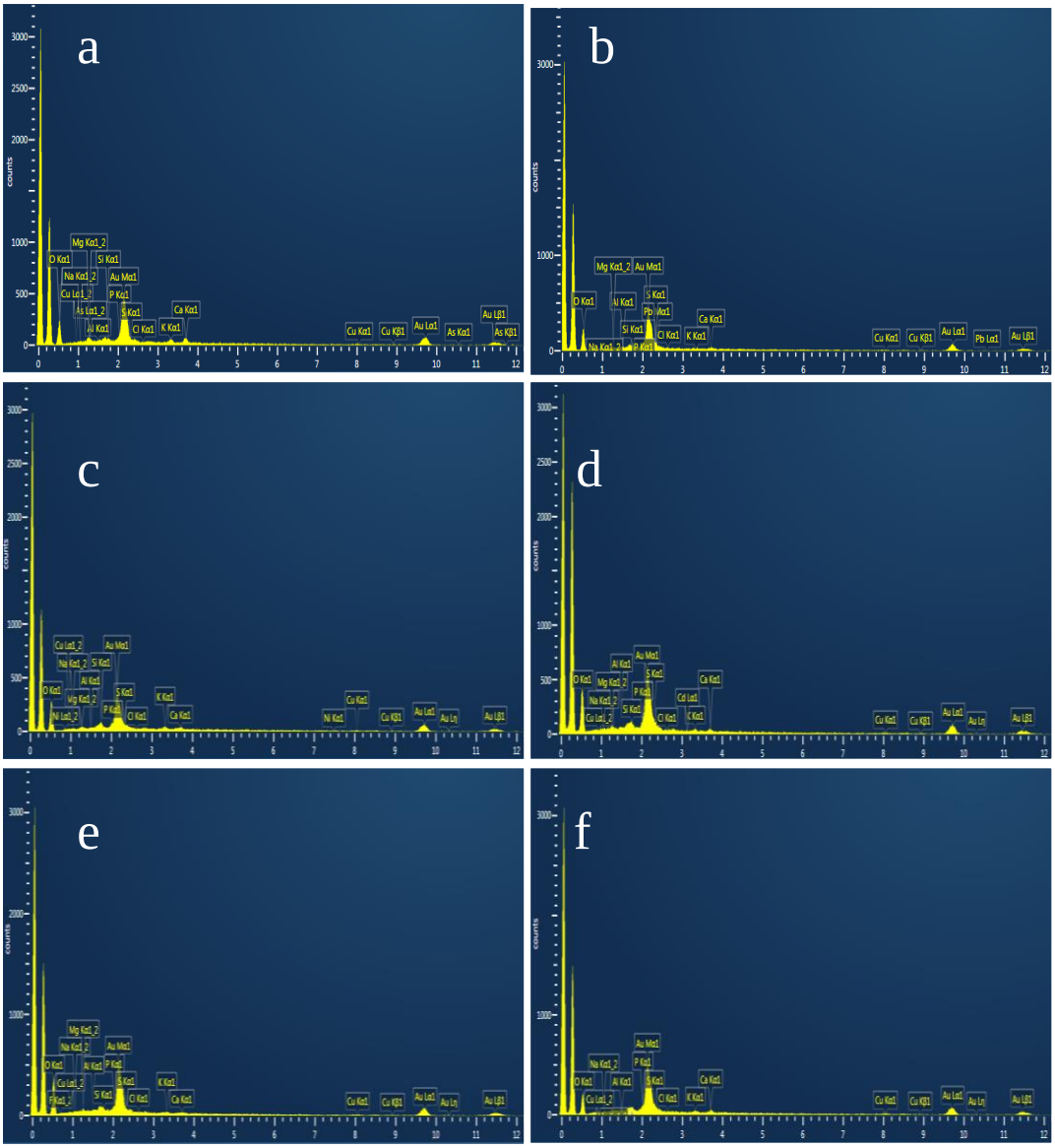

Figure A2.2 EDX spectra of MO+MC loaded with (a) As, (b) Pb, (c) Ni, (d) Cd, (e) fluoride and kaolin (turbidity)

Appendix A3 Elemental composition of unloaded and contaminant-loaded biomass (EDX)

Table A3.1 Elemental composition of unloaded and contaminant-loaded MO

Element	Unloaded		As-loaded		Pb-loaded		Ni-loaded		Cd-loaded		Fluoride-loaded		Kaolin-loaded	
	N=5		N=5		N=4		N=5		N=4		N=7		N=4	
	Wt%	SD	% Wt	SD	Wt%	SD	% Wt	SD	% Wt	SD	Wt%	SD	Wt%	SD
C	74.21	1.77	68.71	2.32	69.12	1.53	71.25	1.50	67.19	0.40	70.81	1.31	68.30	1.08
O	18.21	1.98	27.84	2.42	27.05	1.96	25.40	1.26	29.98	0.56	27.04	1.33	28.21	1.22
N	2.54	0.09	1.76	0.04	1.84	0.04	1.44	0.02	1.25	0.07	1.38	0.02	1.89	0.05
Na	0.06	0.04	0.04	0.01	0.06	0.04	0.06	0.02	0.03	0.03	0.03	0.02	0.05	0.02
Mg	0.28	0.07	0.07	0.03	0.06	0.03	0.06	0.02	0.10	0.03	0.05	0.01	0.07	0.02
Al	0.08	0.02	0.03	0.01	0.04	0.03	0.06	0.03	0.04	0.01	0.02	0.01	0.28	0.12
Si	0.03	0.02	0.06	0.01	0.12	0.05	0.05	0.03	0.05	0.02	0.02	0.02	0.28	0.09
P	0.93	0.08	0.47	0.18	0.55	0.25	0.56	0.27	0.35	0.10	0.14	0.07	0.21	0.07
S	2.65	0.18	0.71	0.09	0.81	0.17	0.79	0.26	0.67	0.17	0.34	0.04	0.44	0.09
Cl	0.04	0.01	0.01	0.01	0.01	0.01	0.01	0.01	0.01	0.01	0.00	0.01	0.01	0.01
K	0.57	0.14	0.01	0.01	0.01	0.01	0.01	0.01	0.01	0.01	0.00	0.01	0.02	0.01
Ca	0.19	0.02	0.16	0.09	0.14	0.03	0.11	0.04	0.17	0.04	0.07	0.01	0.11	0.05
Cu	0.21	0.04	0.12	0.03	0.14	0.03	0.16	0.06	0.13	0.03	0.07	0.02	0.13	0.04
As	0.00	0.00	0.01	0.01	0.00	0.00	0.00	0.00	0.00	0.00	0.00	0.00	0.00	0.00
Pb	0.00	0.00	0.00	0.00	0.05	0.03	0.00	0.00	0.00	0.00	0.00	0.00	0.00	0.00
Ni	0.00	0.00	0.00	0.00	0.00	0.00	0.04	0.02	0.00	0.00	0.00	0.00	0.00	0.00
Cd	0.00	0.00	0.00	0.00	0.00	0.00	0.00	0.00	0.02	0.02	0.00	0.00	0.00	0.00
F	0.00	0.00	0.00	0.00	0.00	0.00	0.00	0.00	0.00	0.00	0.03	0.04	0.00	0.00
Total	100.00		100.00		100.00		100.00		100.00		100.00		100.00	

*N: number of examined sites, %Wt: percentage weight, SD: standard deviation

Table A3.2 Elemental composition of unloaded and contaminant-loaded MC

Element	Unloaded		As-loaded		Pb-loaded		Ni-loaded		Cd-loaded		Fluoride-loaded		Kaolin-loaded	
	N=6		N=6		N=7		N=5		N=5		N=7		N=5	
	Wt%	SD	% Wt	SD	Wt%	SD	% Wt	SD	% Wt	SD	Wt%	SD	Wt%	SD
C	57.22	5.46	63.47	2.16	62.00	3.42	64.12	2.76	63.73	1.06	67.40	2.84	62.41	2.84
O	34.40	6.70	35.13	2.17	36.66	3.36	34.67	2.81	34.77	1.02	31.68	2.91	36.52	2.76
N	0.29	0.04	0.15	0.07	0.14	0.03	0.10	0.08	0.15	0.04	0.18	0.07	0.21	0.03
Na	0.14	0.12	0.08	0.03	0.09	0.02	0.09	0.04	0.07	0.03	0.09	0.04	0.04	0.02
Mg	0.11	0.09	0.13	0.04	0.13	0.04	0.12	0.04	0.09	0.03	0.09	0.04	0.08	0.02
Si	0.08	0.06	0.12	0.04	0.15	0.09	0.14	0.04	0.23	0.06	0.04	0.01	0.17	0.05
P	0.15	0.09	0.06	0.02	0.06	0.02	0.05	0.02	0.05	0.01	0.01	0.01	0.03	0.01
S	0.08	0.05	0.08	0.03	0.08	0.01	0.12	0.06	0.10	0.05	0.10	0.03	0.05	0.02
Cl	0.93	0.53	0.01	0.01	0.01	0.01	0.00	0.01	0.01	0.00	0.01	0.01	0.00	0.01
K	5.63	2.22	0.38	0.11	0.33	0.07	0.27	0.03	0.44	0.10	0.17	0.05	0.25	0.06
Ca	0.67	1.53	0.24	0.10	0.22	0.09	0.17	0.04	0.19	0.05	0.11	0.04	0.16	0.13
Cu	0.30	0.25	0.13	0.04	0.12	0.02	0.14	0.05	0.16	0.04	0.08	0.03	0.08	0.02
As	0.00	0.00	0.02	0.02	0.00	0.00	0.00	0.00	0.00	0.00	0.00	0.00	0.00	0.00
Pb	0.00	0.00	0.00	0.00	0.01	0.01	0.00	0.00	0.00	0.00	0.00	0.00	0.00	0.00
Ni	0.00	0.00	0.00	0.00	0.00	0.00	0.01	0.02	0.00	0.00	0.00	0.00	0.00	0.00
Cd	0.00	0.00	0.00	0.00	0.00	0.00	0.00	0.00	0.01	0.01	0.00	0.00	0.00	0.00
F	0.00	0.00	0.00	0.00	0.00	0.00	0.00	0.00	0.00	0.00	0.04	0.06	0.00	0.00
Total	100.00		100.00		100.00		100.00		100.00		100.00		100.00	

*N: number of examined sites, %Wt: percentage weight, SD: standard deviation

(Appendix A3 Continued)

Table A3.3 Elemental composition of unloaded and contaminant-loaded MO+MC

Element	Unloaded		As-loaded		Pb-loaded		Ni-loaded		Cd-loaded		Fluoride-loaded		Kaolin-loaded	
	N=5		N=7		N=5		N=5		N=5		N=6		N=5	
	Wt%	SD	% Wt	SD	Wt%	SD	% Wt	SD	% Wt	SD	Wt%	SD	Wt%	SD
C	65.67	2.84	69.31	3.84	71.23	4.36	67.25	2.91	71.12	5.42	72.24	5.13	74.32	2.38
O	29.21	3.04	27.73	3.80	25.63	4.51	30.04	2.76	26.02	5.18	24.96	4.99	23.11	2.44
N	2.84	0.18	1.54	0.11	1.47	0.10	1.32	0.18	1.45	0.19	1.62	0.16	1.69	0.09
Na	0.10	0.00	0.10	0.06	0.03	0.04	0.06	0.08	0.06	0.07	0.02	0.05	0.03	0.04
Mg	0.32	0.15	0.21	0.12	0.18	0.12	0.20	0.04	0.17	0.18	0.14	0.08	0.12	0.06
Al	0.08	0.05	0.05	0.04	0.05	0.05	0.02	0.02	0.04	0.02	0.05	0.05	0.06	0.02
Si	0.22	0.20	0.06	0.04	0.13	0.09	0.19	0.17	0.12	0.10	0.07	0.06	0.08	0.04
P	0.26	0.12	0.20	0.09	0.24	0.09	0.18	0.04	0.25	0.08	0.16	0.07	0.08	0.03
S	0.30	0.12	0.22	0.10	0.26	0.17	0.17	0.06	0.34	0.16	0.24	0.08	0.16	0.09
Cl	0.02	0.03	0.02	0.02	0.02	0.02	0.02	0.02	0.01	0.01	0.02	0.02	0.01	0.01
K	0.33	0.12	0.17	0.05	0.24	0.07	0.16	0.02	0.10	0.08	0.07	0.05	0.10	0.02
Ca	0.37	0.11	0.25	0.10	0.22	0.12	0.20	0.06	0.13	0.10	0.10	0.04	0.13	0.01
Cu	0.28	0.16	0.12	0.08	0.23	0.12	0.15	0.04	0.18	0.08	0.14	0.08	0.11	0.04
As	0.00	0.00	0.02	0.03	0.00	0.00	0.00	0.00	0.00	0.00	0.00	0.00	0.00	0.00
Pb	0.00	0.00	0.00	0.00	0.07	0.03	0.00	0.00	0.00	0.00	0.00	0.00	0.00	0.00
Ni	0.00	0.00	0.00	0.00	0.00	0.00	0.04	0.03	0.00	0.00	0.00	0.00	0.00	0.00
Cd	0.00	0.00	0.00	0.00	0.00	0.00	0.00	0.00	0.01	0.01	0.00	0.00	0.00	0.00
F	0.00	0.00	0.00	0.00	0.00	0.00	0.00	0.00	0.00	0.00	0.17	0.18	0.00	0.00
Total	100.00		100.00		100.00		100.00		100.00		100.00		100.00	

*N: number of examined sites, %Wt: percentage weight, SD: standard deviation

Appendix A4 EDX elemental mapping images of contaminant-loaded MC and MO+MC

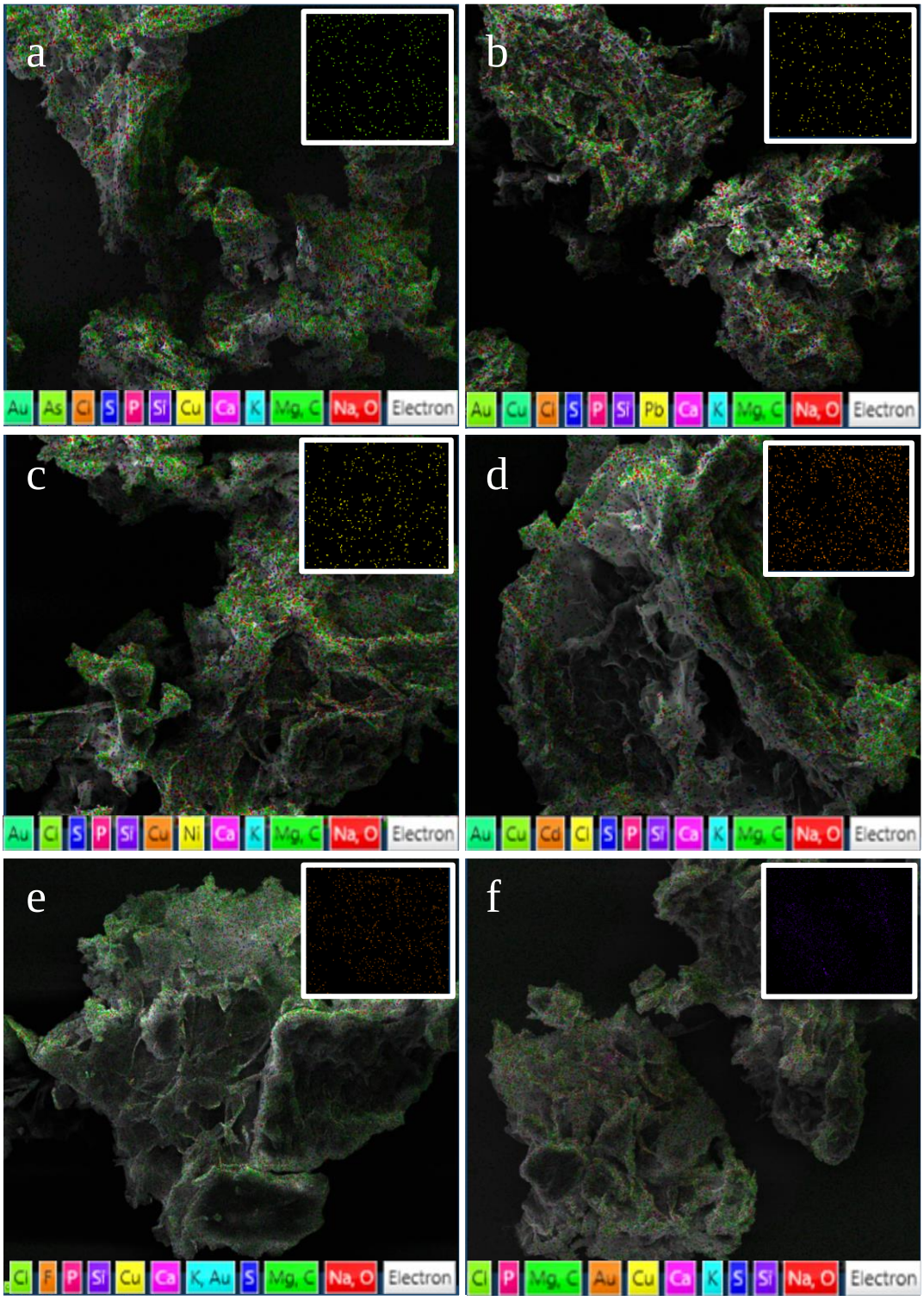

Figure A4.1 EDX elemental mapping images of MC loaded with (a) As, (b) Pb, (c) Ni, (d) Cd, (e) fluoride and (f) kaolin (turbidity)

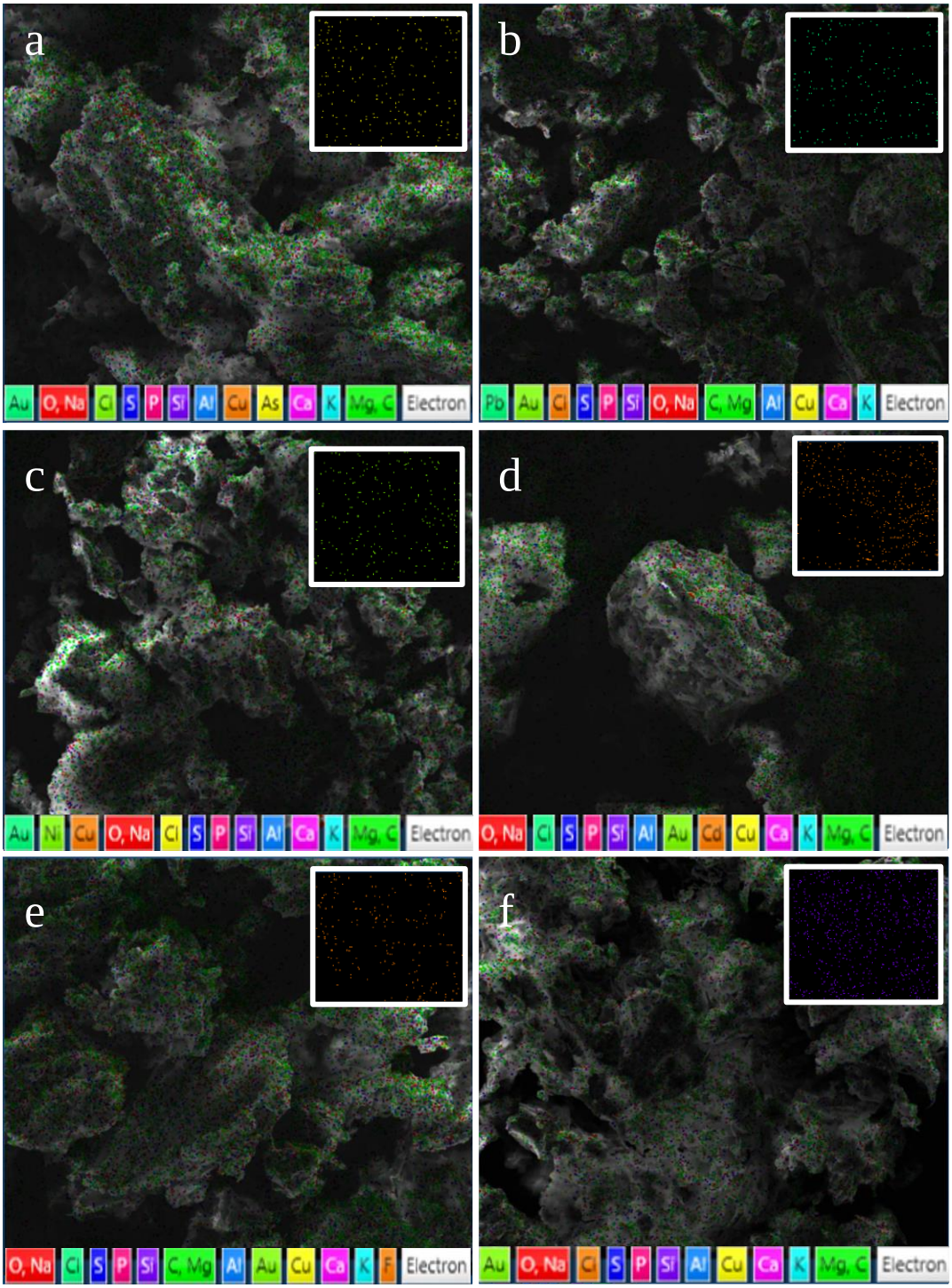

Figure A4.2 EDX elemental mapping images of MO+MC loaded with (a) As, (b) Pb, (c) Ni, (d) Cd, (e) fluoride and (f) kaolin (turbidity)